TECHNISCHE UNIVERSITÄT MÜNCHEN

TUM School of Life Sciences der Technischen Universität München

Lehrstuhl für Tecchnische Mikrobiologie

Identification of assertiveness-strategies of meat-associated *Lactobacillus sakei* and *Lactobacillus curvatus* by comparative genomics

Lara Eisenbach

Vollständiger Abdruck der von der TUM School of Life Sciences der Technischen Universität München zur Erlangung des akademischen Grades eines

Doktors der Naturwissenschaften

genehmigten Dissertation.

Vorsitzender:	Prof. Dr. Wilfried Schwab
Prüfer der Dissertation:	1. Prof. Dr. Rudi F. Vogel
	2. Prof. Dr. Wolfgang Liebl

Die Dissertation wurde am 20.01.2021 bei der Technischen Universität München eingereicht und durch die TUM School of Life Science am 21.04.2021 angenommen.

Vorwort / Danksagung

Die vorliegende Arbeit entstand im Rahmen eines durch Haushaltsmittel des BMWi über die AiF-Forschungsvereinigung Forschungskreis der Ernährungsindustrie geförderten Projektes (AiF 18552 N).

Teilergebnisse der vorliegenden Arbeit wurden vorab in Fachzeitschriften publiziert (Siehe „List of Publications“).

Mein ganz besonderer Dank gilt meinem Doktorvater Prof. Dr. Rudi F. Vogel sowohl für die Bereitstellung des Themas als auch für die Sicherstellung der Finanzierung des Forschungsprojektes. Imbesonderen danke ich ihm für die umfassende Betreuung und Unterstützung sowie fachlichen Diskussionen zu jeder Zeit.

Desweiterern meinen persönlichen Dank an Prof. Dr. Wolfgang Liebl für die Begutachtung der Dissertation sowie Prof. Dr. Wilfried Schwab für die Übernahme des Prüfungsvorsitzes.

Darüber hinaus bedanke ich mich bei Prof. Dr. Matthias Ehrmann, Prof. Dr. Ludwig Niessen, Angela Seppeur und dem gesamten Team der technischen Assistentinnen sowie all meinen Kollegen und Projektpartnern für die fachliche und organisatorische Unterstützung.

Mein Dank gilt auch meinen Studenten Barbara Knauer, Joshua Fäth und Ursula Rambold für die gute Zusammenarbeit und die erzielten Ergebnisse, die auch in diese Arbeit eingeflossen sind.

Ein besonderer Dank gilt meiner Familie, allen voran meinem Ehemann Roman Sternagel, der mich durch jedes Hoch und Tief während der Promotionszeit begleitet hat. Darüber hinaus waren meine Eltern, meine Geschwister sowie deren Partner und meine Schwiegereltern immer eine wertvolle Stütze.

Acronym	Meaning
AgmP	Agmatine putrescine antiporter
ANI	Average Nucleotide Identity
ara	Arabinose
B.	*Bacillus*
BADGE	BlAst Diagnostic Gene findEr
BCCP	Biotin carboxyl carrier protein
BRIG	BLAST Ring Image Generator
CAP	Cold acclimation proteins
CDM	Chemically defined medium
CDS	Coding sequences
CFU	Colony forming units
CimH	Citrate permease
CIP	Cold induced proteins
CitC	[citrate [pro-3S]-lyase] ligase
CitD	Citrate lyase γ -chain
CitE	Citrate lyase β -chain
CitF	Citrate lyase α -chain
CitG	ATP: dephospho-CoA 5'-triphosphoribosyltransferase
CitI	Citrate lyase transcriptional regulator
CitM	Mg^{2+}/citrate complex transporter
CitT	Apo-citrate lyase phosphoribosyl-dephospho CoA transferase
CK	Carbamate kinase
CSP	Cold shock proteins
DCM	Decarboxylation test medium
DNA	Desoxyribonucleoidacid
E.	*Escherichia*

Acronym	Meaning
EPS	Exopolysaccharides
frc	Fructose
g	Gramm
glc	Glucose
Gtf	Glycosyltransferase
h	hour
HePS	Heteropolysaccharide
HoPS	Homopolysaccharide
HPLC	High pressure liquid chromatography
L	Litre
L.	*Lactobacillus*
LAB	Lactic acid bacteria
LPS	Lipidpolysaccachride
MAMP	Microbe associated pattern
man	Mannose
ml	Millilitre
MRS	de Man, Rogosa and Sharpe
NCBI	National Centre for Biotechnology Information
nm	Nanometer
oadA	Oxaloacetate decarboxylase
oadB	Oxaloacetate decarboxylase β-subunit
oadC	Oxaloacetate decarboxylase γ-subunit
OD_{590}	Optic density at 590nm
orf	Openreading frame
PBS	Phosphate-Buffered Saline
PTS	Phosphotransferase System

Acronym	Meaning
PTS Man^{IIC}	PTS mannose/fructose/sorbose transporter subunit IIC
RAST	Rapid Annotation Subsystem Technology
RNA	Ribonucleinacid
S.	Streptococcus
SMRT	Single-molecule real-time sequencing
SU	Subunit
suc	Sucrose
TLR5	Toll-like receptor
TMW	Technische Mikrobiologie Weihenstephan
µl	Mikrolitre

1 INTRODUCTION 1

1.1 SAUSAGE FERMENTATION 1

1.2 MEAT STARTER CULTURES 1

1.3 LACTOBACILLUS SPECIES: *L. SAKEI* AND *L. CURVATUS* 2

1.4 GENOME SEQUENCES OF *L. SAKEI* AND *L. CURVATUS* 3

1.5 STRESS RESISTANCE AND RESPONSE 3

1.5.1 Cold stress adaptation 3

1.5.2 Oxidative stress 5

1.6 METABOLISM 7

1.7 BACTERIAL MOTILITY 10

1.8 CELL WALL PROPERTIES AND BIOPOLYMERS 12

1.8.1 Bacterial Capsule 13

1.8.2 Exopolysaccharides 13

1.8.3 Exopolysaccharides in bacterial biofilms 14

1.9 MOTIVATION, AIM AND WORKING HYPOTHESES 15

2 MATERIAL AND METHODS 16

2.1 BACTERIAL STRAINS AND CULTIVATION 16

2.2 GROWTH EXPERIMENTS 19

2.3 HPLC ANALYSIS 20

2.4 COLD SHOCK INDUCTION AND DETECTION OF RECOVERY AFTER COLD SHOCK 20

2.4.1 Determination of Colony forming Units 21

2.4.2 Fluorescence measurement to detect membrane damage 21

2.5 DECARBOXYLATION TEST MEDIUM 22

2.6 DNA ISOLATION 22

2.7 GENOMIC DNA SEQUENCING AND ANNOTATION 23

2.7.1 Genomic analysis by special (web-based) tools 24

2.8 MOTILITY EXPERIMENT 25

2.9 DETECTION OF BACTERIOCIN/ANTIMICROBIAL PEPTIDE PRODUCTION 26

3 RESULTS 27

3.1 PRESELECTION OF REPRESENTATIVE STRAIN SETS OF *L. CURVATUS* AND *L. SAKEI* 27

3.2 GENOMICS 29

3.2.1 Average Nucleotide Identity (ANI) 32

3.2.2 Genomic Comparison and gene distribution based on RAST Annotation and Seed Viewer 35

3.3 GENOMIC COMPARISON AND BIODIVERSITY 38

3.3.1 Pan and Core-genomes of L. sakei and L. curvatus 38

3.3.2 Accessory-genome of L. sakei and L. curvatus 43

3.3.3 Plasmidome of L. curvatus and L. sakei 46

3.3.4 Prophage gene clusters 51

3.3.5 CRISPR/Cas-systems 51

3.4 COLD SHOCK RESPONSE 54

3.5 OXIDATIVE STRESS RESPONSE 60

3.6 BACTERIOCIN PRODUCTION AND IMMUNITY 63

3.6.1 Detection of predicted bacteriocin gene clusters and genes, which are associated with bacteriocin immunity 63

3.6.2 Bacteriocin production assay 65

3.6.3 Bacteriocin sensitivity 66

3.7 METABOLIC PATHWAYS 69

3.7.1 Glycolysis 71

3.7.2 Glycerolipid metabolism 74

3.7.3 Adenosine and inosine metabolism 80

3.7.4 Amino acid metabolism and biosynthesis 82

3.7.5 Two different citrate clusters are encoded in a few strains of L. sakei 89

3.7.6 Growth experiments reveals different efficiency of citrate utilization based on genomic differences 92

3.7.7 Ribose metabolism *94*

3.7.8 Growth experiment of L. curvatus in presence of ribose in CDM *95*

3.8 ADHESION PROPERTIES / CELL WALL CHARACTERISTICS 98

3.8.1 Motility gene cluster *98*

3.8.2 EPS gene cluster *105*

3.8.3 EPS production in presence of sucrose *114*

3.8.4 Adhesion to different surfaces *115*

4 DISCUSSION 118

4.1 BIO- AND GENETIC-DIVERSITY OF *L. SAKEI* AND *L. CURVATUS* 119

4.2 COMPARATIVE GENOMICS; GENETIC DIVERSITY 120

4.3 EXOGENOUS DNA: CRISPR/CAS AND PHAGES/PLASMIDS 121

4.4 BACTERIOCIN PRODUCTION AND SENSITIVITY 123

4.5 PRECONDITIONING OF COMPETITIVE STARTER STRAINS BY COLD SHOCK 128

4.6 METABOLIC PROPERTIES/DIFFERENCES 130

4.6.1 Glycolysis *130*

4.6.2 Glycerolipid metabolism *131*

4.6.3 Adenosine and inosine metabolism *132*

4.7 RIBOSE METABOLISM 133

4.8 ACID STRESS; ADI-PATHWAY 135

4.9 CITRATE METABOLISM 137

4.10 FLAGELLAR GENE CLUSTER AND MOTILITY 140

4.11 ADHESION AND CELL WALL PROPERTIES 143

4.12 EXPRESSION OF COLONIZATION RESISTANCE 146

4.13 CONCLUSION 148

5 SUMMARY 151

6 ZUSAMMENFASSUNG 155

7 REFERENCES I

8 SUPPLEMENTARY VIII

8.1 MALDI-TOF MS VIII

8.2 AMINO ACID MATRICES AND CODON USAGE HEAT MAPS IX

8.3 SUPPLEMENTARY 2: PROTEOMIC COMPARISON XIII

9 APPENDIX XV

10 LIST OF PUBLICATIONS AND STUDENT THESES XXXVII

1 Introduction

1.1 Sausage fermentation

Raw fermented sausages are traditional food. The ripening process is complex, because a large variety of different parameters influence this process. A main component, besides the meat, is the fermentative microbiota and namely starter cultures derived thereof, which help to control the ripening process and ensure a tasty, biohazard-free product. Dominating lactic acid bacteria (LAB) are *Lactobacillus (L.) sakei* and *L. curvatus* (Hammes, Bantleon, & Min, 1990) at meat environment. It is known that strains of both species ensure the dominance of starters during the whole ripening process (Villani et al., 2007).

Recently, most species within the genus *Lactobacillus* have been re-designated, with *Lactobacillus sakei* and *Lactobacillus curvatus* being renamed to *Latilactobacillus* (Zheng et al., 2020). In this thesis the term "*Lactobacillus (L.)*" is used throughout for consistency with papers derived from parts of this thesis.

During the ripening process exogenous and endogenous parameters influence the fermentation of raw sausage (Hammes et al., 1990). Endogenous factors include raw materials, like meat type and quality, fat content, particle size, and casing material, diameter of sausage, curing agents, like salt, nitrate and nitrite, and spices and other additives. Exogenous parameters include climate, including temperature, relative humidity, movement of air, and smoke.

The aim of the ripening process is lowering of the pH, with concomitant effects of enhancement of shelf life, prevention of pathogen growth, slice-ability, as well as reddening and acquisition of flavour to result in a tasty non-biohazard raw sausage (Hammes et al., 1990).

1.2 Meat starter cultures

In traditional fermentation processes bacteria, yeast and fungi interact to contribute to the quality of the fermented sausages. Nevertheless, traditional spontaneous fermentation could result in off-flavor and biogenic amine formation. Therefore, starter cultures have been

developed to control the ripening process. As example, *L. plantarum* was introduced as starter organism in Europe 1966. Indeed, *L. sakei* and *L. curvatus* are known to be the most competitive LAB in sausage fermentation, and to ensure good quality sausages. Others are *L. brevis, L. alimentarius, L. casei, L. farciminis, L. viridescens* together with unspecified leuconostocs and pediococci (Benito et al., 2007; Cocolin L., 2011; Hammes W.P., 1998; Kröckel, 2003).

Interestingly, some meat-borne lactobacilli exhibit the essential activities like nitrate- and nitrite reductase, catalase activity, lipase and protease (Hammes et al., 1990). These observations suggest that meat-associated strains and meat starter strains are well adapted to such a complex environment. Moreover, such adaptations should be detectable at the genomes.

1.3 Lactobacillus species: *L. sakei* and *L. curvatus*

Both *L. sakei* and *L. curvatus* are often used as starter strains at raw sausage fermentation. Moreover, the facultatively heterofermentative, anaerobic and gram-positive *L. sakei* and *L. curvatus* are adapted to different habitats (Klein et al., 1996) and both species are well described. Torriani *et al.* (Torriani et al., 1996) investigated both species and the results suggest that there is a low level of DNA homology, which predicts that both species should not be closely related based on genomic level, whereas investigations on their physiology suggest that strains are phenotypically closely related. There are only a few differences based on fermentation of few carbohydrates. Moreover, strains of *L. sakei* as well as strains of *L. curvatus* are genomicly homogenous (Torriani et al., 1996). For *L. sakei* 18 strains were compared by microarray hybridization (Nyquist et al., 2011) with the genome *L. sakei* 23K, described by Chaillou *et al.* (Chaillou et al., 2005) used as reference. Interestingly, no significant differences of biodiversity within this species were detectable. However, the genome of *L. sakei* 23K is one of the smallest genomes within the investigated *L. sakei* strains, which display genomes sizes between 1815 kbp and 2310 kbp (Chaillou et al., 2009; McLeod, Nyquist, Snipen, Naterstad, & Axelsson, 2008). Interestingly, it was shown that the genome size does not correlate with physiological diversity of the tested strains.

The main physiological criteria to differentiate strains of *L. sakei* and *L. curvatus* are fermentation of melibiose, and arginine hydrolysis because *L. curvatus* has been declared as negative for both (Klein et al., 1996).

1.4 Genome sequences of *L. sakei* and *L. curvatus*

The first whole genome sequencing of *L. sakei* 23K was described by Chaillou *et al*. (Chaillou et al., 2005). Interestingly, the results suggest that the sequenced strain is auxotrophic for all amino acids except glutamic and aspartic acid. Moreover, a few systems are present for carbohydrate uptake. In detail, there are phosphotransferase systems associated with glucose, mannose, N-acetylglucosamine, fructose, sucrose, trehalose, cellobiose. Indeed, catabolic pathways were predicted, which are responsible for fermentation of melibiose, gluconate, galactose, arabinose, ribose, glycerol, malate, citrate.

1.5 Stress resistance and response

In a complex environment like meat and raw sausage fermentation microorganisms are subjected to different stress conditions, e.g., cold stress or oxidative stress. To overcome these conditions microorganisms developed a wide range of response reactions or stress resistance mechanisms. Interestingly, it was observed by Rallu *et al.* (Rallu, Gruss, Ehrlich, & Magnin, 2000) that stress resistance mechanisms can induce cross-tolerance to different stress qualities. For example, a few *Lactococcus lactis* mutants, which had been classified as acid-stress-resistant, were also characterized as more oxidative-stress-resistant.

1.5.1 Cold stress adaptation

Lactic acid bacteria undergo low temperature during industrial process, e.g., storage of fermented products, low temperature during fermentations (raw sausage fermentation, cheese ripening) or frozen storage of starter preparations (van de Guchte et al., 2002). To overcome these conditions, which are below the optimal growth temperature, the microorganisms need effective strategies for cold stress response. Indeed, such effective strategies are indispensable for assertive starter strains, especially for starter strains, which are used for raw sausage fermentation. On the one hand, these starter strains were freeze-

dried for storage. On the other hand, the cultures are added to a frozen meat matrix and the subsequent sausage fermentation and ripening process is characterized by low temperature. Interestingly, LAB are able to adapt to temperature downshift rapidly (van de Guchte et al., 2002). It was shown that cold shock adapted cells synthesize cold induced proteins (CIP) involved in membrane fluidity, DNA supercoiling, transcription and translation. Moreover, these proteins are associated with different cellular processes, e.g., sugar metabolism, chromosome structuring, signal transduction.

Graumann *et al.* (Graumann & Marahiel, 1996) showed for *Escherichia (E.) coli* and *Bacillus (B.) subtilis,* that bacteria express different classes of proteins at different temperatures. Moreover, proteins, which are present in higher level at low temperature, have been defined as cold acclimation proteins (CAPs). Whereas, proteins, which were synthesized after a sudden decrease of temperature, have been called cold shock proteins (CSPs) (Graumann & Marahiel, 1996). Interestingly, a diversity of the number of CSPs has been detected between subspecies and strains (Champomier-Vergès , Maguin , Mistou , Anglade, & Chich 2002; Champomier-Vergès, Maguin, Mistou, Anglade, & Chich, 2002). Some of the described CSPs are known as CspA, CspB, CspC and CspD (Graumann & Marahiel, 1998; Jones, Van Bogelen, & Neidhardt, 1987). It was shown that these proteins regulate each other's synthesis, directly as well as indirectly. Moreover, a back-up system has been established, this means, that a loss of one or two CSPs lead to an increase in synthesis of the others CSPs (Graumann & Marahiel, 1998). Phadtare *et al.* (Phadtare, Janivette, & Inouye, 1999) showed that *Lactococcus lactis* encoded three genes, which are related to *cspA* gene of *E. coli*. It has been supposed that CSPs function as general RNA and DNA chaperons, stabilize single-stranded regions in RNA and DNA. The outcome of this is an efficient translation, transcription and DNA replication at low temperature. Moreover, it is known that the small acidic CSPs are highly induced in response to cold shock like CspA, -B, -G and -I in *E. coli* (Derzelle, Hallet, Ferain, Delcour, & Hols, 2002; Derzelle et al., 2000). The presence of CSPs in *L. plantarum* was described by Mayo *et al.* (Mayo et al., 1997) and Darzelle *et al.* (Derzelle et al., 2000).

To conclude, there are a high number of cold stress-associated proteins, which enable strains to overcome cold shock as exogenous factor during raw sausage fermentation.

1.5.2 Oxidative stress

Bacteria of different species developed many resistance mechanisms to overcome oxidative stress. One strategy could be the reducing intracellular environment. Pebay *et al.* (Pebay, Holl, Simonet, & Decaris, 1995) described a *gor* gene, which encoded a glutathione reductase within the genome of *Streptococcus (S.) thermophilus*. Interestingly, an aeration results in duplication of reductase activity. Moreover, for *E. coli* it was shown that cells of these species used either the glutathione/glutaredoxin pathway or the thioredoxin pathway (Stewart, Aslund, & J., 1998). Indeed, the *trxB* gene encoding the thioredoxin reductase has been also identified in the genome of *L. bulgaricus* (van de Guchte et al., 2006; van de Guchte et al., 2002). Interestingly, the expression regulation of these enzymes may be different in microorganisms. In *E. coli* it was shown that the OxyR, which is one key regulator in oxidative stress resistance (Prieto-Alamno et al., 2000) is activated by H_2O_2. Whereas, neither the addition of catalase nor H_2O_2 induced transcription of *trxB* in *S. thermophilus* (van de Guchte et al., 2002). Another resistance mechanism was identified for *L. fermentum*: The L-cystein uptake system (Turner, Woodberry, Hafner, & Giffard, 1999). The intracellular cysteine breakdown results in production of reducing free sulfhydryl compound thiocysteine.

A second strategy to overcome oxidative stress may the prevention of reactive oxygen species formation, which means the elimination of free oxygen. *L. delbrueckii* ssp. *bulgaricus* encoded an NADH oxidase, which catalyzes a reaction resulting in elimination of oxygen (Marty-Teysset, de la Torre, & Garel, 2000; Yi, Kot, & Bezkorovainy, 1998). However, this reaction results in production of H_2O_2, which is also toxic to cells (Condon, 1987; Marty-Teysset et al., 2000; van de Guchte, Ehrlich, & Magnin, 2001) but could be eliminated by a catalase. Still, other lactobacilli, e.g. *L. sanfransiscensis*, express NADH oxidase 2, which reduces oxygen directly to water without producing intermediate H_2O_2 (Jänsch, Freiding, Behr, & Vogel, 2011). Another strategy to eliminate free oxygen was described for *L. helveticus* by Guerzoni *et al.* (Guerzoni, Lanciotti, & Cocconcelli, 2001). Oxidative stress

induced a change of composition of fatty acids in the cell membrane. The fatty acid desaturase system, which consumes oxygen is increased and reduces cell damage caused by free radicals.

A third resistance mechanism is the elimination of reactive oxygen species. Many lactobacilli are able to produce H_2O_2 and some of them encode a catalase to overcome the toxicity of hydrogenperoxide (Engesser & Hammes, 1994). There are two different type of catalases described for lactobacilli. On the one hand, there is the heme-dependent catalase and on the other hand, the pseudocatalase which is also known as Mn-containing pseudocatalase. The former is also described as true catalase and is produced by *L. sakei* LTH677 (Knauf, Vogel, & Hammes, 1992), and Chaillou *et al.* (Chaillou et al., 2005) showed that this catalase is also encoded within the genome of *L. sakei* 23K. Moreover, it was observed that transcription of the *katA* gene encoding the catalase was induced by addition of H_2O_2 or aeration (Hertel, Schmidt, Fischer, Oellers, & Hammes, 1998). The Mn-containing catalase of *L. plantarum* ATCC14431 is well known and described (Igarashi, Kono, & Tanaka, 1996; Kono & Fridovich, 1983). Moreover, Archibald *et al.* (Archibald & Fridovich, 1981) described a high intracellular Mn-concentration for *L. plantarum*, and *L. casei* compared to *L. bulgaricus,* which may correlate with the functionality of Mn-containing pseudocatalase (van de Guchte et al., 2002). Interestingly, the high Mn-concentration and the activity of the Mn-containing pseudo catalase enable to counterbalance the lack of superoxide dismutase (Archibald & Fridovich, 1981).

Finally, the putatively most efficient stress response is the repair of (oxidative) stress-induced damage. In *L. lactis* a *recA* (protein RecA) mutant was more sensitive to oxidative stress than the wildtype (Duwat, Ehrlich, & Gruss, 1995). This result suggests that *recA* genes effect a stress resistance caused by its role in DNA repair or its regulatory effect to other genes associated with repair of stress-induced damages. Indeed, the concentration of chaperone proteins was reduced in a *recA* mutant strain.

1.6 Metabolism

Meat as environment is a rich and complex medium, and glucose is only available in small amounts, whenever (mostly) exogenously added for sausage fermentation. But glycogen, lipids and nucleosides are present in high concentrations and they can be used as energy source. Therefore, the glycerol-metabolism, phosphoketolase pathway, nucleoside scavening and the pyruvate metabolism are important for persistence in the meat/sausage environment as well as the glycolysis as main pathway (Chaillou et al., 2005; McLeod, Zagorec, Champomier-Verges, Naterstad, & Axelsson, 2010). The summary of these connected pathways is shown in Figure 1.

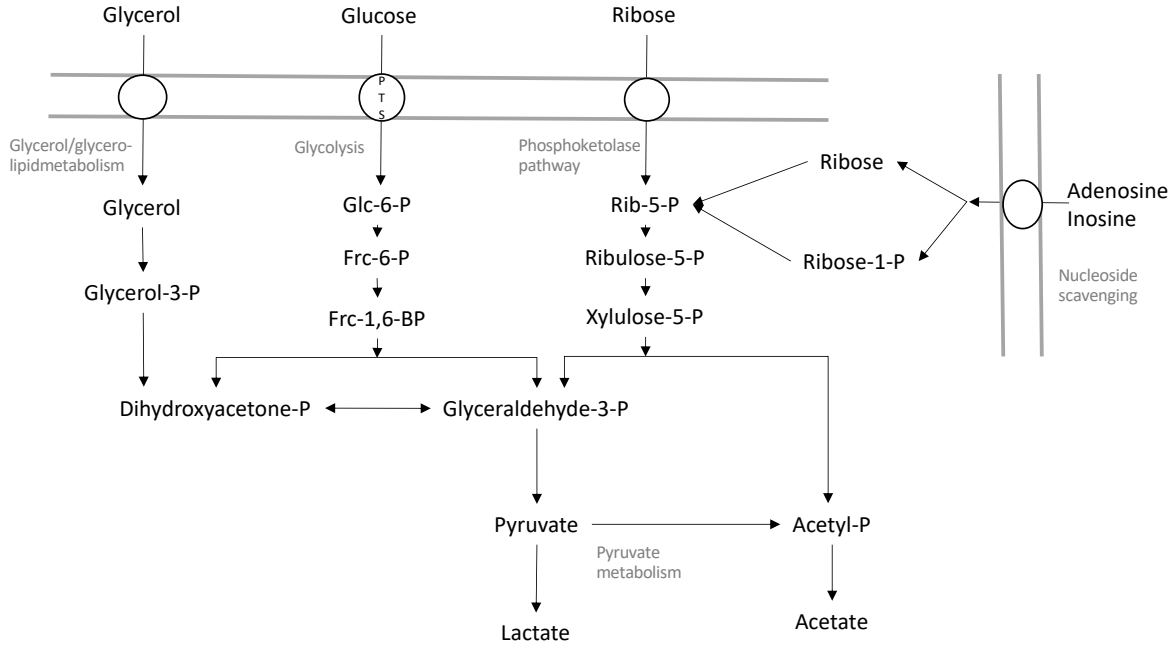

Figure 1: Important metabolisms for strains which are adapted to meat environment like *L. sakei* and *L. curvatus*. This metabolic overview was adapted and modified from (McLeod et al., 2010).

First of all, glycolysis is one of the main hexose fermentations (Koort, Vandamme, Schillinger, Holzapfel, & Bjorkroth, 2004; McLeod et al., 2010). Both *L. sakei* and *L. curvatus* are able to take up glucose by a phosphotransferase system (PTS). Afterwards glucose is converted to dihydroxyacetone-phosphate and glyceraldehyde-3-phospahte by several steps (Figure 1) (McLeod et al., 2010). Both triosephosphates are in an equilibrium to each other. This stage of equilibrium is catalysed by the triosephosphate-isomerase.

The catabolism of glycerol results in formation of dihydroxyacetone-phosphate, too (McLeod et al., 2010). Upon uptake of glycerol, it will be converted to dihydroxyacetone-phosphate by serveral steps of glycerol/glycerolipid-metabolism. Moreover, ribose is converted to glyceraldehyde-3-phosphate and acetyl-phosphate by the phosphoketolase pathway. Acetyl-phospahte is degraded to acetate by the acetate kinase and glyceraldehyde-3-phosphate is degraded to pyruvate. Pyruvate can be degraded to acetyl-phosphate, which is converted to acetate by acetate kinase like described before, or to lactate by the pyruvate metabolism.

Another important energy source are nucleosides. Chaillou *et al.* (Chaillou et al., 2005) showed that *L. sakei* 23K is able to grow in presence of adenosine and inosine, but not in presence of IMP, as energy source. Both, adenosine and inosine, are degraded to ribose under generation of a purine base. Ribose can go through the phosphoketolase pathway or is converted to ribose-1-phosphate to ribose-5-phosphate, which is an intermediate of the phosphoketolase pathway (Chaillou et al., 2005).

Interestingly, there is one metabolic characteristic, which allows to differentiate between *L. curvatus* and *L. sakei*: The arginine-deiminase-(ADI)-pathway (Champomier Verges et al., 1999), which is illustrated in Figure 2.

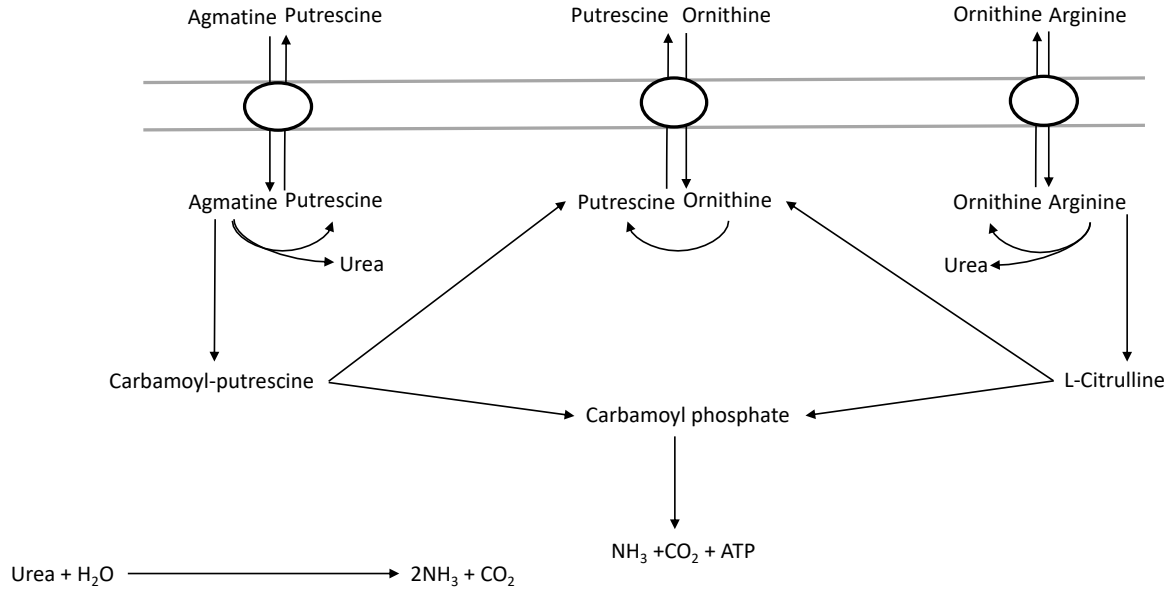

Figure 2: Arginine deiminase (ADI) pathway and agmatine-deiminase (AgDI) pathway which both are described for *L. sakei* (Champomier Verges et al., 1999; Rimaux et al., 2012)

This pathway is associated with the degradation of arginine, which is transported by an arginine-ornithine-antiporter and converted to L-citrulline by the arginine deiminase. In the next two steps L-citrulline is converted to carbamoyl phosphate and ornithine by the ornithine carbamoyl-transferase. Finally, carbamoyl phosphate is degraded to NH_3 and CO_2 under generation of ATP by carbamate kinase (Rimaux et al., 2012). Generated NH_3 results in an increase of intra- and extracellular pH. An important metabolism, which can be connected to arginine metabolism, is the agmatine deiminase (AgDI) pathway. Agmatine passes the membrane by an agmatine-putrescine-antiporter. Afterwards it is converted to carbamoyl-putrescine, this reaction is catalysed by the agmatine deiminase. Carbamoyl-putrescine is degraded to putrescine and carbamoyl-phosphate by the putrescine carbamoyl-transferase, and carbamoyl-phosphate is degraded by the carbamate kinase like described before (Rimaux et al., 2012).

Another important metabolism is the catabolic pathway of citrate (Drider, Bekal, & Prevost, 2004) (Figure 3). For *Lactococcus lactis* and *Leuconostoc mesenteroides* it was shown that citrate will be converted to pyruvate by three steps catalysed by enzymes, which are encoded in their genomes. Moreover, these *cit* genes are regulated by either citrate or pH. The interaction of the citrate metabolism and glycolysis is influenced by the redox state, e.g., in *Leuconostoc,* or by the end products of glycolysis, e.g., in *Lactococcus* (Hugenholtz, 1993; Starrenburg & Hugenholtz, 1991). For *Lactococcus* and *Leuconostoc* the citrate uptake works like a substrate/product exchange system. Lactate is generated by citrate catabolism as well as by glycolysis. The outcome of this is, that the citrate uptake is only efficient if lactate is produced by another (sugar) metabolism (Drider et al., 2004) (Figure 3). Alternatively, whenever less effective, citrate can enter the bacterial cell by diffusion at low pH, when the citrate is uncharged.

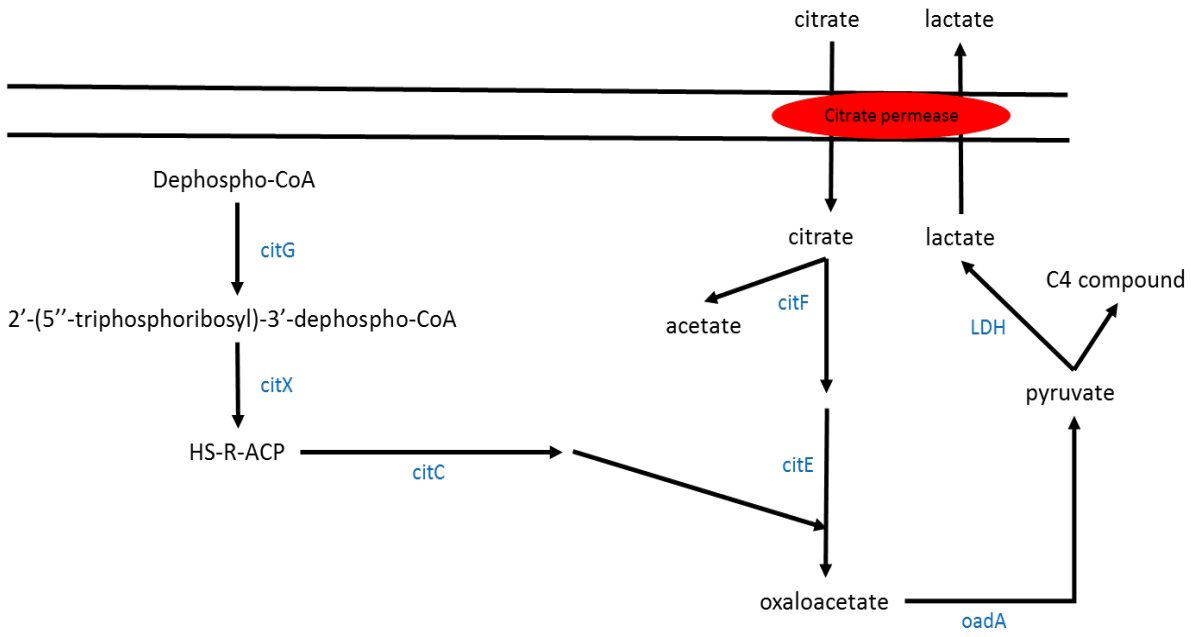

Figure 3: Citrate metabolic pathway like it is described for lactic acid bacteria by Drider et al. (Drider et al., 2004). This pathway is catalyzed by citrate permease, citG (ATP:dephospho-CoA 5'-triphosphoribosyl transferase), citX (holo-acyl carrier protein (ACP) synthase, citC (acetate: SH-citrate lyase ligase), citF (citrate lyase α-subunit citrate:acetyl-ACP transferase, citE (citrate lyase β-subunit citryl-S-ACP lyase), oadA (oxaloacetate decarboxylase), LDH (lactate dehydrogenase).

1.7 Bacterial Motility

The bacterial flagellum is the best-studied prokaryotic motility structure (Bardy, Ng, & Jarrell, 2003; Harshey, 2003; Kaiser, 2000; Macnab, 2003; Szurmant & Ordal, 2004), which is depictured in Figure 4.

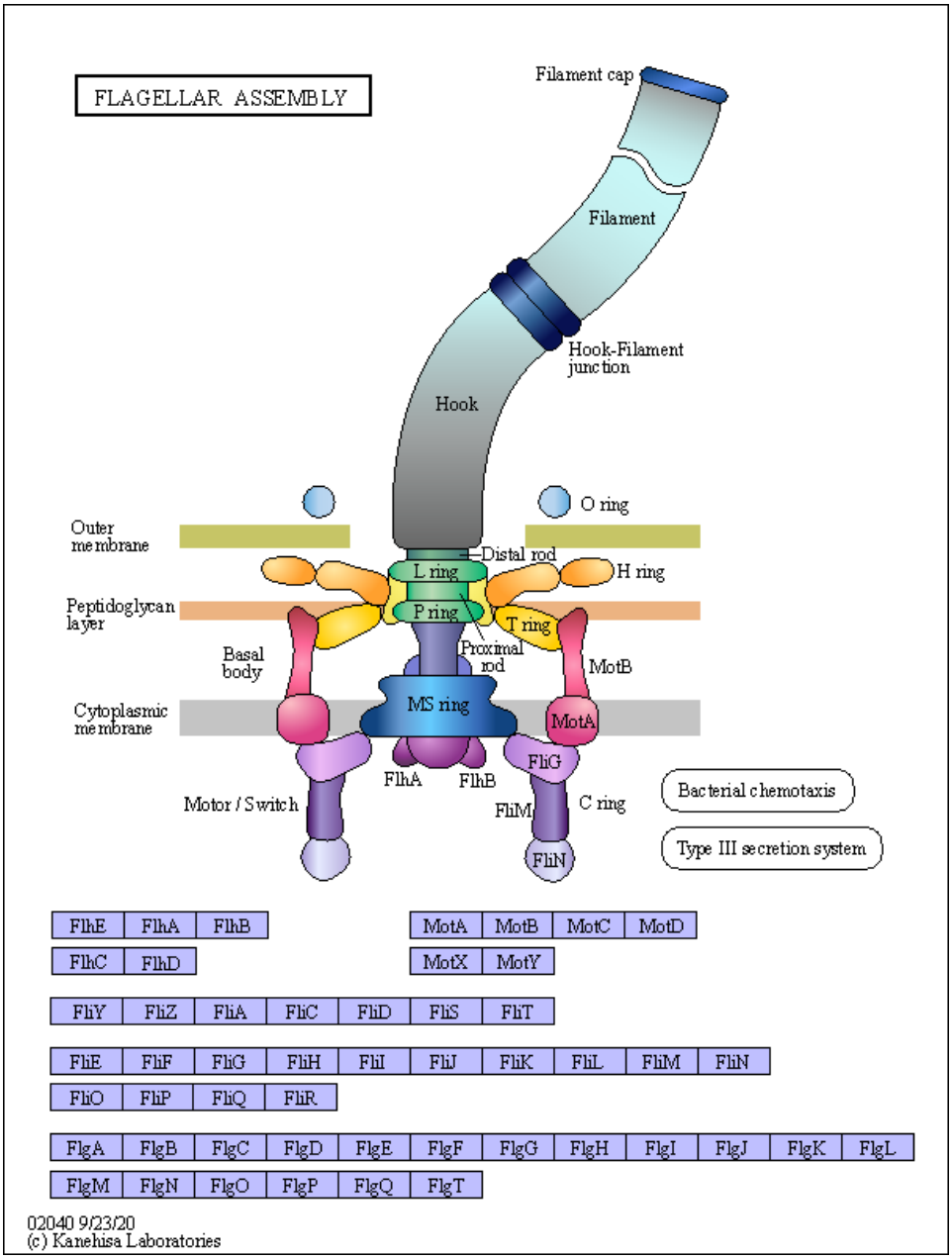

Figure 4: Flagellar assembly by KEGG, which pictured the structure of a flagellar and all involved enzymes.

This rotary structure consists of three major substructures: the basal body, the hook and the filament. The latter consists of thousands of copies of flagellin, which is mostly a single protein, but the flagellum also could be composed of several different flagellins. These proteins are a microbe associated pattern (MAMP), which is recognized by the host Toll-like receptor 5 (TLR5) (Cousin et al., 2015). The hook region connects the filament to the basal body and is one single protein. The connection of this central region and the filament requires two hook-associated proteins (Figure 4). The basal structure is more complex

(Bardy et al., 2003; Macnab, 2003): First, it consists of a rod, a series of rings, which anchor the flagellum to the cytoplasmic membrane, the peptidoglycan and the outer membrane (Figure 4). The last two rings could be missing in gram-positive bacteria. Moreover, there are switch proteins, which allow the bacteria to switch rotation and as a result change the direction of swimming in response to environmental effects. The direct contact of the phosphorylated CheY protein with the FliM switch protein results of environmental sensing (Bourret, Charon, Stock, & West, 2002). Additionally, the Mot proteins forms a proton channel. This results in a proton motive force, which enables the rotation of the flagellum (Bardy et al., 2003). In detail, the flagellar motor could be divided into two major components: the stator and the rotor (Macnab, 2003). The first one is arranged around the basal body and consists of multiple copies of two proteins MotA and MotB. The rotor is non-covalently attached to the MS ring and consists of multiple copies of a protein (FliG). Finally, both rotor and stator, are responsible for the torque generation (Macnab, 2003). Interestingly, the molecular structure of the flagellum, is self-assembled (Cousin et al., 2015; Macnab, 2003).

Flagellum-mediated motility may be a competitive advantage with focus of niche colonization, adhesion to defined surfaces and biofilm formation in an ecosystem like raw meat (Chagnot et al., 2017; Cousin et al., 2015; Macnab, 2003; Neville et al., 2012).

Cousin *et al.* (Cousin et al., 2015) described a motility locus organization within the genome of *L. curvatus* NRIC 0822 compared to *L. ruminis* ATCC 27782 and *L. acidipiscis* KCTC 13900. Moreover, it was possible to show that *L. curvatus* NRIC 0822 is motile.

1.8 Cell wall properties and biopolymers

It is known that bacteria are able to produce biopolymers. They vary based on chemical properties and use of substrates. Moreover, the function of such biopolymers is diverse as well (Nwodo, Green, & Okoh, 2012). There are intracellular and extracellular biopolymers. Only a few intracellular biopolymers are described, and their association with cellular functions is hardly described. In contrary, extracellular biopolymers are a large group, which could be classified into four groups: polyesters, polyamides, inorganic polyanhydrides, e.g., polyphosphates) and polysaccharides (Annous, Kozempel, & Kurantz, 1999; Axelsson &

Ahrne, 2000). The first identified bacterial exopolysaccharide, which was characterized from wine, was produced by *Leuconostoc mesenteroides* (Axelsson & Ahrne, 2000; Dal Bello, Walter, Hammes, & Hertel, 2003).

1.8.1 Bacterial Capsule

A bacterial capsule is characterized by polysaccharides covalently bound at outer cell surface (Nwodo et al., 2012). Moreover, the composition and nature of these molecules are highly strain dependent (Delauney, Cheon, Snyder, & Verma, 1990). Indeed, capsular properties are associated with different characters, like adhesion properties, water binding capacity to overcome dehydration of the cell, and phage resistance (Nwodo et al., 2012).

1.8.2 Exopolysaccharides

Exopolysaccharides are polysaccharides, which are either synthesized intracellulary and secreted, or synthesized extracellulary by enzymes, which are anchored to the cell wall. These heterogenic group of biopolymers could be characterized based on chemical structure, molecular weight and functionality, e.g., redox-active, surface properties, informative (Nwodo et al., 2012). Overall, the exopolysaccharides could be grouped into homo- and heteropolysaccharides (Berthier, Zagorec, Champomier-Verges, & Morel-Deville, 1996). Homopolysaccharides are built with from one type of monosaccharide, whereas heteropolysaccharides is built with di- to heptasaccharides in repeating units. Moreover, homopolysaccharides specifically need sucrose for their biosynthesis. Heteropolysaccharides are synthesized intracellulary, and a isoprenoid carrier molecule is needed for transport of the repeating unit through the cell membrane by flippase. Finally, the polymerization is completed extracellulary (Fernandez Murga, Bernie, Font de Valdez, & Disalvo, 1999). The yield of the exopolysaccharides is influenced by diverse factors, e.g. pH, medium, temperature, incubation time (Fu, Beeler, & Dunn, 1994). The surface active heteropolysaccharides, which varies in chemical structure and surface properties, could be involved in surface adhesion, e.g., charged molecules, which influenced the cell surface interaction, biofilm formation, and may act as antibacterial or antifungal protection (Fu et al., 1994; Gottesman, Roche, Zhou, & Sauer, 1998; Gryllos, Levin, & Wessels, 2003).

1.8.3 Exopolysaccharides in bacterial biofilms

Bacterial biofilms enable strains to colonize and accumulate on surfaces (Nwodo et al., 2012). As example, the biofilm enables the initial steps of adhesion to and colonization of surfaces. Moreover, the exopolysaccharides promote a cell aggregation and hydrophilic exopolysaccharides are characterized by a high ability of water retention. Indeed, biofilms build with exopolysaccharides can also serve as source of nutrients (e.g., carbon, phosphorous, nitrogen). Finally, a biofilm could be also a protective barrier against phages, bacteriocins or other toxic substances, or physical stress conditions like oxidative stress, acid stress or cold shock (Prechtl, Wefers, Jakob, & Vogel, 2018).

1.9 Motivation, aim and working hypotheses

Todays typical strategies of starter culture development for sausage fermentation follows the idea of a one multitalent strain of *L. sakei* or *L. curvatus*, which should outcompete autochtonous strains with unknown/unwanted properties and reliably enable a safe and tasty product. Genomic data have not yet been systematically established and exploited to assist and accelerate this process and transform this mostly empirical process to a science based-one, and possibly predict assertive strains.

Against this background the general aim of this thesis was to establish genomes of a representative strain set of *L. sakei* and *L. curvatus*, delineate by comparative genomics strain/group specific differences, and predict candidate genes for their assertiveness of strains under the conditions in fermenting sausage. To achieve this, these working hypotheses were followed:

- A representative set of *L. sakei* and *L. curvatus* strains can be selected and their genome sequences established
- Comparative genomics allows the identification of species-, strain-, and group-specific traits in *L. sakei* and *L. curvatus*
- Genes can be identified, which can be allocated to assertive / non-assertive strains
- Predicted metabolic traits from the genomes can be verified by physiological and/or biochemical tests
- The roles of sugar-, citrate and arginine metabolism in the assertiveness of *L. sakei* and *L. curvatus* can be delineated
- Specific traits including bacteriocin and exopolysaccharide formation and their roles in the assertiveness of *L. sakei* and *L. curvatus* can be predicted
- The assertiveness of strains can be predicted from their genomes
- The behavior can be explained of strains performing as winners, loosers or partners in sausage fermentation and referred to a genomic level

2 Material and Methods

2.1 Bacterial strains and cultivation

Strains of *L. curvatus* and *L. sakei* were taken from strain collection of Technische Mikrobiologie Weihenstephan (TMW) as listed in Table 1. The strains were cultivated in MRS medium (20 g/L glucose, 10 g/L casein pepton, 10 g/L meat extract, 5 g/L yeast extract, 1 g/L Tween 80, 2 g/L K_2HPO_4, 5 g/L Na-Acetate, 2 g/L $(NH_4)_2$ citrate, 0.2 g/L $MgSO_4*7H_2O$, 0.05 g/L $MnSO_4*H_2O$) (de Man, 1960). The bacterial cultures were incubated at 30°C under anaerobic conditions. For isolation of genomic DNA precultures were incubated for 14 h and 2.5 ml were used to inoculate a main culture (45 ml MRS), which was incubated for 8 h at 30°C under anaerobic conditions.

Table 1: Strain selection for first experiments to determine the biodiversity of both species. Starter preparation in this context means a preparation with an intended use in sausage fermentation.

Species	Strain	Source of isolation	Comments
L. sakei	TMW 1.2	Sausage (Spain)	
	TMW 1.3	Sausage (Spain)	
	TMW 1.4	Sausage (Spain)	
	TMW 1.13	Starter preparation	
	TMW 1.22	Starter preparation	LTH 677
	TMW 1.23	Sausage	LTH 673
	TMW 1.30	Unknown	
	TMW 1.46	Starter preparation	
	TMW 1.114	Starter preparation	
	TMW 1.147	sausage	CTC 335
	TMW 1.148	Unknown	
	TMW 1.149	Unknown	
	TMW 1.150	Unknown	

Species	Strain	Source of isolation	Comments
	TMW 1.151	Unknown	
	TMW 1.152	Unknown	
	TMW 1.153	Unknown	
	TMW 1.154	Unknown	
	TMW 1.155	Unknown	
	TMW 1.161	Starter preparation	
	TMW 1.162	Starter preparation	
	TMW 1.163	Starter preparation	
	TMW 1.165	Unknown	
	TMW 1.402	Sauerkraut	
	TMW 1.411	Sauerkraut	
	TMW 1.412	Sauerkraut	
	TMW 1.417	Starter preparation	
	TMW 1.454	Sausage	
	TMW 1.578	Starter preparation	
	TMW 1.579	Starter preparation	
	TMW 1.587	Starter preparation	
	TMW 1.588	Starter preparation	
	TMW 1.589	Starter preparation	
	TMW 1.1189	DSM 20017^{T}	
	TMW 1.1239	Sourdough	
	TMW 1.1240	Sourdough	
	TMW 1.1290	Sausage	
	TMW 1.1322	Meat	23K
	TMW 1.1366	Starter preparation	
	TMW 1.1383	Starter preparation	

Species	Strain	Source of isolation	Comments
	TMW 1.1385	Starter preparation	
	TMW 1.1386	Starter preparation	
	TMW 1.1388	Starter preparation	bitter aroma
	TMW 1.1392	Starter preparation	mild aroma
	TMW 1.1393	Starter preparation	
	TMW 1.1395	Starter preparation	
	TMW 1.1396	Starter preparation	
	TMW 1.1397	Starter preparation	
	TMW 1.1398	Starter preparation	bitter aroma
	TMW 1.1399	Starter preparation	mild aroma
	TMW 1.1474	Sauerkraut	LTH 2076
	TMW 1.1407	Fermented fish	
L. curvatus	TMW 1.7	DSM 20019^T	
	TMW 1.17	Sausage	
	TMW 1.27	Unknown	
	TMW 1.48	Starter preparation	
	TMW 1.49	Starter preparation	
	TMW 1.50	Starter preparation	
	TMW 1.51	Starter preparation	
	TMW 1.158	Starter preparation	
	TMW 1.166	Unknown	
	TMW 1.167	Unknown	
	TMW 1.401	Sauerkraut	LTH 2053
	TMW 1.407	Sauerkraut	
	TMW 1.408	Sauerkraut	
	TMW 1.421	Sausage material	

Species	Strain	Source of isolation	Comments
	TMW 1.439	Sausage	
	TMW 1.440	Hungarian salami	
	TMW 1.591	Unknown	
	TMW 1.593	Starter preparation	
	TMW 1.594	Starter preparation	
	TMW 1.595	Starter preparation	
	TMW 1.596	Starter preparation	
	TMW 1.624	Italian sausage	
	TMW 1.1291	Sausage	
	TMW 1.1365	Unknown	
	TMW 1.1381	Starter preparation	
	TMW 1.1382	Starter preparation	
	TMW 1.1384	Starter preparation	
	TMW 1.1389	Starter preparation	
	TMW 1.1390	Starter preparation	
	TMW 1.1391	Starter preparation	
	TMW 1.1408	Fermented fish	

2.2 Growth experiments

Precultures of the bacteria were cultivated in MRS and incubated for 16 h at 30°C under anaerobic conditions. Subsequently 1ml of the cell suspension were washed two times with 1 mL 0.9% NaCl until MRS was completely removed. Afterwards, the cells were incubated for 24h in PBS-Buffer (8 g/L NaCl, 0.2 g/L KCl, 1.42 g/L Na_2HPO_4 or 1.78 g/L $Na_2HPO_4*2H_2O$, 0.27 g/L KH_2PO_4). In the next step, the cells were inoculated in chemically defined medium (CDM) (Hebert, Raya, & de Giori, 2004; Morishita, Deguchi, Masako, Sakurai, & Yura, 1981) at a start OD_{590} of 0.1. For HPLC analysis samples of 500 µl were taken at defined time points (0 h, 24 h, 48 h, 72 h, 96 h)

2.3 HPLC analysis

Metabolism was observed based on utilization of substrates and production end-products of each strain with two biological replicates by HPLC as well as a negative control, which was not inoculated. For HPLC analysis of sugars and acids in the medium 500 µl of cell suspension was used and prepared for the following analysis. For sugar analysis, 250 µl 10% (w/v) $ZnSO_4*7H_2O$ (Sigma-Aldrich, St. Louis, USA) were added to a sample of 500 µl cell suspension for precipitation of proteins. Afterwards 250 µl 0.5 M NaOH (Carl Roth, Karlsruhe, Germany) were added and the suspension was mixed well by vortexing before an incubation at room temperature for 20 min. In the next step the suspension was centrifuged (10 min, max. speed with approx. 13,000 g) to pellet the precipitate. The supernatant was used for the analysis, which was done with REMEX^{TM} RPM Pb^{2+} column (Phenomenex, Aschaffenburg, Germany) (heated at 85°C), a Dionex UltiMate 3000 Pump (Dionex, Idstein, Germany) and a Shodex RI-71 detector (Showa Denko Shodex, Munich, Germany).

For acids analysis within the metabolic products, 1 ml sample of the incubated cells was used and was incubated with 50 µl 70% (v/v) perchloric acid (Sigma-Aldrich, St. Louis, USA) overnight at 4°C. Afterwards, the precipitates were removed by centrifugation of the samples (10 min, max. speed approx. 13,000 g). For analysis a Rezex ROA-Organic AcidH+ (Phenomenex, Aschaffenburg, Germany) (heated at 85°C), a Dionex UltiMate 3000 Pump (Dionex, Idstein, Germany) and a Shodex RI-71 detector (Showa Denko Shodex, Munich, Germany) was used to identify the detectable sugar molecules. Standards of lactate, acetate, citrate, ribose (Sigma Aldrich, St. Louis, USA) and glucose (Sigma Aldrich, St. Louis, USA) were used for quantification and the results were evaluated by Chromeleon evaluation software version 6.80 (Dionex, Idstein, Germany).

2.4 Cold shock induction and detection of recovery after cold shock

Each strain was cultivated in precultures (MRS), which were incubated overnight at 30°C under anaerobic conditions. These cultures were used to inoculate the main cultures (MRS 0.02% Glucose). The OD_{590} was set on 1. After inoculation a sample was used to analyse the cells before cold shock induction by determination of the colony forming units (CFU) and

fluorescence microscopy, which enables the detection of membrane damages. The other culture was stored for 3h at -20°C (cold shock induction). A second sample was taken after the cold shock induction and a third sample was taken after a following cultivation for 2h at 20°C. As positive control a culture without any cold shock was used, and as negative control a culture was incubated for 30min at 80°C.

2.4.1 Determination of Colony forming Units

The determination of the colony forming units were done by dilution steps (10^{-3} down to 10^{-5}) in MRS. 100 µl of each dilution was plated at MRS-agar. The plates were incubated at 30°C for two days. Afterwards the colonies were counted and the CFU per 1 ml was determined.

2.4.2 Fluorescence measurement to detect membrane damage

The membrane damage was detected by the LIVE/DEAD® BacLight™ Bacterial viability Kit L13152 (ThermoFischer Scientific, Waltham, USA). The protocol was done like described by the company with the following optimizations:

The bacteria were cultured in 50 ml MRS with 0.02% glucose and the OD_{590} was set on 1. The cultures were centrifuged at 3000 g for 15 min. The supernatant was discarded. The cell pellet was resuspended in 2 ml NaCl (0.8%). 400 µl was transferred in a new reaction tube and NaCl (0.8%) solution was added up to a final volume of 1800 µl. The cell suspension was centrifuged at 3000 g for 15 min., the supernatant was discarded, and the pellet was resuspended in 1800 µl NaCl (0.8%) solution. The cell suspension was centrifuged at 3000 g for 15 min and the supernatant was discard. The pellet was resuspended in 1400 µl NaCl (0.8%) solution and used for the following dyeing.

For staining 50 µl cell suspension was added with 25 µl SYTO 9 solution and 25 µl propidiumiod solution.

For fluorescent microscopy 5 µl of coloured cell suspension was used. The 100th oil-objective was used. To differentiate SYTO 9 and propidiumiodide two different filters were used listed in Table 2.

Table 2: Used stain and filter during fluorescent microscopy by using LIVE/DEAD® BacLight™ Bacterial viability Kit L13152 (ThermoFischer Scientific, Waltham, USA)

fluorescent stain	absorption	beam splitter	emission	fluorescent colour
SYTO 9	BP450-490	FT510	LP515	green
propidiumiodid	BP546/12	FT580	LP590	red

For quantification 10 pictures of each sample with both filters were evaluated. The red and green glowing cells were counted, and the percentages of dead and live cells were calculated.

2.5 Decarboxylation Test medium

Decarboxylation medium (DCM), which has been described by Bover-Cid *et al.* (Bover-Cid, Hugas, Izquierdo-Pulido, & Vidal-Carou, 2001), was used to confirm the ability of the strains of *L. sakei* to decarboxylate arginine, agmatine and ornithine. 1 ml of liquid DCM was used to cultivate the strains in triplicates. The cell cultures, which were inocluated with one colony were incubated at 30°C under anaerobic conditions. At five defined timepoints (24 h, 48 h, 72 h, 96 h and after 7 days) the coulour of each cell suspension was determined. A change of suspension's colour, caused by the added pH-indicator, remarks a change of the pH. A colour-change from yellow to purple, which indicates a increased pH, is defined as positive reaction.

2.6 DNA isolation

For whole genome sequencing high molecular DNA was isolated. The Qiagen Genomic-tip 100/G (Qiagen, Germany) and Qiagen Genomic DNA kit (Qiagen, Germany) was employed to isolate the high molecular DNA of the 20 selected strains of *L. sakei* and *L. curvatus*. 9 ml of cell suspension were used to collect cells of the late exponential growth phase by centrifugation for 10 min at 5,000 g. Afterwards, the supernatant was removed, and the cell pellet was resolved and washed in 1 ml of TE-buffer. In next step, the cell suspension was centrifuged for 5 min at 5,000 g. The washed bacterial cells were lysed like described by the manual of Qiagen Genomic DNA kit (Qiagen, Germany) with the following modifications.

Lysis of the cells was promoted by adding 80 µl mutanolysin (0.5 mg/ml). The lysate suspension was incubated at 37°C for 30 min up to 24 h, depending on the lysation of the cells, which was positive if the cell suspension became clear. After lysis was successful, the isolation of genomic DNA was done like described in the protocol. Finally, the isolated and precipitated genomic DNA was dissolved in 200 µl TE-Buffer.

2.7 Genomic DNA sequencing and annotation

The isolated high molecular genomic DNA was sequenced by the Single-molecule real-time sequencing (SMRT) (Eid et al., 2009; McCarthy, 2010) (PacBio RS II), based on a library size of 8 to 12 kb, and which finally resulted in not less than 200 Mb of raw data from SMRT cells (1x120-min movies) applying P4-C2 chemistry was done by GATC Biotech (Konstanz, Germany).

The collected sequencing data were used for draft genome assembly by using SMRT-Analysis (Pacific Biosciences, Menlo Park, USA), which was executed by SMRT® Portal. At first step the hierarchical genome assembly process (HGAP2 and HGAP3), which are developed by Chin *et al*. (Chin et al., 2013), was applied.

Further assemblies of the sequences with the aim to get complete genomes was done like described by an online manual (https://github.com/PacificBiosciences/Bioinformatics-Training/wiki/Finishing-Bacterial- Genomes) and advised by PacBio. The assemblies done by RS_HGAP_Assembly_3 protocol were used to generate contigs by BioPerl (https://bioperl.org/), which were controlled to be redundant by NCBI BLAST (Altschul, Gish, Miller, Myers, & Lipman, 1990; Camacho et al., 2009; SF, W, W, EW, & DJ, 1990). Non-sense and redundant contigs were discarded. Moreover, overlapping ends of the assembled sequences were identified by Gepard (Krumsiek, Arnold, & Rattei, 2007), a dotplot tool. The contigs with identified overlapping ends were circularized by an introduction of an *in silico* break within the contig (fasta) and a circularization was performed by minimus2 (AMOS, http://amos.sourceforge.net). A successful circularization was controlled by Gepard and a NCBI BLAST against the original contigs, to guarantee that 100% of the initial sequence was kept.

To finish the assembly of the genomes a resequencing was performed by using RS-Resequencing_1 protocol of SMRT-Analysis. This procedure was repeated until 100% of average reference consensus accordance was reached. The generated fasta-files are the input for all following genomic analysis.

For further analysis the whole genomes were annotated by two different platforms. On the one hand the DNA sequences were annotated by National Centre for Biotechnology Information (NCBI) and is listed under Bioproject ID: PRJNA317414, and on the other hand the RAPID Annotation Subsystem Technology (RAST) server was used to annotate the whole genome sequences and generate the E.C. numbers for following metabolic analysis (Aziz et al., 2008).

2.7.1 Genomic analysis by special (web-based) tools

First the genomic relationship of the sequenced strains of both species was calculated based on the Average Nucleotide Identity (ANI) by using the web-based tool ANI calculator (http://enve-omics.ce.gatech.edu/ani/). The calculated data were used to create a dendogram by R-studio Version 3.2.1 and the package “pvclust” which illustrated the relationship within each species.

Furthermore, the genomes were checked for gene clusters associated with prophages, CRISPR/Cas systems and bacteriocin production/immunity. For this, the following web based tools were used: PHASTER (http://phaster.ca), which is able to identify putative prophage gene clusters (Arndt et al., 2016), CRIPSRdb (http://crispr.i2bc.paris-saclay.fr), which enables identification of CRISPR/Cas gene cluster (Grissa, Vergnaud, & Pourcel, 2007) and BAGEL (http://bagel4.molgenrug.nl), which was used to detect genes associated with bacteriocin production or immunity (de Jong, van Hijum, Bijlsma, Kok, & Kuipers, 2006).

For a more detailed genomic analysis and comparison the pan-, core- and accessory-genome of both *L. sakei* and *L. curvatus* were calculated by using the BlAst Diagnostic Gene findEr (BADGE) (Behr, Geissler, Schmid, Zehe, & Vogel, 2016). The Calculation was performed with default settings with exception of “megablast percent identity cut” changed to

90 and “megablast within group qscov” set on 0.9 and “min DMG occurrence” was definded as 0.1.

To visualize the genomic comparison of both *L. sakei* and *L. curvatus* the genomic tool Blast Ring Image Generator (BRIG) (Alikhan, Petty, Zakour, & Beatson, 2011) was used with the annotated ORFs of calculated pan-genome as reference. Furthermore, the ORFs of pan-genome were sorted in the category core-genome (present in all sequenced strains) and accessory-genome (present in at least one strain, but not all strains) to get a clearer and detailed overview.

A more detailed genomic analysis was done by smart BLAST (https://blast.ncbi.nlm.nih.gov/smartblast/). This webbased tool enables the control of each single sequence of predicted enzymes and identified paralougs of each gene.

Another webbased tool the TMHMM (http://www.cbs.dtu.dk/services/TMHMM/) enables to check the transmembrane structure of putative transporters based on the amino acid sequence. This tool was used to identifiy differences based on the transporter’s structure.

2.8 Motility experiment

The experiment was performed in biological triplicates. The motility was tested with an motility agar (cfMRS) (10 g/L bacterial peptone from meat, 5 g/L yeast extract, 5 g/L sodium acetate, 2 g/L ammonium citrate, 2 g/L potassium phosphate, 1 ml/L Tween 80, 0.2 g/L $MgSO_4$, 0.05 g/L $MnSO_4$, 0.4% Agar (w/v), 0.5% carbon source (w/v) (glucose, ribose, glycerol) and one without any carbon source. 10 ml of the motility agar was prepared in test tubes. Precultures of tested bacteria were incubated over night at 30°C under anaerobic conditions. Afterwards, the main culture (10 ml of cfMRS w/o Agar) was inoculated by 400 µl of the preculture and incubated at 30°C under anaerobic conditions. After 6 h, during exponential growth, an inoculation loop was dropped into the main culture and was cut in the motiliy agar. The motility was tested under different conditions. First, it was observed at 30°C, 20°C and 15°C. Second, different carbohydrates were present: glucose, ribose, glycogen and no carbohydrate.

2.9 Detection of bacteriocin/antimicrobial peptide production

The bacteriocin immunity and production was tested by an inhibition assay. Firstly, putative bacteriocin producers were cultivated in precultures in MRS (Table 15 and Table 16). In the next step, 5 µl of the cell culture was dropped onto MRS-Agar (0.2% glucose). This assay plates were incubated overnight at 30°C under aerobic conditions. Afterwards, an overlay agar, which was inoculated with 200 µl of a preculture of the indicator strains (Table 17, Table 18 and Table 19), was overlaid over the colonies. Then, the bacteriocin assay plates were incubated 30°C under aerobic conditions, and after 48 h inhibition zones around the colonies, which indicated a bacteriocin production, were observed and documented. *L. curvatus* TMW 1.624 was used as positive control based on the results described by Janßen *et al.* (Janßen, Eisenbach, Ehrmann, & Vogel, 2018) which suggest that this strain produce at least one bacteriocin.

3 Results

3.1 Preselection of representative strain sets of *L. curvatus* and *L. sakei*

For the preselection of a representative group, which reflects the biodiversity of both species, some physiological experiments were done. Firstly, the RAPD-Fingerprinting (Freiding, Gutsche, Ehrmann, & Vogel, 2011) was used. Moreover, MALDI-TOF-MS were used to group strains based on the Sub-Proteome (Janßen, Eisenbach, et al., 2018). Additionally, the physiology of the strains was tested. As example, the growth in MRS with and without prior cold shock induction were measured in presence of a lower glucose concentration (0.02% glucose). Finally, the oxidative stress response was evaluated by a growth experiment in presence of the H_2O_2 (data not shown).

All generated data were calculated by a DAPC analysis, which is shown by Figure 5. Selected criteria are growth parameters like the length of the growth phase (with and without cold shock), maximal growth rate, maximal OD, growth in presence of H_2O_2, predicted competitiveness (strong, weak, average) and source of isolation (data not shown).

Interestingly, *L. sakei* strains grouped into 6 groups based on the physiological data, whereas *L. curvatus* grouped in two main groups. For *L. sakei* and *L. curvatus* (DAPC grouping set to three groups instead of two groups) the DAPC was performed with the grouping criteria, e.g., source of isolation as well as predicted competitiveness (supplementary Figure 9, supplementary Figure 10, supplementary Figure 11, supplementary Figure 12, supplementary Figure 13). There was no correlation between either source of isolation or the six physiological groups, which were identified based on the preselection.

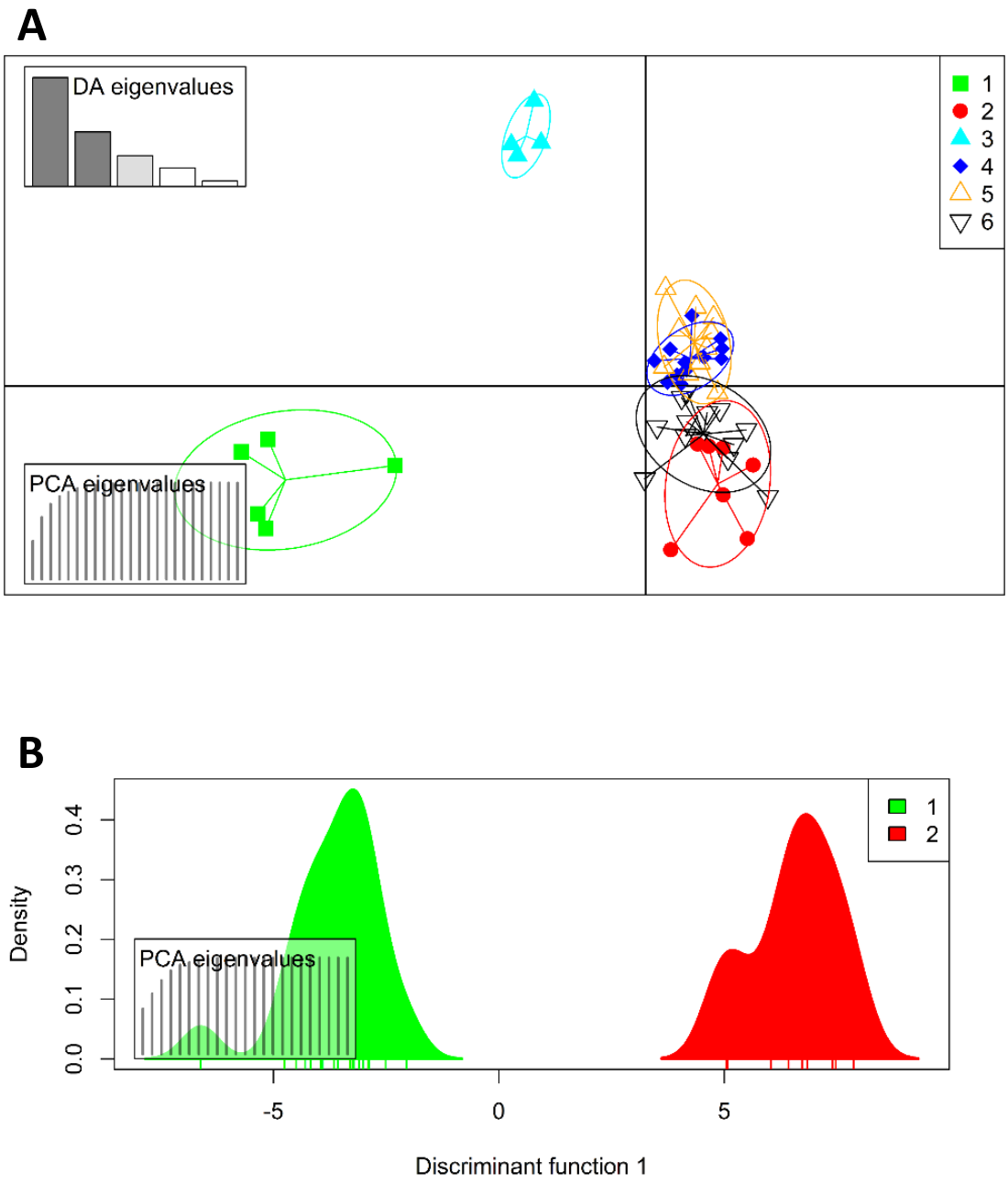

Figure 5: DAPC analysis of the physiological screening of *L. sakei* and *L. curvatus* (B). (A) *L. sakei* strains could be grouped into 6 groups, but 3 main groups could be defined. (B) *L. curvatus* strains were grouped into two main groups. For further analysis the DAPC analysis was grouped by defined main criteria (supplementary Figure 9, supplementary Figure 10, supplementary Figure 11, supplementary Figure 12, supplementary Figure 13).

Finally, 10 strains of each species were selected. The strain selection should represent the physiological and genomic biodiversity, so strains with different characteristics like DAPC cluster, RAPD-Group, MALDI-TOF-MS-Group were selected. The final strain set is presented in Table 3.

Table 3: Strain selection for further experiments and genomics. “Starter culture” in this context means a preparation with an intended use in sausage fermentation.

L. sakei	*source*	*L. curvatus*	*Source*
TMW 1.3	Sausage (spain)	TMW 1.27	Unknown
TMW 1.46	Starter culture	TMW 1.167	Unknown
TMW 1.114	Starter culture	TMW 1.401	Sauerkraut
TMW 1.417	Starter culture	TMW 1.407	Sauerkraut
TMW 1.578	Starter culture	TMW 1.421	Sausage material
TMW 1.1189	DSM 20017^T	TMW 1.439	Sausage
TMW 1.1239	Sourdough	TMW 1.595	Starter culture
TMW 1.1322	23K (INRA, France)	TMW 1.624	Italian sausage
TMW 1.1396	Starter culture	TMW 1.1381	Starter culture
TMW 1.1398	Starter culture	TMW 1.1390	Starter culture

3.2 Genomics

In total 19 genomes of *L. sakei* and *L. curvatus* were sequenced by SMRT sequencing (Eid et al., 2009; McCarthy, 2010) and assembled by SMRT-Analysis (Pacific Biosciences, Menlo Park, USA) and circularized. Finally, the assembled genomes were annotated by RAST (Aziz et al., 2008; Overbeek et al., 2014) and NCBI (National Center for Biotechnology Information, Bethesda, Maryland, USA). All sequenced whole genomes were described as ‘complete’. Moreover, the complete whole genome sequence of *L. sakei* TMW 1.1322 (23K) was downloaded from NCBI (Chaillou et al., 2005).

The sequence data as well as the basic genomic data are listed in Table 4 (*L. curvatus*) and Table 5 (*L. sakei*). To conclude, the genome size of both *L. sakei* and *L. curvatus* ranged between 1.8Mb and 2.0Mb. There are strains carried no plasmids or up to three plasmids, but it could be that smaller plasmids not detected by this sequence method caused by the sample preparation. Both species has a GC content of around 41% or 42%.

Furthermore, coding density and number of CDS (coding sequences), RNAs were calculated and are listed in Table 4 and Table 5.

Table 4: Summary of the general features of the sequenced genomes of L. curvatus.

	L. curvatus									
Genome	TMW 1.421	TMW 1.439	TMW 1.624	TMW 1.595	TMW 1.1381	TMW 1.1390	TMW 1.401	TMW 1.407	TMW 1.27	TMW 1.167
number of Contigs	2	1	3	2	1	1	2	3	3	2
Genome size (bp)	1,994,091	1,947,550	2,131,532	2,032,028	1,948,585	1,977,421	1,885,790	1,886,130	2,056,372	1,951,420
GC content (%)	41.97	42.04	41.63	41.95	42.05	42.07	42.00	42.01	41.86	42.03
Number of CDS	1,961	1,939	2,148	1,991	1,933	1,949	1,83	1,831	2,027	1,94
Total CDS length (bp)	1,715,035	1,674,641	1,835,409	1,746,212	1,677,999	1,710,135	1,617,590	1,630,147	1,763,844	1,680,664
coding density (%)	86.01	85.99	86.11	85.93	86.11	86.48	85.78	86.43	85.77	86.13
Number of plasmids	1	0	2	1	0	0	1	2	2	1
Number of RNAs	83	84	87	88	84	88	85	84	91	84
origin	sausage	sausage	sausage	starter culture	starter culture	starter culture	sauerkraut	sauerkraut	unknown	unknown
Accession number (chr)	CP016221	CP015489	CP015490	CP016470	CP015493	CP015494	CP016216	CP016218	CP016467	CP016472

Table 5: Summary of the general features of the sequenced genomes of *L. sakei*.

	L. sakei									
Genome	TMW 1.3	23K	TMW 1.46	TMW 1.114	TMW 1.417	TMW 1.578	TMW 1.1396	TMW 1.1398	TMW 1.1239	DSM 20017^T
number of Contigs	2	1	2	2	2	2	2	4	1	1
Genome size (bp)	1,930,337	1,884,661	2,079,718	1,976,338	1,980,463	1,976,312	1,935,698	2,066,572	1,975,742	1,942,056
GC content (%)	41.12	41.26	41.1	41.19	41.18	41.18	41.28	41.17	41.2	41.18
Number of CDS	1,861	1,844	2,03	1,901	1,887	1,898	1,873	2,015	1,880	1,863
Total CDS length (bp)	1,669,711	1,627,920	1,816,491	1,713,165	1,714,895	1,712,580	1,680,893	1,791,826	1,717,616	1,691,532
coding density (%)	86.50	86.38	87.34	86.68	86.59	86.66	86.84	86.71	86.94	87.10
number of plasmids	1	0	1	1	1	1	1	3	0	0
Number of RNAs	87	85	84	87	87	87	87	87	87	84
origin	sausage (spain)	meat	starter culture	starter culture	starter culture	starter culture	starter culture	starter culture	sourdough	type strain
accession number (chr)	CP016465	NC_007576	CP015487	CP017566	CP017568	CP017570	CP017273	CP017275	CP017272	CP017271

3.2.1 Average Nucleotide Identity (ANI)

The genomic relationship between species as well as strains could be identified by the average nucleotide identity (ANI). For *L. curvatus* strains results revealed an ANI diversity between 98.98 % and 99.99 %. The ANI calculation was clustered with R studio. The result suggests that *L. curvatus* strains are grouped in two groups like it is shown in Figure 6. The genomic relationship of the strains, calculated by ANI, does not correlate neither with genome sizes nor with the source of isolation.

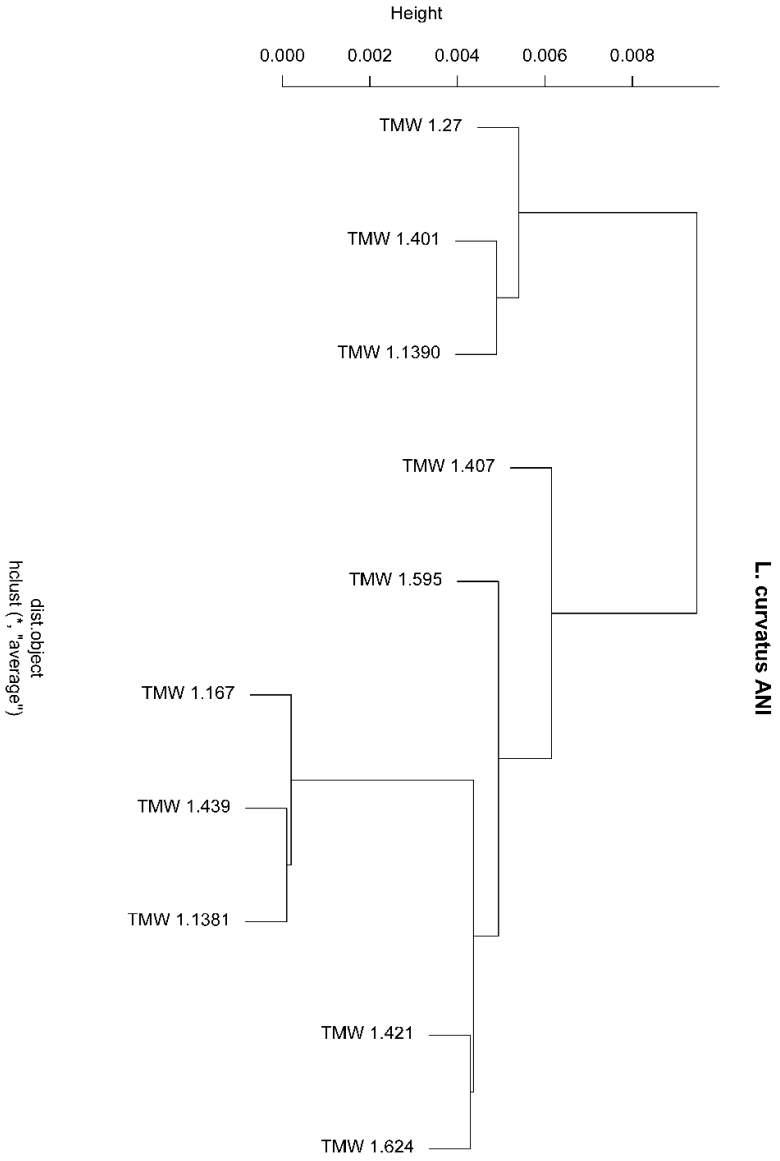

Figure 6: Dendogram of ANI calculation illustrates the genomic based relationship within *Lactobacillus curvatus*. Calculated ANI were clustered with R-Studio using “pvclust” script. The dendogram illustrated the genomic relationship between the sequenced genomes.

For *L. sakei* strains the intra species ANI diversity range between 100% up to 97.05%. Strains of this species were clustered based on the ANI diversity like described before for *L. curvatus*. This clustering method suggests that strains of *L. sakei* forms two main groups which could be sub-devided into sub-groups (Figure 7). Interestingly, meat associated strains seem to be genomicly closely related based on the results of the dendogram. But there is *L. sakei* TMW 1.46, which was isolated from meat environment. Indeed, results suggest a close genomic relationship with *L. sakei* TMW 1.1189 and TMW 1.1239, which were isolated from plant related environment, e.g., sake-starter, or sourdough.

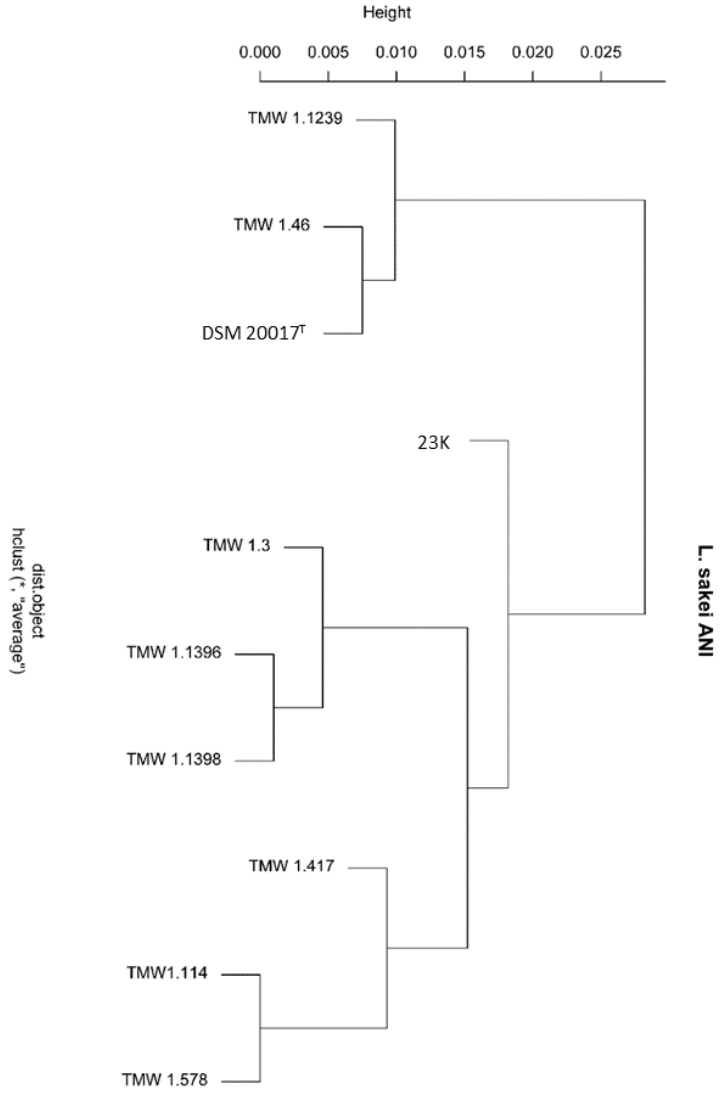

Figure 7: Dengoram of ANI calculation illustrates the gentical based relationship within *Lactobacillus sakei*. Calculated ANI were clustered with R-Studio using “pvclust” script. The dendogram illustrated the genomic relationship between the sequenced genomes.

Moreover, the interspecies ANI diversity of *L. curvatus* and *L. sakei* ranged between 82.76% and 84.84% (supplementary Table 1). As depicted in Figure 8, both species are closely related, but clearly separated.

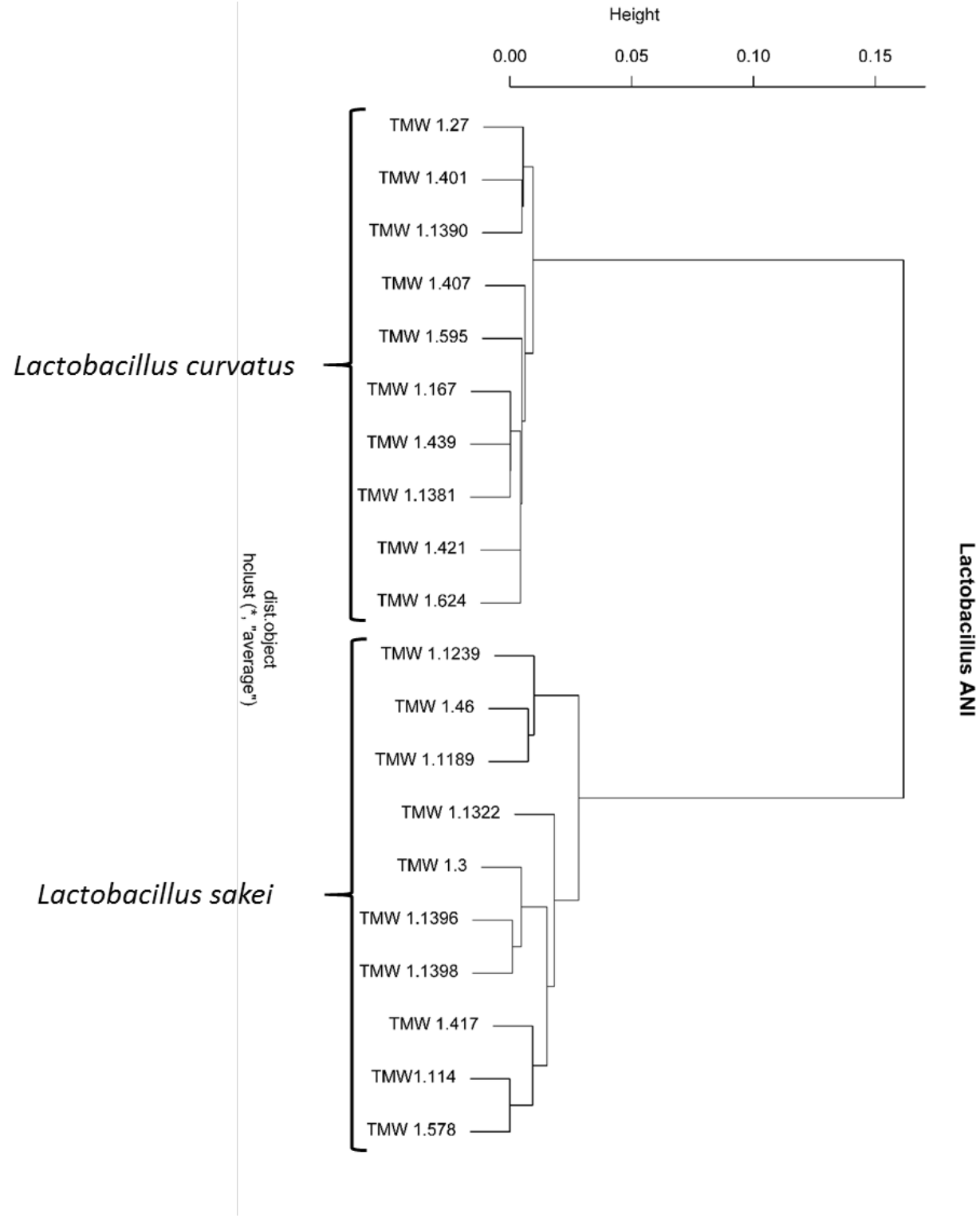

Figure 8: Dendogram of ANI calculation revealed a genomic relationship between both species. Moreover, strains of both species could be separate clearly. Calculated ANI were clustered with R-Studio using “pvclust” script. The dendogram illustrated the genomic relationship between the sequenced genomes.

3.2.2 Genomic Comparison and gene distribution based on RAST Annotation and Seed Viewer

The summary of encoded genes in correlation with defined categories, like metabolic pathways, cell wall etc., reflects the diversity as well as the similarity of strains within one species, and is given in Figure 9 and Figure 10 for *L. curvatus* and *L. sakei*, respectively.

For *L. curvatus* strains a maximum of encoded genes was detected of 1127 genes (*L. curvatus* TMW 1.1390) and a minimum of 1060 (*L. curvatus* TMW 1.407) encoded genes. Detailed analysis revealed a highly similarity in the number of genes associated with cofactors, vitamins, prosthetic groups, pigments, membrane transport, iron acquisition and metabolism, DNA metabolism, protein metabolism, and stress response. But there is detectable diversity based on the categories of cell wall and capsule, nucleosides and nucleotides, fatty acids, lipids and isoprenoids, amino acids and derivatives, carbohydrates.

For *L. sakei* differences were observed of genes involved in protein metabolism, and for carbohydrates, whereas there are less differences for nucleosides and nucleotides, fatty acids, lipids and isoprenoids, amino acids and derivates and stress response. In total, strains of *L. sakei* encoded in least 1097 (*L. sakei* TMW 1.1322) up to 1152 (*L. sakei* TMW 1.1398) genes, which were correlated with different categories of SEED.

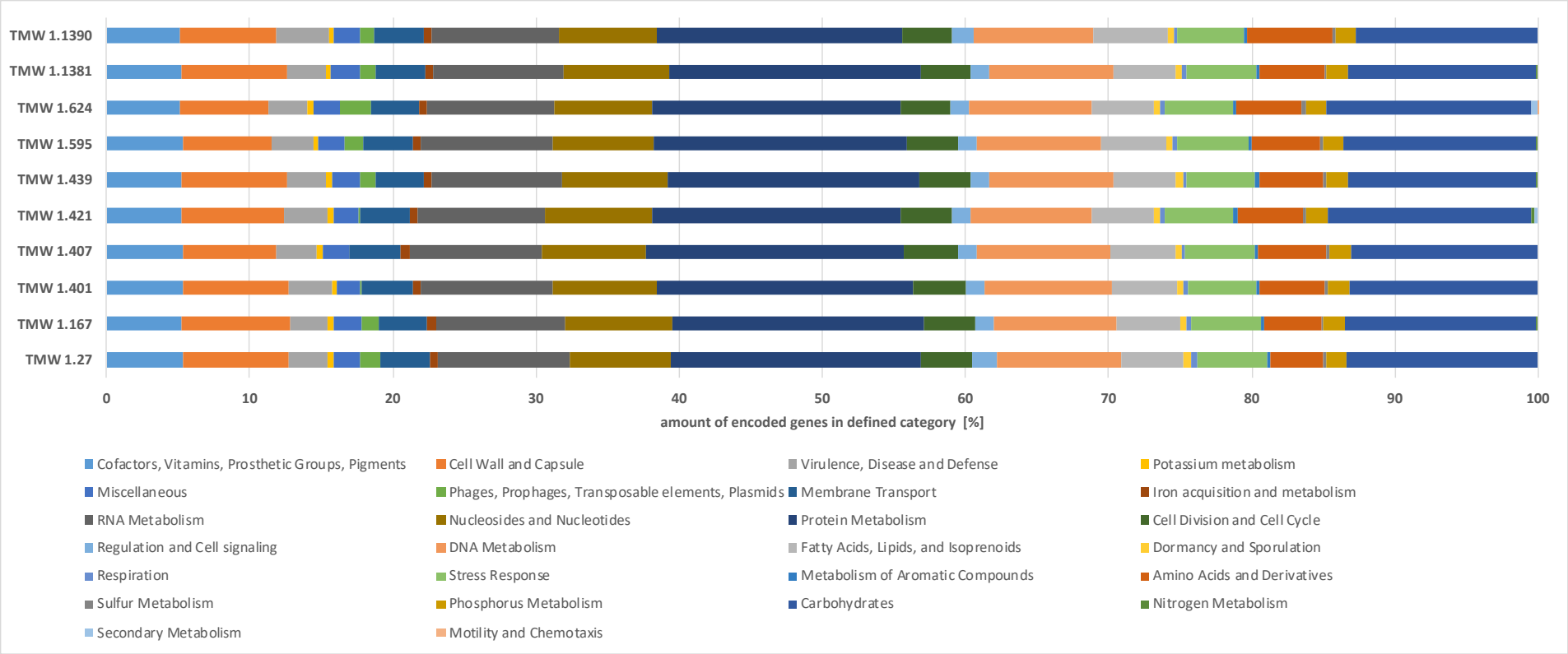

Figure 9: Relative gene distribution based on defined categories based on RAST annotation and Seed viewer for *L. curvatus*. The encoded genes were sorted by their predicted function of encoded gene products.

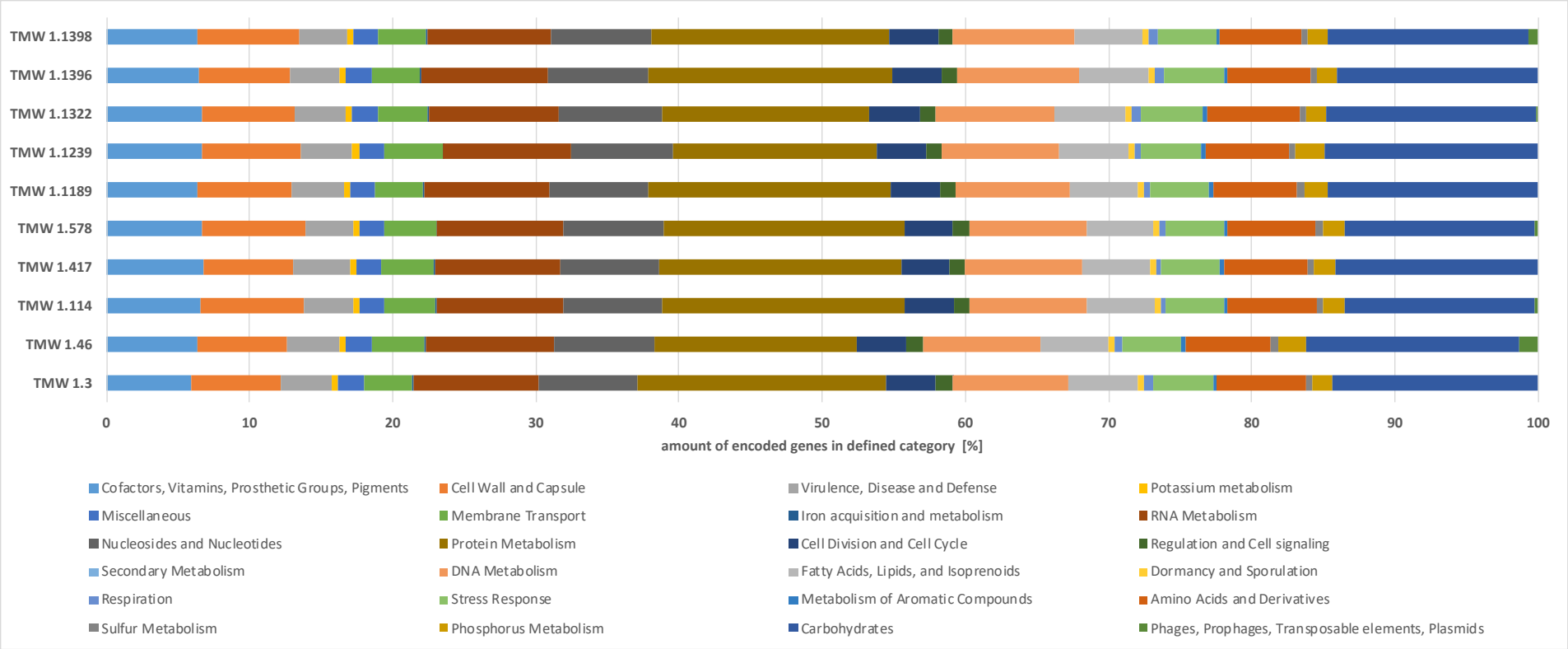

Figure 10: Relative gene distribution based on defined categories based on RAST annotation and Seed viewer for *L. sakei*. The encoded genes were sorted by their predicted function of encoded gene products.

3.3 Genomic comparison and biodiversity

3.3.1 Pan and Core-genomes of *L. sakei* and *L. curvatus*

Determination of the size of pan and core-genomes was done by CMG biotools. The calculation is depicted in Figure 11, and results revealed that around half of the pan-genome of *L. curvatus* is part of the core-genome.

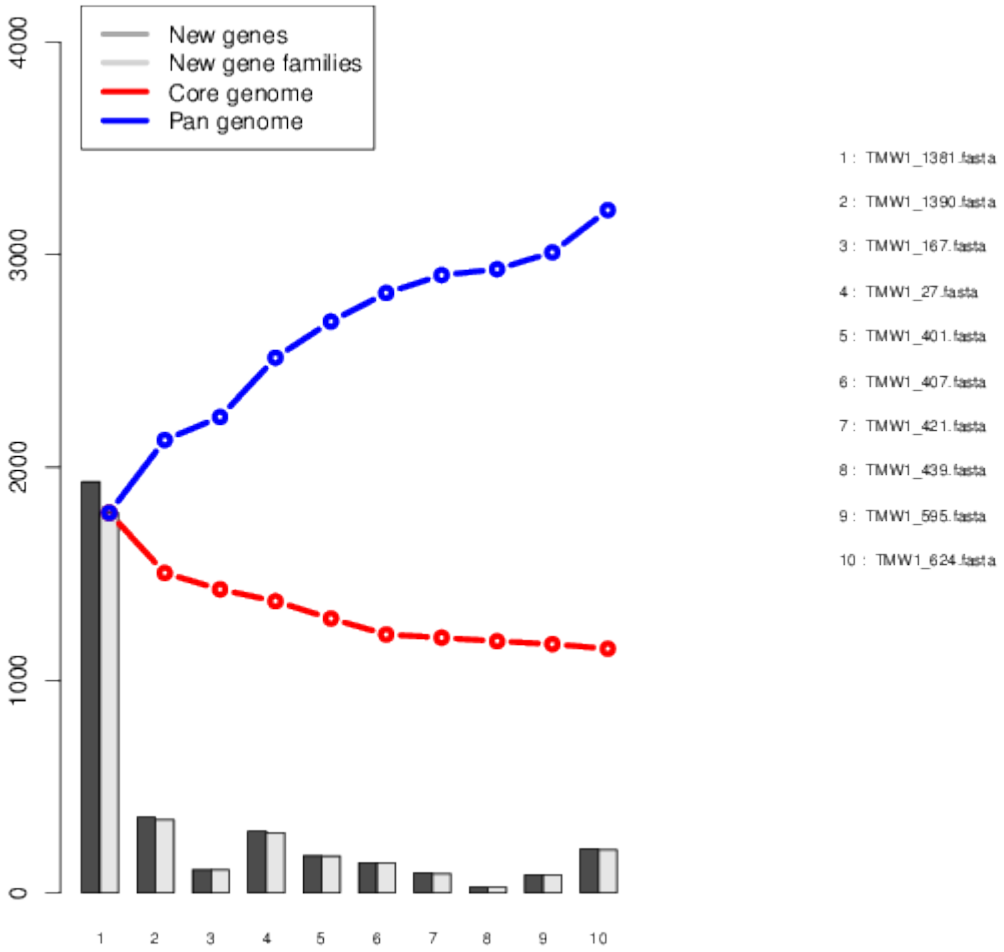

Figure 11: Pan-Core plot of *L. curvatus* calculated by CMG Biotool. Red-line marks the core-genome and blue-line marks the pan-genome. Moreover, the dark-grey bars show the identified new genes and the light-grey bars illustrate the identified new gene families.

Interestingly, the number of new genes or new gene families upon addition of single genomes varies. *L. curvatus* TMW 1.439 (No. 8, Figure 11) has only less new genes compared to the other strains, whereas *L. curvatus* TMW 1.624 (No. 10, Figure 11) has a high number of new genes or new gene families compared to all other 9 strains, which are

not part of the core-genome. Figure 11 also shows that the core-genome does not significantly shrink anymore upon addition of new genomes of more strains. This is indicative for a representative strain selection comprising most of the biodiversity within *L. curvatus*. Based on the pan-genomic calculation a pan-genomic dendrogram was generated (supplementary Figure 14), and there are three strains *L. curvatus* TMW 1.27, TMW 1.401 and TMW 1.1390, which form a separate group. Moreover, the dendrogram revealed a close relationship of *L. curvatus* TMW 1.167, TMW 1.439 and TMW 1.1381. Indeed, comparison of all strains of *L. curvatus* by using BADGE based on the encoded orfs (open reading frames), (visualization by BRIG, Figure 12) illustrates the close relationship between *L. curvatus* TMW 1.167, TMW 1.439 and TMW 1.1381, like it was observed based on the pan-genomic dendrogram (supplementary Figure 14). Moreover, the pan-genome analysis revealed that *L. curvatus* TMW 1.401 and TMW 1.1390 as well as *L. curvatus* TMW 1.421 and TMW 1.624 are closely related based on the genome sequences. The visualized pan-genome of *L. curvatus* revealed that both chromosome- and plasmid-encoded strain specific genes are detectable.

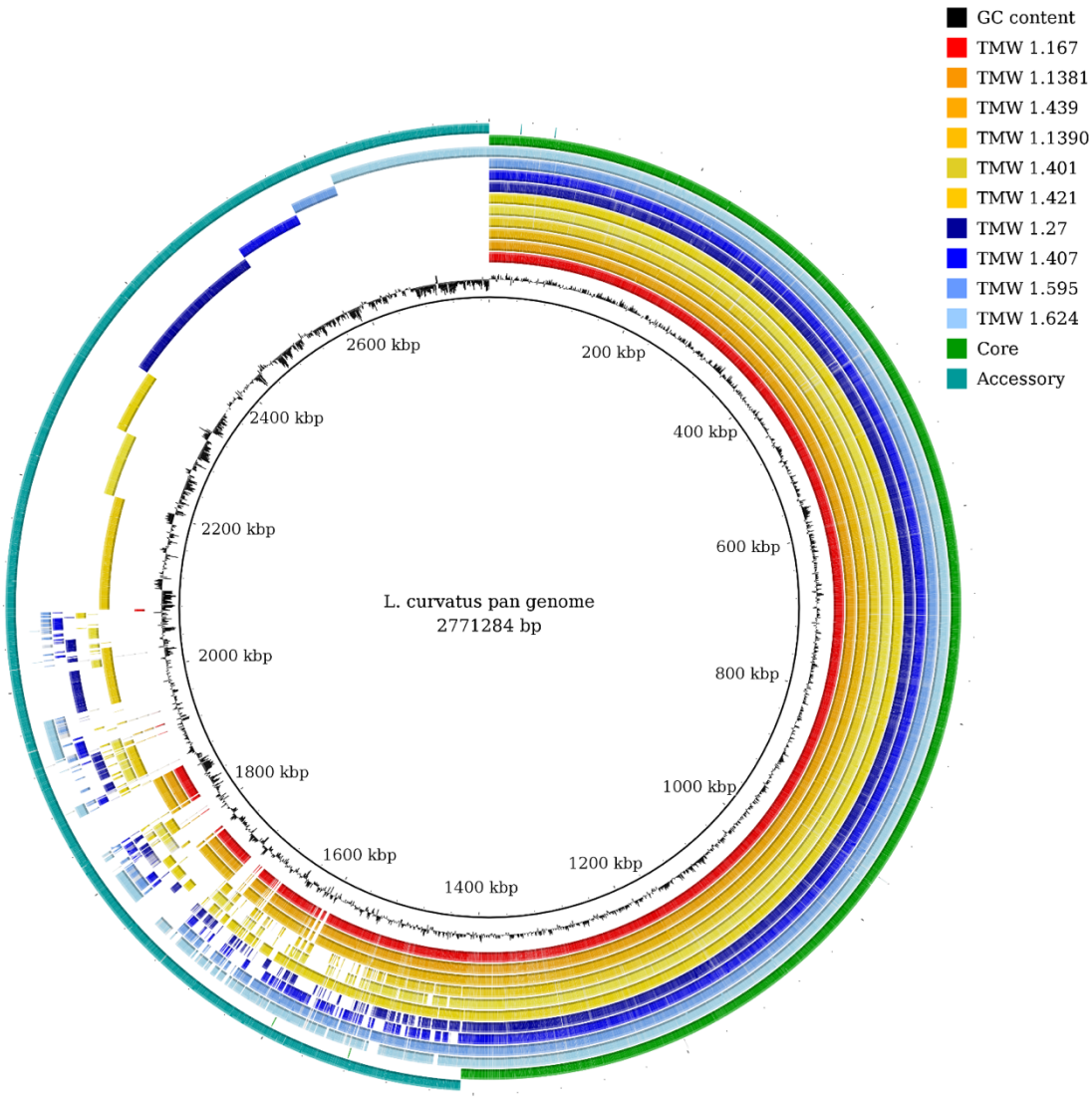

Figure 12: BRIG (Alikhan et al., 2011) was used to visualize the genomic comparison of sequenced genomes of *L. curvatus*. The identified orfs of the pan-genome were used as reference for the comparison of all sequenced genomes of the *L. curvatus* strains. For better overview the orfs of pan-genome were sorted, so the image enables the identification of similarities and differences, and strain specific genes.

Furthermore, the visualization of the genomes by BRIG enables the illustration of GC-content within the depictured pan-genome. On the one hand it suggests a higher variability of the GC-content within the accessory-genome, whereas, on the other hand, there is a highly conserved GC content shown within the core-genome.

The pan and core-genome plot of *L. sakei* revealed that all strains have a similar number of new genes or new gene families, except of *L. sakei* TMW 1.578 (No. 10, Figure 13). Based

on these pan and core determination a dendrogram was calculated (supplementary Figure 15).

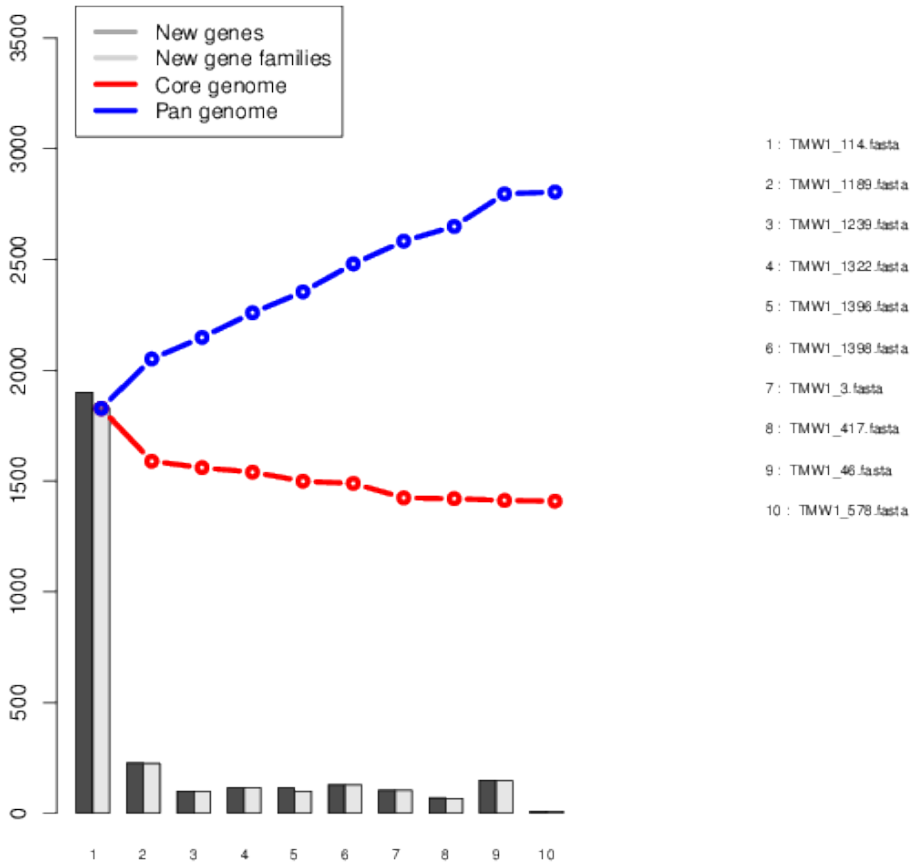

Figure 13: Pan-Core plot of *L. sakei* calculated by CMG Biotool. Red-line marks the core-genome and blue-line marks the pan-genome. Moreover, the dark-grey bars show the identified new genes, and the light-grey bars illustrate the identified new gene families.

Figure 13 also shows that the core-genome does not significantly shrink anymore upon addition of new genomes of more strains. This is indicative for a representative strain selection comprising most of the biodiversity within *L. sakei*. *L. sakei* TMW 1.46, TMW 1.1189 and TMW 1.1239 form a single group, whereas the second main group can be subdivided into two groups. Group A concludes *L. sakei* TMW 1.3, TMW 1.1396 and TMW 1.1398 and group B concludes *L. sakei* TMW 1.114, TMW 1.417, TMW 1.578 and TMW 1.1322. Additionally, the pan- and core-genome were calculated by BADGE and illustrated by BRIG (Figure 14) like described for *L. curvatus*. This genomic comparison, which enables pan-genomic analysis, revealed that *L. sakei* TMW 1.1396 and TMW 1.1398 are closely related based on the genomic properties. The same could be observed for the strains *L.*

sakei TMW 1.46, TMW 1.1239 and TMW 1.1189, as well as *L. sakei* TMW 1.114 and TMW 1.578.

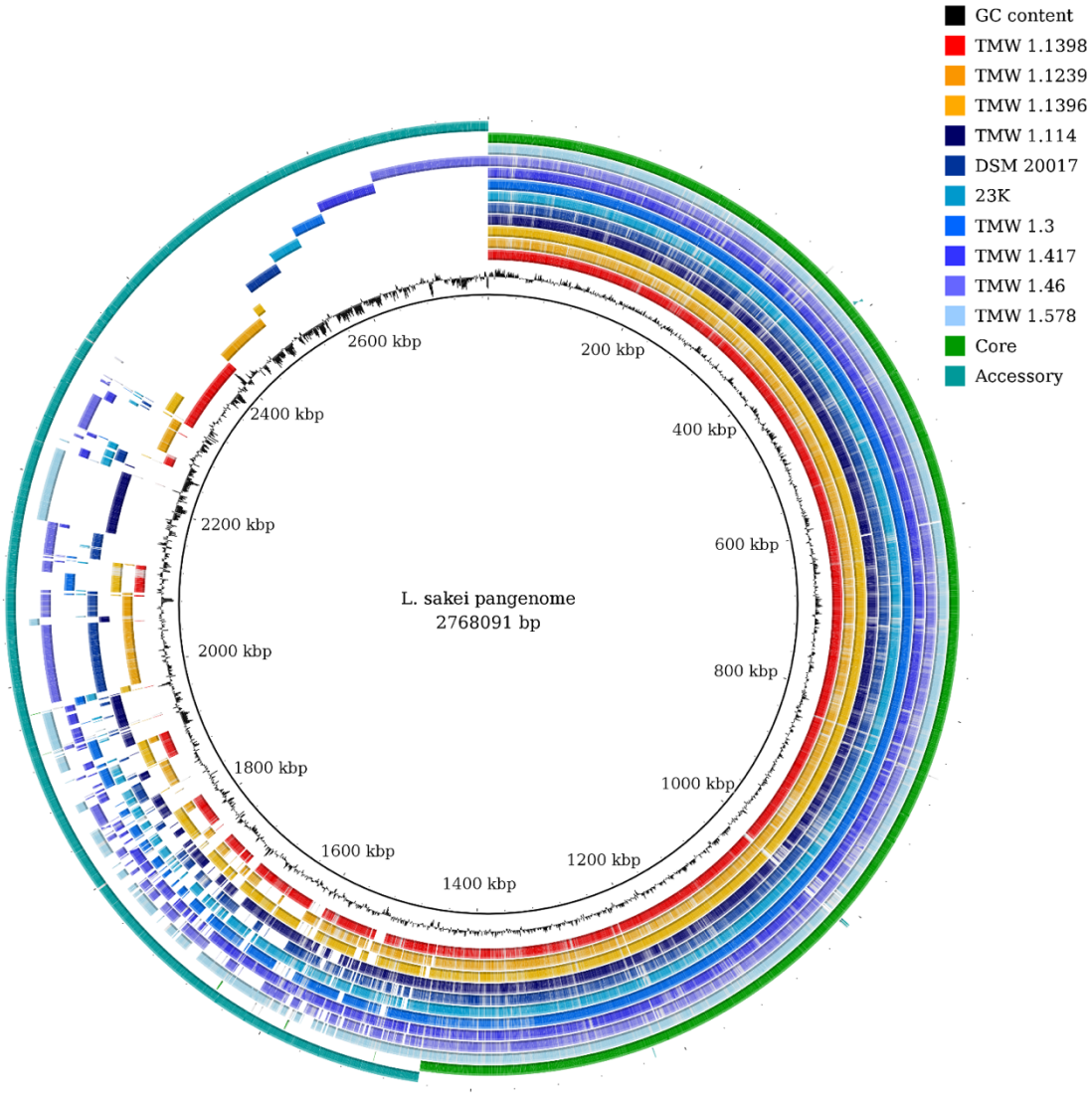

Figure 14: BRIG (Alikhan et al., 2011) was used to visualized the genomic comparison of sequenced genomes of *L. sakei*. The identified orfs of the pan-genome were used as reference for the comparison of all sequenced genomes of the *L. sakei* strains. For better overview the orfs of pan-genome were sorted, so the image enables the identification of similarities and differences, and strain specific genes.

The genomic diversity within *L. sakei* is reflected in the accessory-genome. This part of the pan-genome is influenced by environmental factors and includes the adaptation to a habitat of the strains at the genomic level. Indeed, strain specific genes could be detected. These genes are either plasmid or chromosome encoded. The GC-content, calculated and depictured by BRIG, suggests a highly conserved GC-content within the core-genome,

whereas the diversity of accessory-genome results in a high variable GC-content at this part of pan-genome.

The diversity of accessory-genomes of both *L. curvatus* and *L. sakei* has to be investigated more detailed because this part of the pan-genome encoded the genomic differences within a species.

3.3.2 Accessory-genome of *L. sakei* and *L. curvatus*

L. curvatus and *L. sakei* are species, which appear to be well adapted to different habitats or environments, because strains of both species could be isolated from a wide range of different sources. These environments are associated with meat, e.g., starter cultures or sausages, or with plants like sauerkraut or sourdough. Moreover, some strains of this study were isolated from an unknown source (Table 3). Finally, strains appear to be adapted to overall two different ecological niches (meat- and plant-associated). This should be reflected in genetic diversity within each species, namely within the accessory-genome.

The genomic intraspecies diversity of *L. curvatus*, which is encoded in the accessory-genome, is shown in Figure 15. Interestingly, the result suggests genomic differences between *L. curvatus* TMW 1.401 and TMW 1.407, which were both isolated from sauerkraut (Figure 15; blue genomes). Indeed, *L. curvatus* TMW 1.401, which were isolated from sauerkraut, and *L. curvtaus* TMW 1.1390, which were isolated from a starter culture preparation intended for sausage fermentation, appear to encode similar genes, like it is depicted at the regions of approximately 500 and 600kbp of the accessory-genome. Additionally, *L. curvatus* TMW 1.421 shows less genomic correlation with strains, which are isolated from meat environment, although this strain was isolated from meat, e.g., between 100kbp and 200kbp of the accessory-genome.

To conclude, apparently there is no correlation detectable between genomic properties and source of isolation within the accessory-genome of *L. curvatus.*

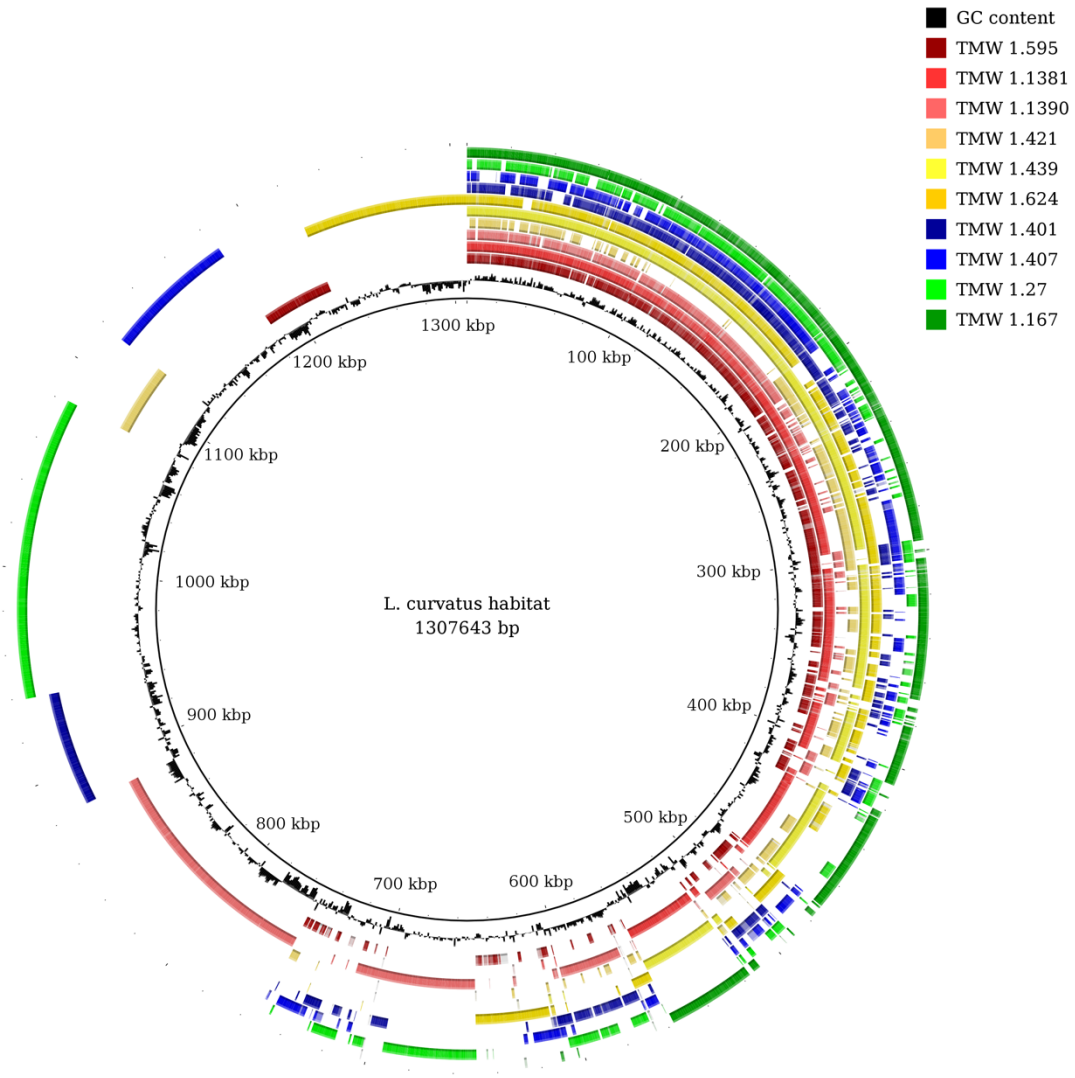

Figure 15: Accessory-genome of *L. curvatus*. Genomes of 10 sequenced strains of *L. curvatus* were mapped against the accessory-genome of *L. curvatus*. The strains are coloured based on the source of isolation: red starter preparation; yellow meat or raw sausage; blue sauerkraut and green unknown source.

The accessory-genome of *L. sakei* revealed a high genetic diversity within the species, but there are strains, which seem close related based on the genomic properties (Figure 16). First, at the regions of approximately 500kbp and 600kbp of the accessory-genome (Figure 16), a close genomic relationship between *L. sakei* TMW 1.46, TMW 1.1189 and TMW 1.1239 is detectable. Additionally, this result suggests a significantly genomic difference between these three strains and the other strains of *L sakei*. A second region of accessory-genome (between 400 kbp and 500 kbp) including genomes of *L. sakei* TMW 1.46, TMW

1.1322, TMW 1.1189 and TMW 1.1239 revealed a set of genes, which are encoded purely by these strains. Interestingly, *L. sakei* TMW 1.46 has been isolated from a starter culture preparation and TMW 1.1322 has benn isolated from meat, whereas *L. sakei* TMW 1.1189, which has been isolated from sourdough and *L. sakei* TMW 1.1239, which has been isolated from sake starter culture, are associated with plant environment. Indeed, the genomic comparison revealed a close relationship between *L. sakei* TMW 1.114, TMW 1.417 and TMW 1.578, and between *L. sakei* TMW 1.1396 and TMW 1.1398. Moreover, *L. sakei* TMW 1.3 and 23K are similar to these five strains, and there are genomic regions, which reflect similarity, but no close genomic relationship could be identified.

In conclusion, the results suggest that there is no correlation detectable in *L. sakei* between source of isolation and genomic properties.

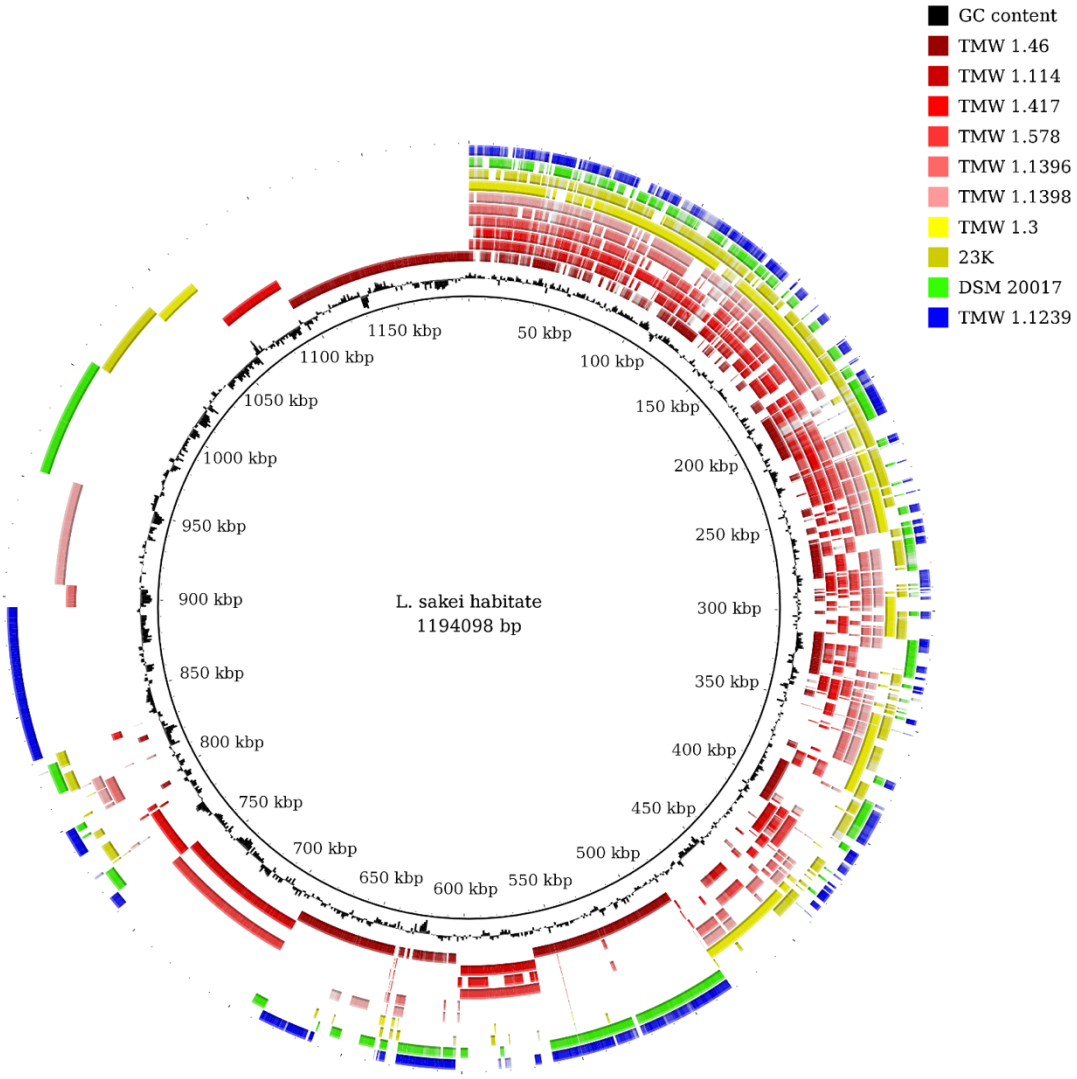

Figure 16: Genomes of 10 sequenced strains of *L. sakei* were mapped against the accessory-genome of *L. sakei* based on these 10 sequenced genomes. The structures of the accessory-genome and the genomes did not reflect the physical structure of the chromosomes and plasmids. The strains are coloured based on the source of isolation: red starter preparation; yellow meat or raw sausage; blue sourdough and green sake starter strain.

3.3.3 Plasmidome of *L. curvatus* and *L. sakei*

Genomic analysis revealed that *L. curvatus* and *L. sakei* strains harbor plasmids, listed in Table 6 and

Table 7, respectively. There are strains, which carry no or up to two plasmids based on the genomic data. There are plasmids, which are carried by only one strain only, and these plasmids appear to be unique. The genomic analysis of the plasmids of *L. curvatus* results in a heterogenic plasmidome based on the encoded genes as well as genome size, coding

density and GC content (Table 6). Genomic comparison revealed a relationship between plasmids pL127-2 and pL1401-1 as well as pL1624-2 and pL1595-1 by using MAUVE (supplementary Figure 16, supplementary Figure 17). These plasmids encode an electron transfer flavoprotein gene cluster and ribonucleotide-diphosphate reductase. Moreover, the genetic data revealed pL127-1 carried a protein homologous to a bacteriocin immunity protein and genes of a toxin-antitoxin system depending on the Xre family. Finally, the genomic data suggest that there is a further, partially sequenced plasmid, described as pL1407-1.

Table 6: General features of *L. curvatus* plasmids.

	L. curvatus									
plamids	pL1167-1	pL127-1	pL127-2	pL1401-1	pL1407-1	pL1407-2	pL1421-1	pL1595-1	pL1624-1	pL1624-2
Contigs	1	1	1	1	1	1	1	1	1	1
Genome lenght (bp)	3,213	220,332	44,118	48,281	11,242	2,799	61,429	50,304	84,447	43,639
GC content (%)	34,67	42,06	38,14	40,44	38,71	35,3	40,89	40,52	34,55	41,34
Number of CDS	7	211	48	54	11	3	63	53	88	45
Total CDS length (bp)	2666	174407	37780	41898	8299	1651	52002	43373	70066	38506
coding density (%)	82,98	79,16	85,63	86,78	73,82	58,99	84,65	86,22	82,97	88,24
accession number	CP016473	CP016468	CP016469	CP016217	CP016219	CP016220	CP016222	CP016471	CP015491	CP015492

Genetic analysis of the plasmidome of *L. sakei* revealed that this is heterogenous (
Table 7). There are strains which carry no plasmids, whereas other strains carry up to three plasmids. The detailed analysis of the plamsidome suggests a close relationship between pL146-1, pL1114-1, pL11396-1, pL11398-2, pL11398-3 and pL1578-1 (supplementary Figure 18, supplementary Figure 19). Nevertheless, based on analysis using MAUVE, this group of plasmids could be subdivided into two subgroups concluding on the one side pL11396-1, pL11398-2 and pL11398-3, and on the other side pL1114-1 and pL1578-1. Still, these plasmids encode the same genes: (1) electron transfer flavoprotein (2) ribonucleotide-diphosphate reductase. Indeed, these genes are also encoded in the chromosome of *L. sakei* TMW 1.1189 and TMW 1.417. Nevertheless, the electron transfer flavoprotein is also encoded on plasmid pL13-1, which was classified as a different plasmid compared to the other sequenced plasmids. Interestingly, the ribonucleotide-diphosphate reductase is not encoded in neither the plasmid nor the chromosome of *L. sakei* TMW 1.3.

Table 7: General features of *L. sakei* plasmids.

	L.sakei								
plasmids	pL1114-1	pL11396-1	pL11398-1	pL11398-2	pL11398-3	pL13-1	pL1417-1	pL146-1	pL1578-1
Contigs	1	1	1	1	1	1	1	1	1
Plasmid length (bp)	34,136	40,197	27,120	40,209	40,107	35,983	64,141	68,079	34,136
GC content (%)	41.69	39.75	40.16	39.74	39.62	36.66	38.54	40.48	41.69
Number of CDS	37	43	27	44	40	36	69	69	37
Total CDS length (bp)	26,373	34,926	20,555	34,746	33,770	28,727	53,162	58,470	26,373
coding density (%)	77.26	86.89	75.79	86.41	84.20	79.83	82.88	85.89	77.26
accession number	CP017567	CP017274	CP017276	CP017277	CP017278	CP016466	CP017569	CP015488	CP017571

3.3.4 Prophage gene clusters

Gene clusters of prophages are a frequent part of bacterial genomes. Therefore, the genomes of both species *L. sakei* and *L. curvatus* were analysed to identify such gene clusters associated with prophages. The prophage gene clusters were detected by PHASTER, which classified the gene clusters to be “intact”, “incomplete” or “questionable” like it is listed in supplementary Table 2 and supplementary Table 3. “questionable” described CDSs, which associated with prophage gene clusters, but they did not describe a prophage correctly. Most strains of *L. curvatus* encoded in least one prophage classified as intact (supplementary Table 2). A few prophage gene clusters encoded lysins, which are introduced in the genome of *L. curvatus* TMW 1.167, TMW 1.439, TMW 1.595, TMW 1.624, TMW 1.1381 and TMW 1.1390. Moreover, these lysin-encoding prophages are introduced into the chromosome, and they are classified as questionable or intact. For *L. sakei* strains it was shown that all strains carry at least one incomplete putative prophage gene cluster, and maximally six putative prophage gene clusters, which were classified as questionable, incomplete or intact. To conclude, all identified prophages are encoded within plasmids or chromosomes, and at least one prophage gene cluster is encoded in each *L. sakei* genome.

3.3.5 CRISPR/Cas-systems

CRISPR/CAS systems are associated with the bacterial immune system. These genomic clusters are influenced by the uptake of foreign DNA, e.g., plasmids or phage-DNA. This could result in phage tolerance and/or an adaptation to a defined ecological niche, and that could influence the assertiveness of each single strain in a special habitat. Indeed, nine different CRISPR/CAS clusters were detected in *L. curvatus* genomes, which are listed in Table 8 and the spacers are described in Table 9. There are CRISPR/CAS clusters (CRISPR-1 to CRISPR-5) identified in a few strains, but there are also CRISPR/CAS systems, which appear to be strain specific. *L. curvatus* TMW 1.624 encoded CRISPR-6 and CRISPR-7, and *L. curvatus* TMW 1.401 carry CRISPR-8 and CRISPR-9, which appears to be strain specific. Interestingly, the close related strains *L. curvatus* TMW 1.167, TMW 1.439 and TMW 1.1381 encoded three identical CRISPR/Cas clusters, but CRISPR-4 is only

identified at the genome of *L. curvatus* TMW 1.167 and TMW 1.1381 and not at the one of *L. curvatus* TMW 1.439.

Table 8: List of detected CRISPR/Cas cluster in *L. curvatus.* + marks the identification of the specific CRISPR/Cas cluster; - markes the missing of a cluster. All defined clusters were numbered consecutively.

CRISPR	TMW 1.167	TMW 1.1381	TMW 1.1390	TMW 1.624	TMW 1.595	TMW 1.439	TMW 1.421	TMW 1.407	TMW 1.401	TMW 1.27
CRISPR_1	+	+	-	+	-	+	+	-	-	+
CRISPR_2	+	+	-	+	-	+	+	-	-	-
CRISPR_3	+	+	-	-	-	+	+	-	-	-
CRISPR_4	+	+	-	-	-	-	-	-	-	-
CRISPR_5	-	-	+	-	-	-	-	+	+	+
CRISPR_6	-	-	-	+	-	-	-	-	-	-
CRISPR_7	-	-	-	+	-	-	-	-	-	-
CRISPR_8	-	-	-	-	-	-	-	-	+	-
CRISPR_9	-	-	-	-	-	-	-	-	+	-

Table 9: Repeat sequences of identified CRISPR/Cas systems

CRISPR	CRISPR_id	repeat sequence
TMW 1.27	926_158106_1	GTTGAACTACTCATTGATTTGATACTCTTCTAAAAC
	926_158106_2	TAATTGTTGTAAGCCACCTGAAAG
TMW 1.167	926_158104_1	CTTTCAGATGGCTTACAACAATTA
	926_158104_2	GTTTTAGAAGAGTATCAAATCAATGAGTAGTTCAAC
	926_158104_3	GTTTTAGAAGAGTATCAAATCAATGAGTAGTTCAAC
	926_158104_4	TTAGTTTGTATTCAGTTTGACCA
TMW 1.401	926_158103_1	GTTGAACTACTCATTGATTTGATACTCTTCTAAAAC
	926_158103_2	ATTTAACGTTTGTAAACCTGTGTTTAATTGACCAGCACCGT
	926_158103_3	ATTTAACGTTTGTAAACCTGTGTTTAATTGACCAGCACCGT
TMW 1.407	926_158102_1	TACTCATTGATTTGATACTCTTCTAAAAC
TMW 1.421	926_158101_1	GTTGAACTACTCATTGATTTGATACTCTTCTAAAAC
	926_158101_2	GTTGAACTACTCATTGATTTGATACTCTTCTAAAAC
	926_158101_3	TAATTGTTGTAAGCCACCTGAAAG
TMW 1.439	926_158100_1	GTTGAACTACTCATTGATTTGATACTCTTCTAAAAC
	926_158100_2	GTTGAACTACTCATTGATTTGATACTCTTCTAAAAC
	926_158100_3	TAATTGTTGTAAGCCACCTGAAAG
TMW 1.624	926_158098_1	TTATATGGTAGATTGTAAAATTAA
	926_158098_2	TGGCTAACTTGTTCTTGCAATTT
	926_158098_3	GTTGAACTACTCATTGATTTGATACTCTTCTAAAAC
	926_158098_4	TAATTGTTGTAAGCCACCTGAAAG
TMW 1.1381	926_158096_1	CTTTCAGATGGCTTACAACAATTA
	926_158096_2	GTTTTAGAAGAGTATCAAATCAATGAGTAGTTCAAC
	926_158096_3	GTTTTAGAAGAGTATCAAATCAATGAGTAGTTCAAC
	926_158096_4	TTAGTTTGTATTCAGTTTGACCA
TMW 1.1390	926_158097_1	GTTTTAGAAGAGTATCAAATCAATGAGTAGTTCAAC

At genomes of *L. sakei* also CRISPR-clusters were identified. The four detected clusters are listed in Table 10 and the spacer sequences are described in Table 11. Only *L. sakei* TMW 1.1398 did not encode any detectable CRISPR-Cluster. Furthermore, *L. sakei* TMW 1.417 encoded a strain specific CRISPR-cluster, described as CRISPR-4. Finally, there are the identified clusters CRISPR-1 to CRISPR-3, which could be detected in different strains. Interestingly, only *L. sakei* TMW 1.1239 is the only strain, which encoded more than one CRISPR/Cas gene cluster.

Table 10: List of detected CRISPR/Cas cluster in *L. sakei.* + marks the identification of the specific CRISPR/Cas cluster; - markes the missing of a cluster. All defined clusters were numbered consecutively.

CRISPR	TMW 1.3	TMW 1.46	TMW 1.114	TMW 1.417	TMW 1.578	DSM 20017^T	TMW 1.1239	23K	TMW 1.1396	TMW 1.1398
CRISPR_1	+	-	-	-	-	-	+	-	+	-
CRISPR_2	-	+	-	-	-	+	+	+	-	-
CRISPR_3	-	-	+	-	+	-	-	-	-	-
CRISPR_4	-	-	-	+	-	-	-	-	-	-

Table 11: Repeat sequences of identified CRISPR/Cas systems of *L. sakei* strains.

strain	CRISPR_ID	Repeat sequence
TMW 1.3	926_158107_1	CTAGCACTAATGGCACGTTTAAA
TMW 1.46	926_158105_1	TTAGATGTTTCAAATTGGGATAC
TMW 1.114	926_163477_1	GTTGAACCACTCATTGATTTGATACTCTTCTAAAAC
TMW 1.417	926_163482_1	GGTTGAACTACTCATTGATTTGATACTCTTCTAAAGC
TMW 1.578	926_163483_1	GTTGAACCACTCATTGATTTGATACTCTTCTAAAAC
DSM 20017^T	926_163485_1	TTAGATGTTTCAAATTGGGATAC
TMW 1.1239	926_163486_1	TTAGATGTTTCAAATTGGGATAC
	926_163486_2	TTTAAACGTGCCATTAGTGCTAG
23K	926_163488_1	TTAGATGTTTCAAATTGGGATAC
TMW 1.1396	926_163490_1	CTAGCACTAATGGCACGTTTAAA
TMW 1.1398	-	-

3.4 Cold shock response

Selected strains of both species were screened for their cold shock response as a suspected main characteristic for starter strains in raw fermented sausages. The screening was based on membrane damage and colony forming units (CFU) per ml to characterize the reaction to cold shock of the single strains (Figure 17 and Figure 18). The CFU reflected the number of survived cells, which were able to form a new colony, and enable identification of recovery ability after cold shock induction.

Most *L. curvatus* strains showed a stable CFU after cold shock induction compared to the CFU before cold shock induction. *L. curvatus* TMW 1.407 was able to increase the CFU after cold shock. However, *L. curvatus* TMW 1.401, TMW 1.407, TMW 1.439 and TMW 1.1381 were able to increase significantly the CFU upon a time of recovery (Figure 17).

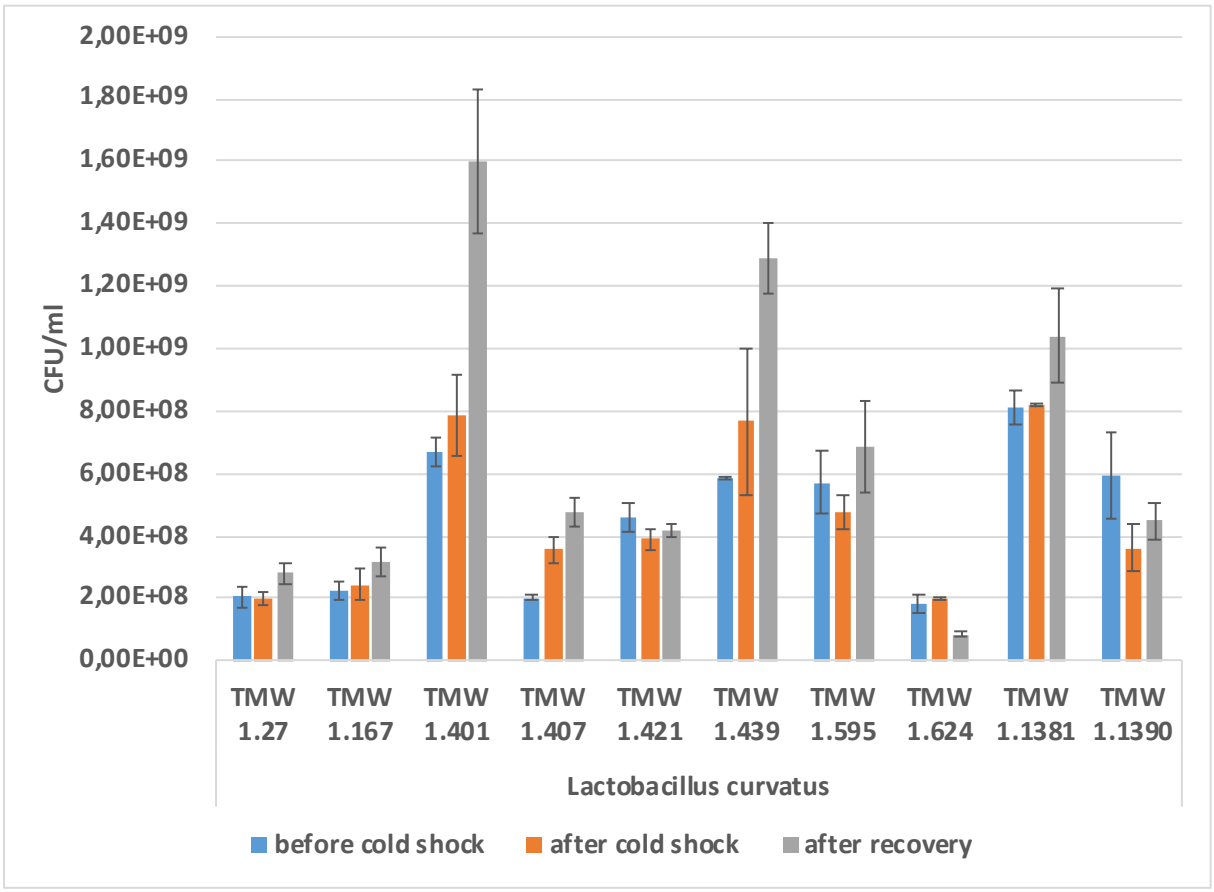

Figure 17: Determination of CFU/ml of *L. curvatus* strains before and after cold shock as well as after 2 h recovery. Several strains are able to increase the CFU after cold shock or suggest a stable CFU after cold shock (orange bars). Most strains of *L. curvatus* show an ability to recover after cold shock, defined as increase of the CFU/ml (grey bars) except *L. curvatus* TMW 1.421 (stable CFU/ml) and *L. curvatus* TMW 1.624 (decrease CFU/ml).

For *L. sakei* similar results could be observed (Figure 18). More than half of the tested strains of *L. sakei* did not increase the CFU after cold shock, whereas *L. sakei* TMW 1.417, TMW 1.578 and TMW 1.1398 are able to increase number of CFU. Indeed, *L. sakei* TMW 1.1239 decreased the CFU after cold shock induction. Upon 2 h of recovery *L. sakei* TMW 1.3, TMW 1.114, TMW 1.578 and TMW 1.1189 revealed a significant increase of CFU/ml. The rest strains showed a stable CFU/ml after 2 h of recovery (Figure 18).

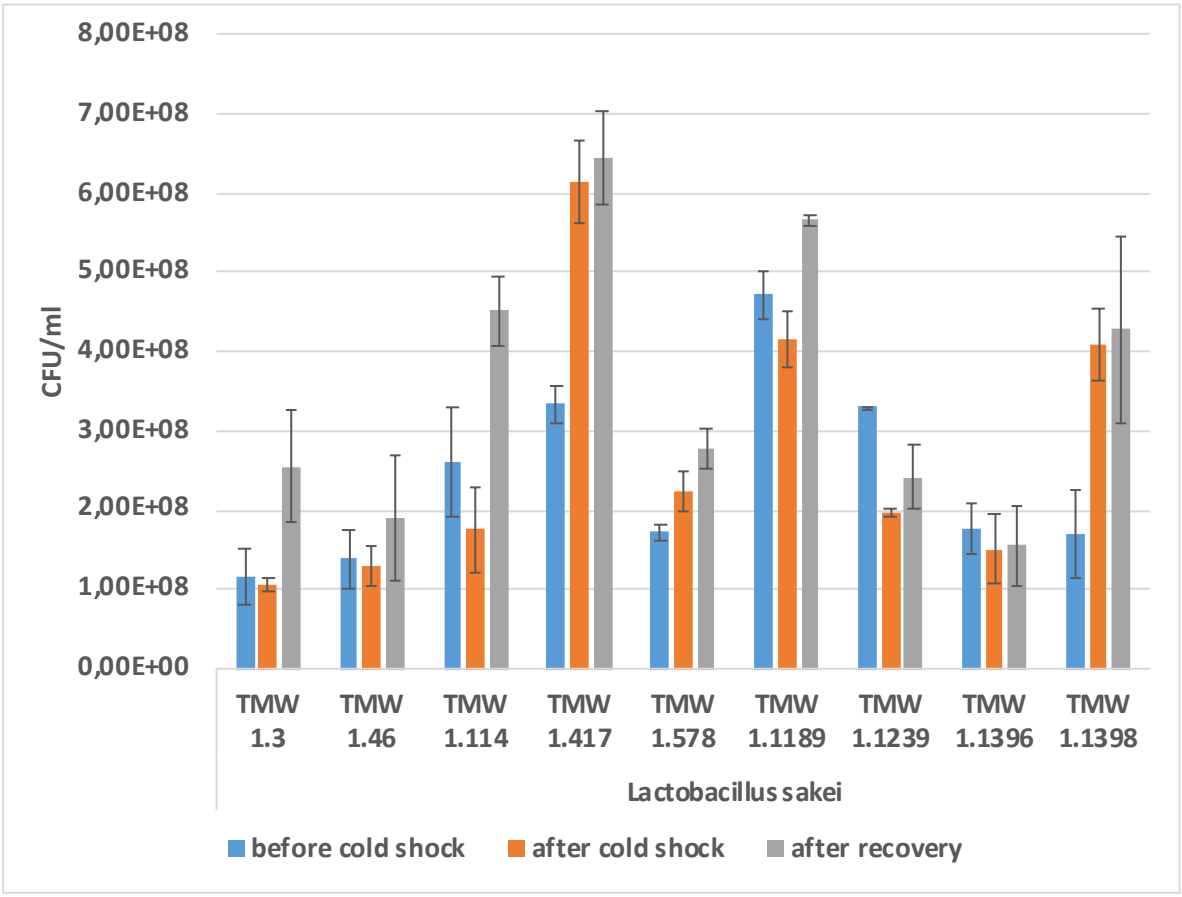

Figure 18: Determination of CFU/ml of *L. sakei* strains before and after cold shock as well as after 2 h recovery. Few strains are able to increase the CFU/ml after cold shock induction, whereas the rest of the strains shows a stable CFU/ml with exception of *L. sakei* TMW 1.114 and TMW 1.1239 (orange bars). Nevertheless, all strains suggest an ability to recover after cold shock induction except *L. sakei* TMW 1.1396 which shows a stable CFU/ml (grey bars).

Cold shock induction could result in membrane damage of stressed cells. Such damage influenced the viability of the microorganisms, which was verified by the determination of the CFU per ml. Fluorescence microscopy in combination with LIVE/DEAD® BacLight™ Bacterial viability Kit L13152 (ThermoFischer Scientific, Waltham, USA) was used to identify

the quantity of damaged cell membranes of stressed cells (used stain and filter listed in Table 2).

Interestingly, all strains showed a regeneration of the membrane damages upon 2 h of recovery time after cold shock induction. Moreover, it is possible to differentiate two different groups based on the membrane damage for both species.

There are strains, which showed no increase of membrane damage or only less. And there are other strains, which have a high increase of detectable membrane damage like it is shown in Figure 19 and Figure 20. For *L. curvatus* it was observed that *L. curvatus* TMW 1.421 (Figure 19, A), TMW 1.439, TMW 1.595, TMW 1.1381 and TMW 1.1390 have no or less increase of membrane damage after cold shock induction, whereas *L. curvatus* TMW 1.27, TMW 1.167, TMW 1.401, TMW 1.407 (Figure 19, B) and TMW 1.624 have a high membrane damage. Strains of *L. sakei* was grouped into two groups as well. The first groups comprise *L. sakei* TMW 1.114 (Figure 20, A), TMW 1.417, TMW 1.578, TMW 1.1396 and TMW 1.1398, which show less than an increase of 10% of membrane damage after cold shock induction. The second group comprises strains, which show an increase of 11% or more after cold shock induction. *L. sakei* TMW 1.3 (Figure 20, B), TMW 1.46, TMW 1.1189 and TMW 1.1239 belong this group.

A

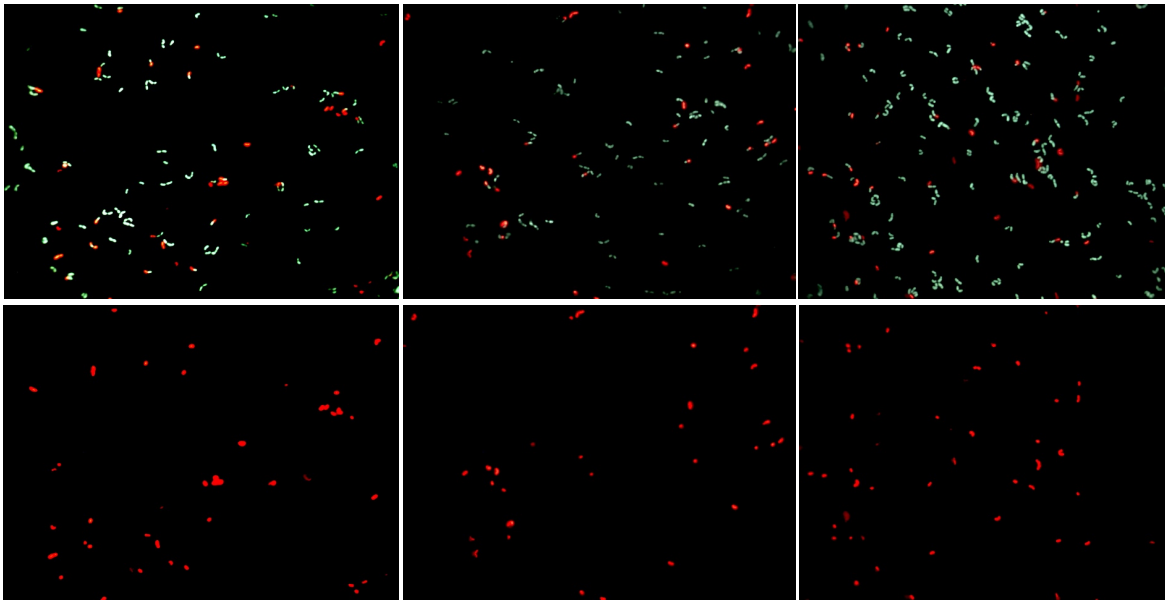

Before cold shock | After cold shock | After 2h of recovery

L. curvatus TMW 1.421

B

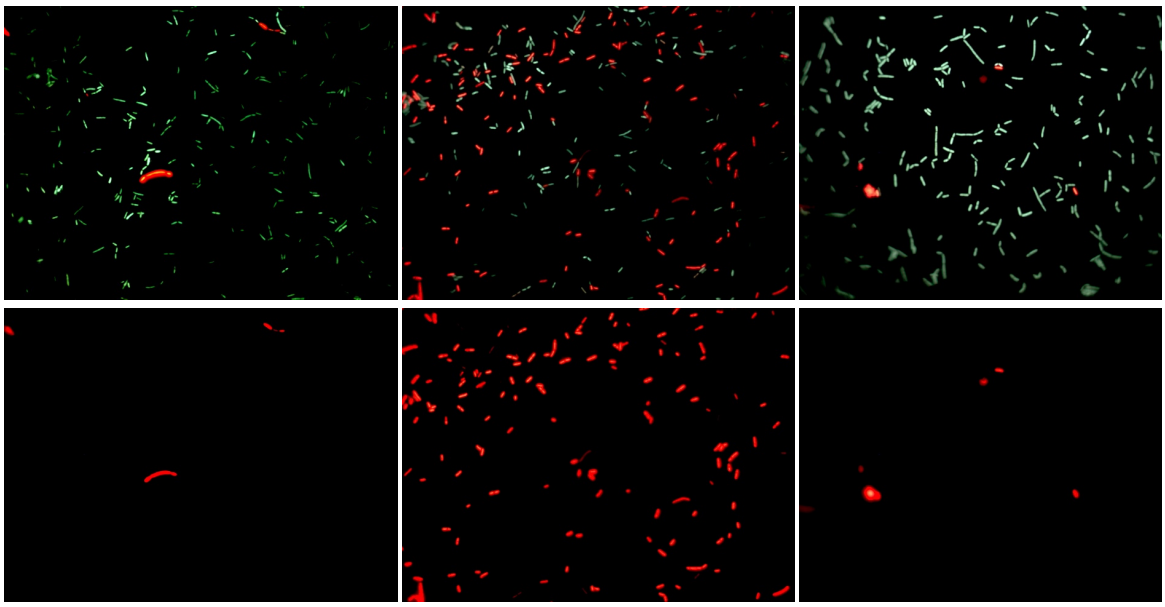

Before cold shock | After cold shock | After 2h of recovery

L. curvatus TMW 1.407

Figure 19: Fluorescence assay of membrane damage revealed differences between *L. curvatus's* strains. Half of the stressed strains shows no or less membrane damage (A, *L. curvatus* TMW 1.421), whereas other half of the strains exhibits a high rate of membrane damage (B, *L. curvatus* TMW 1.407). Green fluorescent cells have no membrane damage, whereas red fluorescence cells have a damaged cell membrane. Positive control is a unstressed cell sample ("before cold shock") and negative control is a sample of cell suspension, which was incubated for 30 min at 80°C (data not shown).

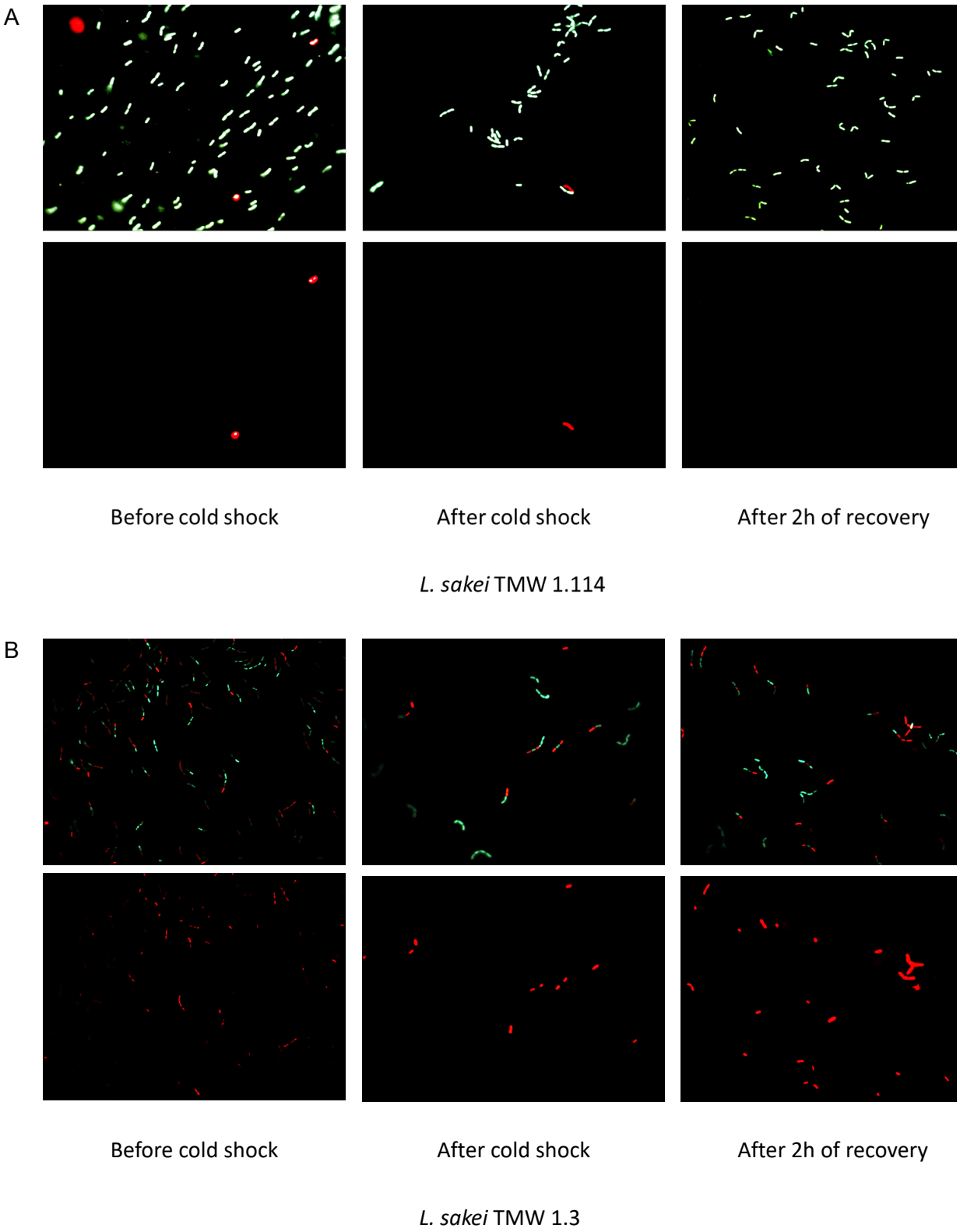

Figure 20: Fluorescence assay of membrane damage revealed differences between strains of *L. sakei*. Half of the stressed strains shows no or less membrane damage (A, *L. sakei* TMW 1.114), whereas other half of the strains exhibits a high rate of membrane damage (B, *L. sakei* TMW 1.407). Green-fluorescent cells have no membrane damage, whereas red fluorescence cells have a damaged cell membrane. Positive control is a unstressed cell sample ("before cold shock") and negative control is a sample of cell suspension, which was incubated for 30 min at 80°C (data not shown).

In the view on these physiological groups (membrane damage high or low) genomes of strains of both species were compared by BADGE (Table 12 and Table 13) to identify related genomic features within the respective groups.

For the group of *L. curvatus* strains, which show less or no membrane damage (Table 12) 3 putative DMGs were detectable: (1) lipotheichoic acid synthase family protein; (2) bacteriocin immunity protein; (3) hypothetical protein, which is a putative isopeptide forming domain-containing fimbrial protein. Lipotheichoic acid is part of the bacteria cell wall, so the lipotheichoic acid synthase family protein is involved in the cell wall synthesis.

For the groups of *L. sakei* (Table 13) more than 5 putative DMGs could be defined, which are associated with less membrane damage after cold shock induction. (1) IS30 family transposases; (2) DUF956 family protein; (3) cell surface protein; (4) filamentation induced by cAMP protein fic; (5) different hypothetical proteins.

Table 12: Strains of *L. curvatus* were grouped based on their detectable membrane damage after cold shock.

No or less membrane damage	**Membrane damage**
TMW 1.421	TMW 1.27
TMW 1.439	TMW 1.167
TMW 1.595	TMW 1.401
TMW 1.1381	TMW 1.407
TMW 1.1390	TMW 1.624

Table 13: Strains of *L. sakei* were grouped based on their detectable membrane damage after cold shock.

membrane damage ≤ 10%	**Membrane damage ≥ 11%**
TMW 1.114	TMW 1.3
TMW 1.417	TMW 1.46
TMW 1.578	TMW 1.1189
TMW 1.1396	TMW 1.1239
TMW 1.1398	

3.5 Oxidative stress response

Based on the pan-genome analysis it was shown that a catalase is part of the core-genome of *L. sakei*. Moreover, most *L. curvatus* strains encoded a catalase, which is highly conserved, with the exception of *L. curvatus* TMW 1.407, which encoded no catalase. The catalase encoded by *L. sakei* and *L. curvatus* is known to be heme-dependent or a manganese-dependent pseudocatalase. Knauf *et al*. (Knauf et al., 1992) described the *katA* gene for *L. sakei* LTH677. Annotated catalase genes of tested strains of *L. sakei* and *L. curvatus* were compared to *katA* gene of *L. sakei* LTH677 by using Blast (blastn and blastp). The comparison of the sequences suggests that the encoded catalases at the core-genome of both species are identical with *katA* gene of *L. sakei* LTH677 like it is illustrated in supplementary Figure 22 and supplementary Figure 23. This indicates that these strains carry a gene encoding a heme catalase.

Therefore, the oxidative stress response of the strains was experimentally probed along an improved growth behaviour in presence or absence of hematin, and with or without oxidative stress (2 mM or 0 mM H_2O_2).

The growth of the strains and the length of the lag-phase (λ) reflects differences between the strains of each species like it is shown in Table 14. All strains of *L. curvatus* show a shorter

lag-phase in presence of hematin under oxidative stress conditions (Table 14). Interestingly, there is a group of strains, which are able to grow after 6h up to 9h shorter lag-phase than without hematin. A second group of strains has a reduction of λ around 12 h up to 24 h in presence of hematin.

For a few strains of *L. sakei* a reduction of λ was observed, too. But the reduction of the lag-phase was between 5h and 9h. Nevertheless, there is one group of strains, which have a shorter lag-phase in absence of hematin. The results revealed that the λ with hematin was 6h or 36h longer with hematin than without. This group comprise *L. sakei* TMW 1.114, TMW 1.417 and TMW 1.1239. Moreover, there are two strains, *L. sakei* TMW 1.1322 and TMW 1.1398, which suggest no difference of oxidative stress tolerance in presence or absence of hematin.

Table 14: Length of the lag-phase during growth in presence of 2 mM H_2O_2 and with or without hematin.

species	strain	length lag-phase (λ) [h]	
		With Hematin	Without Hematin
L. curvatus	TMW 1.27	24	30
	TMW 1.167	39	45
	TMW 1.401	12	24
	TMW 1.407	21	45
	TMW 1.421	21	40
	TMW 1.439	24	39
	TMW 1.595	27	51
	TMW 1.624	27	39
	TMW 1.1381	39	57
	TMW 1.1390	24	33
L. sakei	TMW1.3	36	45
	TMW 1.46	42	49
	TMW 1.114	33	27
	TMW 1.417	45	39
	TMW 1.578	30	36
	TMW 1.1189	4	9
	TMW 1.1239	60	24
	TMW 1.1322	45	45
	TMW 1.1396	24	32
	TMW 1.1398	15	15

3.6 Bacteriocin production and immunity

3.6.1 Detection of predicted bacteriocin gene clusters and genes, which are associated with bacteriocin immunity

The web-based tool BAGEL was used to identify bacteriocin-associated gene clusters as well as putative immunity genes, because the strategy of bacteriocin production and immunity is a powerful property for assertiveness in a competitive habitat. The detected putatively produced bacteriocins are listed in Table 15. The results suggest that most strains of *L. curvatus* carried a gene cluster associated with sakacin Q, whereas *L. curvatus* TMW 1.407 and TMW 1.1390 carry no gene cluster which is associated with bacteriocin production. On the other hand, analysis of genome of *L. curvatus* TMW 1.624 carry multiple bacteriocin gene clusters which associated with Sakacin Q, Sakacin Tα, Enterocin NKR-5-3a, a Lanthipeptide class II and a putative functional type-A Lantibiotic. The latter is also identified in the genome of *L. curvatus* TMW 1.401 and TMW 1.595.

Table 15: Bacteriocin gene clusters encoded in the genome were identified using BAGEL. Five gene clusters were detected at the sequenced genomes of *L. curvatus* strains and they are associated with the production of Sakacin Q, Sakacin Tα, Enterocin NKR-5-3A, Lanthipeptid class II and type-A Lantibiotic. "+" remarks the identification of a gene cluster, whereas "–"remarks the missing of a gene cluster.

strain		Sakacin Q	Sakacin Tα	Enterocin NKR-5-3A	Lanthipeptid class II	type-A Lantibiotic
L. curvatus	TMW 1.27	+	-	-	-	-
	TMW 1.167	+	-	-	-	-
	TMW 1.401	+	-	-	-	+
	TMW 1.407	-	-	-	-	-
	TMW 1.421	+	-	-	-	-
	TMW 1.439	+	-	-	-	-
	TMW 1.595	+	-	-	-	+
	TMW 1.624	+	+	+	+	+
	TMW 1.1381	+	-	-	-	
	TMW 1.1390	-	-	-	-	-

However, genomic analysis using BADGE revealed that *L. curvatus* TMW 1.27, TMW 1.167, TMW 1.401, TMW 1.421, TMW 1.439, TMW 1.595, TMW 1.624 and TMW 1.1381 encoded in least one immunity protein, which is homologous to the enterocin A immunity protein (supplementary Table 4), which is not encoded in the genomes of neither *L. curvatus* TMW 1.407 nor TMW 1.1390. These identified proteins could cause an immunity for class IIa, class IIb and class IId bacteriocins without the ability to produce the respective bacteriocin.

Also, within the genomes of *L. sakei* a putative bacteriocin gene cluster could be detected by the web-based tool BAGEL. The results, listed in Table 16, revealed that less such gene clusters are encoded than it was observed for *L. curvatus*. In detail, for *L. sakei* TMW 1.46 a gene cluster associated with production of carnocin. Moreover, in the genome of *L. sakei* TMW 1.3 a gene cluster was identified, which appears to be homologous with lactocin-S. Finally, a bacteriocin gene cluster, which encoded the production of peptides belonging to the COMC family was detected within the genome of *L. sakei* TMW 1.114 and TMW 1.578. Moreover, these four strains, which are putative bacteriocin producers, encoded immunity proteins homologous to enterocin A immunity protein (supplementary Table 5).

Table 16: Bagel was used to identify putative bacteriocin gene clusters at the genomes of *L. sakei*. Three gene clusters were detected associated with the production of carnocin CP52, predicted lactocin-S and homologous peptides of COMC family. + marks the presence, whereas - marks the absence of a gene cluster.

strain		Carnocin CP52	lactocin-S	peptide of COMC family
L. sakei	TMW 1.3	-	+	-
	TMW 1.46	+	-	-
	TMW 1.114	-	-	+
	TMW 1.417	-	-	-
	TMW 1.578	-	-	+
	DSM 20017^T	-	-	-
	TMW 1.1239	-	-	-
	23K	-	-	-
	TMW 1.1396	-	-	-
	TMW 1.1398	-	-	-

3.6.2 Bacteriocin production assay

The presence of the bacteriocin gene clusters predicted that a few strains of both species are able to produce bacteriocins. Therefore, the strains were tested towards their ability to inhibit growth of other closely related strains listed in Table 17.

L. sakei TMW 1.3, TMW 1.46, TMW 1.114 and TMW 1.578 encoded bacteriocin gene clusters, but no inhibitory effect against the selected strains of both *L. sakei* and *L. curvatus* was identified (Table 17). On the other hand, *L. curvatus* TMW 1.624 appears to be an effective bacteriocin producer. It encoded five different bacteriocin gene clusters and the results of the bacteriocin assay suggest they enable *L. curvatus* TMW 1.624 to inhibit the growth of all tested strains (Table 15 and Table 17).

Table 17: The functionality of the detected bacteriocin gene cluster was tested by a bacteriocin inhibitory assay. A positive reaction results in inhibitory zones: "–" indicates no inhibitory effect; "+" indicates detectable inhibitory effect.

		***L. sakei* TMW 1.3**	***L. sakei* TMW 1.46**	***L. sakei* TMW 1.114**	***L. sakei* TMW 1.578**	***L. curvatus* TMW 1.624**
L. sakei	**TMW 1.3**	-	-	-	-	+
	TMW 1.46	-	-	-	-	+
	TMW 1.114	-	-	-	-	+
	TMW 1.417	-	-	-	-	+
	TMW 1.578	-	-	-	-	+
	TMW 1.1189	-	-	-	-	+
	TMW 1.1239	-	-	-	-	+
	TMW 1.1322	-	-	-	-	+
	TMW 1.1396	-	-	-	-	+
	TMW 1.1398	-	-	-	-	+
L. curvatus	**TMW 1.27**	-	-	-	-	+
	TMW 1.167	-	-	-	-	+
	TMW 1.401	-	-	-	-	+
	TMW 1.407	-	-	-	-	+
	TMW 1.421	-	-	-	-	+
	TMW 1.439	-	-	-	-	+
	TMW 1.595	-	-	-	-	+
	TMW 1.624	-	-	-	-	-
	TMW 1.1381	-	-	-	-	+
	TMW 1.1390	-	-	-	-	+

3.6.3 Bacteriocin sensitivity

Pediococcus (P.) acidilactici produces a class IIa bacteriocin called pediocin PA-1, which inhibits *Listeria monocytogenes*. Moreover, *P. acidilactici* could be isolated from meat. So, the immunity against pediocin PA-1 of both *L. sakei* and *L. curvatus* could increase their assertiveness in presence PA-1 producers. Moreover, there are several strains, which encoded an enterocin A immunity gene (3.6.1, supplementary Table 4 and supplementary Table 5).

3.6.3.1 Bacteriocin sensitivity of *L. curvatus* against Pediocin PA-1

The results of the bacteriocin sensitivity assay are listed in Table 18**Fehler! Verweisquelle konnte nicht gefunden werden.**. Interestingly, most strains of *L. curvatus* are resistant. Nevertheless, *L. curvatus* TMW 1.407, TMW 1.439 and TMW 1.1398 are sensitive to PA-1 after incubation in presence of glucose as well as mannose, whereas *L. curvatus* TMW 1.421 is resistant against PA-1 in presence of glucose. Still, this strain is sensitive against PA-1 if it is grown in presence of mannose.

Table 18: Bacteriocin-resistance assay against class II bacteriocin pediocin PA-1 for *L. curvatus*. A positive reaction results in inhibitory zones: "–" indicates no inhibitory effect; "+" indicates detectable inhibitory effect.

		Glucose	Mannose
L. curvatus	TMW 1.27	-	-
	TMW 1.167	-	-
	TMW 1.401	-	-
	TMW 1.407	+	+
	TMW 1.421	-	+
	TMW 1.439	+	-
	TMW 1.595	-	-
	TMW 1.624	-	+
	TMW 1.1381	+	+
	TMW 1.1390	-	-

Genomic comparison of the strains revealed that the three sensitive strains encoded four genes, which are not encoded by the resistant strains. (1) ABC transporter substrate-binding protein (A4W71_00975) (2) PTS mannose/fructose/sorbose transporter subunit IIC (PTS Man^{IIC}) (A4W71_01930) (3) amino acid permease (A4W71_00610) and (4) D-alanyl-

lipotheichoicacid biosynthesis protein (DltB) (A4W71_01460). Interestingly, *L. curvatus* TMW 1.421 encoded only (1) and (2), but either the amino acid permease or D-alanyl-lipotheichoicacid biosynthesis protein. Detailed analysis of PTS Man^{IIC} revealed a high similarity to the sequence of two different PTS Man^{IIC} genes (PTS Man^{IIC-1}, PTS Man^{IIC-2}) encoded by *Listeria monocytogenes* EGD-e (Glaser et al., 2001) (Figure 21). The transmembrane structure analysis revealed that the structure of PTS Man^{IIC} encoded by *L. curvatus* strains was more similar to PTS Man^{IIC-1} than to PTS Man^{IIC-2} (Figure 21).

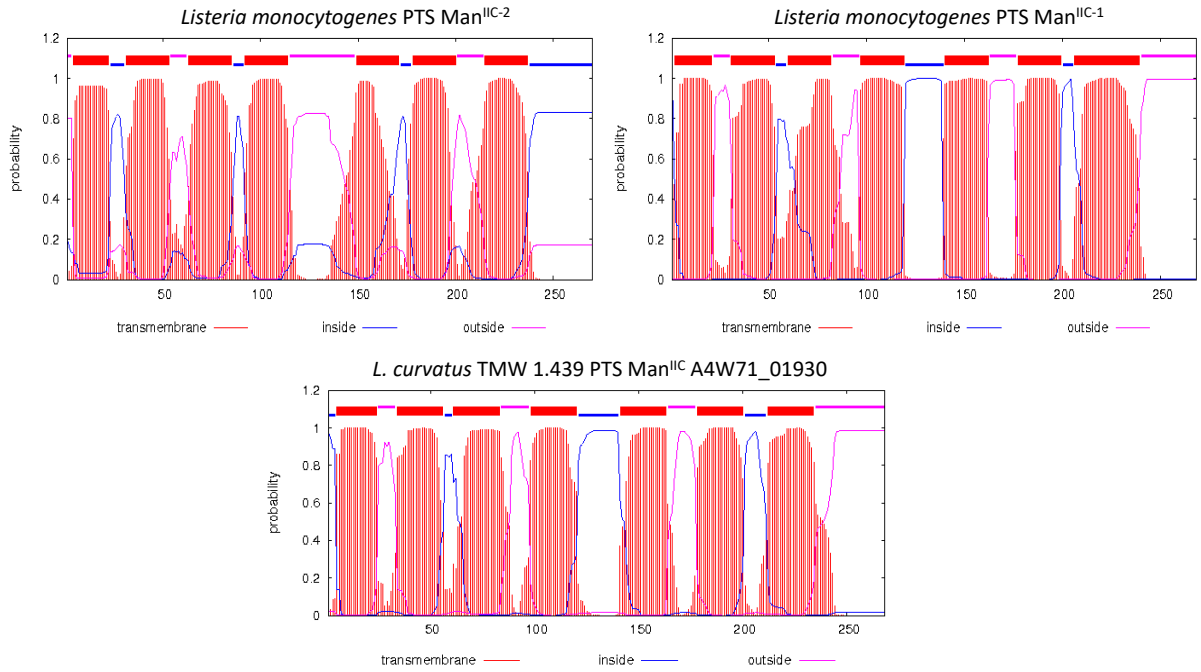

Figure 21: The transmembrane structure of PTS Man^{IIC} encoded in *L. curvatus* TMW 1.439 was compared with the two identified PTS Man^{IIC} (PTS Man^{IIC-1} and PTS Man^{IIC-2}) encoded in *Listeria monocytogenes* EGD-e (Glaser et al., 2001).

The pan-genome analysis based on amino acid sequences revealed, that different bacteriocin immunity proteins are part of the accessory-genome. In detail, there are three diagnostic marker genes (DMG_443, DMG_5404 and DMG_5725), which encoded an Enterocin A immunity protein. All resistant strains encoded in least one of these genes (supplementary Table 4). But *L. curvatus* TMW 1.439 and TMW 1.1381 encoded one immunity protein, too.

3.6.3.2 Bacteriocin sensitivity of *L. sakei* against Pediocin PA-1

The strains of *L. sakei* show different sensitivity/resistance against PA-1 shown in Table 19. Most strains of *L. sakei* are sensitive, but only *L. sakei* TMW 1.3, TMW 1.114, TMW 1.417 and TMW 1.578 are sensitive in presence of glucose and mannose, whereas *L. sakei* TMW 1.1239, TMW 1.1322, and TMW 1.1398 are sensitive in presence of mannose, but not in presence of glucose. Indeed, *L. sakei* TMW 1.1189 is sensitive against PA-1 in presence of glucose and resistant in presence of mannose.

Table 19: Bacteriocin-resistance assay against class II bacteriocin pediocin PA-1 for *L. sakei*. A positive reaction results in inhibitory zones: "–" indicates no inhibitory effect; "+" indicates detectable inhibitory effect.

		Glucose	Mannose
L. sakei	TMW 1.3	+	+
	TMW 1.46	-	-
	TMW 1.114	+	+
	TMW 1.417	+	+
	TMW 1.578	+	+
	TMW 1.1189	+	-
	TMW 1.1239	-	+
	TMW 1.1322	-	+
	TMW 1.1396	-	-
	TMW 1.1398	-	+

Genomic comparison of the strains suggest that the sensitive strains are different based on a few transporter systems and cell wall properties. They encoded UDP-N-acetylmuramoyl-tripeptide –D-alanyl-D-alanine ligase, which catalyses the reaction during lysine biosynthesis and peptidoglycan biosynthesis. Moreover, there are amino acid permease, hydrolase and short-chain hydrolase, which are encoded in the most genomes of sensitive strains. Interestingly, sensitive strains *L. sakei* TMW 1.3, TMW 1.114, TMW 1.417, TMW 1.578 and TMW 1.1322, which is only sensitive in presence of mannose, encoded a peptide ABC transporter permease, which is known as a bacteriocin exporter and could be involved in the resistance of the strain.

Moreover, strains, which are sensitive under all conditions, encoded (1) penicillin-binding protein, (2) short chain dehydrogenase, (3) peptidase C69 and (4) MFS transporter.

3.7 Metabolic pathways

Metabolic properties and adaptions are highly important for survival on a raw meat matrix as well as beeing competitive during raw sausage fermentation. Meat is a rich medium, which harbors a lot of different niches, which can be occupied by the strains. Interesting substrates are different carbon sources like glucose, ribose, sucrose. On the other hand, there are lipids, which are sources of fatty acids and glycerol, proteins, nucleosides, which are sources of ribose, amino acids, citrate and others. All these substrates are metabolized in different pathways, which are summarized in Figure 22. Moreover, the core-genome of both *L. curvatus* and *L. sakei* encodes glutamine-fructose-6-phosphate aminotransferase, UDP-N-acetylglucosamine diphosphorlylase, and phosphate dikinase, which are known to be key traits of cell wall biosynthesis from pyruvate and gluconeogenesis.

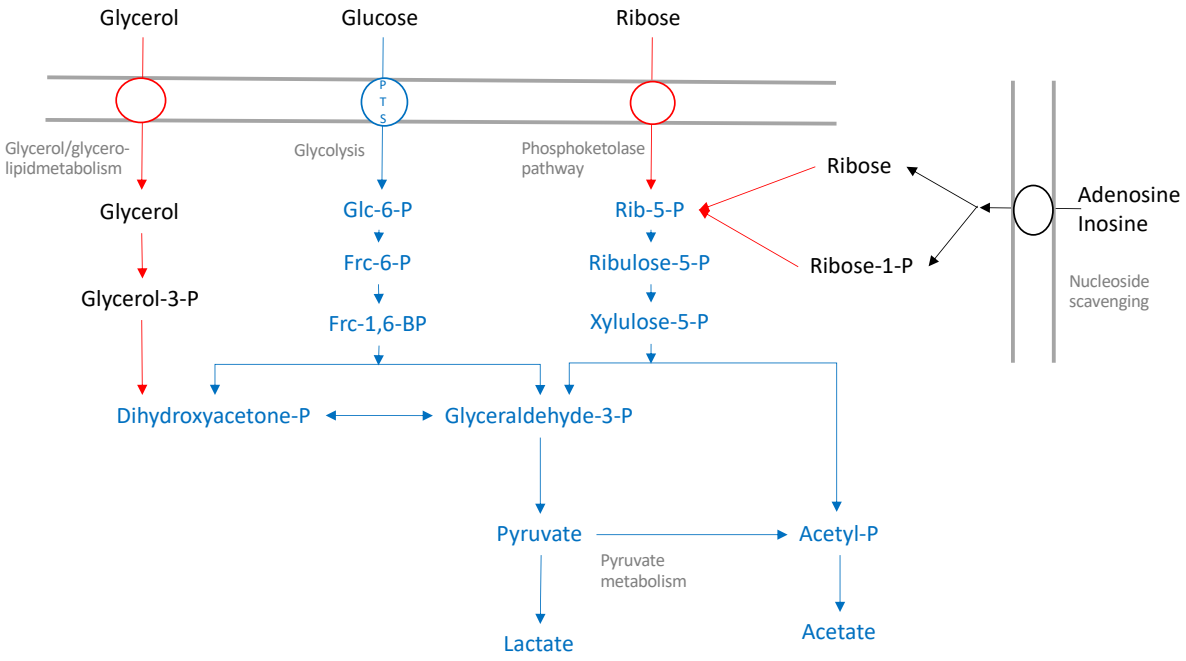

Figure 22: Pathways encoded in the genomes of *L. sakei* and *L. curvatus*. This metabolic overview was adapted and modified from (McLeod et al., 2010). Blue marks steps of pathways, which are encoded in the core-genome, whereas red marks the steps, which are part of the accessory-genome if they are at least part of one accessory-genome of either *L. curvatus* or *L. sakei*.

For adaptation to a habitat the metabolism is the most obvious, if not prominent property of bacteria. A well-adapted metabolism could result in assertiveness in a special environment

and occupation of an ecological niche. Therefore, the pan-genomes of both species were analyzed to identify respective metabolic properties.

Apart from general pathways of glycolysis, the pathway for the fermentation of melibiose is part of the core-genome of both species. Furthermore, all enzymes, which are associated with the metabolism of galactose, gluconate, arabinose, ribose, and glycerol, are encoded in the genomes of all strains of both *L. sakei* and *L. curvatus*. Moreover, the gene sequences of these enzymes are generally well conserved. However, several mutations were identified within the gene encoding a glycerol-3-phosphate dehydrogenase in the genome of *L. sakei* TMW 1.1398. This mutation leads to an introduction of an earlier stop codon in the amino acid sequence at amino acid position 38 rendering it non-functional. Another gene, *araA*, which encodes L-arabinose-isomerase, was also identified at all sequenced genomes, but the sequence analysis revealed that the nucleotide sequence is not well conserved. Indeed, in *L. sakei* TMW 1.417 the *araA* gene is different from other ones. The sequence comparison suggests that the first 304bp is missing in the gene *araA* in the genome of *L. sakei* TMW 1.417. Still, the alignment and analysis of amino acid sequence shows that the predicted functional part of the gene is apparently intact. These results were confirmed by smart BLAST. Genome sequencing shows that a trehalose specific IIA subunit of PTS system, which is involved to the phosphorylation of extracellular trehalose to trehalose-6-phosphate, is part of the core-genome of *L. sakei*. Furthermore, the genomic data suggests that the trehalose-6-phosphatase or alpha, alpha-phosphotrehalase, which catalyses the conversion of trehalose-6-phosphate to D-glucose and D-glucose-6-phosphate, is encoded by all sequenced strains.

Furthermore, sucrose metabolism is found in the core genome of *L. sakei* and is outlined in Figure 23.

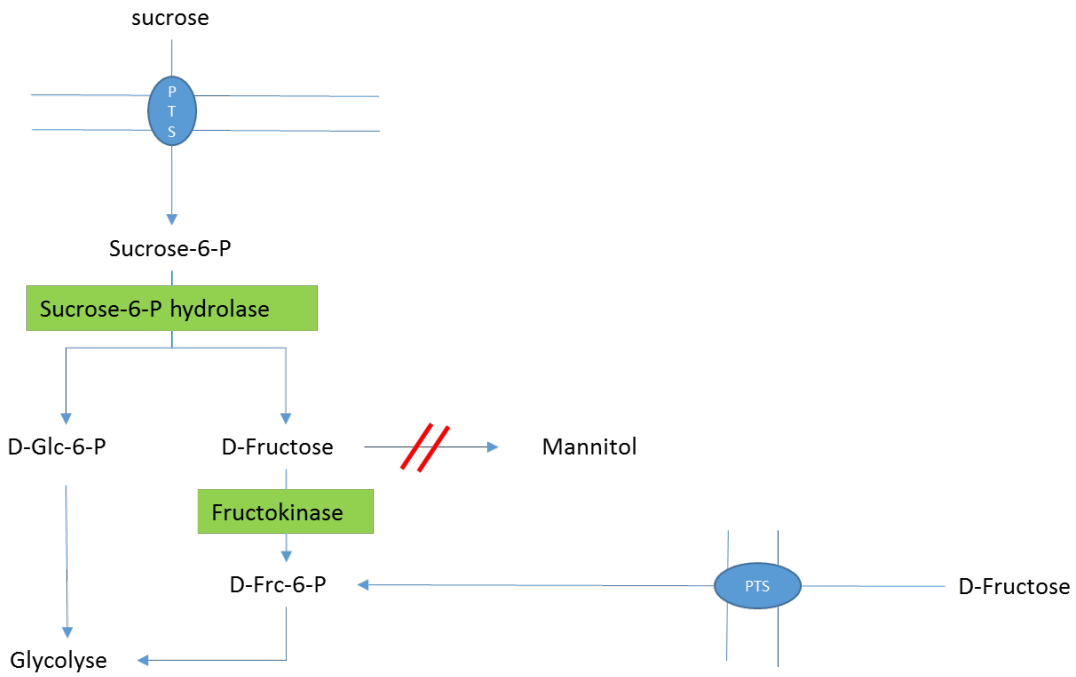

Figure 23: Sucrose metabolism: genes are part of the core-genome of *L. sakei.*

Genes involved in this metabolism are encoded within a sucrose operon, which is detected at the core-genome of *L. sakei*. The strains are able to take up sucrose by a sucrose PTS. Subsequently, sucrose-6-phosphate hydrolase catalyses the reaction form sucrose-6-phosphate to D-glucose-6-phosphate and D-fructose. In the following step, D-fructose is phosphorylated to D-fructose-6-phosphate by fructokinase, whereas D-glucose-6-phosphate will further metabolize by the glycolysis. Indeed, a fructose associated PTS was detected at the core-genome, so the *in silico* prediction suggest there is the ability to take up extracellular fructose by a PTS. Interestingly, the strains are predictively unable to use fructose as electron acceptor and produce mannitol in the recycling of NAD.

3.7.1 Glycolysis

Genomic comparison revealed that all genes, which encoded enzymes involved in glycolysis, are part of the core-genome of both species (Figure 22). The gene sequences are highly conserved, and no mutations are detectable.

Transporter system (PTS) for glucose, glucokinase, phosphoglucoisomerase, fructose-1,6-bisphosphatase, 6-phosphofructokinase, aldolase is encoded in the genomes of both species, and they are part of core-genome of *L. sakei* as well as *L. curvtaus*.

Interestingly, four different L-lactate dehydrogenases were encoded by the strains of *L. sakei*, but only two of these genes are part of the core-genome. Whereas strains of *L. curvatus* encoded two different L-lactate dehydrogenases. Moreover, the pyruvate dehydrogenase of *L. curvatus* TMW 1.421 is different based on the amino acid sequence compared to the other strains.

The growth of all genome-sequenced strains was tested in presence of glucose in CDM (Figure 24 and Figure 25). The physiology of all strains shows differences, although all strains are able to grow well in presence of glucose as single carbon source.

L. curvatus strains could be separated to three groups based on their growth behaviour on glucose. *L. curvatus* TMW 1.595 and TMW 1.1381 reached the stationary growth phase after 24 h. Indeed, the strains *L. curvatus* TMW 1.167, TMW 1.439, TMW 1.624 and TMW 1.1390 show after 24 h late exponential growth and only after 48 h stationary growth phase. Moreover, *L. curvatus* TMW 1.27, TMW 1.401, TMW 1.407, TMW 1.421 grow slower. These strains show exponential growth after 24 h and stationary growth after 48 h.

For strains of *L. sakei* similar results were observed. *L. sakei* TMW 1.417, TMW 1.1239 and TMW 1.1322 reached the stationary growth phase after 24 h, whereas *L. sakei* TMW 1.46, TMW 1.114, TMW 1.578, TMW 1.1396 and TMW 1.1398 showed late exponential growth after 24 h and stationary growth after 48 h. However, *L. sakei* TMW 1.3 and TMW 1.1189 showed exponential growth after 24 h and stationary growth after 48 h.

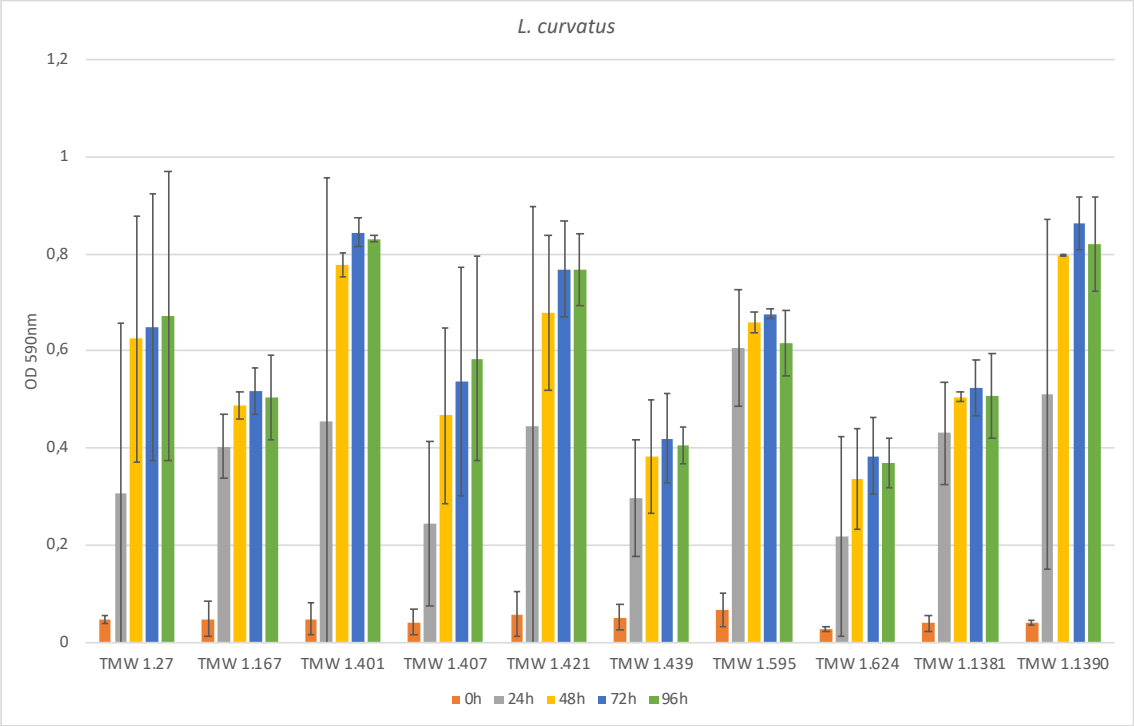

Figure 24: Growth of *L. curvatus* in CDM with glucose (25 mM). All necessary enzymes associated with the glycolysis are part of the core-genome. Based on *in silico* prediction all strains are able to use glucose by their catabolic pathway.

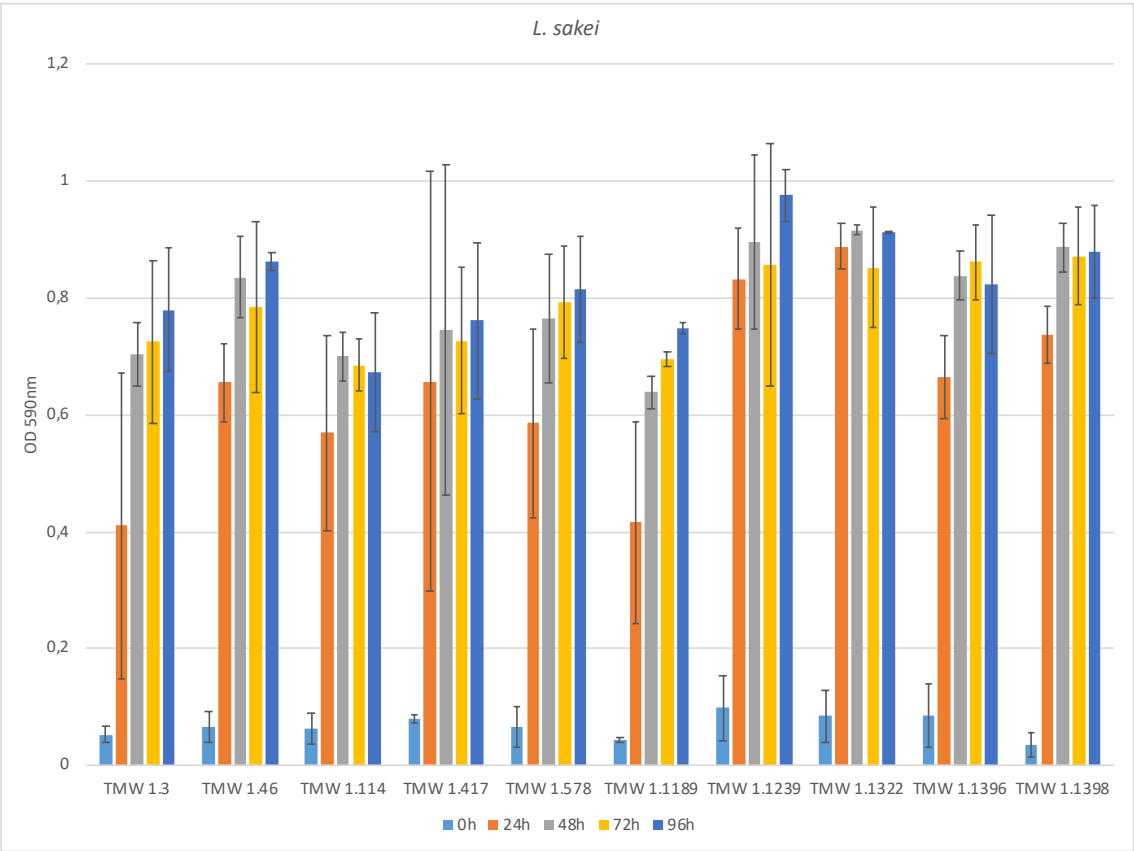

Figure 25: Growth of *L. sakei* in CDM in presence of glucose (25 mM) as energy source. The genomic analysis of the core-genome suggest that genes encoding all necessary enzymes associated with the glycolysis are part of their core-genome.

3.7.2 Glycerolipid metabolism

Glycerolipid metabolism is one of the important pathways for adaptation to and surviving in meat environment. Glycerolipid is one of the main substrates within meat matrix. Interestingly, there are detectable differences in the amino acid sequences of protein homologous to enzymes, which are involved in this pathway.

The pan-/core-genome analysis revealed a lot of differences based on the glycerol metabolism within strains of *L. curvatus,* which are listed in Table 20.

Table 20: List of identifed enymes associated with glycerollipid metabolism in *L. curvatus*. "+" marks yes or functional and "-" marks no or non-functional.

L. curvatus	**genetic characteristics**	**glycerol-3-phosphate dehydrogenase**	**glycerol kinase**	**glycerol transporter**	**aquaporin**
TMW 1.27	encoded	+	+	+	+
	mutated	-	-	-	-
	predicted functionality	+	+	+	+
TMW 1.167	encoded	+	+	+	+
	mutated	-	+	+	-
	predicted functionality	+	-	-	+
TMW 1.401	encoded	+	+	-	+
	mutated	+	+	-	-
	predicted functionality	-	-	-	+
TMW 1.407	encoded	+	+	+	+
	mutated	+	-	-	-
	predicted functionality	-	+	+	+
TMW 1.421	encoded	+	+	+	+
	mutated	-	-	-	-
	predicted functionality	+	+	+	+

L. curvatus	genetic characteristics	glycerol-3-phosphate dehydrogenase	glycerol kinase	glycerol transporter	aquaporin
TMW 1.439	encoded	+	+	+	+
	mutated	-	-	-	-
	predicted functionality	+	+	+	+
TMW 1.595	encoded	+	+	+	+
	mutated	-	-	+	-
	predicted functionality	+	+	-	+
TMW 1.624	encoded	+	+	+	+
	mutated	-	-	+	-
	predicted functionality	+	+	-	+
TMW 1.1381	encoded	+	+	+	+
	mutated	-	-	-	-
	predicted functionality	+	+	+	+
TMW 1.1390	encoded	+	+	+	+
	mutated	-	-	-	-
	predicted functionality	+	+	+	+

There are three important enzymes, which are involved in the metabolism: glycerol transporter, glycerol kinase and glycerol-3-phosphate dehydrogenase. The transporter of glycerol is not part of the core-genome, because *L. curvatus* TMW 1.401 does not encode a glycerol transporter based on results of sequence comparison and annotation. Moreover, there are *L. curvatus* TMW 1.167, TMW 1.595 and TMW 1.624, which are different based on the sequences of the respective genes. More detailed analysis suggests that there are mutations within the nucleotide sequences, which result in introductions of early stop codons, rendering these genes non-functional. The analysis of the final transmembrane structure, which was done by TMHMM, showed that the mutated transporters have one single transmembrane structure at the beginning of the sequence, whereas the non-mutated transporter has more transmembrane structures (Figure 26). Moreover, the genetic analysis

revealed that all strains of both species encoded an aquaporin, which is associated with glycerol uptake, too.

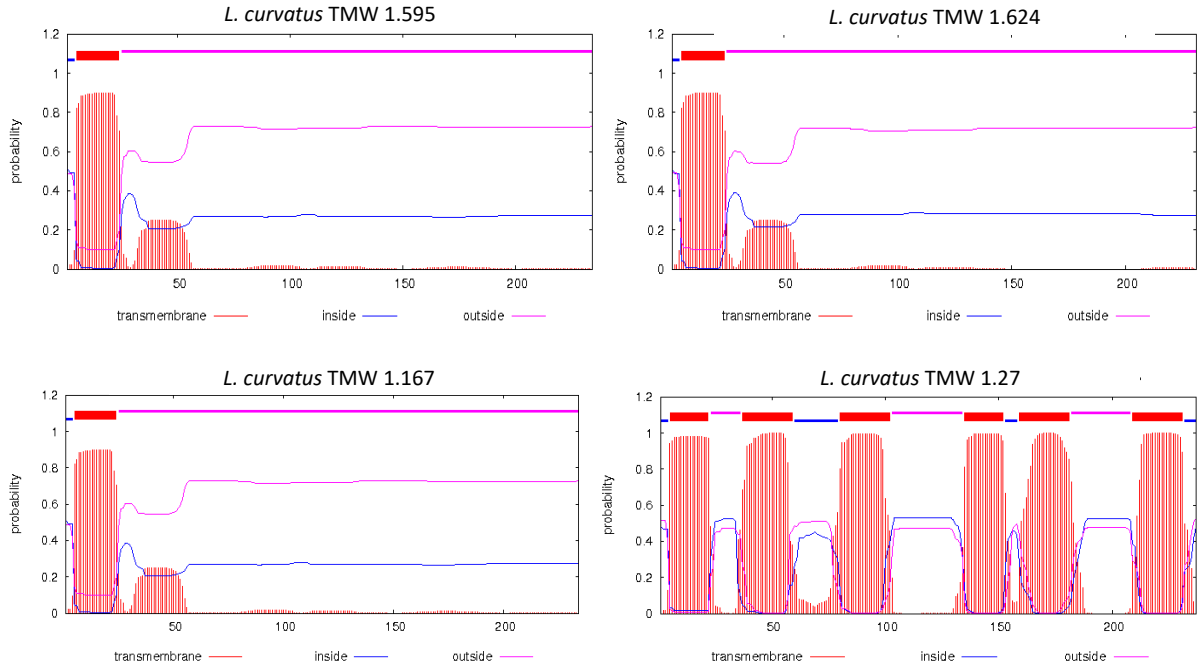

Figure 26: TMHMM analysis of glycerol transporter encoded in genomes of *L. curvatus* TMW 1.595, TMW 1.624, TMW 1.167 and TMW 1.27. Genetic analysis revealed that the gene of glycerol transporter at the genome of *L. curvatus* is not mutated, whereas the same gene in the genomes of the other three strains appears to be mutated. These mutations result in a changed transmembrane structure.

The glycerol kinase is encoded by all strains of *L. curvatus*, but there are differences based on the sequence. *L. curvatus* TMW 1.407, TMW 1.439, TMW 1.595, TMW 1.624, TMW 1.1381 and TMW 1.1390 encoded the same glycerol kinase with an orf length of 1518 bp. The amino acid sequence revealed that there are no stop codons within the sequence. Furthermore, *L. curvatus* TMW 1.27, TMW 1.167, TMW 1.401 and TMW 1.421 have different glycerol kinases. First, *L. curvatus* TMW 1.421 encoded a gene, which is closely similar to glycerol kinase of other strains based on the nucleotide sequence, but the amino acid sequence differs significantly. Moreover, there is no early stop codon introduced, and the same can be observed for *L. curvatus* TMW 1.27, whereas *L. curvatus* TMW 1.167 and TMW 1.401 have mutated sequences, which results in introduction of early stop codons. The third enzyme of the glycerol metabolism is the glycerol-3-phosphate dehydrogenase. It is part of the core-genome of *L. curvatus,* but *L. curvatus* TMW 1.401 and TMW 1.407 have mutated sequences with an early stop codon.

All three described enzymes (glycerol transporter, glycerol kinase, glycerol-phosphate dehydrogenase) are part of the core-genome of *L. sakei* based on the nucleotide sequences like it is listed in Table 21. Comparison of amino acid sequences revealed only single exchanges of amino acids which may not influence the function of the genes, with the exception of the glycerol-3-phosphate dehydrogenase, which is mutated in *L. sakei* TMW 1.1398. This mutation results in an introduction of a stop codon.

Table 21: List of identifed enzymes associated with glycerollipid metabolism in *L. sakei*. "+" marks yes or functional and "-" marks no or non-functional.

L. sakei	**genetic characteristics**	**glycerol-3-phosphate dehydrogenase**	**glycerol kinase**	**glycerol transporter**	**aquaporin**
TMW 1.3	encoded	+	+	+	+
	mutated	-	-	-	-
	predicted functionality	+	+	+	+
TMW 1.46	encoded	+	+	+	+
	mutated	-	-	-	-
	predicted functionality	+	+	+	+
TMW 1.114	encoded	+	+	+	+
	mutated	-	-	-	-
	predicted functionality	+	+	+	+
TMW 1.417	encoded	+	+	+	+
	mutated	-	-	-	-
	predicted functionality	+	+	+	+
TMW 1.578	encoded	+	+	+	+
	mutated	-	-	-	-
	predicted functionality	+	+	+	+
TMW 1.1189	encoded	+	+	+	+
	mutated	-	-	-	-
	predicted functionality	+	+	+	+

L. sakei	genetic characteristics	glycerol-3-phosphate dehydrogenase	glycerol kinase	glycerol transporter	aquaporin
TMW 1.1239	encoded	+	+	+	+
	mutated	-	-	-	-
	predicted functionality	+	+	+	+
TMW 1.1322	encoded	+	+	+	+
	mutated	-	-	-	-
	predicted functionality	+	+	+	+
TMW 1.1396	encoded	+	+	+	+
	mutated	-	-	-	-
	predicted functionality	+	+	+	+
TMW 1.1398	encoded	+	+	+	+
	mutated	+	-	-	-
	predicted functionality	-	+	+	+

The genomic comparison and analysis are an *in silico* prediction, so the physiology was tested by growth experiments for strains of both species.

The growth experiment revealed that *L. curvatus* TMW 1.401 and TMW 1.595 are able to use glycerol as source of energy to grow, whereas *L. curvatus* TMW 1.407 and TMW 1.624 has no specific detectable growth (Figure 27). The OD_{590} of *L. curvatus* TMW 1.624 is stable. The OD_{590} of *L. curvatus* TMW 1.407 declined over 96h. The other tested six strains have a small, but detectable growth.

The growth experiment in CDM with glycerol revealed that all strains of *L. sakei* are able to grow in presence of glycerol as only source (Figure 28). Two strains, *L. sakei* TMW 1.1189 and TMW 1.1398, show less growth compare to the other strains of *L. sakei*.

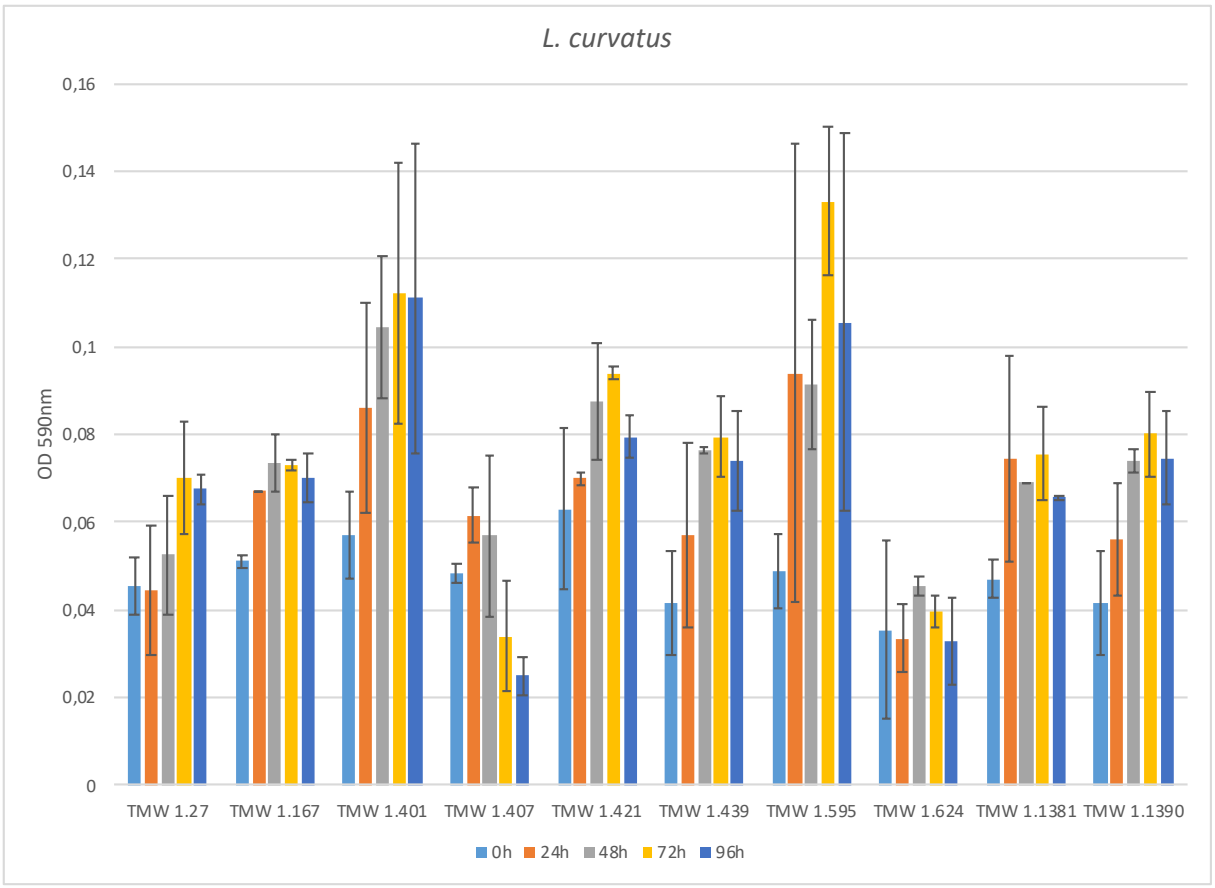

Figure 27: Growth of *L. curvatus* in CDM with glycerol (25 mM) as carbon source. Genetic analysis revealed that the catabolic pathway of glycerol is not encoded in core-genome of *L. curvatus* strains. Moreover, *in silico* prediction suggest that there are differences between the strains based on the ability using glycerol as single carbon source.

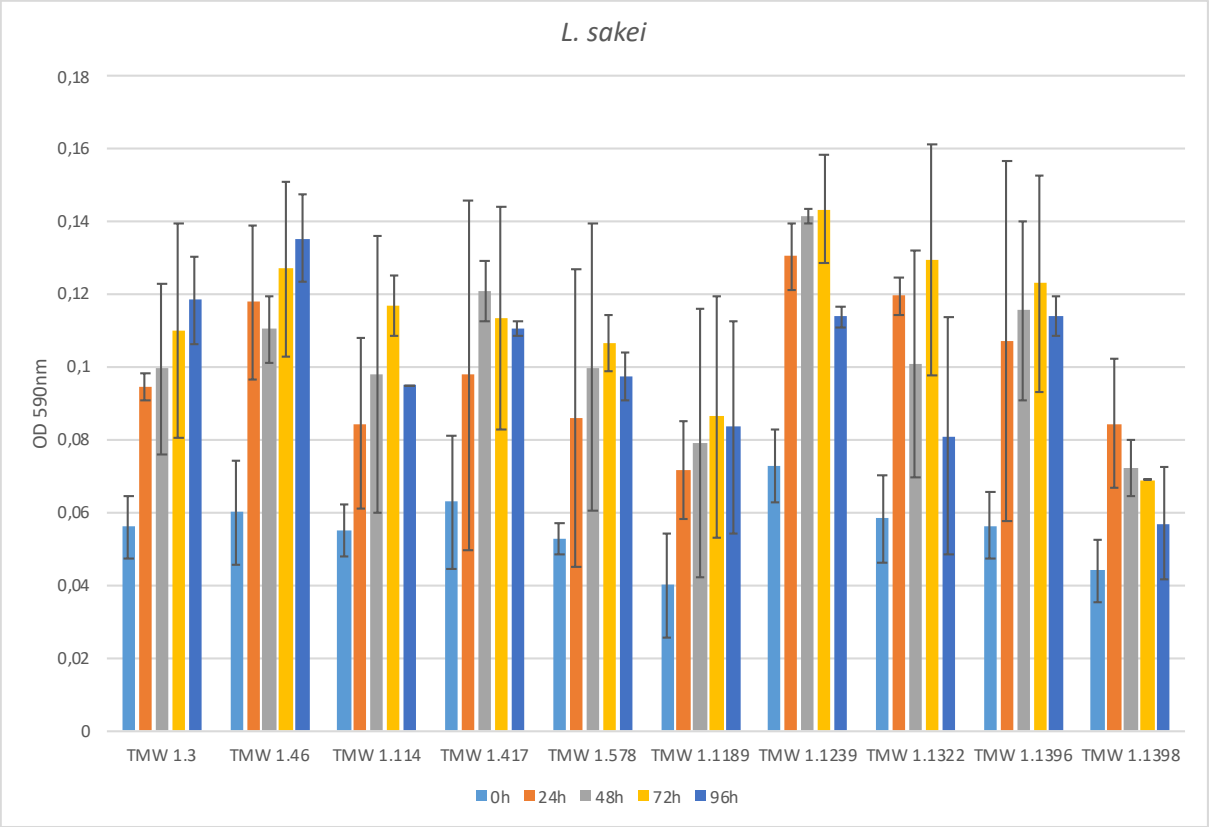

Figure 28: Growth of *L. sakei* strains in CDM in presence of glycerol (25 mM) as carbon source. Genomic comparison revealed that most strains encoded all necessary enzymes involved in catabolic pathway. Only for *L. sakei* TMW 1.1398 a mutation at the gene of glycerol-3-phosphate dehydrogenase was detected.

3.7.3 Adenosine and inosine metabolism

Purine nucleosides are important sources for meat-associated strains. Nucleoside scavenging is important to generate ribose as shown in Figure 22. Genomics revealed that all strains of *L. sakei* are able to degrade inosine and adenosine to ribose. Indeed, all strains encoded an adenosine deaminase, which catalyzes the degradation of adenosine to inosine and NH_3, nucleoside phosphorylases, which catalyzes the phosphorylation reaction of inosine to ribose-1-phosphate, and phosphopentomutase, which catalyzes the reaction of ribose-1-phosphate to ribose-5-phosphate.

The described enzymes are not part of the core-genome of *L. curvatus*. All strains of *L. curvatus* encoded a ribonucleoside hydrolase, but *L. curvatus* TMW 1.407 encoded a different sequence. Overall, two different ribose transporters were detected within the pan-genome of *L. curvatus* (3.7.7). The adenosine deaminase is encoded by all strains of *L.*

curvatus. But the nucleoside phosphorylases and phosphopentomutase are only encoded in the genomes of *L. curvatus* TMW 1.167, TMW 1.421, TMW 1.439 and TMW 1.1381.

Further growth experiments were performed to detect the differences of physiology based on adenosine utilization (Figure 29).

First, *L. curvatus* TMW 1.407 is not able to grow in presence of adenosine. Most other strains show significant growth after three days (72h), except of *L. curvatus* TMW 1.1390 which show significant increase of OD_{590} after 24h.

The growth experiment was performed in CDM with adenosine to detect the ability to grow in presence of adenosine.

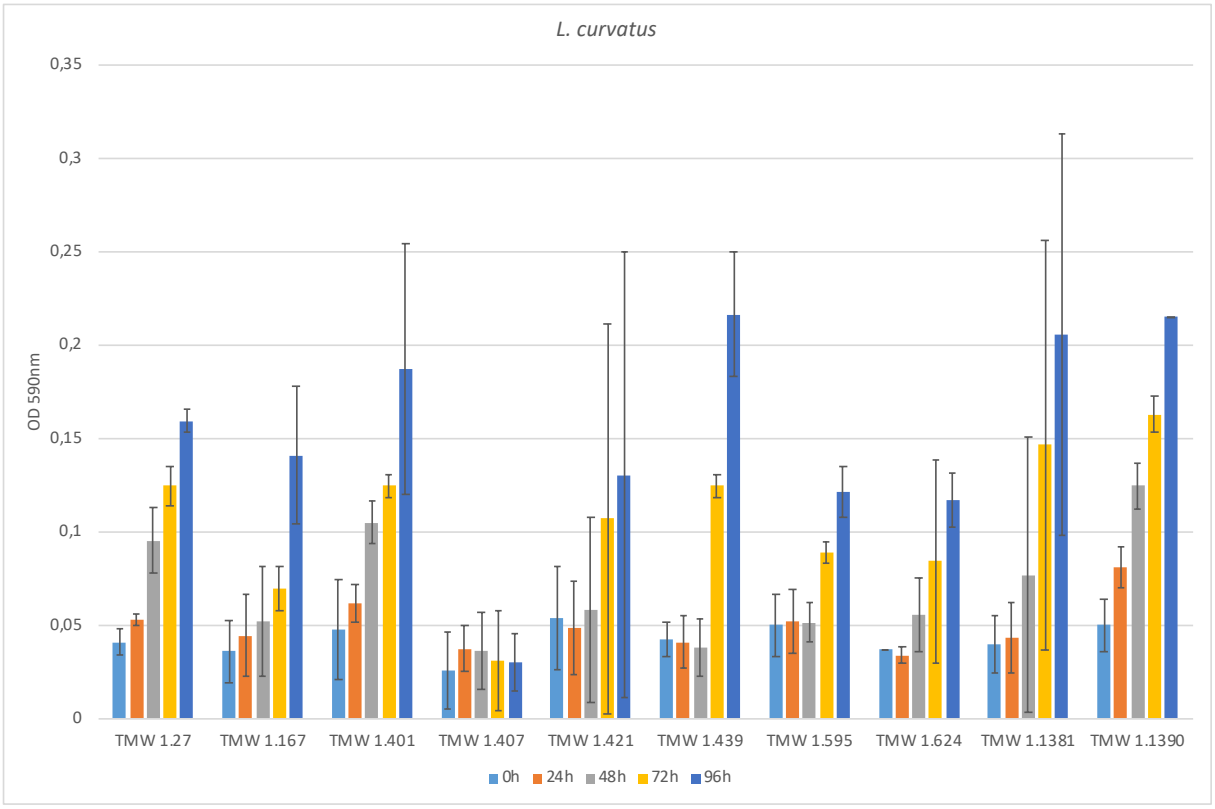

Figure 29: Growth of *L. curvatus* in CDM in presence of adenosine (25 mM)

Most strains of *L. sakei* are able to grow in presence of adenosine (Figure 30). But *L. sakei* TMW 1.1322 show less growth than the other strains. Moreover, *L. sakei* TMW 1.3 and TMW 1.46 show no clear detectable growth.

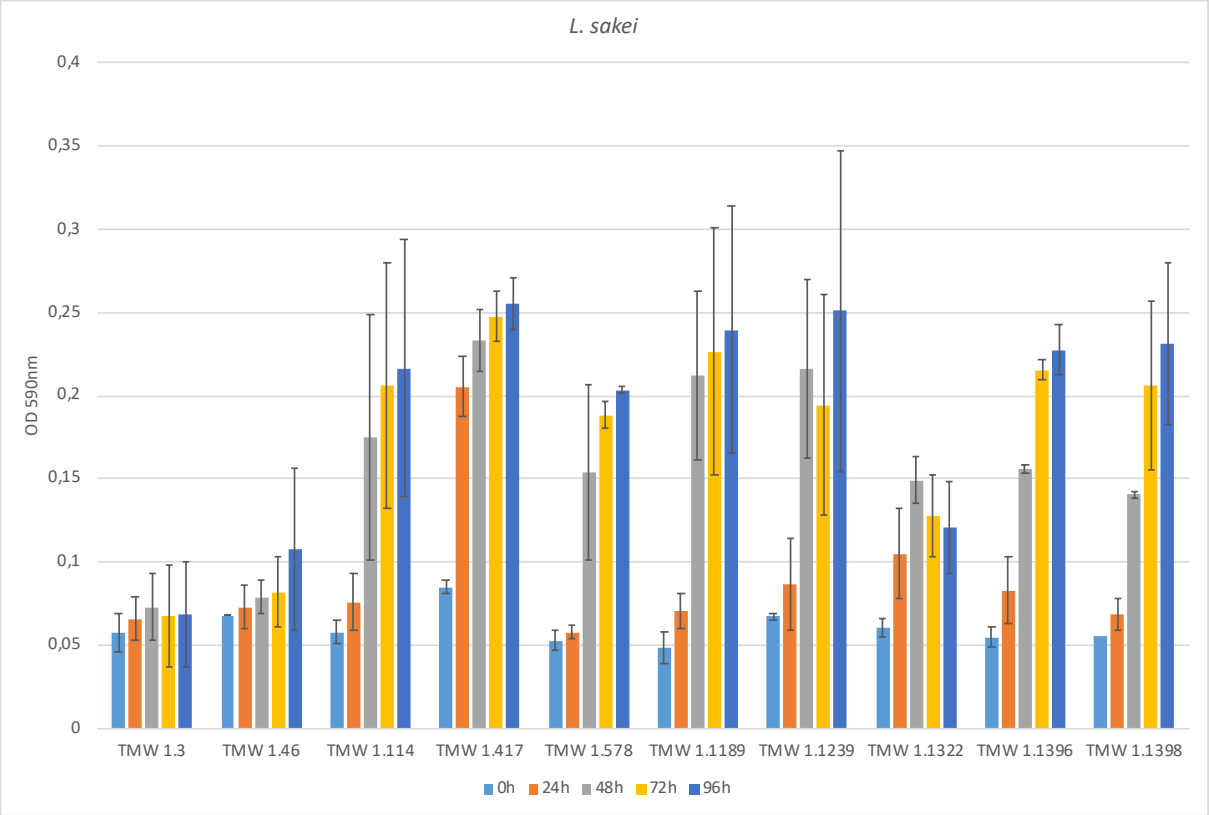

Figure 30: Growth of *L. sakei* in CDM in presence of adenosine.

3.7.4 Amino acid metabolism and biosynthesis

Proteins of the meat are degraded by different enzymes, e.g., cathepsins from meat or bacterial peptidases, to peptides and single amino acids. The metabolism and biosynthesis ability of these components are important based on the adaptation of the strains to meat as habitat. Based on the RAST annotation and KEGG database all strains of both *L. sakei* and *L. curvatus* were tested on their ability to metabolize amino acids. No metabolism of histidine was detectable for all strains of both species.

3.7.4.1 Alanine, Aspartate and glutamate

Genomic analysis suggests that all strains encoded enzymes, which are associated with different reactions of L-aspartate (Figure 31). All strains of both species are able to convert L-aspartate to D-aspartate by an aspartate racemase based on *in silico* prediction. Furthermore, the aspartate carbamoyl transferase is part of the core-genome of both *L. sakei* and *L. curvatus* and enables conversion of L-aspartate to N-carbamoyl-L-aspartate. Moreover, L-aspartate could be degraded to fumarate by two enzymes adenylosuccinate

synthase, which catalyses the GTP-dependent reaction of L-aspartate and IMP to adenylosuccinate, and adenylosuccinate lyase, which catalyses the following reaction of adenylosuccinate to fumarate and AMP. Indeed, the adenylosuccinate synthase is a really important enzyme because of its important role in purine biosynthesis, especially the reaction is part of the de-novo-synthese of AMP.

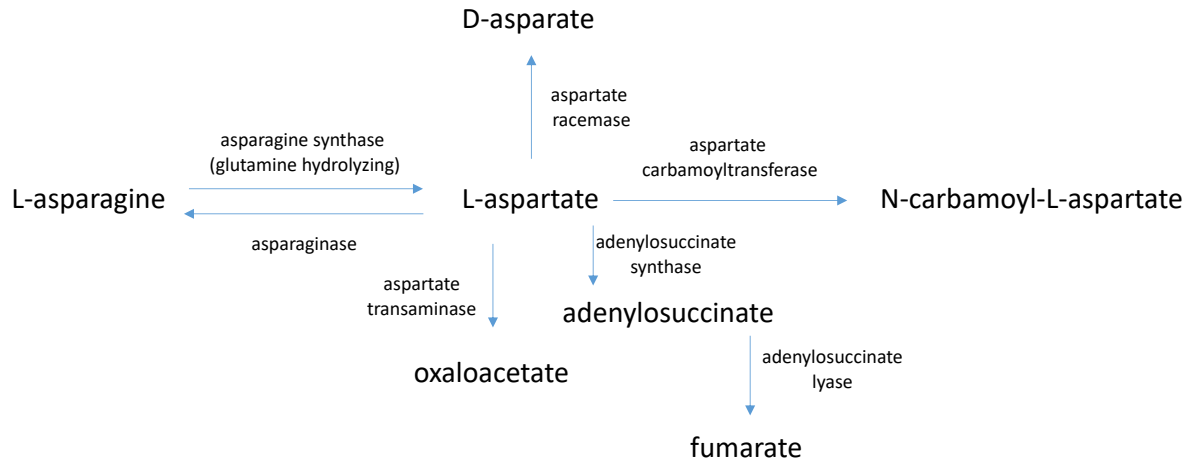

Figure 31: Reactions of L-aspartate, which are encoded in the genomes of sequenced strains of both species *L. curvatus* and *L. sakei.*

All strains are able to synthesize L-asparagine by the reaction of L-aspartate and L-glutamine with use of ATP and H_2O to L-asparagine and L-glutamate, AMP and PP_i which is catalysed by the asparagine synthase (glutamine hydrolysing) (Figure 32). However, asparaginase, which catalyses the hydrolysing of L-asparagine to L-aspartate is encoded within the core-genomes of both species. Another enzyme, the pyridoxal phosphate (PLP)-dependent aspartate transaminase, is part of both core-genomes, too. It catalyses the reaction of L-aspartate and α-ketoglutarate to oxaloacetate and L-glutamate. All genome sequenced strains encoded the glutamine synthetase, which catalyses the condensation of L-glutamate and NH_3 with use of ATP to L-glutamine, phosphate and ADP. Interestingly, only a few strains of *L. curvatus* encoded a glutamate synthase, which catalyses the reaction of L-glutamine and 2-oxoglutarate plus NADPH and H^+ into two L-glutamate plus $NADP^+$ (reaction marked with red arrows in Figure 32). Nevertheless, there are three enzymes encoded by all strains, which are associated with the degradation of L-glutamine: (1) glutamine-fructose-6-

phosphate transaminase, which catalyses the reaction of L-glutamine and D-fructose-6-phosphate to L-glutamate and D-glucosamine-6-phosphate, (2) amidophosphoribosyltransferase which catalyses the conversion of PRPP and L-glutamine to 5-phosphoribosylamine, and L-glutamate. The products of this reaction can only be used for IMP synthesis. Moreover, the reaction could be inhibited by IMP, GMP and AMP. (3) carbamoyl phosphate synthase catalyses the reaction of L-glutamine to carbamoylphosphate and L-glutamate. The enzyme is activated by ATP and PRPP, whereas UMP inhibits it.

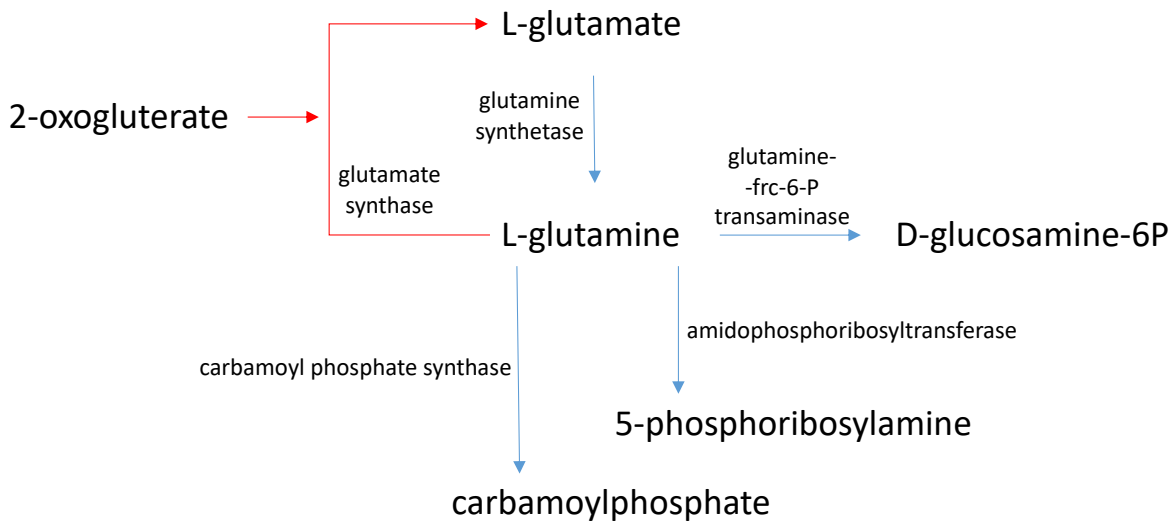

Figure 32: Pathways of L-glutamine which are encoded in the genomes of sequenced strains of *L. curvatus* and *L. sakei*. The red arrows mark a reaction step, which is not encoded in the core-genome of *L. curvatus.*

3.7.4.2 Serine, Threonine and Methionine metabolism

Genomic analysis suggests that the genomes of strains of *L. curvatus* and *L. sakei* encode enzymes associated with catabolism of serine, threonine and methionine, which is summarized in Figure 33.

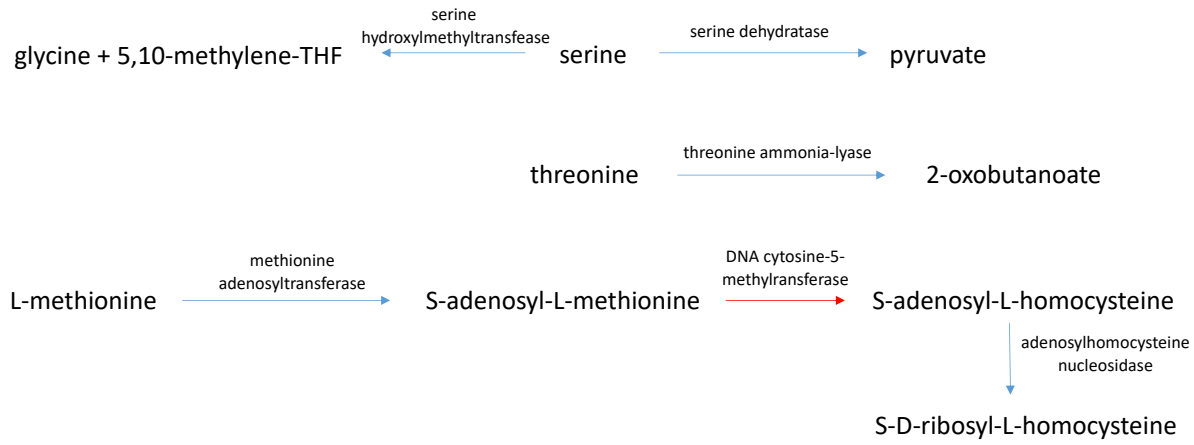

Figure 33: The metabolism of serine, threonine and methionine encoded in the genomes of *L. curvatus* and *L. sakei.* The red arrows remark a reaction step, which is not encoded in the core-genome of *L. curvatus* and *L. sakei*.

All strains encoded a serine dehydratase which is an PLP-dependent enzyme and catalyses the reaction of serine to pyruvate and NH_3. Pyruvate is an important product, which can be metabolized under energy generation in further reactions. Nevertheless, the PLP-dependent enzyme serine hydroxyl-methyltransferase, which is encoded in both core-genomes, plays an important role in one-carbon pathways and catalysed the reaction of L-serine to glycine and 5,10-methylene-tetrahydrofolate (THF).

Moreover, all strains encoded a threonine ammonia-lyase, which catalyses the reaction of threonine to α-ketobutyrate and NH_3.

L-methionine plus ATP could be converted to S-adenosyl-methionine by methionine adenosyltransferase, which is encoded by all strains. But the DNA cytosine-5-methyltransferase is part of the accessory-genome und is encoded in the genomes of *L. sakei* TMW 1.46, TMW 1.417, TMW 1.1239 and TMW 1.1398, as well as *L. curvatus* TMW1.167, TMW 1.401, TMW 1.439 and TMW 1.1381. DNA cytosine-5-methyltransferase catalyses the reaction of S-adenosyl-methionine to S-adenosyl-homocysteine. However, the adenosylhomocysteine nucleosidase, which catalyses the reaction of S-adenosyl-homocysteine to S-D-ribosyl-homocysteine and adenine is part of the core-genome.

3.7.4.3 Agmatine and ADI-pathway

Champomier Verges et al. (Champomier Verges et al., 1999), described the arginine-deiminase (ADI)-pathway of *L. sakei* and the advantage of this pathway in a meat

environment. So, the genomes of both species were investigated to identify the genes associated with the ADI-pathway (Figure 34). A major difference between *L. sakei* and *L. curvatus* could observed. The ADI-pathway is encoded in the core-genome of *L. sakei*, whereas no genome-sequenced strain of *L. curvatus* encoded this pathway (Figure 35). Furthermore, the agmatine pathway is not encoded by any strain of *L. curvatus*, too.

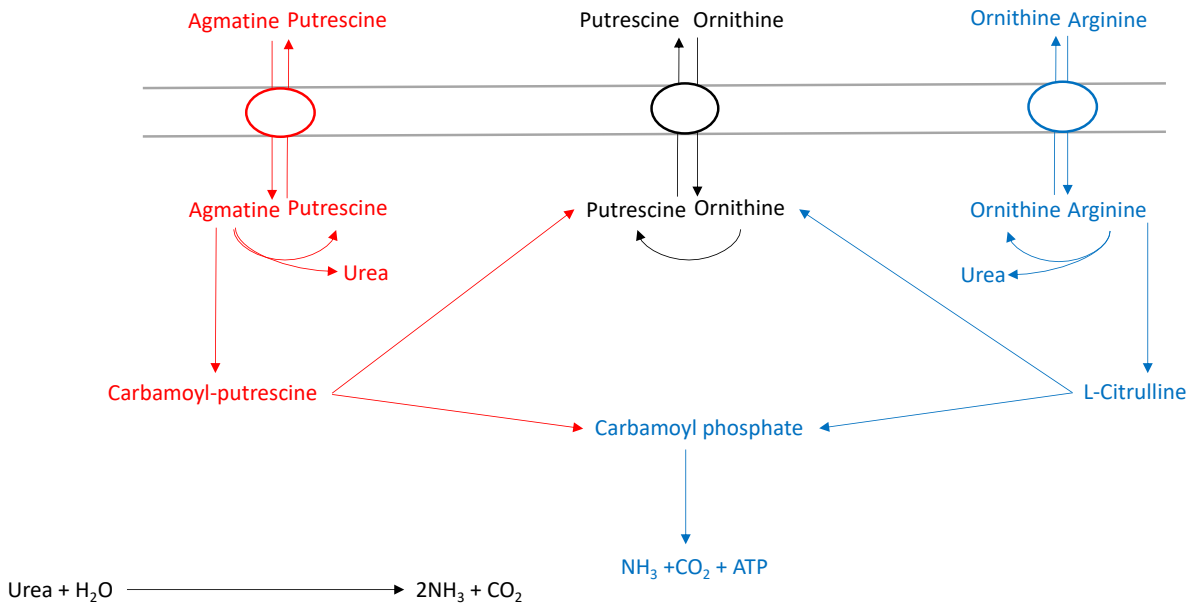

Figure 34: Metabolism of Agmatine, Ornithine and Arginine.

Moreover, *L. sakei* TMW 1.3, TMW 1.114, TMW 1.578 and TMW 1.1322 encode genes associated with the agmatine metabolism (Figure 35). This pathway is encoded in the accessory-genome of *L. sakei*. Moreover, the detailed genomic analysis of this gene cluster suggests differences between the strains.

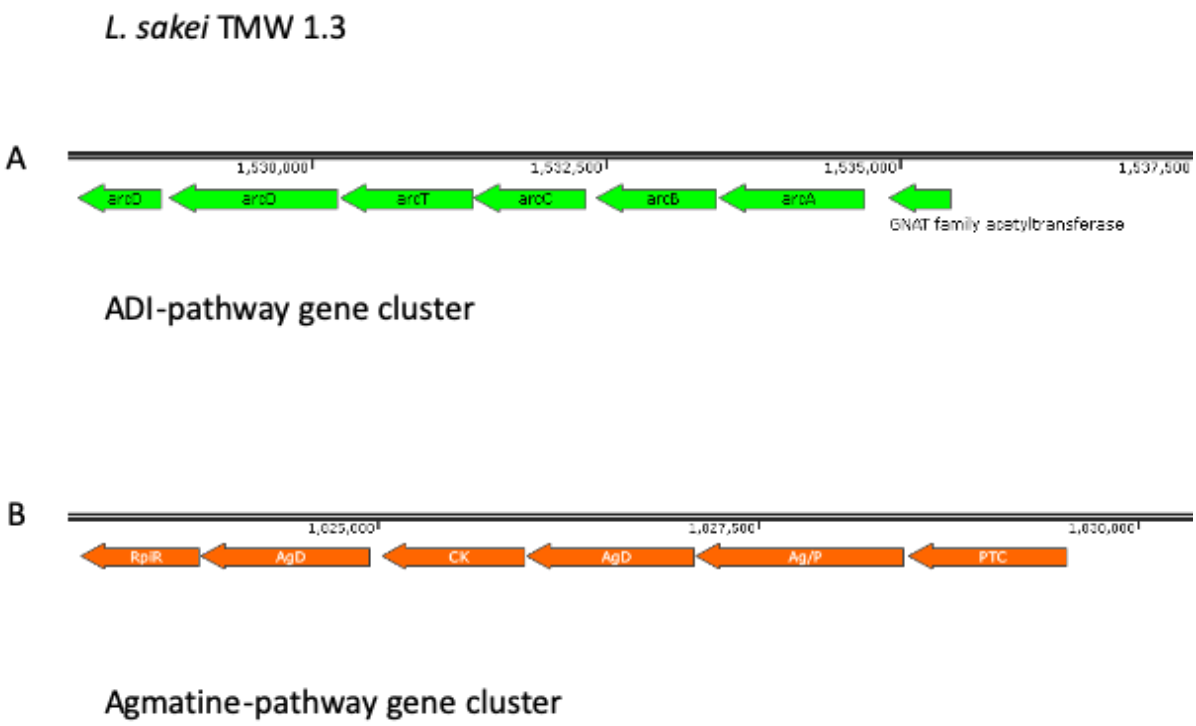

Figure 35: Gene clusters encoded by *L. sakei* TMW 1.3, which are associated with ADI-pathway (A) and agmatine pathway (B).

On the one hand, *L. sakei* TMW 1.114 and TMW 1.578 encoded an identical agmatine deiminase gene cluster. Indeed, the same gene cluster structure was identified in the genome of *L. sakei* TMW 1.3 and TMW 1.1322. But the sequence analysis shows mutations at the genes carried by *L. sakei* TMW 1.3 and TMW 1.1322. First, a mutation within the sequence of *aguD* encoding agmatine-putrescine antiporter (AgmP). The results of the web-based tool TMHMM, which analysis the transmembrane structure of a protein, suggest a changed structure of the antiporter, caused by the detected mutation. Another mutation was identified within the gene sequence of *aguC* encoding the carbamate kinase (CK) at the genome of *L. sakei* TMW 1.3. Carbamate kinase is involved in the degradation of carbamoyl phosphate to NH_3 and CO_2 under the generation of ATP.

If the mutations influenced the function of the encoded genes, it could be verified by physiological experiments. The strains were cultivated in DCM with agmatine or arginine and at day 0 and 5 the pH was measured, and the color of the cultures were documented,

because the pH-indicator shows if the pH changed from acidic environment to basic one (Figure 36).

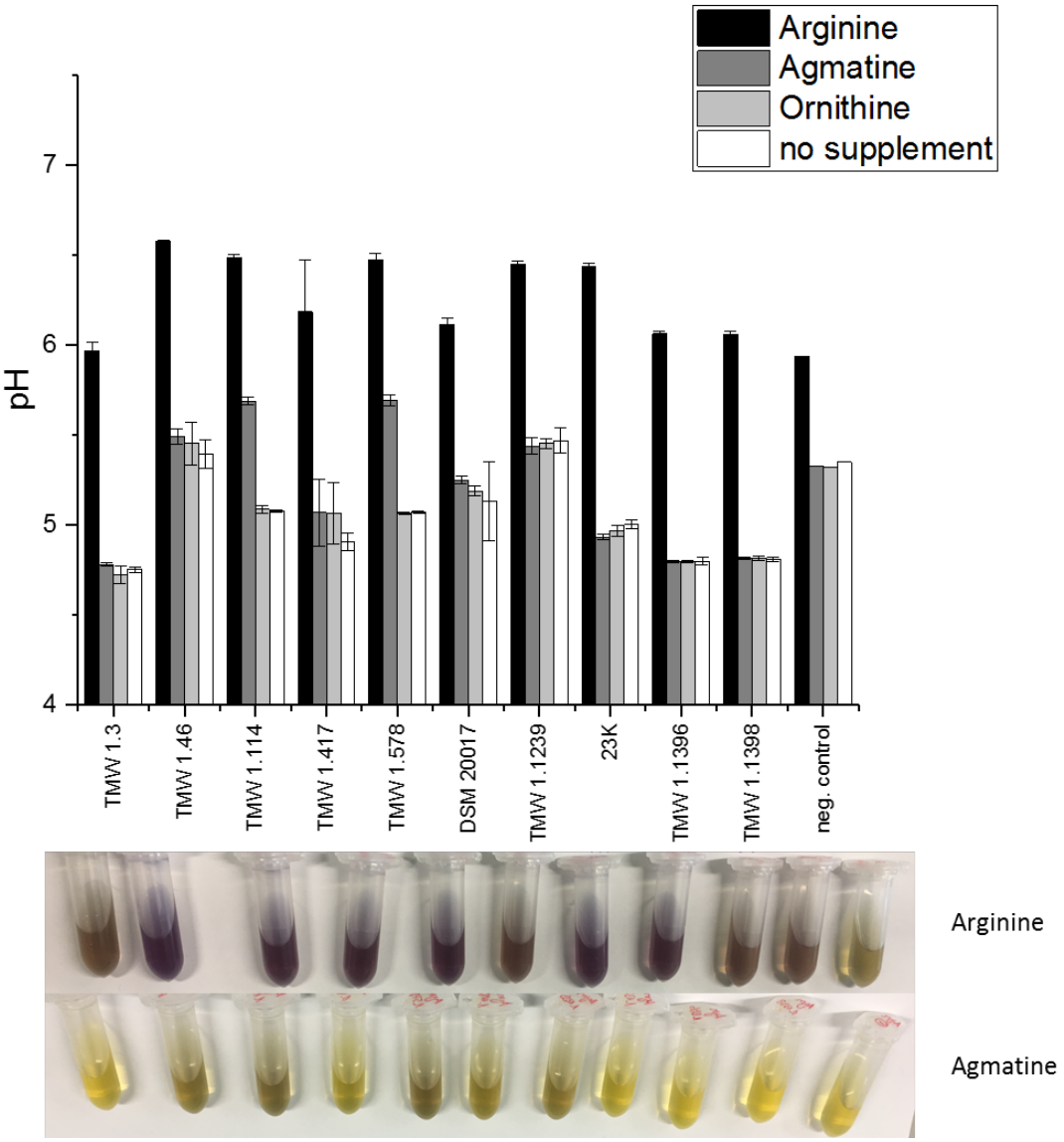

Figure 36: Influence of arginine, agmatine and orinithin metabolism on the pH of the media. Upper part: pH upon addition of the different substrates; lower part: colour change from yellow to purple as a result of pH increase.

The results suggest that all *L. sakei* strains tested were able to form a basic environment, as indicated by the purple color (Figure 36). The comparison of the four strains, encoding gene clusters associated with agmatine deiminase pathway, revealed physiological differences. On the one hand, *L. sakei* TMW 1.114 and TMW 1.578 were able to increase the pH in presence of agmatine, but *L. sakei* TMW 1.3 and TMW 1.1322 (synonym for 23K) shows a decrease of pH in presence of agmatine.

3.7.5 Two different citrate clusters are encoded in a few strains of *L. sakei*

Metabolic and genomic analysis revealed that the metabolism of malate and citrate is not part of the core-genome. Malate dehydrogenase is carried by *L. sakei* TMW 1.46, TMW 1.1189 and TMW 1.1239. This enzyme catalyses the reaction of L-malate to oxaloacetate. Enzymes, which are associated with the citrate metabolism, are organized in a gene cluster. For *L. sakei* strains two different citrate clusters could be identified. So, there are strains which encode either citrate cluster I or citrate cluster II, like they are visualized in Figure 37. Moreover, there are also strains of *L. sakei,* which did not carry any citrate gene cluster in their genomes. This group of strains conclude *L. sakei* TMW 1.114, TMW 1.417 and TMW 1.578.

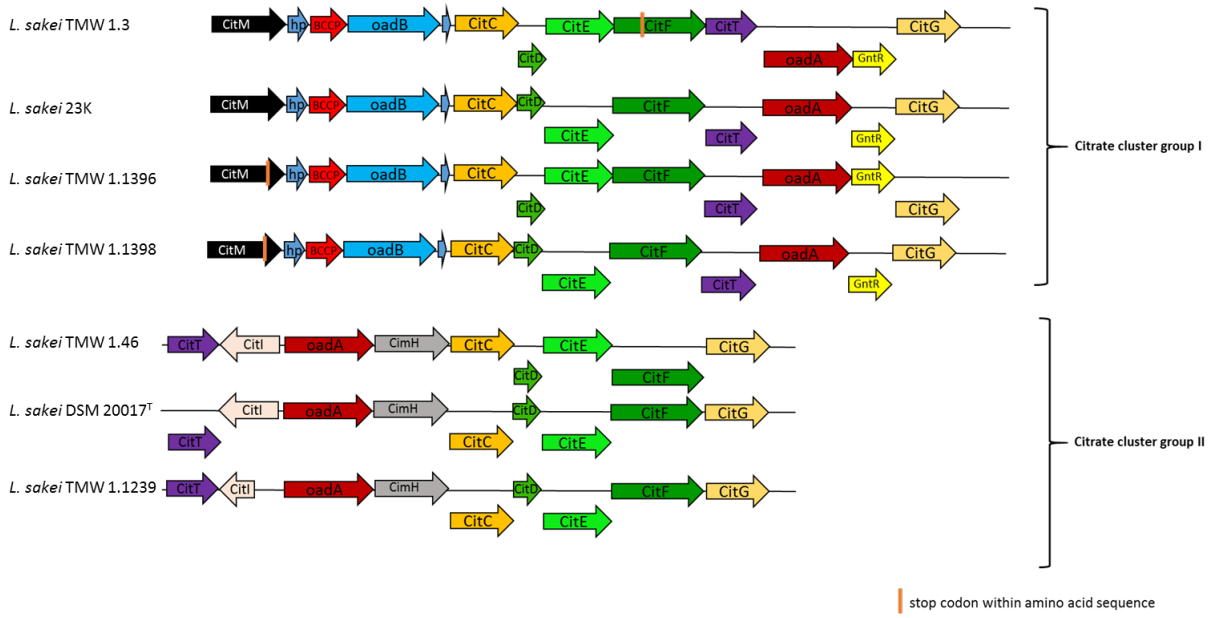

Figure 37: Citrate gene clusters, which are encoded within the accessory-genome of *L. sakei*

Genomic comparison of both gene clusters revealed that the nucleotide sequences of both gene clusters are different. Indeed, all relevant metabolic genes associated with the citrate gene cluster are encoded by both citrate gene clusters. One main difference of both gene clusters refers to the transporter systems.

In detail, group I (citrate cluster I) comprise *L. sakei* TMW 1.3, TMW 1.1322, TMW 1.1396 and TMW 1.1398, and this group carried a Mg^{2+}/citrate complex transporter (CitM) as

transporter. The cluster is structured like described below: In the middle of the cluster CitC ([citrate [pro-3S]-lyase] ligase), CitD (citrate lyase ɣ-chain), CitE (citrate lyase ß-chain), CitF (citrate lyase α-chain) are encoded. Downstream of CitF the genes CitT (Apo-citrate lyase phosphoribosyl-dephospho CoA transferase), oadA (Oxaloacetate decarboxylase) and the transcriptional regulator GntR and CitG (ATP: dephospho-CoA 5'-triphosphoribosyl transferase; EC 2.7.5.25) are carried. Upstream of CitC the transporter CitM, BCCP (Biotin carboxyl carrier protein), oadB (oxaloacetate decarboxylase ß-subunit) and oadC (oxaloacetate decarboxylase ɣ-subunit) are located. Genomic comparison revealed that there are differences between the strains of group I. First in *citF,* encoded in genome of *L. sakei* TMW 1.3, a mutation was identified. The sequence analysis, which was done by smart blast, suggests that this mutation results in a non-functional enzyme.

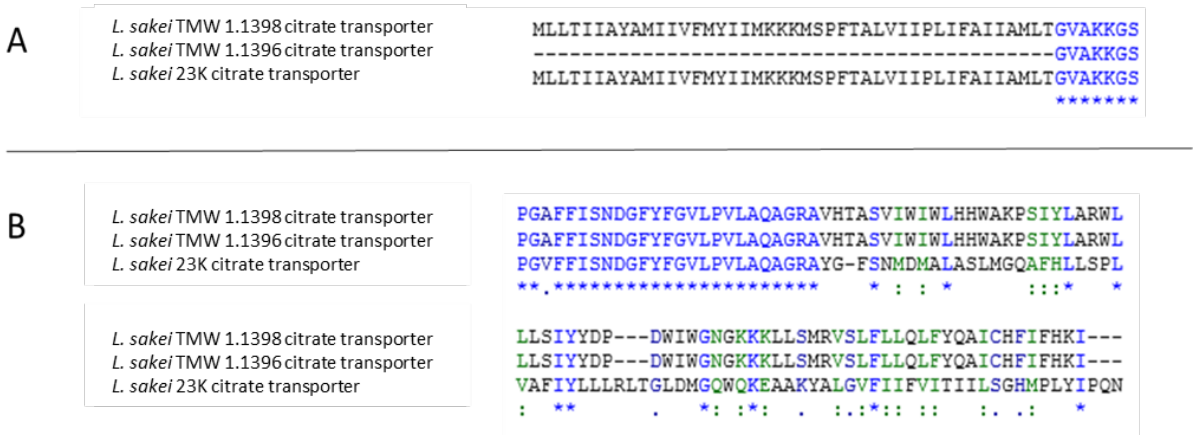

Figure 38: Amino acid sequence comparison of citrate transporter encoded by *L. sakei* TMW 1.1396, TMW 1.1398 and TMW 1.1322 (23K). Differences within the amino acid sequence of citrate transporter could be detect.

Furthermore, mutations were detected within the sequence of transporter CitM of both *L. sakei* TMW 1.1396 and TMW 1.1398. Sequence analysis results revealed that there are stop codons introduced at earlier positions. Comparison of encoded CitM at the genome of *L. sakei* TMW 1.1322 (Figure 38, B) and the CitM genes encoded by *L. sakei* TMW 1.1396 and TMW 1.1398 results in *in silico* prediction that transport function is changed.

Moreover, sequence alignment suggests that sequence of the transporter encoded by *L. sakei* TMW 1.1396 is less long than sequences of the transporters are carried at genome of

L. sakei TMW 1.1322 and TMW 1.1398 (Figure 38, A). The structure of the encoded transporter CitM was verified by the web-based tool TMHMM (Figure 39). The results suggest that transporters encoded by *L. sakei* TMW 1.3 and TMW 1.1322 are identical based on the transmembrane structure. Interestingly, the structure of transporter CitM, encoded in genome of *L sakei* TMW 1.1398, shows differences at amino acid position 266. The same could be observed for transporter of *L. sakei* TMW 1.1396, which shows a shorter sequence compared to the other three ones and the structure looks different at the first 100 amino acids (Figure 39). But overall, the results suggest an intact transmembrane structure, so all transporters should be functional. Nevertheless, the transporter efficiency has to be tested by a phyiological experiment based on *in silico* prediction.

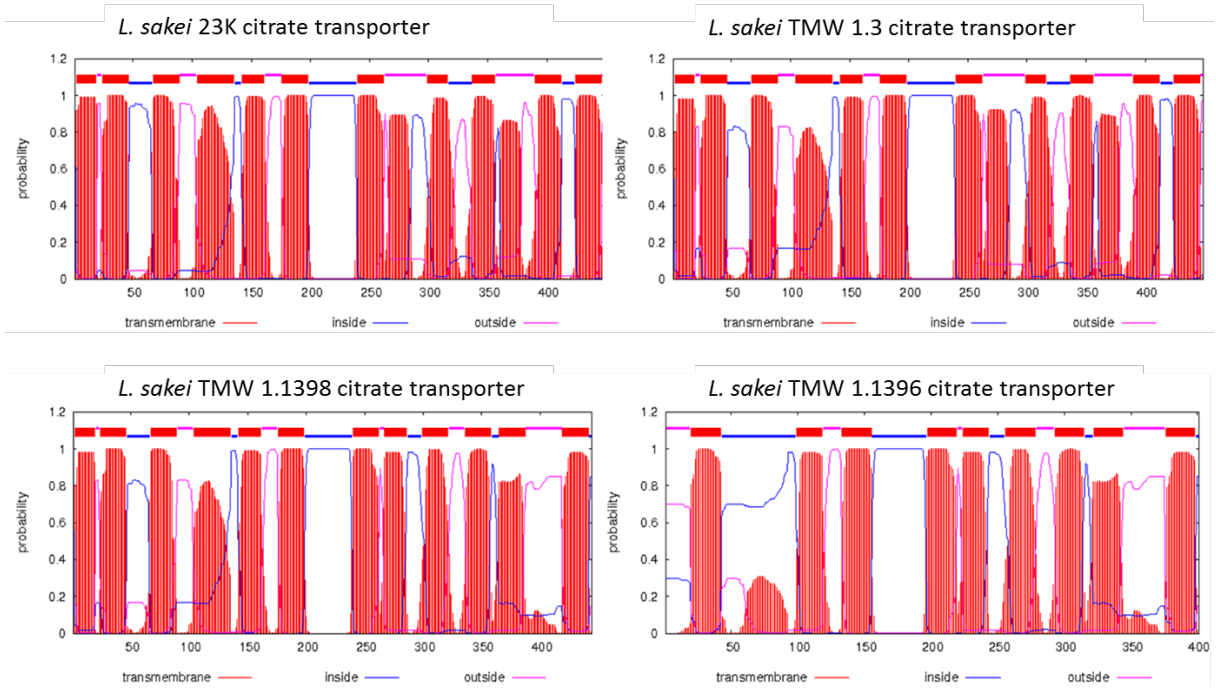

Figure 39: TMHMM analysis of citrate transporter. The structure of citrate transporters revealed differences between compared strains *L. sakei* TMW 1.1322, TMW 1.3, TMW 1.1396 and TMW 1.1398.

Group II encoded a citrate permease (CimH) as transporter (Figure 37). This group includes *L. sakei* TMW 1.46, TMW 1.1189 and TMW 1.1239. The transporter is encoded by the gene *cimH,* which is located upstream of the *citCDEFG* gene cluster. This structure is also different from the structure of citrate cluster I (Figure 37). Upstream of the described genes

citT, citI (encoding citrate lyase transcriptional regulator) and *oadA* are identified. The *citI* gene encoded in the genome of *L. sakei* TMW 1.1239 revealed a shorter sequence of this gene compared to the one of the other strains encoding citrate gene cluster II.

3.7.6 Growth experiments reveals different efficiency of citrate utilization based on genomic differences

The described differences of the two citrate gene clusters, both the two gene clusters and the detected mutations and differences within one describe group, could result in differences in physiology. So, the functionality and efficiency of both citrate gene clusters were verified by physiological tests. Both gene clusters encoded genes, which are associated with the citrate metabolism like it is described and shown in 1.5.2. All strains of *L. sakei* were cultivated in a CDM (citrate, glucose and citrate or glucose as single carbon source), and after 48 h the growth of cultures was verified as well as the metabolic changes of the media was measured by HPLC.

The results suggest that there are differences in the uptake of glucose and citrate. Moreover, the secretion of lactate and acetate, which are products of both citrate metabolism and glycolysis appears to be different (Table 22). Indeed, no differences were detectable if strains were incubated in presence of only citrate. Results suggest that no citrate-uptake could be measured for all strains. Moreover, there were also no differences of glucose-uptake detectable if the strains were incubated in presence of only glucose or glucose in combination with citrate (Table 22). Nevertheless, within the group differences were identified as well as differences between the groups. For group I and group II, which both encoded a citrate gene cluster, a higher acetate concentration was measured in presence of glucose and citrate than in presence of only glucose. This could not be observed for the third group including *L. sakei* TMW 1.114, TMW 1.417 and TMW 1.5787 which encoded no citrate gene cluster. But the results revealed that *L. sakei* TMW 1.3 takes up 9.72% of citrate, simultaneously no significant higher acetate concentration was measureable. For group II also differences of the efficiency of citrate metabolism were detectable. On the one hand, *L. sakei* TMW 1.1396 shows the highest citrate uptake rate with 30.32%. On the other hand,

results suggest that *L. sakei* TMW 1.1239 take up citrate faster and more efficient, because after 48h no citrate was detectable by HPLC. Nevertheless, HPLC results revealed no high differences on production of acetate and lactate for strains of group II. Interestingly, *L. sakei* TMW 1.1189 showed a smaller uptake rate of citrate as well as a lower lactate concentration as product of the metabolisms than the other strains of group II.

Table 22: The concentration of citrate, lactate, acetate and glucose were detected by HPLC. The concentration was determined at time point 0 h (control) and after 48 h of incubation under anaerobic conditions.

		strain	citrate [mM]	acetate [mM]	lactate [mM]	glucose [mM]
citrate		control	8.36 ± 2.19	28.52 ± 4.71	0.00 ± 0.00	0.00 ± 0.00
	no cluster	TMW 1.114	8.55 ± 0.54	28.94 ± 2.47	0.00 ± 0.00	0.00 ± 0.00
		TMW 1.417	7.59 ± 1.16	24.45 ± 2.84	0.00 ± 0.00	0.00 ± 0.00
		TMW 1.578	8.27 ± 0.25	28.35 ± 1.31	0.00 ± 0.00	0.00 ± 0.00
	cluster I	TMW 1.3	8.81 ± 0.72	27.73 ± 0.54	0.00 ± 0.00	0.00 ± 0.00
		23K	8.65 ± 0.62	27.81 ± 0.62	0.00 ± 0.00	0.00 ± 0.00
		TMW 1.1396	7.52 ± 0.11	28.36 ± 0.61	0.00 ± 0.00	0.00 ± 0.00
		TMW 1.1398	6.94 ± 0.64	26.96 ± 3.16	0.00 ± 0.00	0.00 ± 0.00
	cluster II	TMW 1.46	7.78 ± 1.29	25.70 ± 3.78	0.00 ± 0.00	0.00 ± 0.00
		DSM 20017^T	8.28 ± 0.16	27.57 ± 0.36	0.00 ± 0.00	0.00 ± 0.00
		TMW 1.1239	6.43 ± 0.24	28.14 ± 1.72	0.00 ± 0.00	0.00 ± 0.00
glucose		control	0.00 ± 0.00	26.81 ± 4.80	0.00 ± 0.00	19.04 ± 0.98
	no cluster	TMW 1.114	0.00 ± 0.00	27.66 ± 3.81	25.34 ± 11.54	11.74 ± 1.45
		TMW 1.417	0.00 ± 0.00	32.42 ± 1.99	28.75 ± 4.60	11.93 ± 1.42
		TMW 1.578	0.00 ± 0.00	29.46 ± 4.55	29.73 ± 10.55	10.86 ± 1.07
	cluster I	TMW 1.3	0.00 ± 0.00	26.63 ± 4.72	22.45 ± 7.48	12.77 ± 1.47
		23K	0.00 ± 0.00	28.06 ± 3.64	44.20 ± 13.96	6.55 ± 2.04
		TMW 1.1396	0.00 ± 0.00	28.39 ± 4.22	36.15 ± 12.90	9.37 ± 2.46
		TMW 1.1398	0.00 ± 0.00	27.22 ± 4.22	37.97 ± 14.23	8.67 ± 2.85
	cluster II	TMW 1.46	0.00 ± 0.00	28.08 ± 3.34	38.14 ± 21.76	8.23 ± 5.26
		DSM 20017^T	0.00 ± 0.00	29.02 ± 3.02	26.84 ± 9.44	11.15 ± 1.92
		TMW 1.1239	0.00 ± 0.00	28.65 ± 4.13	37.87 ± 19.04	8.99 ± 4.16
citrate + glucose		control	7.85 ± 0.55	24.08 ± 2.40	0.00 ± 0.00	16.86 ± 1.25
	no cluster	TMW 1.114	7.82 ± 0.09	28.10 ± 0.91	26.70 ± 0.74	9.81 ± 0.05
		TMW 1.417	8.83 ± 0.70	28.45 ± 1.54	27.65 ± 1.26	8.66 ± 0.27
		TMW 1.578	7.54 ± 5.90	33.81 ± 6.21	32.91 ± 11.90	8.28 ± 3.19
	cluster I	TMW 1.3	7.72 ± 1.19	24.36 ± 3.70	13.27 ± 2.55	12.46 ± 0.28
		23K	9.13 ± 0.78	30.09 ± 3.06	42.66 ± 5.21	5.86 ± 0.57
		TMW 1.1396	5.83 ± 0.57	31.02 ± 0.94	31.25 ± 0.05	8.78 ± 0.84
		TMW 1.1398	8.05 ± 0.00	32.40 ± 4.50	35.04 ± 12.33	8.48 ± 2.03
	cluster II	TMW 1.46	1.16 ± 0.08	31.11 ± 0.41	40.43 ± 0.50	6.91 ± 0.59
		DSM 20017^T	7.48 ± 0.48	28.73 ± 2.03	17.53 ± 1.56	11.27 ± 2.15
		TMW 1.1239	0.00 ± 0.00	31.27 ± 0.84	38.74 ± 0.68	5.67 ± 0.25

3.7.7 Ribose metabolism

Meat contains another important energy source, which is ribose, a sugar, which is part of the ribonucleotides, and its metabolism results in generation of ATP and pyruvate via glycolysis. So, this metabolism is very important for *L. sakei* and *L. curvatus* in the meat environment like for every other bacteria associated with meat. Genomic comparison revealed that all strains are able to utilize ribose as carbon source, but for *L. curvatus* not all genes, which are associated with the ribose metabolism are part of the core-genome. In detail, there are two ribose transporters detectable at the accessory-genome. Moreover, the structure of both ribose operons (*rbsUDKR* and *rbsRDACBK*) is different. These results enable clustering of the strains in two different groups, like it is shown in Figure 40.

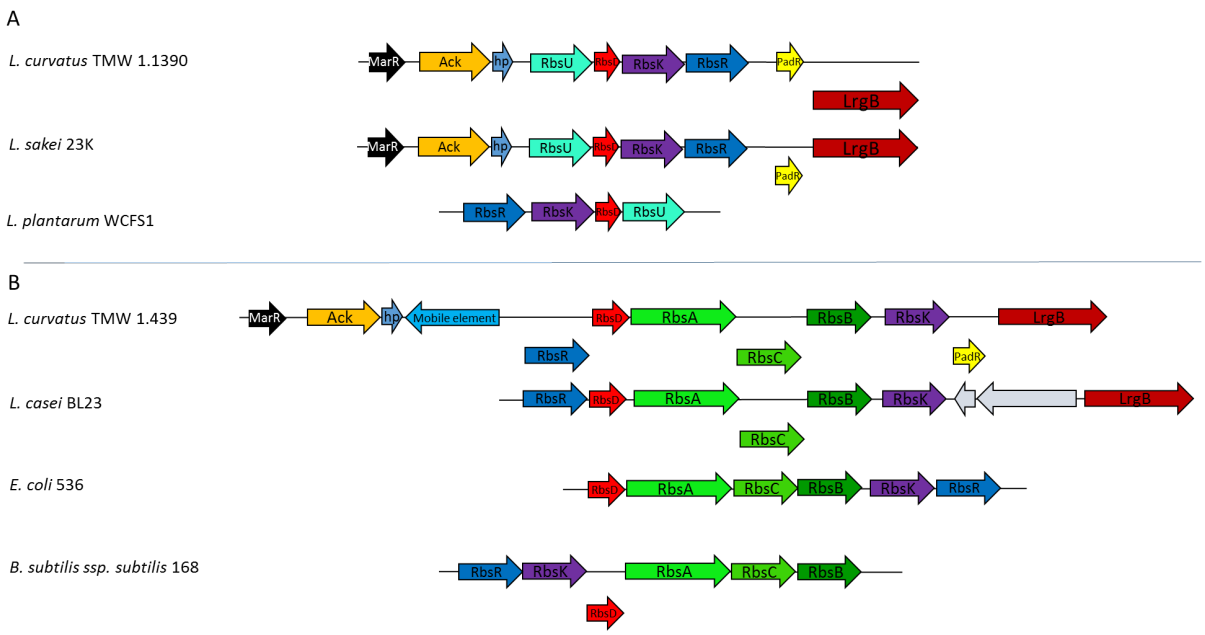

Figure 40: Ribose operon encoded within the accessory-genome of *L. curvatus*. Two different ribose operons are detected at the genomes of sequenced strains of *L. curvatus*.

L. curvatus TMW 1.401, TMW 1.407, TMW 1.421 and TMW 1.1390 forms group I (Figure 40, A). This identified ribose operon is identical with the one which was described by Chaillou *et al.* (Chaillou et al., 2005) for *L. sakei* 23K. *L. curvatus* TMW 1.27, TMW 1.167, TMW 1.439, TMW 1.595, TMW 1.624 and TMW 1.1381, which forms the group II, encoded genes, which are associated with the ribose operon, which was described for *L. casei* BL23 (Figure 40, B)

(Maze et al., 2010). In detail the transporter *rbsACB* was identified and described for *Bacillus subtilis* ssp. *subtilis* and *Escherichia coli* (Stentz & Zagorec, 1999).

The main difference of both identified ribose operons is the transporter system. On the one hand, gene *rbsU* encoded a phosphotransferase transporter system (PTS) and is part of *rbsUDKR* which is encoded by the strains of group I. On the other hand, genes *rbsACB* encoded an ATP binding cassette (ABC) transporter and part of the ribose operon *rbsRDACBK* which was identified at the genome of the strains of group II. Furthermore, both ribose operons are also different based on the gene position of *rbsR*. At the ribose operon *rbsUDKR* the *rbsR* is encoded downstream of the ribose operon (Figure 40, A) and at the *rbsRDACBK* operon the *rbsR* gene is upstream of the operon (Figure 40, B). Moreover, the transcriptional regulator *padR* is downstream of both identified ribose operons. Interestingly, at all other identified ribose operons within the genomes of *L. plantarum, L. casei* and *E. coli* and *B. subtilis* ssp. *subtilis* this regulator is downstream located. Indeed, acetate kinase (*ack*) is encoded downstream of the transcriptional regulator *marR*, and it is upstream encoded of both ribose operons identified in strains of *L. curvatus*. This structure appears to be special and unique for *L. sakei* and *L. curvatus*.

3.7.8 Growth experiment of *L. curvatus* in presence of ribose in CDM

As the genetic differences of both identified ribose operons may influence the efficiency of the utilization of ribose as single carbon source, the metabolic activity and ribose uptake were detected by a growth experiment and HPLC analysis. The strains were cultivated in chemically defined medium (CDM) in presence of ribose as single energy source.

The growth behaviour of two strains, which differs in the ribose operon, was compared (Figure 41): *L. curvatus* TMW 1.624 encoded the ABC transporter system *rbsACB* (Figure 40, B), and *L. curvatus* TMW 1.401, which encoded the ribose PTS *rbsU* (Figure 40, A). Interestingly, for *L. curvatus* TMW 1.401 a higher optical density was measured than for *L. curvatus* TMW 1.624.

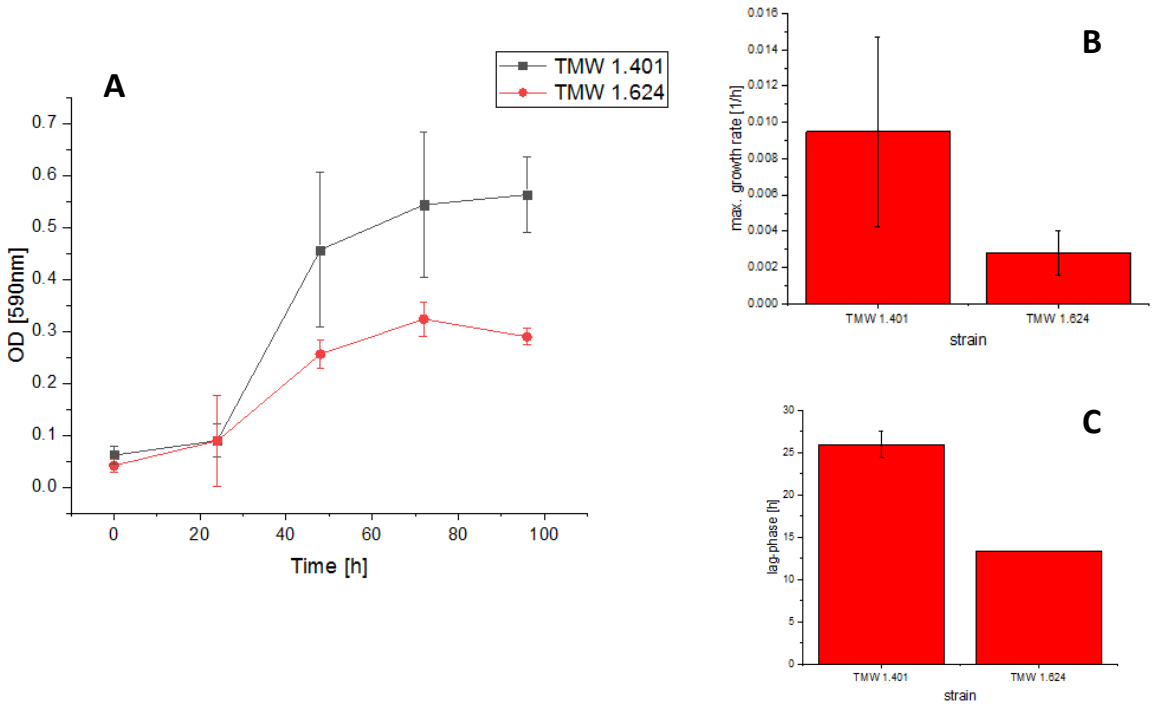

Figure 41: Growth of *L. curvatus* TMW 1.401 and TMW 1.624 in CDM with ribose (A). There are detectable differences between both strains based on growth rate (B) and length of lag-phase (C).

Moreover, for *L. curvatus* TMW 1.401 was a higher growth rate (μ_{max}) (0.009 ± 0.005 h^{-1}) was detected than for *L. curvatus* TMW 1.624 (0.003 ± 0.001 h^{-1}) (Figure 41, B). Nevertheless, for *L. curvatus* TMW 1.624 a shorter lag-phase (20.59 ± 4.3 h) was observed than for *L. curvatus* TMW 1.401 (24.47 ± 0.64) (Figure 41, C). The outcome of this is, that *L. curvatus* TMW 1.624 grow earlier but slower than *L. curvatus* TMW 1.401.

Subsequently, HPLC was used to determine the ribose concentration (25 mM at time point 0 h) during the cultivation of the strains at defined time points (0 h, 24 h, 48 h, 72 h, 96 h). The detected ribose concentrations are depicted for all investigated strains in Figure 42. Indeed, for strains of group I (encoding the PTS) the ribose concentration was decreased to a concentration between 12.79 mM and 4.08 mM after 48 h of cultivation. After 72 h (late exponential growth phase) the ribose concentration decreased to a concentration between 7.51 mM and 1.98 mM and furthermore, the ribose concentration reached a less detectable concentration at stationary phase (96 h).

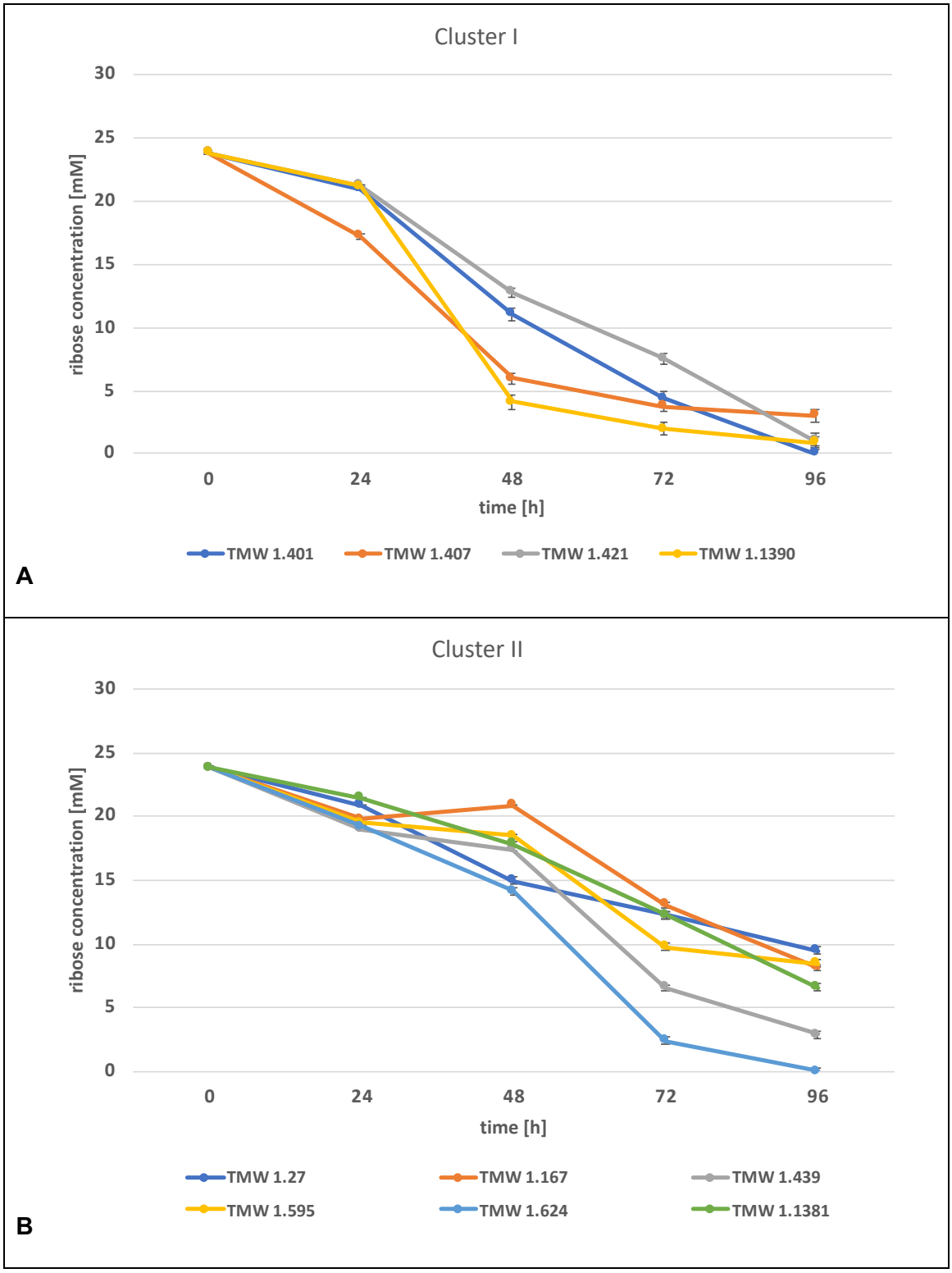

Figure 42: Uptake of ribose by *L. curvatus* strains in CDM. There are differences identified between strains encoding cluster I (A) and strains encoding cluster II (B).

Interestingly, for group II (encoding ABC transporter) the ribose concentration was decreased to a ribose concentration between 20.90 mM and 14.13 mM after 48 h. At late exponential growth phase (72 h) a ribose concentration between 17.84 mM and 2.38 mM was

measurable. Finally, at the stationary (96 h) the concentration of ribose was decreased between 9.48 mM and 0.00 mM.

To conclude, there are differences between both groups based on the ribose uptake. After 48h of cultivation strains of group I take up 50 % to 80 %, whereas strains of group II take up 20 % to 44 % of the presence ribose.

3.8 Adhesion properties / cell wall characteristics

3.8.1 Motility gene cluster

Another important trait is the ability to adhere to different surfaces. The adhesion is influenced by special cell surface properties. Among many others, the flagellin proteins can interact with other surface molecules as they are ranging out wide off the surface. As a consequence, the flagella could enable initial contact and adhesion to special surfaces.

Genomic analysis identified a motility gene cluster within the genome of *L. curvatus* TMW 1.27 and TMW 1.1390, no strain of *L. sakei* encoded a motility gene cluster. A motility gene cluster is encoded by *L. curvatus* TMW 1.27 and TMW 1.1390 and was compared to *L. curvatus* NRIC 0822 (Cousin et al., 2015) (Figure 43).

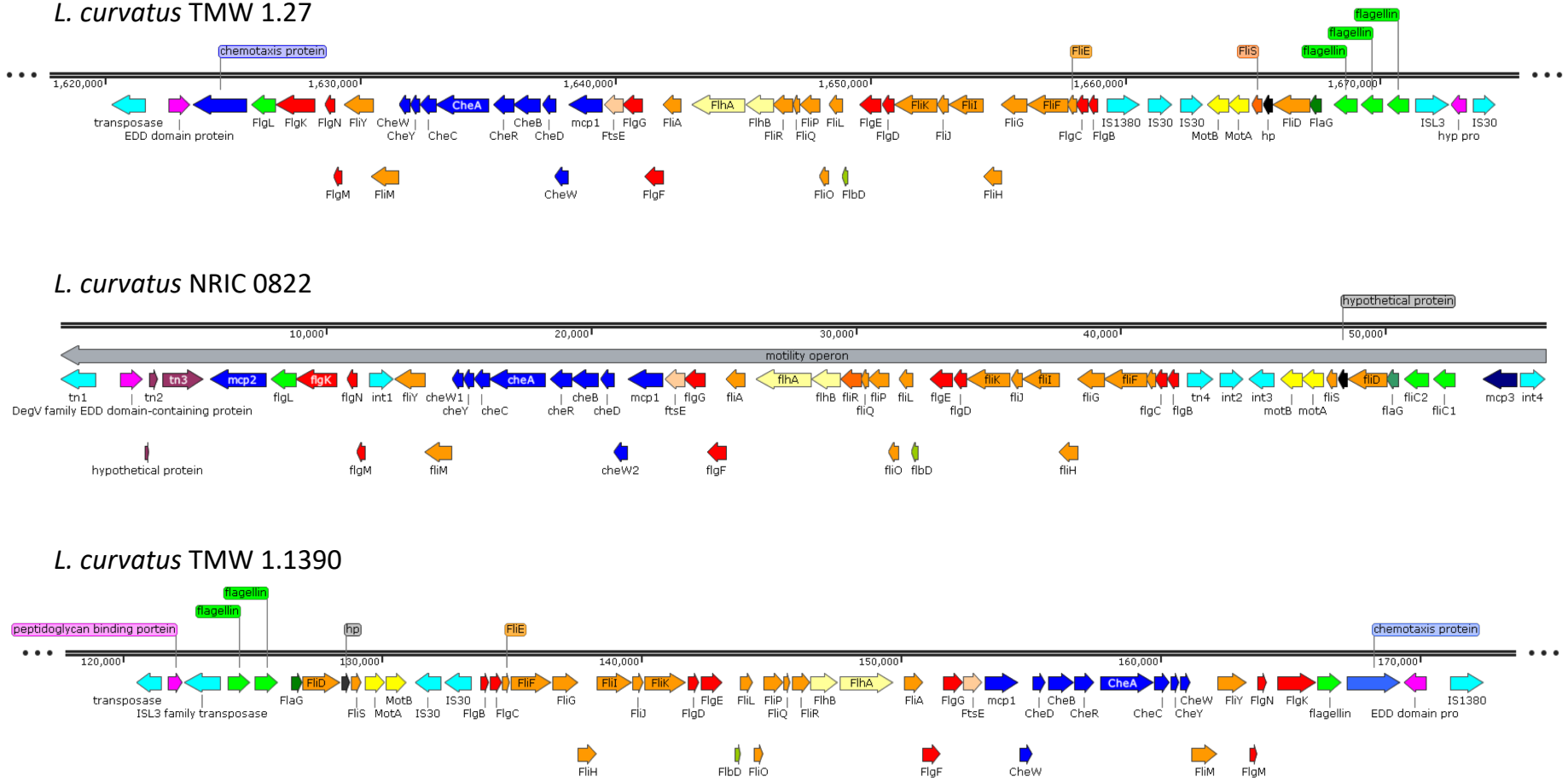

Figure 43: Comparison of motility gene clusters encoded in the genomes of *L. curvatus* TMW1.27 and TMW 1.1390 and *L. curvatus* NRIC 0822.

The structure of the three clusters is closely similar and most of the gene sequences are highly conserved, which means a query cover of 100% and identity of 97% up to 100%. Invertases and transposases are different in structure and position within the gene cluster. In detail, there is no homologous protein of *tn2* and *tn3* gene encoded in the motility gene cluster of *L. curvatus* TMW 1.27 and TMW 1.1390. On the other hand, there are homologous proteins of *int1, tn4* and *int3* gene, but the position within the gene cluster is different.

Indeed, the functional genes are mostly identical in structure and position. Upstream of the *mcp2* gene (*L. curvatus* NRIC 0822), which encodes a methyl-accepting chemotaxis protein, a protein with an EDD domain is encoded. Downstream of the chemotaxis protein gene *flgLKNM* (flagellin protein) and *fliYM,* which encodes the flagellar switch phosphatase/protein, but between both, *int1* is only introduced within the gene cluster of *L. curvatus* NRIC0822. Downstream of *fliYM, cheWYCARBDW*, genes encoded chemotaxis proteins, and *mcp1*, which encodes a methyl-accepting chemotaxis protein, are located. So, these genes formed a genomic region, which is involved in chemotaxis (Figure 44).

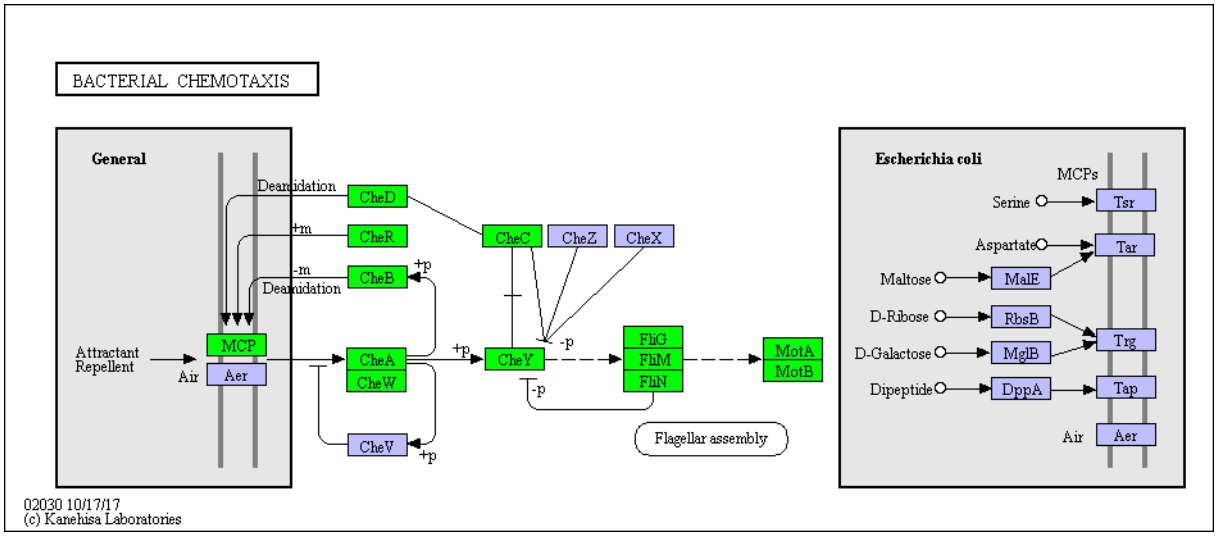

Figure 44: Bacterial chemotaxis encoded by *L. curvatus* TMW 1.27 and TMW 1.1390

Behind *ftsE,* which encodes a protein homologue to the cell division ATP-binding protein, *flgGF,* proteins are encoded, which are associated with flagellar *fliA* (RNA polymerase, σ-factor) and *flhAB*, which encode proteins associated with EscV-YscV-HrcV family type III

secretion system export apparatus (switch) protein. Downstream of the *fliR* gene, which encodes a flagellar biosynthetic protein, is located, which is diverse in all three strains. Afterwards *fliQ*, encoding a EscV-YscV-HrcV family type III secretion system export apparatus protein, *fliPOL,* which encode flagellar biosynthetic proteins, *flbD* (endoflagellar protein)*, flgED,* which encode flagellar basal-body rod proteins, *fliK* (flagellar hook-length control protein), *fliJ* (flagellar protein), *fliI* (EscN-YscN-HrcN family type III secretion system ATPase) *fliH* (flagellar assembly protein), *fliG* (flagellar motor switch protein), *fliF* (flagellar M-ring protein), *fliE* (flagellar hook-basal body protein) and *flgC* (flagellar basal-body rod protein) are encoded and these genes are highly conserved. Downstream of these genes ther *flgB* gene (flagellar basal-body rod protein) is located, which reflects differences based on the amino acid sequence. Downstream of gene *flgB* mobile elements, like transposases and integrases, which are highly diverse between all three gene-clusters of the three strains, are encoded. The following part concluding *motBA* is highly conserved and encodes chemotaxis proteins. The following gene *fliS*, which encodes a flagellar protein, is highly conserved between *L. curvatus* TMW 1.1390 and NRIC0822, but it appears diverse compared to the sequence of *L. curvatus* TMW 1.27. Downstream of *fliS* and upstream of *fliD* (flagellar hook-associated protein) a predicted gene with unknown function (hypothetical protein) is encoded. The sequence of this gene is highly conserved. At the final end of the gene cluster *flaG, fliC1C2, mcp3* and *int4* genes are encoded. In detail *flaG* is highly conserved and encoded a flagellar protein, whereas *fliC1C2* genes, which encoded flagellin, are diverse and *mcp3* of *L. curvatus* NRIC 0822 is similar to *mcp1* and *mcp2* of *L. curvatus* TMW 1.27 and 1.1390.

To conclude, *L. curvatus* TMW 1.27 and TMW 1.1390 encodes a motility gene cluster, which is complete and should enable the synthesis and secretion of a flagellar based on genomic properties. The encoded genes are remarked green in Figure 45.

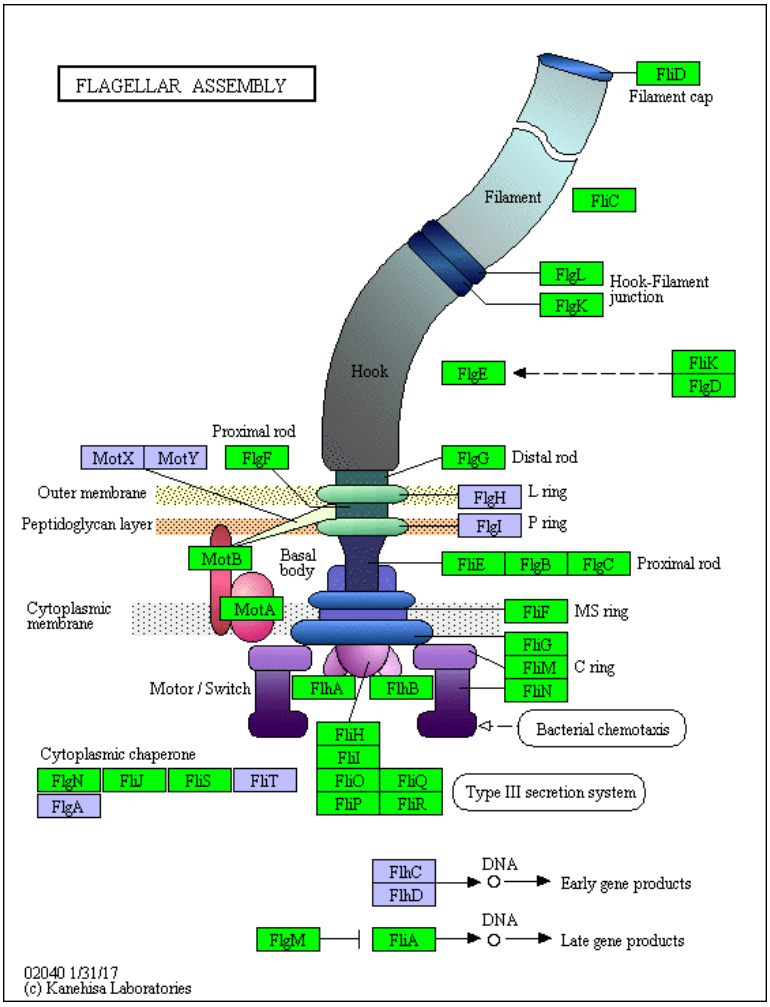

Figure 45: Flagellar assembly by KEGG. Green marks encoded genes, which associated with components of flagellar encoded by *L. curvatus* TMW 1.27 and TMW 1.1390.

The functionality of the motility gene cluster was investigated by a motility agar assay, the results of which are shown in Figure 46. Different conditions were tested like 15°C, 20°C and 30°C and in presence of glucose, glycogen, ribose or no carbon source. The results reflect differences between *L. curvatus* TMW 1.27, TMW 1.1390, whose genomes encode a motility gene cluster, and the genomically closely related *L. curvatus* TMW 1.401, which does not encode a motility gene cluster. First of all, *L. curvatus* TMW 1.401 shows no motility under all conditions. At 30°C *L. curvatus* TMW 1.27 and TMW 1.1390 shows motility in presence of all sugars and in absence of any carbon source. But, upon incubation at 20°C differences were detectable. *L. curvatus* TMW 1.27 shows weak motility in presence of glycogen and in absence of any carbon source. Whereas, in presence of ribose and glucose motility was detectable. In contrast, *L. curvatus* TMW 1.1390 revealed weak/less motility in presence of

glucose, glycogen and in absence of any carbon source. At 15°C no motility could be observed for all tested strains.

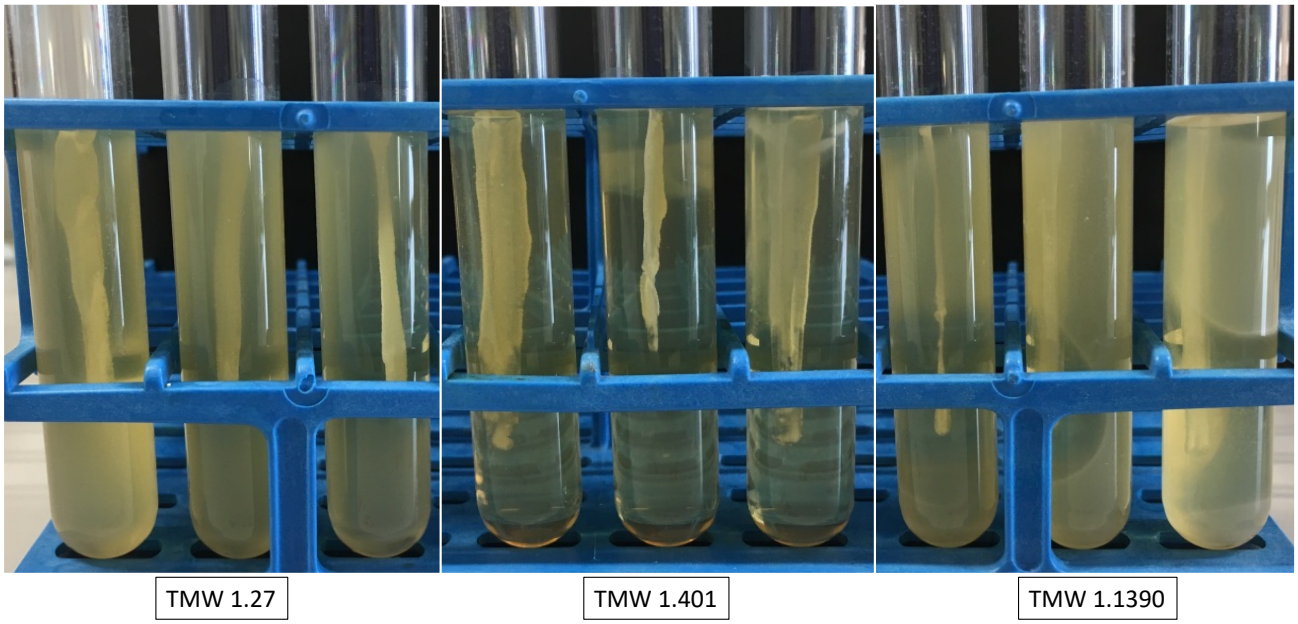

Figure 46: Motility assay of *L. curvatus* TMW 1.27, TMW 1.1390 and TMW 1.401 (negative control). Strains were incubated in cfMRS with glucose at 30°C.

Adhesion characteristics of *L. curvatus* TMW 1.27 and TMW 1.1390 were tested in comparison with *L. curvatus* TMW 1.401, which was shown to be not motile. The results are shown in Figures 47 and 48.

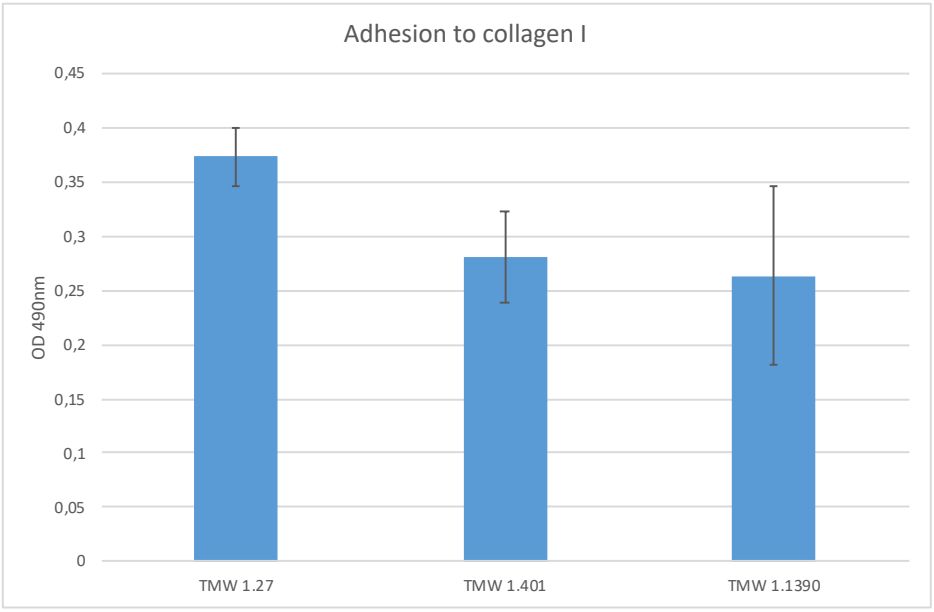

Figure 47: Adhesion to collagen I was tested. *L. curvatus* TMW 1.27 and TMW 1.1390, which encoded the motility gene cluster, were compared to *L. curvatus* TMW 1.401, which was used as negative control.

The adhesion to collagen I suggest that *L. curvatus* TMW 1.27 is able to adhere more efficiently to collagen I compared to *L. curvatus* TMW 1.1390, which has a flagellar gene cluster and appears to be motile, and TMW 1.401, which has no flagellar gene cluster and no motility.

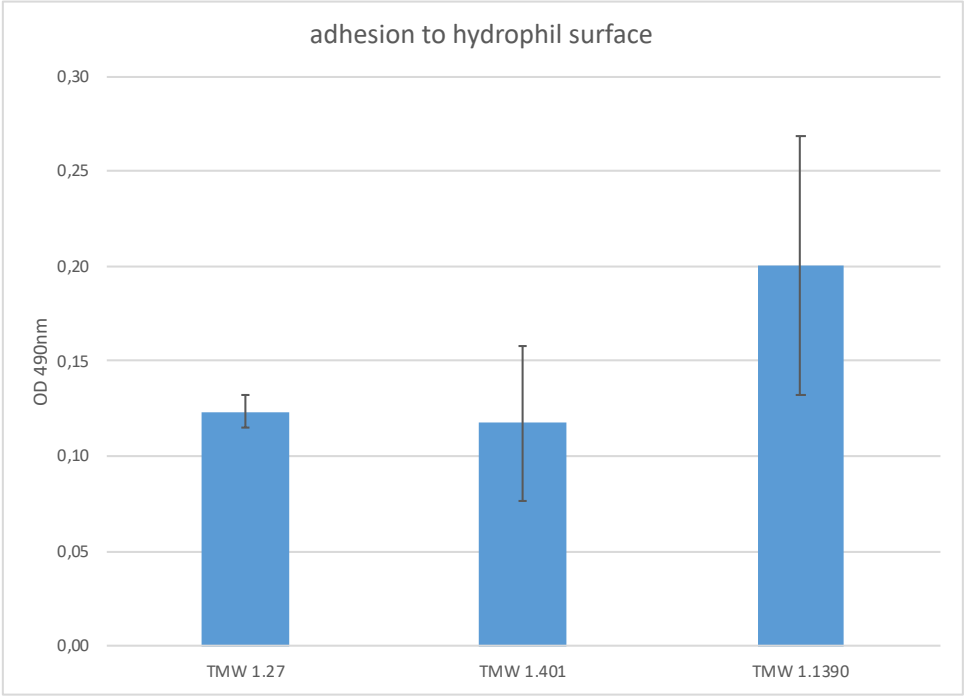

Figure 48: Adhesion to a hydrophilic surface. *L. curvatus* TMW 1.27 and TMW 1.1390, which encoded the motility gene cluster are compared to *L. curvatus* TMW 1.401 which was used as negative control.

Furthermore, the adhesion to a hydrophilic surface was tested. The results suggest that *L. curvatus* TMW 1.1390 is able to adhere to a hydrohpilic surface more efficiently than *L. curvatus* TMW 1.27 and TMW 1.401. Indeed, it was shown that *L. curvatus* TMW 1.1390 cell surface appears to be 100% hydrophilic, whereas the cell surfaces of *L. curvatus* TMW 1.27 and TMW 1.401 are less hydrophilic (~90%) (oral description by Janßen).

3.8.2 EPS gene cluster

Exopolysaccharides (EPS) can be important surface characteristics of bacteria because these structures or the enzymes producing them can influence the adhesion to surfaces like meat and they could be part of a stress response strategy like acid, cold or oxidative stress. EPS-mediated surface adhesion could be mediated by capsule-forming β-glucans or heteropolysaccharides (HePS) as well as surface-displayed glycosyltransferases producing homopolysaccharides (HoPS) from sucrose. Therefore, respective gtf genes encoding gylcosyltransferases and HePS genomic gene clusters were characterized in strains of *L. sakei* and *L. curvatus*. Basically, HePS formation overlaps with cell wall biosynthesis in the undecaprenyl-carrier molecule, which acts as anchor for the growing repeating unit of the HePS. The major difference lies in the use of dTTP-rhamnose, which is a frequent component of HePS, as well as an array of different glycosyltransferases and the flippase transporter.

The genomic comparison based on RAST annotation revealed that the strains of both species are different based on the genetic properties associated with cell wall and capsule, like it is listed Table 23.

Table 23: List of genomic comparison of genes involved in “cell wall characteristics” (here: HePS biosynthesis) based on RAST annotation identified at the genome of strains of *L. sakei*.

	TMW 1.3	TMW 1.46	TMW 1.114	TMW 1.417	TMW 1.578	TMW 1.1189	TMW 1.1239	TMW 1.1322	TMW 1.1396	TMW 1.1398
Cell Wall and capsule										
Capsular and extracellular polysacchraides										
dTDP-rhamnose synthesis										
dTDP-4-dehydrorhamnose reductase (EC +.+.+.+33)	-	-	+	-	+	-	+	-	-	+
dTDP-glucose 4,6-dehydratase (EC 4.2.+.46)	-	-	+	-	+	+	+	-	-	+
dTDP-rhamnosyl transferase RfbF (EC 2.-.-.-)	-	-	+	-	+	-	-	-	-	-
dTDP-4-dehydrorhamnose 3,5-epimerase (EC 5.+.3.+3)	-	-	+	-	+	-	+	-	-	+
Glucose-+-phosphate thymidylyltransferase (EC 2.7.7.24)	-	-	+	-	+	+	+	-	-	+
Rhamnose containing glycans										
UDP-glucose 4-epimerase (EC 5.+.3.2)	-	-	+	-	+	+	+	-	-	+
dTDP-4-dehydrorhamnose reductase (EC +.+.+.+33)	-	-	+	-	+	-	+	-	-	+
Alpha-L-Rha alpha-+,3-L-rhamnosyltransferase (EC 2.4.+.-)	-	-	-	-	-	-	+	-	-	-
dTDP-glucose 4,6-dehydratase (EC 4.2.+.46)	-	-	+	-	+	+	+	-	-	+
dTDP-4-dehydrorhamnose 3,5-epimerase (EC 5.+.3.+3)	-	-	+	-	+	-	+	-	-	+
Glycerol-3-phosphate cytidylyltransferase (EC 2.7.7.39)	-	-	+	-	+	+	+	-	-	+
Glucose-+-phosphate thymidylyltransferase (EC 2.7.7.24)	-	-	+	-	+	+	+	-	-	+
Exoplysaccharide Biosynthesis										
Exopolysaccharide biosynthesis glycosyltransferase EpsF (EC 2.4.+.-)	+	+	+	-	+	-	-	-	-	-
Manganese-dependent protein-tyrosine phosphatase (EC 3.+.3.48)	-	-	+	-	+	-	-	-	-	-
Glycosyl transferase, group 2 family protein	-	-	+	-	+	+	-	-	-	-
Tyrosine-protein kinase transmembrane modulator EpsC	+	+	+	+	+	+	-	+	+	+
Tyrosine-protein kinase EpsD (EC 2.7.+0.2)	+	+	+	+	+	+	-	+	+	+
Undecaprenyl-phosphate galactosephosphotransferase (EC 2.7.8.6)	+	+	+	+	+	+	-	+	+	+

The genomes of *L. sakei* strains TMW 1.114, TMW 1.578, TMW 1.1189, TMW 1.1239 and TMW 1.1398 encode genes, which are associated with capsular and extracellular polysaccharides, namely rhamnose-containing HePS. However, in *L. sakei* TMW 1.1239 and TMW 1.1398 the dTDP-rhamnosyl transferase RfbF, and *L. sakei* TMW 1.114, TMW 1.578 and TMW 1.1398 lack alpha-L-Rha alpha-+,3-L-rhamnosyltransferase. Other strains, e.g., TMW 1.1189 lack several enzymes of this pathway, or do not contain any of these TMW 1.3, TMW 1.46, TMW 1.417, TMW 1.1322, TMW 1.1396.

Finally, the RAST annotation revealed differences in the HePS biosynthesis listed as "Exopolysaccharide Biosynthesis" in Table 23. *L. sakei* TMW 1.1239 did not encode any of these genes, while *L. sakei* TMW 1.114 and TMW 1.578 all of them. The other strains only had some of these.

Taken together, for *L. sakei* TMW 1.114 and TMW 1.578 a complete EPS gene cluster were identified, which is shown for *L. sakei* TMW 1.114 in Figure 49, and are predicted to form a capsular HePS.

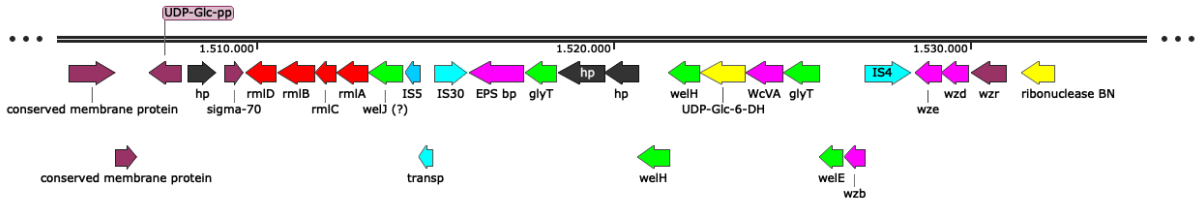

Figure 49: HePS gene cluster of *L. sakei* TMW 1.114.

The gene cluster include *rmlABCD*, which encoded dTDP-glucose pyrophosphorylase (*rmlA*), dTDP-glucose 4,6-dehydratase (*rmlB*), TDP-6-deoxy-D-xylo-4-hexulose-3,5-epimerase (*rmlC*), and NADPH:TDP-6-deoxy-D-xylo-4-hexulase-4-reductase (*rmlD*). These encoded enzymes catalyzed reactions, which are involved in the conversion of glucose-1-phosphate to dTDP-rhamnose, and the intermediates dTDP-glucose and TDP-4-keto-6-deoxy-hexulose. dTDP-rhamnose is part of the cell wall associated EPS biosynthesis and a component of the final EPS like UDP-glucose and UDP-galactose.

The RAST annotation revealed that strains of *L. curvatus* are different based on the genomic properties associated with cell wall and capsule, like it is listed in Table 24.

Table 24: List of genomic comparison of genes involved in “cell wall characteristics” (here: HePS biosynthesis) based on RAST annotation identified at the genome of strains of *L. curvatus*.

	TMW 1.27	TMW 1.167	TMW 1.401	TMW 1.407	TMW 1.421	TMW 1.439	TMW 1.595	TMW 1.624	TMW 1.1381	TMW 1.1390
Cell Wall and capsule										
Capsular and extracellular polysacchraides										
dTDP-rhamnose synthesis										
dTDP-4-dehydrorhamnose reductase (EC 1.1.1.133)	+	+	+	-	+	+	-	-	+	+
dTDP-glucose 4,6-dehydratase (EC 4.2.1.46)	+	+	+	-	+	+	-	-	+	+
dTDP-rhamnosyl transferase RfbF (EC 2.-.-.-)	-	-	-	-	-	-	-	-	-	-
dTDP-4-dehydrorhamnose 3,5-epimerase (EC 5.1.3.13)	+	+	+	-	+	+	-	-	+	+
Glucose-1-phosphate thymidylyltransferase (EC 2.7.7.24)	+	+	+	-	+	+	-	-	+	+
Phosphorylcholine incorporation in LPS										
Choline permease LicB	-	+	-	-	-	+	-	-	+	-
Choline kinase (EC 2.7.1.32)	-	+	-	-	-	+	-	-	+	-
Cholinephosphate cytidylyltransferase (EC 2.7.7.15)	-	+	-	-	-	+	-	-	+	-
Polysaccharide deacetylases										
Peptidoglycan N-acetylglucosamine deacetylase (EC 3.5.1.-)	-	-	-	-	+	-	-	-	-	-
Rhamnose containing glycans										
UDP-glucose 4-epimerase (EC 5.1.3.2)	+	+	+	-	+	+	-	-	+	+
dTDP-4-dehydrorhamnose reductase (EC 1.1.1.133)	+	+	+	-	+	+	-	-	+	+
Alpha-L-Rha alpha-1,3-L-rhamnosyltransferase (EC 2.4.1.-)	+	+	+	-	+	+	-	-	+	+
dTDP-glucose 4,6-dehydratase (EC 4.2.1.46)	+	+	+	-	+	+	-	-	+	+
dTDP-4-dehydrorhamnose 3,5-epimerase (EC 5.1.3.13)	+	+	+	-	+	+	-	-	+	+
Alpha-D-GlcNAc alpha-1,2-L-rhamnosyltransferase (EC 2.4.1.-)	+	-	-	-	-	-	-	-	-	+
capsular polysaccharide biosynthesis protein	-	+	-	-	-	-	-	-	+	-
Glycerol-3-phosphate cytidylyltransferase (EC 2.7.7.39)	-	-	+	-	-	-	-	-	-	-
Glucose-1-phosphate thymidylyltransferase (EC 2.7.7.24)	+	+	+	-	+	+	-	-	+	+

	TMW 1.27	TMW 1.167	TMW 1.401	TMW 1.407	TMW 1.421	TMW 1.439	TMW 1.595	TMW 1.624	TMW 1.1381	TMW 1.1390
Exoplysaccharide Biosynthesis										
Exopolysaccharide biosynthesis glycosyltransferase EpsF (EC 2.4.1.-)	-	-	-	-	-	-	-	-	-	-
Manganese-dependent protein-tyrosine phosphatase (EC 3.1.3.48)	-	-	-	-	-	-	-	-	-	-
Glycosyl transferase, group 2 family protein	-	+	-	-	-	-	-	-	-	-
Tyrosine-protein kinase transmembrane modulator EpsC	+	+	+	+	+	+	+	+	+	+
Tyrosine-protein kinase EpsD (EC 2.7.10.2)	+	+	+	+	+	+	+	+	+	+
Undecaprenyl-phosphate galactosephosphotransferase (EC 2.7.8.6)	+	+	+	+	+	+	+	+	+	+
Lipopolysaccharide cholinephosphotransferase LicD3 (EC 2.7.8.-)	-	-	-	+	-	-	-	-	-	-
Glycosyl transferase, group 1 family protein	-	-	-	-	-	+	-	-	+	-

First, there are strains encoded genes which associated with the dTDP-rhamnose synthesis. *L. curvatus* TMW 1.27, TMW 1.167, TMW 1.401, TMW 1.421, TMW 1.439, TMW 1.1381 and TMW 1.1390 encoded dTDP-4-dehydrorhamnose reductase, dTDP-glucose-4,6-dehydratase, dTDP-4-dehydrorhamnose-3,5-epimerase and glucose-1-phosphate thymidylyltransferase. Interestingly, the dTDP-rhamnosyl transferase RfbF is not encoded by the *L. curvatus* strains, but it was identified in genomes of a few strains of *L. sakei*. Genomic data revealed that *L. curvatus* TMW 1.167, TMW 1.439 and TMW 1.1398 encode choline permease LicB, choline kinase and cholinephosphate cytidylyltransferase. Moreover, *L. curvatus* TMW 1.421 encoded the peptidoglycan N-acetylglucosamine deacetylase, which appears to be strain specific. However, genes, which are associated with the rhamnose containing glycans are part of the accessory-genome, so *L. curvatus* TMW 1.407, TMW 1.595 and TMW 1.624 do not encoded any genes of this category. On the other hand, *L. curvatus* TMW 1.27, TMW 1.167, TMW 1.401, TMW 1.421, TMW 1.439, TMW 1.1381 and TMW 1.1390 encoded UDP-glucose-4-epimerase, dTDP-4-dehydrorhamnose reductase, α-L—Rha α-1,3-L-rhamnosyltransferase, dTDP-glucose 4,6-dehydratase, dTDP-4-dehydrorhamnose 3,5-epimerase and glucose-1-phosphate thymidylyltransferase. *L. curvatus* TMW 1.27 and TMW 1.1390 encoded α-D-GlcNAc α-1,2-L-rhamnosyltransferase. Furthermore, *L. curvatus* TMW 1.167 and TMW 1.1381 encoded a capsular polysaccharide biosynthesis protein. *L. curvatus* TMW 1.401 encoded glycerol-3-phosphate cytidylyltransferase, which appears to be a strain specific gene.

Above the rhamnosyl biosynthetic pathways, genes were identified, which are involved in HePS biosynthesis. Tyrosine-protein kinase transmembrane modulator EpsC, tyrosine-protein kinase EpsD and undecaprenyl-phosphate galactosephosphotransferase is part of the core-genome of *L. curvatus*. On the other hand, *L. curvatus* TMW 1.439 and TMW 1.1381 encoded a glycosyl transferase (group 1 family protein). Furthermore, *L. curvatus* TMW 1.167 encoded a glycosyl transferase (group 2 family protein) and *L. curvatus* TMW 1.407 encoded a lipopolysaccharide cholinephosphotransferase. Both genes appear to be strain specific.

Genomic analysis based on NCBI annotation enables a more detailed analysis of the gene clusters or genes, which are involved in cell wall and capsular synthesis. *L. curvatus* strains encoded genes, which are associated with EPS biosynthesis (Figure 50). But the genes *rmlABCD* are not part of the core-genome of *L. curvatus*. Actually, *rmlB* is part of the core-genome, whereas *rmlA, rmlC* and *rmlD* are only encoded by *L. curvatus* TMW 1.167, TMW 1.401, TMW 1.421, TMW 1.439, TMW 1.1381 and TMW 1.1390. Moreover, *L. curvatus* TMW 1.27 encodes *rmlD*.

To conclude, *L. curvatus* TMW 1.167, TMW 1.401, TMW 1.421, TMW 1.439, TMW 1.1381 and TMW 1.1390 encode complete genes *rmlABCD*, which are involved in the biosynthesis of dTDP-rhamnose, which is associated with the cell wall EPS biosynthesis and part of the EPS build with UDP-glucose and UDP-galactose and are predicted to produce a capsular HePS.

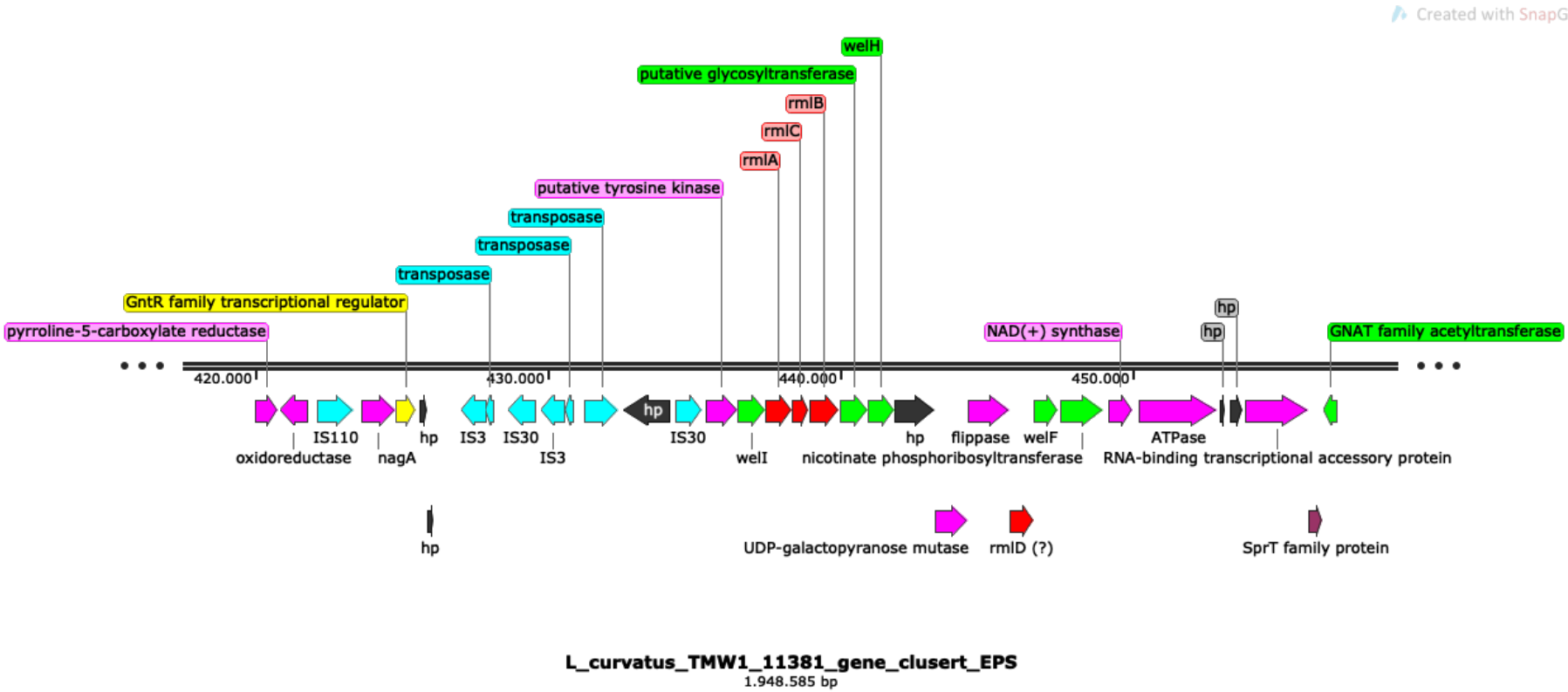

Figure 50: EPS gene cluster in genome of *L. curvatus* TMW 1.1381. This gene cluster was also found in *L. curvatus* 1.167, TMW 1.421 and 1.439.

3.8.3 EPS production in presence of sucrose

HoPS production from sucrose frlies on a cell wall-bound Gtf, which mostly has been found on small plasmids (R. M. Prechtl et al., 2018). These, however, are lost in the SMART sequencing procedure as a result of size selection of fragments before sequencing. Therefore, the HoPS production of *L. sakei* and *L. curvatus* strains was tested physiologically in presence of sucrose. Production of EPS could affect behavior in meat, the assertiveness in the meat environment or stress tolerance. The production of dextran was shown by a plate assay, like it is shown in Figure 51. As positive control the well described strain *L. sakei* TMW 1.411 was used. The results are listed in Table 25.

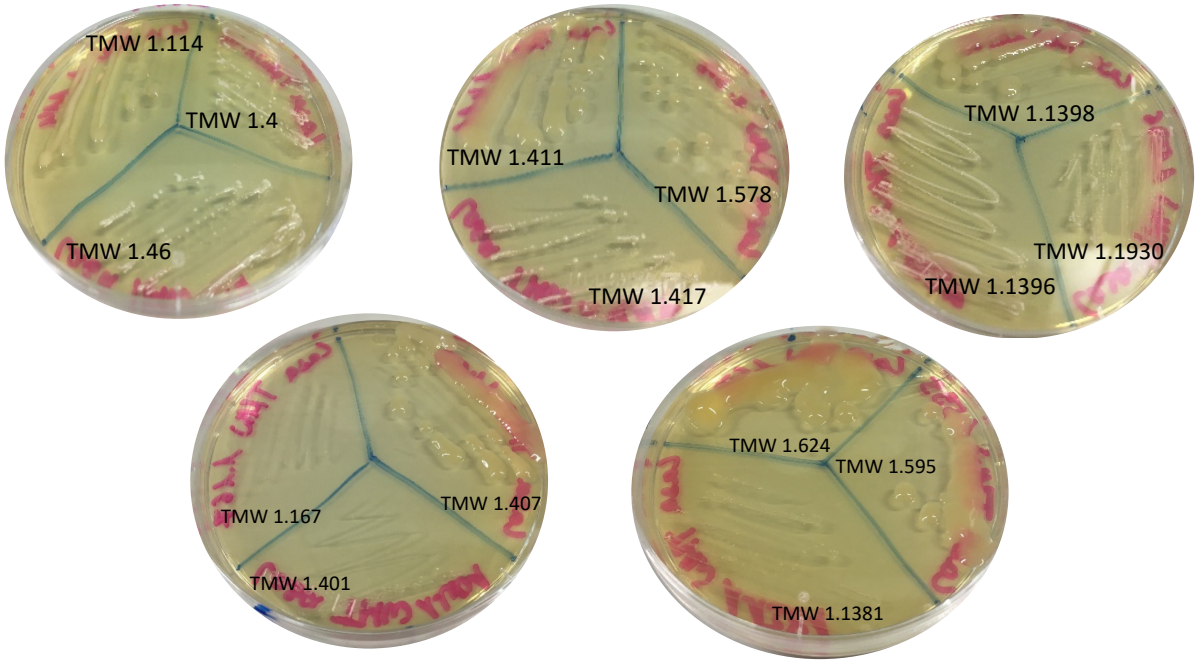

Figure 51: HoPS production plate assay with strains of *L. curvatus* and *L. sakei*.

Table 25: HoPS production of the genome sequenced strains was tested by a plate assay. HoPS producer in presence of sucrose are remark with "+" and "-" remark that strains are not able to produce HoPS.

Lactobacillus sakei	**HoPS producer**	***Lactobacillus curvatus***	**HoPS producer**
TMW 1.3	-	TMW 1.27	-
TMW 1.46	-	TMW 1.167	-
TMW 1.114	+	TMW 1.401	-
TMW 1.417	-	TMW 1.407	+
TMW 1.578	+	TMW 1.421	-
TMW 1.1189	-	TMW 1.439	-
TMW 1.1239	-	TMW 1.595	+
TMW 1.1322	-	TMW 1.624	+
TMW 1.1396	-	TMW 1.1381	-
TMW 1.1398	+	TMW 1.1390	-

The results suggest that *L. sakei* TMW 1.114, TMW 1.578 and TMW 1.1398 as well as *L. curvatus* TMW 1.407, TMW 1.595 and TMW 1.624 are able to produce EPS in presence of sucrose.

3.8.4 Adhesion to different surfaces

For the adaptation to the meat environment, it is important for a bacterium to adhere to meat surface and possibly form a biofilm, which allows persistence on a meat surface.

Therefore, the biofilm formation and adherence to a hydrophobic surface was investigated. The results are shown in Figure 52 and Figure 53. Strains of both species *L. sakei* and *L. curvatus* show no significant differences. Nevertheless, *L. sakei* TMW 1.1189 shows the highest ability to adhere to a hydrophobic surface upon growth in MRS. *L. curvatus* TMW 1.624 showed adherence to all three surface types. It is the only strain of the species, which shows a detectable adhesion to a hydrophobic surface after growing in MRS with sucrose. Interestingly, under this condition *L. curvatus* TMW 1.624 showed HoPS production.

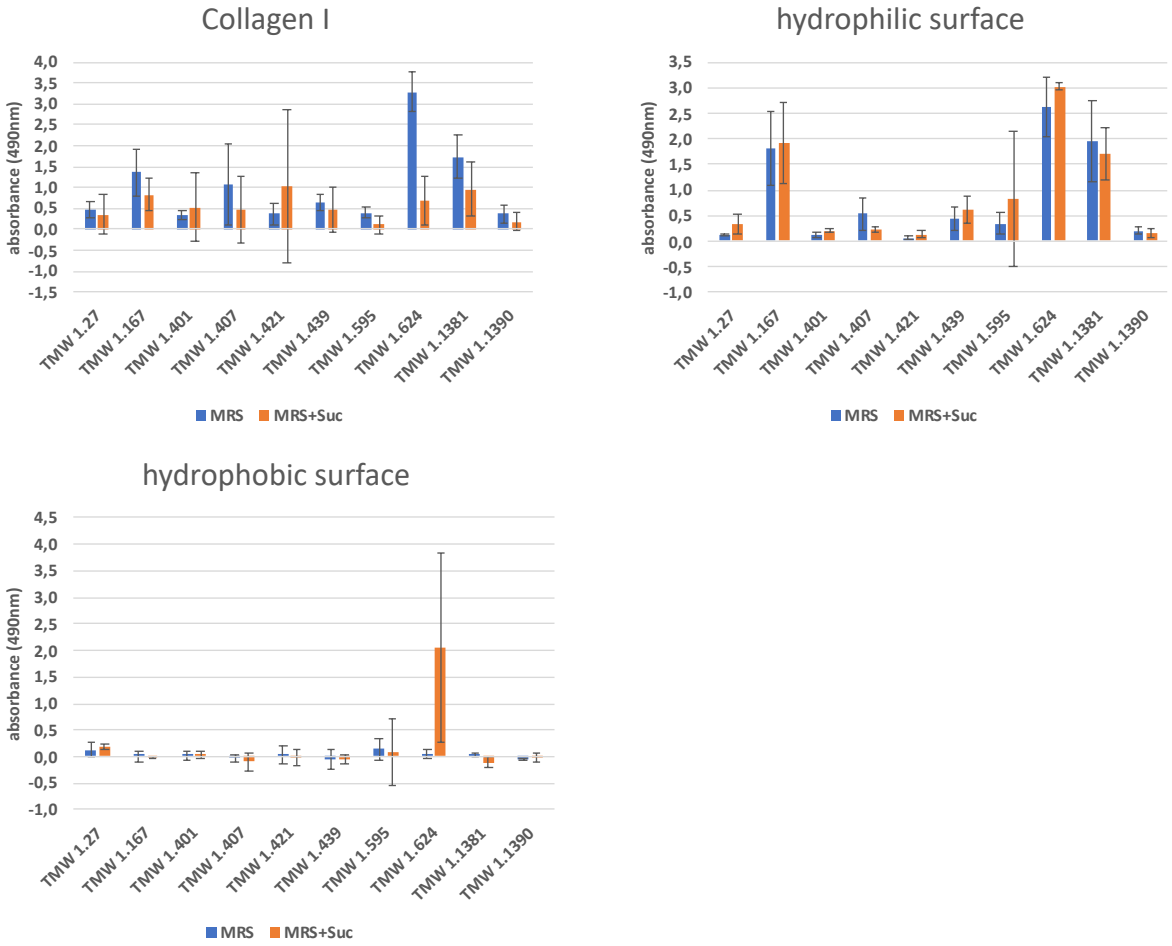

Figure 52: Adhesion of *L. curvatus* strains to different surfaces like hydrophobic, hydrophilic surface or collagen I.

The adhesion to a hydrophilic surface was shown in another experiment. The results are not significant based on statistical analysis (Figure 52 and Figure 53). For *L. sakei* TMW 1.114, TMW 1.1239, TMW 1.1396 and TMW 1.1398 an adhesion to hydrophilic surface could be detected. Moreover, *L. curvatus* TMW 1.167, TMW 1.624 and TMW 1.1381 are suggested to adher to a hydrophobic surface.

Finally, the adhesion to collagen I was investigated. The adhesion characteristics of *L. sakei* strains is not significant different, but it appears that *L. sakei* TMW 1.46, TMW 1.417 and TMW 1.1189 are able to adhere to collagen I. *L. curvatus* strains are different compared to strains of *L. sakei*. The results of the adhesion assay revealed that *L. curvatus* TMW 1.167, TMW 1.407, TMW 1.624 and TMW 1.1381 show an adhesion to collagen I.

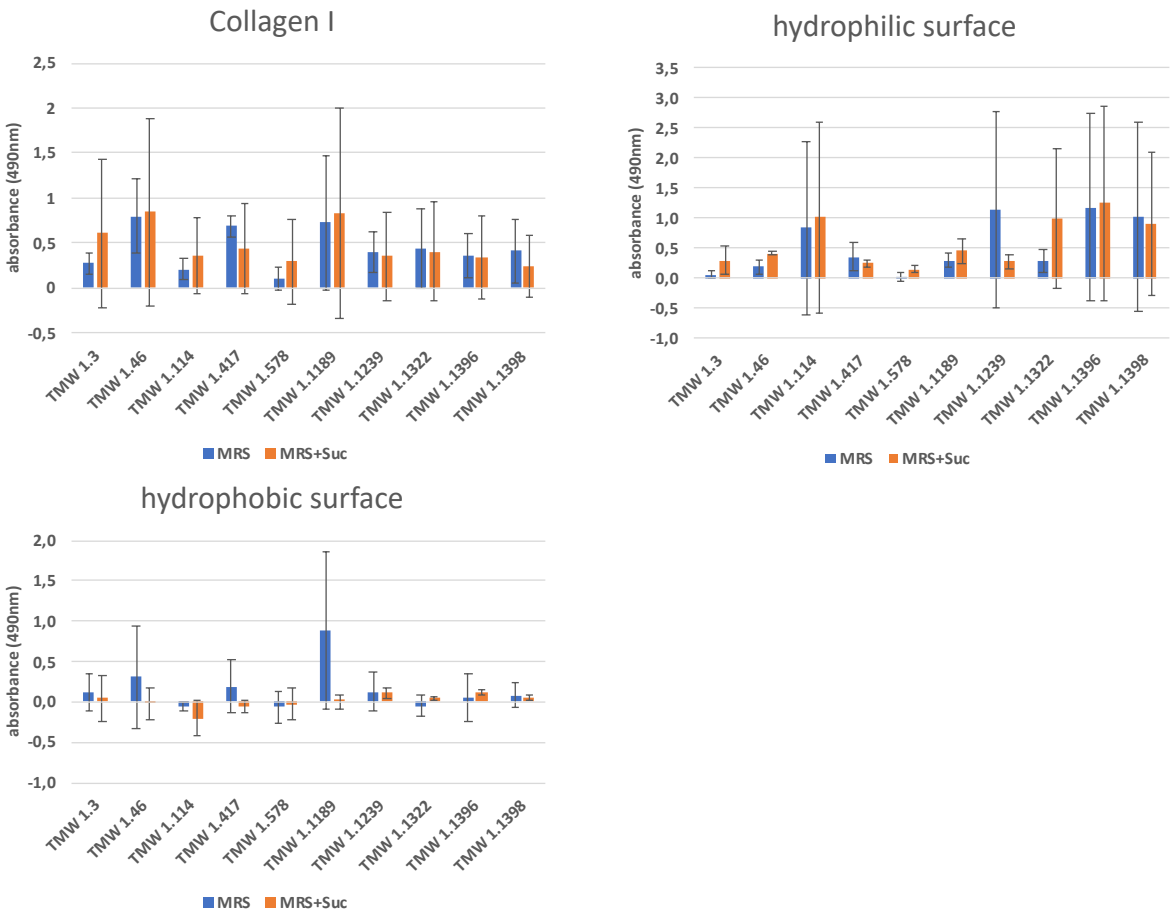

Figure 53: Adhesion of *L. sakei* strains to different surfaces like hydrophobic, hydrophilic surface or collagen I.

4 Discussion

L. sakei and *L. curvatus* are widely used as starter cultures in sausage fermentation. To date, the development of such cultures is mostly based on time-consuming empirical approaches. Mostly, it remains out of the experimental possibilities of the starter culture producers and anyway the meat processing companies, to test or prove at a strain-specific level an assertive performance of the applied strain. Neither would they be able to follow a targeted approach to develop starter strains along traits determining their behavior and assertiveness in the (non-sterile) raw meat environment. Based on the general working hypothesis that assertiveness in sausage fermentation is a multifactorial, strain-specific trait, comparative genomics assisted by physiological testing of predicted traits was used to identify key functions for a knowledge-based starter strain selection. The following theses could be derived from this approach, which are discussed in the subsequent chapters:

- The strain set used in this work was representative for *L. sakei* and *L. curvatus*
- Comparative genomics allows the identification of species-, strain-, and group-specific traits in *L. sakei* and *L. curvatus*
- Assertiveness in meat fermentation is a multifactorial, strain-specific trait
- Genes can be identified, which can be allocated to predictively assertive / non-assertive strains and used for the prediction of single- and multi-strain assertiveness
- Metabolic prediction from the genomes mostly matches physiological testing
- A “positive” cold shock response appears to be an exploitable trait for prediction of assertiveness, pre-selection and possibly also pre-conditioning of competitive starter strains
- Major decisive traits include metabolic functions but also functions involved in the expression of a colonization resistance, namely adhesive functions resulting from surface/flagellar proteins and surface-displayed glycosyltransferases

- Metabolic differences in ribose- citrate and arginine/agmatine metabolism represent complementary key functions for the deliberate combination of strains to assertive partner strains along their complementary accessory genomes
- Apart from bacteriocin production, bacteriocin immunity can contribute as such to the assertiveness of a strain in the meat matrix
- Specific traits including bacteriocin and exopolysaccharide formation and their roles in the assertiveness of *L. sakei* and *L. curvatus* can be predicted
- Neither the adaptation to the meat environment, nor predicted functions of assertiveness are plasmid encoded
- The behavior can be explained of strains in sausage fermentation, which perform as winners, loosers or partners and referred to a genomic level
- Partner strains within one species can be predicted along their complementary accessory genomes

4.1 Bio- and Genetic-diversity of *L. sakei* and *L. curvatus*

Strains of both *L. sakei* as well as *L. curvatus* were isolated from different environments including meat, fermented sausages, moto, sourdough, sauerkraut, and kimchi. These strains apparently are able to adapt to a wide range of different habitats. The ability to adapt to various ecological niches suggest a genetic diversity within both species. Moreover, a co-existence of both species in the same environment suggests, that both species should be different. Further studies revealed within the lactobacilli there are detectable different capabilities for a ubiquitous or specialized lifestyle. As an example, there are on the one side, described as ubiquistic, *L. brevis* and *L. plantarum* and there are on the other side *L. sanfranciscensis* or *L. lindneri*, which are known for their specialized lifestyles caused by well-adapted genomic properties to the habitats of sourdoughs or beer, respectively (Geissler, Celano, Minervini, Gobbetti, & Vogel, 2017). Furthermore, detailed analysis based on genomic comparison revealed that these species defined by either a large pan- and accessory-genome, like it is shown for *L. brevis*, or a small one like it was observed for *L.*

sanfranciscensis (Behr et al., 2015; M.E. Fraunhofer, Geissler, Jakob, & Vogel, 2017; Geissler, Behr, & Vogel, 2016). Indeed, it has been shown that the adaptation of *L. brevis* to the specific ecological niche of beer is carried on plasmids (Behr et al., 2015), which can even be found in different beer-spoiling species and genera. Moreover, plasmids which encode these traits, could transferred between bacteria in different habitats, as an example between bacteria in beer and insects (M. E. Fraunhofer, 2018).

These observations and results of further studies suggest that *L. sakei* and *L. curvatus* developed different strategies to occupy ecological niches, especially meat, in the broad range of environments, where they are able to reach high numbers. Moreover, the putatively variable lifestyle of the strains of both species revealed genetic diversity, which could be detected within the pan-genome by analysing the core and accessory-genome of both species. Indeed, the occupation of a defined ecological niche could be the result of the assertiveness of one strain. In which, assertiveness of strain describes the ability of the strain to reach high cell numbers in a habitat or ecological niche. Traits which enable this assertiveness could base on antimicrobial properties, highly efficient metabolic adaptations like uptake or conversion of nutrients or competitive exclusion by adhesion or biofilm production.

4.2 Comparative genomics; genetic diversity

The genomic comparison of *L. curvatus* and *L. sakei* corroborates their close relationship within the species as well as their genomic diversity. It could be demonstrated for strains of both species, that the core-genome does not significantly shrink anymore upon addition of new genomes of more strains. This is indicative for a representative strain selection comprising most of the biodiversity within *L. sakei* and *L. curvatus.*

Indeed, for both species the core-genome encodes approximately 50% of the pan-genome. Nevertheless, for *L. curvatus* less variability was observed for genome size (2.1 Mb - 1.8 Mb), GC content (42.07% - 41.63%), coding density (86.48% - 85.77%), ANI calculation (99.99% - 98.98%). The genomic comparison of *L. sakei* strains revealed that this species is

also as well closely related, as genomically diverse based with respect to genome size (2.0 Mb - 1.8 Mb), GC-content (41.28% - 41.1%), coding density (87.34% - 86.38%), ANI calculation (100.00% - 97.05%) as well as the diverse number of plasmids in each strain. Moreover, a high genetic diversity within the accessory-genome is caused by plasmids, which could allow an adaptation to different habitats. The outcome of this is, that the core-genome encoded genes related with the general lifestyle of *L. curvatus* and *L. sakei*, and gene content of accessory-genome forms the pool of genetic diversity, which results in intraspecies diversity characterized by assertiveness, co-existence or synergism of strains.

4.3 Exogenous DNA: Crispr/Cas and phages/plasmids

The accessory-genome characterizes the genetic diversity described by genes, which are not encoded within genomes of all strains and, like it was observed in this study, a high variability of the GC-content. These variable GC-contents revealed that the strains take up exogenous DNA possibly by plasmid-transfer or phage-infection. This property enables strain to adapt more efficiently to the meat environment, because “useful” genes encoded by plasmids could be picked up (Geissler, Behr, von Kamp, & Vogel, 2016). Nevertheless, the strains must differentiate between self and foreign DNA. Therefore, bacteria developed a CRISPR/Cas system (Horvath & Barrangou, 2010), which is a microbial adaptive immune system with information about exogenous DNA. The contact with foreign DNA introduces different spacer regions into the CRISPR system, which enable recognition of incoming DNA containing homologous regions. It is suggested that a high rate/number of CRISPR/Cas systems should result in a higher assertiveness as a result of an improved phage defense. However, despite differences based on the number of CRISPR/Cas systems as well as detected clusters in *L. sakei* as well as *L. curvatus,* no correlation was found between detected CRISPR/Cas systems and assertiveness in a competitive setting in a sausage fermentation model performed and described by Janßen *et al.* (Janßen, Eisenbach, et al., 2018). Still, a recently performed even broader analysis of CRISPR/Cas systems in *L. sakei* revealed insights into evolutionary relationships between different strains and illustrated their

usefulness for strain differentiation in assertiveness experiments, or the development of bacteriophage-resistant strains (Schuster, Vogel, & Ehrmann, 2019). Indeed, the genome analyses of strains of both species *L. sakei* and *L. curvatus* revealed that all strains had contact to phages because a high number of prophage gene clusters were identified within the genomes. Detailed analysis suggest that the prophages could be clustered into three groups specificed as “intact”, “incomplete” or “questionable”. Indeed, it was possible to identify genes, which are associated with the production of lysin or lysin modules. Potentially, a (defined) prophage promotes the assertiveness of a strain because the lysin production or the property to release a phage which infected a phage-sensitive strain, enables to overcome the competitors. Moreover, the genetic information of a prophage, independently of the characterization “intact”, “incomplete” or “questionable”, could result in a resistance against phage infection like it was described for bacteriocins (Bobay, Touchon, & Rocha, 2014).

The detailed investigation of the accessory-genome revealed that all strains have taken up exogenous DNA. One typical and well-known procedure of up taking exogenous DNA is the transfer of plasmids, encoding genes, which are associated with the assertiveness in a defined or special ecological niche. So, this mechanism could be also part of the genomic adaptation to a habitat. This strategy of genomic adaptation to a special habitat has been demonstrated for beer spoiling lactobacilli, which encoded traits, which support the adaptation to the habitat beer defined as hop tolerance enabling growth in this special ecological niche, on plasmids (Behr et al., 2015; Behr et al., 2016; M.E. Fraunhofer et al., 2017; Geissler, Behr, von Kamp, et al., 2016)

Nevertheless, in *L. sakei* and *L. curvatus* no traits, associated with neither meat environment and sausage fermentation nor plant-associated habitat, were encoded in the detected plasmids.

4.4 Bacteriocin production and sensitivity

The ability to uptake exogenous DNA results also in uptake of gene clusters, which are associated with bacteriocin production as well as bacteriocin immunity (Claesson, van Sinderen, & O'Toole, 2007). The ability to produce bacteriocins can be a benefit because these antimicrobial peptides enable strains to inhibit the growth of competitors, and this has also been described for strains of the meat environment by Tichaczek *et al.* (Tichaczek, Nissen-Meyer, Nes, Vogel, & Hammes, 1992). Moreover, it was shown that the ability to produce antimicrobial peptides is an industrial advantage, which results in a single strain assertiveness in the meat environment (Janßen, Dworschak, Ludwig, Ehrmann, & Vogel, 2020; Tichaczek et al., 1992).

Furthermore, Claesson *et al.* described the putative resistance of strains against bacteriocins caused by the presence of bacteriocin gene clusters (Claesson et al., 2007) which results in a competitive character to ensure the survival of its own. Interestingly, most strains of *L. curvatus* encoded genes, which are associated with sakacin Q production, with exception of *L. curvatus* TMW 1.407 and TMW 1.1390. Moreover, in this study it was described that *L. curvatus* TMW 1.624 encoded more putative bacteriocin gene clusters than all other strains conclude in this study. In total, this strain appears to carry more than four gene clusters associated with bacteriocin gene clusters, which suggest promoting assertiveness in meat environment and raw sausage fermentation. Several studies described, that *L. curvatus* TMW 1.624 is assertive as single strain either in competitive fermentation in sausage models (Janßen, Eisenbach, et al., 2018) or an industrial ring trail (Janßen, Ehrmann, & Vogel, 2018). These results correlate with the outcome of the bacteriocin production assay, which was done in this study. Moreover, Janßen *et al.* (Janßen, Eisenbach, et al., 2018) shows an inhibitory effect of *L. curvatus* TMW 1.624 against the growth of its competitor strains *in vitro*. Recently, Janßen at al. (Janßen et al., 2020) demonstrated that *L. curvatus* TMW 1.624 could suppresses all *L. curvatus* and most *L. sakei* strains in competitive settings in a sausage fermentation model. This could be referred to its expression of several bacteriocins by proteomic analysis, which revealed peptides mapping to sakacin Q, sakacin Tα and β,

and sakacin X. Lanthicin S, which is also encoded in the chromosome of this strain could not be detected, because it contains lanthionine rings and therefore likely escaped that analysis. To conclude, bacteriocin production appears to be an advantage in meat environment, and further it promotes assertiveness of a single strain during raw sausage fermentation even above other assertiveness traits (Janßen et al., 2020; Janßen, Ehrmann, et al., 2018; Janßen, Eisenbach, et al., 2018).

Claesson *et al.* (Claesson et al., 2007) described that it could also be that putative bacteriocin gene clusters result in a resistance against bacteriocins produced by related bacteria. But, in this study for strains, which were identified to carry single bacteriocin gene clusters without any inhibitory effect against closely related bacteria, no effect of immunity against a closely related bacteriocin producer could observed. This observation correlates with the results described by Janßen *et al*. (Janßen, Eisenbach, et al., 2018). However, this work demonstrates a clear difference between *L. sakei* and *L. curvatus* based on the bacteriocin sensitivity in presence of PA-1, a class IIa bacteriocin. Apparently the observed bacteriocin tolerance does not correlate with predicted bacteriocin production, except for strain *L. curvatus* TMW 1.624. Only strains *L. sakei* TMW 1.3, TMW 1.46, TMW 1.114 and TMW 1.578 encode detectable genes associated with bacteriocin production. Moreover, these putatively produced bacteriocins are classified as class I bacteriocins. Whereas the genomes of strains *L. curvatus* TMW 1.27, TMW 1.167, TMW 1.401, TMW 1.421, TMW 1.439, TMW 1.595, TMW 1.624 and TMW 1.1381 contain genes, which are associated with the production of sakacin Q which is categorized as class II bacteriocin. Compared to the results of the bacteriocin resistance assay in presence of bacteriocin class II pediocin PA-1, it appears that the presence of genes for sakacin Q production could rather provide sensitivity against another class II bacteriocin. This is in contrast to Claesson *et al.* (Claesson et al., 2007) who described the ability of gene clusters associated with bacteriocins to promote the resistance against related bacteriocins. Only strains *L. curvatus* TMW 1.407, TMW 1.421, TMW 1.439 and TMW 1.1381 were sensitive in presence of PA-1, whereas all other *L.*

curvatus strains were resistant. On the other hand, most strains of *L. sakei,* with the exception of *L. sakei* TMW 1.46 and TMW 1.1396, were sensitive against class II bacteriocin PA-1. No strain of *L. sakei* encodes a class II bacteriocin, but *L. sakei* TMW 1.46, which was tested resistant encoded a class I gene cluster. On the other hand, the resistance-tested *L. sakei* TMW 1.1396 encoded no detectable bacteriocin gene cluster. Moreover, PA-1 sensitive-tested strains *L. curvatus* TMW 1.439, TMW 1.421 and TMW 1.1381 encoded class II bacteriocin sakacin Q like other strains, which were resistant. Only *L. curvatus* TMW 1.407, which were sensitive against PA-1, encoded no bacteriocin gene cluster. To conclude, these results suggest that an encoded bacteriocin gene cluster could result in a bacteriocin resistance like described by Claesson *et al.* (Claesson et al., 2007). Nevertheless, genomic comparison suggests that there are more complex mechanisms, which influenced the bacteriocin sensitivity/resistance of *L. sakei* and *L. curvatus* (Table 26).

For the group of sensitive *L. curvatus* strains four marker genes could be identified, which are associated with cell wall characteristics (putatively involved in bacteriocin binding): (1) ABC transporter substrate-binding protein, (2) PTS mannose/fructose/sorbose transporter subunit IIC (PTS Man^{IIC}), (3) amino acid permease, and (4) D-alanyl-lipotheichoicacid biosynthesis protein (DltB). *L. curvatus* TMW 1.421, which was only sensitive in presence of mannose as carbon source, encoded only (1) and (2). Moreover, PTS Man^{IIC} shows a similarity to PTS Man^{IIC} genes encoded by *Listeria monocytogenes* EGD-e, which is known to be sensitive to PA-1 (Glaser et al., 2001). So, it appears that this Mannose PTS subunit C is induced in the presence of mannose and involved in the PA-1 senisitvity of strains as it is a predicted PA-1 binding site rendering the PTS transporter open upon bacteriocin binding (Diep, Skaugen, Salehian, Holo, & Nes, 2007). Indeed, the screening results of *L. curvatus* TMW 1.421 suggest that the expression of this PTS could be influenced by the available carbon source (mannose), and that in turn shows, that the sensitivity of bacteria is influenced by the growth conditions.

Table 26: conclusion of putative bacteriocin producer, identifed bacterioacin immunity protein, and PA-1 sensitivity for *L. curvatus* and *L. sakei.*

	strain sensitivity to PA-1		**predicted class I bacteriocin production**	**predicted class II bacteriocin production**	**predicted immunity protein production**
L. sakei	glucose	mannose			
TMW 1.3	**+**	**+**	-	+	+
TMW 1.46	-	-	-	+	+
TMW 1.114	+	+	-	+	+
TMW 1.417	+	+	-	-	-
TMW 1.578	+	+	-	+	+
TMW 1.1189	+	-	-	-	-
TMW 1.1239	-	+	-	-	-
TMW 1.1322	-	+	-	-	-
TMW 1.1396	-	-	-	-	-
TMW 1.1398	-	+	-	-	-

	strain sensitivity to PA-1		predicted class I bacteriocin production	predicted class II bacteriocin production	predicted immunity protein production
L. curvatus					
TMW 1.27	-	-	-	+	+
TMW 1.167	-	-	-	+	+
TMW 1.401	-	-	+	+	+
TMW 1.407	+	+	-	-	-
TMW 1.421	-	+	-	+	+
TMW 1.439	+	-	-	+	+
TMW 1.595	-	-	+	+	+
TMW 1.624	-	+	+	+	+
TMW 1.1381	+	+	-	+	+
TMW 1.1390	-	-	-	-	-

For all sensitive strains of *L. sakei* also marker genes could be detected, which are associated with cell wall properties or transport systems: (1) UDP-N-acetylmuramoyl-tripeptide –D-alanyl-D-alanine ligase, (2) amino acid permease, (3) hydrolase, (4) short-chain hydrolase, (5) penicillin-binding protein, (6) short chain dehydrogenase, (7) peptidase C69 and (8) MFS transporter. Moreover, in presence of as well glucose as mannose sensitive strains *L. sakei* TMW 1.3, TMW 1.114, TMW 1.417, TMW 1.578 encoded (9) a peptide ABC transporter permease, which is also encoded by *L. sakei* TMW 1.1322, only sensitively tested in presence of mannose.

To conclude, bacteriocin production and resistance can be but need not be connected. On the one hand, bacteriocin gene clusters enable bacteria to produce antimicrobial peptides to combat competing bacteria. The outcome of this is that strains are assertive in a set or as single strain. On the other hand, it was shown that presence of (partial) bacteriocin gene clusters can result in bacteriocin resistance, which could also provide assertiveness in a complex habitat like meat. Moreover, the genomic comparison revealed that sensitivity can also be influenced by presence/absence of transporter systems, namely Man^{IIC}, which is involved in the binding and mechanism of action of class II bacteriocins, whereby the presence of such transporters is influenced by the growth conditions, e.g., presence of special carbon source. Furthermore, other or cell wall properties may influence the sensitivity of bacteria, whose specific function in the binding of bacteriocins have not yet been elucidated.

4.5 Preconditioning of competitive starter strains by cold shock

The cold shock answer as well as the recovery after cold shock could be a main advantage by the assertiveness of strains during the early phase of sausage fermentation.

The selected strains of *L. curvatus* and *L. sakei* were investigated based on their reaction to cold shock induction and recovery after 2 h. The screening based on colony forming units (CFU) and detectable membrane damage after cold shock induction. Interestingly, all strains

of both *L. sakei* and *L. curvatus* show a complete regeneration of membrane damage upon 2h recovery time. So, the main difference could be detected after cold shock. These differences could influence the ability to be assertive in meat environment in the initial phase of sausage fermentation. Genomic comparison revealed that *L. curvatus* strains, which show less, or no membrane damage encoded following marker genes: (1) lipoteichoic acid synthase family protein, (2) bacteriocin immunity protein and (3) hypothetical protein, which is a putative isopeptide forming domain-containing fimbrial protein. These genes are involved in cell wall properties, e.g., lipoteichoic acid synthase family protein. Moreover, *L. sakei* strains, which show less membrane damage encoded the following DMGs (1) IS30 family transposase, (2) DUF956 family protein, (3) cell surface protein, (4) filamentation induced by cAMP protein fic and (5) different hypothetical proteins. Interestingly, there is a cell surface protein part of the DMGs. To conclude, genomic comparison revealed that strains, which show less membrane damage after cold shock, are different in cell wall characteristics based on the genetic properties.

Moreover, the CFU of the strains revealed that strains react differently to cold shock. Some strains show no differences after cold shock, whereas other strains show an increase of CFU after cold shock induction. A third group showed a significant increase of CFU upon 2h of recovery. Janßen et al. (Janßen, Ehrmann, et al., 2018; Janßen, Eisenbach, et al., 2018) described a set or single strains, which were assertive during raw sausage fermentation as well in a sausage model as in a industrial ring trail in raw sausages. Most - as assertive characterized – strains had shown low or no membrane damage after cold shock, with exception of *L. curvatus* TMW 1.624 and *L. sakei* TMW 1.3 and TMW 1.46. Moreover, all strains, which were not assertive had shown high membrane damage after cold shock induction with exception of *L. sakei* TMW 1.114. In fact, *L. sakei* TMW 1.3 and TMW 1.46, which were assertive but had a high increase of membrane damage were able to recover fast and increased the CFU/ml after recovery time. This indicates a strong cold shock response, which results into a fast recovery. Compared to the results of Janßen et al. (Janßen, Eisenbach, et al., 2018) a “positive” cold shock response appears to be an

exploitable trait for prediction of assertiveness, pre-selection and possibly also pre-conditioning of competitive starter strains.

4.6 Metabolic properties/differences

Overall, the classification of annotated genes by RAST Annotation and SEED viewer revealed that strains are different based on their metabolic properties. For both species a wide range of annotated genes by RAST annotation was detectable. Strains of *L. curvatus* encoded 1127 genes down to 1060 genes, and it was observed that strains of *L. sakei* encoded 1152 genes down to 1097. *L. curvatus* and *L. sakei* strains are different based on the number of genes correlated with the metabolism of carbohydrates and nucleosides, fatty acids, amino acids and proteins.

4.6.1 Glycolysis

Genomic analysis based on NCBI annotation and BADGE calculated comparison, as well on nucleotide sequences as amino acid sequences, revealed that the glycolysis is a well conserved metabolism within both species. Still, for *L. curvatus* TMW 1.421 differences of pyruvate dehydrogenase based on amino acid sequence were detected. Moreover, the annotation revealed that strains of both *L. curvatus* and *L. sakei* encoded more than one lactate dehydrogenase. This little surprising *in vitro* prediction revealed that all strains are able to use glucose as energy source by glycolysis. Indeed, for both *L. sakei* and *L. curvatus* it was previously described that these species are able to degrade glucose to pyruvate and lactate or ethanol by glycolysis (Chaillou et al., 2005; McLeod et al., 2010).

Moreover, the fact that glycolysis is encoded within the core-genome suggests that no differences should be detectable for growth of these strains in presence of glucose as single energy source. Indeed, all strains of both *L. curvatus* and *L. sakei* were able to grow under this defined condition, but differences were detectable. The physiology of the strains is different. Interestingly, *L. sakei* strains' physiology appears similar, but not identical, whereas *L. curvatus* strains' growth behaviour is diverse. Indeed, these detectable differences of physiology may result from different expression / redundancy of enzymes and finally

influence the assertiveness of the strains in the sausage fermentation. A strain, which is able to grow fast in presence of glucose, is able to occupy such ecological niche and overgrow other competitors. Indeed, it has recently been demonstrated that a prediction of assertiveness in this environment can be made along the maximum growth rate of *L. sakei* and *L. curvatus* in a modified MRS medium containing glucose (Janßen et al., 2020).

4.6.2 Glycerolipid metabolism

Meat is a substrate-rich environment, which also delivers lipids and fat to bacteria in raw sausage fermentation. So, it was supposed that a well-adapted strain should be able to use glycerol as substrate. McLeod *et al.* (McLeod et al., 2010) described the glycerol metabolism briefly and showed an expression of the described enzymes by proteomic analysis of *L. sakei*. Interestingly, the genome analysis in this work revealed that genes associated with the glycerol metabolism are part of *L. sakei's* core-genome with the exception of the gene, encoding glycerol-3-phosphat dehydrogenase, which is mutated, rendering is possibly non-functional, within the genome of *L. sakei* TMW 1.1398. For *L. curvatus* strains it was observed that the genes, which are associated with the glycerol metabolism are part of the accessory-genome and thus strain / group specific. Firstly, *L. curvatus* TMW 1.401 encoded no glycerol transporter, and the sequences of this gene in *L. curvatus* TMW 1.167, TMW 1.595, and TMW 1.624 is mutated, which results in a changed transmembrane structure. In detail, the structure analysis by TMHMM suggests that the mutation of the sequence caused that the mutated transporters conclude only one transmembrane structure, whereas the non-mutated sequence encoded multiple transmembrane structures. Possibly this causes a impaired functionality or a non-functional transporter. A growth experiment in CDM suggests that there is no clear correlation between the genetic properties and the physiology. Indeed, the results of growth experiments revealed that *L. curvatus* TMW 1.401 and TMW 1.595 are able to grow in presence of glycerol as energy source, although no glycerol transporter could be detected within the genome of *L. curvatus* TMW 1.401 based on the NCBI annotation, and the sequence of the glycerol transporter of *L. curvatus* TMW 1.595 contains a mutation, which should influence the functionality of the transporter. Nevertheless, all strains encoded

an aquaporin, which is associated with glycerol uptake. So, this gene appears to be functional and allows strains take up glycerol, although they encoded a mutated glycerol transporter. Indeed, *L. curvatus* TMW 1.624, whose genome also encodes the mutated transporter, shows no growth in presence of glycerol. Moreover, *L. curvatus* TMW 1.407 showed no growth, too. This strain encoded a glycerol-3-phosphat dehydrogenase, which is part of core-genome based on the nucleotide sequence, but the amino acid sequence revealed an introduction of an earlier stop codon, which may result in a non-functional enzyme. But, for *L. curvatus* TMW 1.401 the same mutation was identified, and this strain was able to grow in presence of glycerol as single energy source.

To conclude, the detected physiological differences of the strains of *L. curvatus* do not correlate with the identified differences at the genetic level. (Point) mutations could result in a changed function of enzymes or transporters, but the *in silico* prediction does not enable reliable prediction of physiological properties.

4.6.3 Adenosine and inosine metabolism

The ability to metabolize purine nucleosides like adenosine and inosine may be a good indicator for adaptation to the meat environment of *L. sakei* and *L. curvatus* (Rimaux, Vrancken, Vuylsteke, De Vuyst, & Leroy, 2011), because these nucleosides are part of the rich medium meat. So, it is not remarkable that the enzymes, which are associated with the purine metabolism are part of the core-genome of *L. sakei*. Chaillou *et al.* (Chaillou et al., 2005) described this metabolism for *L. sakei* 23K because their genomic analysis of this strain showed the presence of the required enzymes. The genomic analysis revealed that all genome sequenced strains are able to use adenosine as single energy source for growth. Indeed, most *L. sakei* strains grow in presence of adenosine, but there are *L. sakei* TMW 1.3 and TMW 1.46, which show no detectable growth, and *L. sakei* TMW 1.1322, which grows slower than the other tested strains. These results suggest that *L. sakei* TMW 1.3 and TMW 1.46 encoded the genes, but may not express these enzymes, wherefore these strains not able to use adenosine as energy source.

Interestingly, the genome analysis of *L. curvatus* revealed that the genes, which are associated with the adenosine and inosine metabolism, are part of the accessory-genome. All strains of *L. curvatus* encoded ribonucleoside hydrolase, but genome analysis revealed a different sequence for *L. curvatus* TMW 1.407. Indeed, *L. curvatus* TMW 1.407 is the one strains, which was unable to grow in presence of adenosine. So, it appears, that the ribonucleoside hydrolase of this strain is not functional or is not expressed under the tested conditions. Moreover, the genome analysis revealed that the strains of *L. curvatus* differs based on the ribose transporter, the nucleoside phosphorylases and phosphopentomutase. But the adenosine deaminase is part of the core-genome. Interestingly, all strains of *L. curvatus* show growth after 72h, in which *L. curvatus* TMW 1.1390 shows significant growth after 24h. To conclude, there is no significant correlation between the genomic properties and the physiology. Nevertheless, the genetic regulation and expression results in physiological differences, which may influence the assertiveness in meat fermentation. Still, the genomic differences of *L. curvatus* TMW 1.407 result in physiological differences, because the mutated gene of ribonucleoside hydrolase results in a non-functional enzyme. Furthermore, *L. curvatus* TMW 1.407 is unable to use adenosine as energy source. This fact may influence the adaptation to meat environment and the prediction revealed that *L. curvatus* TMW 1.407 should not be assertive during raw sausage fermentation. Indeed, this strain proved to be non-assertive in the study of Janßen et al. (Janßen, Eisenbach, et al., 2018) while TMW 1.1390 was among assertive winner strains.

4.7 Ribose metabolism

Ribose is known as important substrate, which could be obtained by the degradation of adenosine and inosine, to generate energy at the meat environment (Chaillou et al., 2005; McLeod et al., 2010; Nyquist et al., 2011; Rimaux, Vrancken, Vuylsteke, et al., 2011). Nyquist *et al.* (Nyquist et al., 2011) described divergent regions in *L. sakei* genomes and detected the *rbs* operon within these regions. Interestingly, all genome-sequenced strains of *L. sakei*, which are included in this study, carried a ribose operon, which is highly conserved

and part of the core-genome of *L. sakei*. So, all *L. sakei* strains encoded the rbs operon *rbsUDKR*, which is homologous to the rbs operon *rbsUDKR* carried by *L. curvatus* TMW 1.401, TMW 1.407, TW 1.421 and TMW 1.1390 (classified as group I). Nevertheless, sequence analysis of transcriptional the regulator *padR* and MFS transporter revealed differences.

Indeed, genomic comparison of *L. curvatus* revealed that the *rbs* operon is part of the accessory-genome. In detail, two different operons could be identified, which differ based on structure and transporter system. On the one hand the efficiency of both transporter systems was tested by growth experiment at CDM and HPLC analysis. The results suggest that the strains carry the operon *rbsUDKR* (classified as group I), which encodes *rbsU* a PTS as transporter system characterized by a higher ribose uptake rate during the first 48 hours (50-80%) compared to the strains belonging to group II encoding *rbsDACBK*, which encodes *rbsACB* an ABC transporter. Moreover, the comparison of the growth curve for *L. curvatus* TMW 1.401 (group I) and TMW 1.624 (group II) revealed that the higher ribose uptake rate results in a higher growth rate. To conclude, the different ribose transporters result in differences of the efficiency of the ribose uptake, and this may influence the growth of the strains. Moreover, the efficiency of ribose uptake and the growth rate will influence the assertiveness of a strain or species, especially during the occupation of the ecological niche “ribose utilization”.

Furthermore, the genetic analysis of both ribose operons revealed differences based on the operon structure. Putatively, the structure differences will influence the operon regulation, which also may influence the efficiency of ribose utilization. For *Escherichia coli* Laikova *et al.* (Laikova, Mironov, & Gelfand, 2001) describes *rbsR* as independent gene, which is located downstream of *rbsDACBK* operon. For the *rbsUDKR* of group I it was observed that *rbsR* gene is located downstream of the operon. Moreover, this gene may be regulated by its own promotor. In contrast, for the *rbsDACBK* operon of group II it was observed that the *rbsR* gene is encoded upstream of the operon and there is one single promotor upstream of *rbsR* gene and the *rbsDACBK* operon.

Finally, the genomic and physiological analysis of the ribose operon and ribose utilization enables to identify differences based on putative regulation and structure of both ribose operons. Moreover, the comparison of ribose uptake and utilization verified by growth experiments and HPLC analysis suggests differences between both defined groups I and II based on the encoded ribose operon. The results revealed clearly identified differences in the efficiency of transporter systems and utilization of ribose, which correlates with a defined ribose transporter system or ribose operon type and a ribose uptake rate. In detail, it appears that strains encoding *rbsUDKR* operon, which carries the ribose PTS, has an advantage over the strains encoding *rbsDACBK* operon, which carries the ABC transporter, based on the efficiency of ribose utilization.

Interestingly, both groups of *L. curvatus* strains (sequenced in this study and published sequences), which address the ribose operon, do not correlate with the source of isolation or putatively preferred habitat, e.g., a plant related environment, which should be rich in pentoses. There is also no correlation with arabinose or xylose pathways (Chaillou et al., 2005; Cousin et al., 2015; Hebert et al., 2012). This may be due to the fact that pentoses in plants are mostly present in polymers, e.g., arabinoxylans, and can only be used upon their degradation or other microbes sharing this environment.

4.8 Acid stress; ADI-pathway

The first whole genome sequencing of *L. sakei* 23K, described by Chaillou *et al.* (Chaillou et al., 2005) suggests a well adaptation to meat environment. This adaptation concludes also the stress response, like acid stress. A well-known acid stress response is the arginine deiminase (ADI) pathway (Chaillou et al., 2005; Nyquist et al., 2011; Rimaux, Vrancken, Pothakos, et al., 2011). Moreover, the ADI pathway generates metabolic energy for the strains (Chaillou et al., 2005; Nyquist et al., 2011). This pathway was described as main criterion of meat adaptation of the strains by the authors. Indeed, in all *L. sakei* strains, which were analysed by further studies, the ADI pathway was encoded within the genomes. Furthermore, the ADI pathway was also detected in the core-genome of *L. sakei* strains of

our study. So, the ADI pathway appears is corroborated as important pathway for a life in the meat environment. However, the analysis of *L. curvatus* strains suggests that the ADI pathway is neither encoded within their core-genome nor accessory-genome, despite the finding of competitive strains in this environment. This result correlates with the description of the main differences between *L. sakei* and *L. curvatus* by Champomier-Verges *et al.* (Champomier Verges et al., 1999). It is known that a low sugar concentration results in an initiation of the arginine catabolism. This means, that the ADI pathway in *L. sakei* will be induced if the available sugar in meat environment is reduced or depleted (Chaillou et al., 2005; Champomier Verges et al., 1999; Rimaux et al., 2012; Rimaux, Vrancken, Pothakos, et al., 2011).

Interestingly, the analysis of the accessory-genome revealed that *L. sakei* TMW 1.3, TMW 1.114, TMW 1.578 and TMW 1.1322 encoded a putative agmatine pathway. The agmatine pathway is known to enable strains to increase the pH and generated energy. Still, the genomic comparison revealed differences of the gene clusters encoded by the strains. Indeed, it was shown that *L. sakei* TMW 1.3 and TMW 1.1322 are not able to increase the pH during cultivation in a defined medium (decarboxylation medium) in presence of agmatine. In contrast, *L. sakei* TMW 1.114 and TMW 1.578 are enabled to neutralize the pH under the same conditions. These results suggest that the gene cluster, which is encoded within the genomes of *L. sakei* TMW 1.114 and TMW 1.578 are functional. Whereas the mutations detected at the gene clusters of *L. sakei* TMW 1.3 and TMW 1.1322 may result in non-functional enzymes. First, the *aguD* gene, which is carried by *L. sakei* TMW 1.1322 and encodes the agmatine/putrescine antiporter appears to be mutated. Additionally, for *L. sakei* TMW 1.3 it was shown that the *aguC*, which encodeds a carbamate kinase appears to be mutated, too. To conclude, the physiological tests revealed that both detected mutations result in non-functional enzyme or transporter. Interestingly, *L. sakei* TMW 1.3 carried a gene, which encodes a carbamate kinase and is part of the ADI pathway. Moreover, it was shown that the ADI pathway is functional for all tested *L. sakei* strains. This leads to the conclusion that both gene clusters may be regulated independent from each other, and the

ADI pathway will be induced by a low sugar concentration and presence of arginine, whereas agmatine is no inducer of the ADI pathway. Still, agmatine should be a putative inducer of the agmatine deiminase gene cluster.

Both described pathways enable strains to overcome acid stress, but they are also a main criterion to differentiate *L. sakei* and *L. curvatus*. So, *L. curvatus* has to develop other strategies to overcome acid stress. One strategy appears to be the tyrosine decarboxylation, like it has been described by Freiding *et al.* (Freiding et al., 2011). They reported that *L. curvatus* TMW 1.167, TMW 1.407, TMW 1.421, TMW 1.439, TMW 1.595, TMW 1.624 and TMW 1.1381 encode a functional tyrosine decarboxylase. Moreover, *L. curvatus* TMW 1.407, TMW 1.421, TMW 1.595 and TMW 1.624 carried also a gene, which encodes a putative ornithine decarboxylase. A more detailed analysis of the *L. curvatus*' core-genome revealed that all strains encoded a L-serine deaminase, which enables the strains to convert L-serine to NH_3 and pyruvate, and they encoded a guanine deaminase, which enables them to degrade guanine to NH_3 and xanthine. Interestingly, both described enzymes are not carried by *L. sakei* TMW 1.1322. Finally, the genome analysis and comparison revealed that cytosine deaminase, D-glucoseamine-6-phosphate deaminase, adenosine deaminase and adenine deaminase are encoded within the core-genome of *L. curvatus* as well as carried by *L. sakei* TMW 1.1322. To conclude, all these described deaminases enable strains to generate NH_3, which is important to increase the pH of the environment and overcome acid stress. So, this strategy allows *L. curvatus* to be tolerant against acid, although this species does not encode ADI pathway or agmatine deiminase pathway.

4.9 Citrate metabolism

Nyquist *et al*. (Nyquist et al., 2011) described the citrate catabolic genes and observed a divergence of these genes. Moreover, a detailed comparison of the genomes of *L. sakei* LS25 and 23K revealed a divergence of the gene cluster within the species *L. sakei* at genomic level. The citrate gene cluster encoded within the genome of *L. sakei* LS25 appears not orthologous to the one, which was identified in *L. sakei* 23K. Indeed, McLeod *et al.*

(McLeod, Brede, Rud, & Axelsson, 2013) identified 250 protein-encoding genes, which were unique to *L. sakei* LS25. Furthermore, genomic comparison and analysis of the core and accessory-genome of *L. sakei* suggest that two different citrate gene clusters are detectable within the analysed genomes of *L. sakei*. Interestingly, there is a group of strains, which encoded no detectable genes associated with the citrate metabolism.

In detail, it is known that one important enzyme of citrate metabolism is encoded by *citP* and is described as citrate permease. Detailed analysis suggest that this enzyme reached highest efficiency at a defined pH. As example, *Lactococcus lactis* citrate permease reached its optimum at the pH of 5.0 and 6.0, and in *L. plantarum* it was observed that the optimum pH for the citrate permease is at pH 4.0. However, at such low pH levels citrate, which is characterized with a pK_a=3.14, 4.77, 5.40, exists in acidic and uncharged form (Hugenholtz, 1993). This means that citrate also easily can diffuse through cell membrane. The comparison of both identified citrate gene clusters revealed that the citrate cluster I, which is encoded by *L. sakei* TMW 1.3, TMW 1.1322, TMW 1.1396 and TMW 1.1398, carries a Mg^{2+}/citrate complex transporter (*citM*), whereas, at citrate cluster II, which was identified in the genomes of *L. sakei* TMW 1.46, TMW 1.1139 and 1.1239, encoded the citrate permease (*cimH*). The Mg^{2+}/citrate complex transporter was identified within the genome of *Bacillus subtilis* and Mg^{2+} ions is the inducer of citrate uptake by this transporter (Boorsma, van der Rest, Lolkema, & Konings, 1996). The first initial step of catabolic citrate metabolism is the conversion of citrate to oxaloacetate and acetate catalysed by citrate lyase. This means that acetate concentration can be used as indicative for an active catabolic citrate metabolism. Additionally, the genomic comparison of all strains of *L. sakei* suggest that citrate lyase is encoded within all detected citrate gene clusters of this species, and the genetic data revealed that this enzyme is unique for the putative citrate utilizers. Indeed, the results of HPLC analysis revealed a higher acetate concentration in presence of citrate for strains, which encoded a citrate gene cluster. Detailed analysis of the nucleotide sequence as well as amino acid sequence of encoded citrate lyase within the gene cluster of *L. sakei* TMW 1.3 identified a point mutation at nucleotide sequence, which should result in an introduction of

an earlier stop codon. So, the mutation should cause a non-functional enzyme. The HPLC data revealed that *L. sakei* TMW 1.3 takes up 9.72% of the available citrate, but there is no detectable significant increase of acetate concentration (1.18%). The outcome of this is that the isocitrate lyase may not be functional, so the initial step of citrate breakdown does not work for *L. sakei* TMW 1.3. Moreover, also within the genome of *L. sakei* TMW 1.1396 and *L. sakei* TMW 1.1398 mutations within the encoded citrate transporter *citM* was detected. These mutations result in the introduction of earlier stop codons. Furthermore, the length of gene sequence of the transporter, which is encoded within the genome of *L. sakei* TMW 1.1396, is less long compared to the homologous sequences identified at the genome of both *L. sakei* TMW 1.1322 and TMW 1.1398. All detected differences at the genes, which encoded the transporter CitM results in a transformation of the structure of transporters, which were analysed by the web-based tool TMHMM, encoded by *L. sakei* TMW 1.1396 and TMW 1.1398. Indeed, the citrate uptake rate of *L. sakei* TMW 1.1396 is the highest rate - with a citrate uptake of 30.32% - in comparison with the uptake rate of the other strains which also encoded the citrate gene cluster I with the Mg^{2+}/citrate complex transporter. The outcome is that first the transporter is functional, and second the changed transmembrane structure and amino acid sequence may cause a more efficient transporter like it was demonstrated with the higher citrate uptake rate after an incubation of 48h. Nevertheless, also *L. sakei* TMW 1.1239 shows a higher citrate uptake rate. This strain encoded the citrate gene cluster II like *L. sakei* TMW 1.46 and TMW 1.1189. This gene cluster appears to be highly conserved, but it was shown that *citI* gene, which encoded the isocitrate lyase transcriptional regulator, is changed within the genome of *L. sakei* TMW 1.1239. In detail, the sequence's length is shorter compared to the sequences of the genes encoded in the genomes of *L. sakei* TMW1.46 and 1.1189. To conclude, the results suggest that the transcriptional regulator influenced the citrate uptake and the mutation within the gene *citI* encoded by *L. sakei* TMW 1.1239 may lead to a higher efficiency of citrate uptake caused by a putative stronger upregulated expression of citrate lyase, which catalyses the initial step of catabolic citrate metabolism/citrate breakdown.

The comparison of the citrate uptake rate of strains encoded citrate gene cluster I *versus* strains encoded citrate gene cluster II suggests that the gene cluster II enables a faster citrate uptake after 48h of incubation/during the first 48h, but no significant differences based on the acetate concentration or production could be identified. So, the advantage of citrate gene cluster II is only based on the transporter system (citrate permease), which may more efficient. A higher efficient substrate or citrate uptake will be causing an assertiveness of the strains during occupation of the ecological niche formed by citrate as useable substrate at meat environment.

4.10 Flagellar gene cluster and motility

The adaptation to ecological niches or defined environments is triggered by different factors, which results from changes within the genome. One part of these adaptations are metabolic properties, which are changed or optimized based on efficient substrate uptake or substrate utilization. Another part comprises different strategies based on the cell properties like cell surface, exopolysaccharide production or the ability to adhere to defined surfaces. All these differences are encoded within the genomes. Moreover, the differences within one species are detectable within the accessory-genome. One of these adaptations to a specialized lifestyle was identified within the accessory-genome of the species *L. curvatus*. The flagella operon described by Cousin *et al.* (Cousin et al., 2015) in *L. curvatus* NRIC 0822, was identified in the genomes of *L. curvatus* TMW 1.27 and TMW 1.1390. Interestingly, it was described that the adhesion is influenced by cell surface proteins like flagellar proteins (Chagnot et al., 2017). First genomic analysis revealed that the operons encoded by *L. curvatus* TMW 1.27, TMW 1.1390 and NRIC0822 are different and there are numerous mobile elements like invertases, and transposases close to the operons. This observation was also described by Cousin *et al.* (Cousin et al., 2015). So, it may possible that the ability to express a functional flagellum will be impaired in different strains and could be an instable characteristic trait. Moreover, it appears that there is no correlation between the source of isolation and the presence/absence of the genomically encoded ability to form a flagellum.

Nevertheless, *L. curvatus* TMW 1.27 and TMW 1.1390 encoded a complete conserved flagellar gene cluster, like it was described by Cousin *et al.* (Cousin et al., 2015), whereas no other strains of *L. curvatus* and no strains of *L. sakei* encoded a gene cluster associated with flagella. The detailed analysis revealed that the most gene sequences are highly conserved, based on the genomic comparison of *L. curvatus* TMW 1.27, TMW 1.1390 and NRIC 0822. The main differences of all three encoded gene clusters based on the invertases and transposases, which differs in structure and position within the gene cluster.

Moreover, the gene *fliS*, which encodes a flagellar protein FliS and is known to be a flagellin-specific T3S chaperone. Buntin *et al.* (Buntin, de Vos, & Hongpattarakere, 2017) has shown and described that FliS is essential for the flagellar assembly. Moreover, it was shown that mutation of *fliS* results in changes of motiliy and flagellar filament assembly. This gene is highly conserved based on genome comparison of *L. curvatus* TMW 1.1390 and NRIC 0822, whereas this gene is different based on the sequence encoded in the genome of *L. curvatus* TMW 1.27. Putatively, these genomic differences may influence the motility or flagellar filament assembly of the strains. So, the motility of both strains was tested. The motility experiment showed that both strains are motile if they are cultivated at 30°C in presence of glucose, ribose, glycogen and no carbon source. Furthermore, no motile activity could be detected if the strains were cultivated at 15°C. Nevertheless, if the strains were cultivated at 20°C the motility characteristics of both strains are different. However, *L. curvatus* TMW 1.27 is not motile in presence of glycogen or in absence of every carbon source, and *L. curvatus* TMW 1.1390 was not motile in presence of glycogen or in absence of every carbon source.

It appears, that on the one hand external factors, e.g., temperature or carbon source, influence the motility of the strains. Moreover, the mutations within the sequence of *fliS* may result in different motility characteristics under defined conditions. The reduced or not detectable motility may indicate a non-functional flagellar filament assembly, which could result in non-functional flagella or an absence of any flagella at the cell surface.

The expressed flagella are at the cell surface and it was described by Chagnot *et al.* (Chagnot et al., 2017) that the flagella could influence the adhesion of bacteria to a defined

surface. So, the adhesion characteristics of *L. curvatus* TMW 1.27 and TMW 1.1390 and the non-motile *L. curvatus* TMW 1.401, which was used as negative control, were determined. First, collagen I was used as surface for adhesion and the results suggest that *L. curvatus* TMW 1.27 adhere more efficient than *L. curvatus* TMW 1.1390 and TMW 1.401. However, there are genes *fliC$_1$C$_2$,* which are not highly conserved, and the genomic comparison revealed differences within the sequences encoded in the genomes of *L. curvatus* TMW 1.1390 and TMW 1.27. FliC is known as flagellin, which is a subunit protein, which is part of the filament of bacteria flagella. The genomic differences may influence the structure of the protein which are of the flagella. The change of protein structure may change the cell surface characteristics and the ability to adhere to meat surface.

Interestingly, differences based on the adhesion could be detected for *L. curvatus* TMW 1.27, TMW 1.1390 and TMW 1.401 which was used as negative control based on *in vitro* experiments. Results suggest that *L. curvatus* TMW 1.27 is able to adhere more efficiently to collagen I than *L. curvatus* TMW 1.1390 and TMW 1.401. But *L. curvatus* TMW 1.1390 appears to adhere more efficiently to a hydrophilic surface. Indeed, further experiments revealed that the cell surface of *L. curvatus* TMW 1.1390 is 100% hydrophilic, whereas the cell surface of both *L. curvatus* TW 1.127 and TMW 1.401 is less hydrophilic (~90%).

To conclude, the hydrophilic cell surface appears to influence the ability to adhere to hydrophilic surfaces. Moreover, the divers flagellin proteins, encoded by *fliC*, could influence the adhesion characteristics of the strains. The flagellin proteins of *L. curvatus* TMW 1.27 should promote the adhesion to collagen I.

In summary, the differences which were detected within the flagellar gene cluster may results in differences of motility under defined conditions, but the conditions during raw sausage fermentation should enable the strains to form flagella. Furthermore, the cell surface characteristics appear to be influenced, which results in different adhesion characteristics. Moreover, the results suggest that the property to express a flagellar could result in

assertiveness at raw fermented sausages, because the strains are able to adhere at the meat surface and putatively occupy an ecological niche.

4.11 Adhesion and cell wall properties

Apart from the influence of flagellar proteins residing on the cell surface to an adhesion ability, the occupation of a niche within the meat matrix can also by influenced by the formation of EPS, which, depending on the type, can affect cell surface properties. Actually, in the case of capsule-forming β-glucans or heteropolysaccharides (HePS), the EPS can mediate the adhesive function, while homopolysaccharides (HoPS), formed by cell envelope-bound glycosyltransferases from sucrose and released into the surrounding medium should not mediate direct adhesive functions. Still, the surface-displayed glycosyltransferases could mediate adhesion and HoPS can found the establishment and be constituents of biofilms. Furthermore, EPS production is known to be part of the stress response. So, a capsular HePS or extracellulary formed HoPS may result in a higher adaptation to conditions stress, e.g., cold stress, acid stress or salt stress (R.M. Prechtl et al., 2018).

To test the ability of the strains to produce a HoPS from sucrose, all strains were tested for their HoPS production in presence of sucrose. Interestingly, for both species *L. sakei* and *L. curvatus* three of ten strains were identified as HoPS producer. Moreover, no correlation was detected for assertiveness and the ability to produce HoPS. Interestingly, all strains of *L. sakei* encoded a sucrose operon, which enables strains to use sucrose as energy source. Moreover, this operon is not part of the core-genome of *L. curvatus.* Only *L. curvatus* TMW 1.27 and TMW 1.421 are able to use sucrose as carbon source. But both strains are unable to produce HoPS. Actually, the ability to metabolise sucrose does not (and need not) correlate with the ability to produce HoPS. Moreover, Prechtl *et al.* described that genes associated with the HoPS production are plasmid encoded and the HoPS of *L. sakei* TMW 1.411 is a dextran (R. M. Prechtl et al., 2018). Thus, the ability to produce HoPS could be transferred between strains by plasmids or the ability will be lost by losing this small plasmid.

Interestingly, the genomic analysis revealed more differences between the genome sequenced strains based on their cell wall properties. For *L. curvatus* it was shown that *L. curvatus* TMW 1.407, TMW 1.595 and TMW 1.624 no genes were encoded, which are associated capsular HePS or β-glucans. Furthermore, all strains, with exception of *L. curvatus* TMW 1.407, TMW 1.595 and TMW 1.624, encoded genes, which are associated with rhamnose containing glycans. This is indicative for gene clusters encoding HePS biosynthesis, because rhamnose anabolic pathways are mostly exclusive for HePS repeating unit builtup. Indeed, further genomic analysis, based on the NCBI annotation, revealed that *L. curvatus* TMW 1.167, TMW 1.421, TMW 1.439 and TMW 1.1381 encoded an EPS gene cluster, which is homologous to a HePS gene cluster encoded within the genome of *L. rhamnosus* ATCC 9595. Interestingly, *L. curvatus* TMW 1.439 (set II) and *L. curvatus* TMW 1.421 and TMW 1.1381 (set I modified) were described as assertive and an assertive pair, respectively, during raw sausage fermentation (Janßen, Ehrmann, et al., 2018; Janßen, Eisenbach, et al., 2018). It appears, that the production of these EPSs contributes to the assertiveness of the tested strains, but there are also strains like *L. curvatus* TMW 1.624, which does not encode any genes associated with the production of HePS, this strain proved assertive in raw sausage fermentation (Eisenbach, Janßen, Ehrmann, & Vogel, 2018; Janßen, Ehrmann, et al., 2018; Janßen, Eisenbach, et al., 2018). However, *L. curvatus* TMW 1.624 produced HoPS on sucrose. Still, the respective Gtf could not be fond in the genome, which could be referred to the loss of small plasmids in the SMART sequencing procedure, as this Gtf resides on a small plasmid (R. M. Prechtl et al., 2018). Above this, the prominent assertiveness of this strain can be explained by the production of several bacteriocins by *L. curvatus* TMW 1.624, which obviously overrides other assertiveness determinants, namely because *L. curvatus* TMW 1.421 and TMW 1.1381 proved only assertive in the absence of strain TMW 1.624. To conclude, the ability to produce HePS may result in an assertiveness of strains, but assertiveness will be not be exclusively caused by HePS production.

For *L. sakei* the genomic data also revealed differences based on the HePS production. First, *L. sakei* TMW 1.114 and TMW 1.578 encoded genes, which are associated with dTDP-rhamnose synthesis and rhamnose-containing glycans as well as with exopolysaccharide biosynthesis. Interestingly, *L. sakei* TMW 1.1189, TMW 1.1239 and TMW 1.1398 encoded also genes associated with dTDP-rhamnose synthesis and rhamnose-containing glycans as well as with exopolysaccharide biosynthesis, but *L. sakei* TMW 1.1239 is the only strain without other detectable genes associated with HePs biosynthesis.

A more detailed genomic comparison based on the NCBI annotation revealed that *L. sakei* TMW 1.114 and TMW 1.578 also encoded an HePS gene cluster, which is homologous to the HePS gene cluster identified at the genome of *L. rhamnosus* ATCC 9595. Moreover, *L. sakei* TMW 1.1189 and TMW 1.1239 encoded also genes associated with this special gene cluster, but not the complete gene cluster. In comparison to the assertiveness experiments, described by Janßen *et al.* (Janßen, Ehrmann, et al., 2018; Janßen, Eisenbach, et al., 2018), only *L. sakei* TMW 1.578 is assertive and encoded the HePS gene cluster. So, again it may be advantageous to produce a HePS for assertiveness as observed for *L. curvatus* strains TMW 1.421 and TMW 1.1381. Still, *L. sakei* TMW 1.1396, which was assertive as single strain and suppressed the growth of *L. sakei* TMW 1.578 during raw sausage fermentation, encoded no HePS gene cluster. Taken together, HePS production does not solely promote the assertiveness of strains during raw sausage fermentation but can contribute to it.

Finally, the adhesion characteristics of the strains of both species *L. curvatus* and *L. sakei* were investigated. The adhesion properties of the strains to hydrophilic or hydrophobic surface and collagen I show no correlation to the described assertiveness during raw sausage fermentation (Janßen, Ehrmann, et al., 2018; Janßen, Eisenbach, et al., 2018). Moreover, the adhesion characteristics did not correlate with the cell wall characteristics. But, for *L. curvatus* TMW 1.167, TMW 1.407, TMW 1.439 and TMW 1.1381 glycosyl transferases were detected based on RAST annotation, which appear to be strain specific and may influence the ability to adhere to hydrophobic surface or collagen I. Also, Gtfs involved in HoPS production from sucrose, are surface displayed and could mediate adhesion.

Whenever these could not be proven in the genome sequences as a result of the loss of small plasmids in the sequencing procedure, the physiological tests on HoPS clearly predict that they are expressed in the respective strains.

4.12 Expression of colonization resistance

Adaptation to a specific habitat and suppression of competing strains of the autochthonous microbiome generally relies on the expression of colonization resistance. This term is widely discussed in the context of intestinal microbiota, and surprisingly virtually unknown in the community of researchers on food fermentation. Still, this principle follows some intrinsic logics and at the same time is naturally connected with functions of assertiveness. The raw sausage batter presents a wide variety of ecological niches, which are defined by many different substrates, decreasing pH, specific redox potential influenced by oxygen and nitrate (reduction), hydrophilic and hydrophobic surfaces and meat enzymes, namely proteases and lipases and last not least inhibitory functions, resulting from the fermentative action, bacteriocin formation, as well as biofilm and EPS formation. It appears as unlikely that one multitalented starter strain can be found, which can occupy all these niches alone, i.e., by combining all identified assertiveness functions of this work and thus realize competitive exclusion of autochthonous strains. Such a strain should e.g., effectively use citrate, ribose, arginine, agmatine, and produce HePS, Gtf, flagella and bacteriocin. Therefore, it is not surprising that the competitive sausage model study of Janßen et al. (Janßen et al., 2018) revealed the expression of colonization resistance promoting competitive exclusion as regularily achieved by pairs of partner strains as a frequent principle. Indeed, these authors showed that upon omission of a partner strain can have the effects of (i) loss of the assertiveness of the remaining partner, e.g., *L. curvatus* TMW 1.439 without partner TMW 1.1390, or (ii) adoption of another new partner strain to re-gain assertiveness, e.g., *L. curvatus* TMW 1.1390 cooperate with *L. curvatus* TMW 1.595, if *L. curvatus* TMW 1.439 is missing. A closer look into the accessory genomes of such partner strains showed that they possess complementary accessory genomes encoding different assertiveness, i.e., niche

occupying, traits, e.g complementary citrate or ribose metabolism like it is illustrated in Figure 54. This offers the possibility to predict fitting partner strains along their complementary accessory genomes.

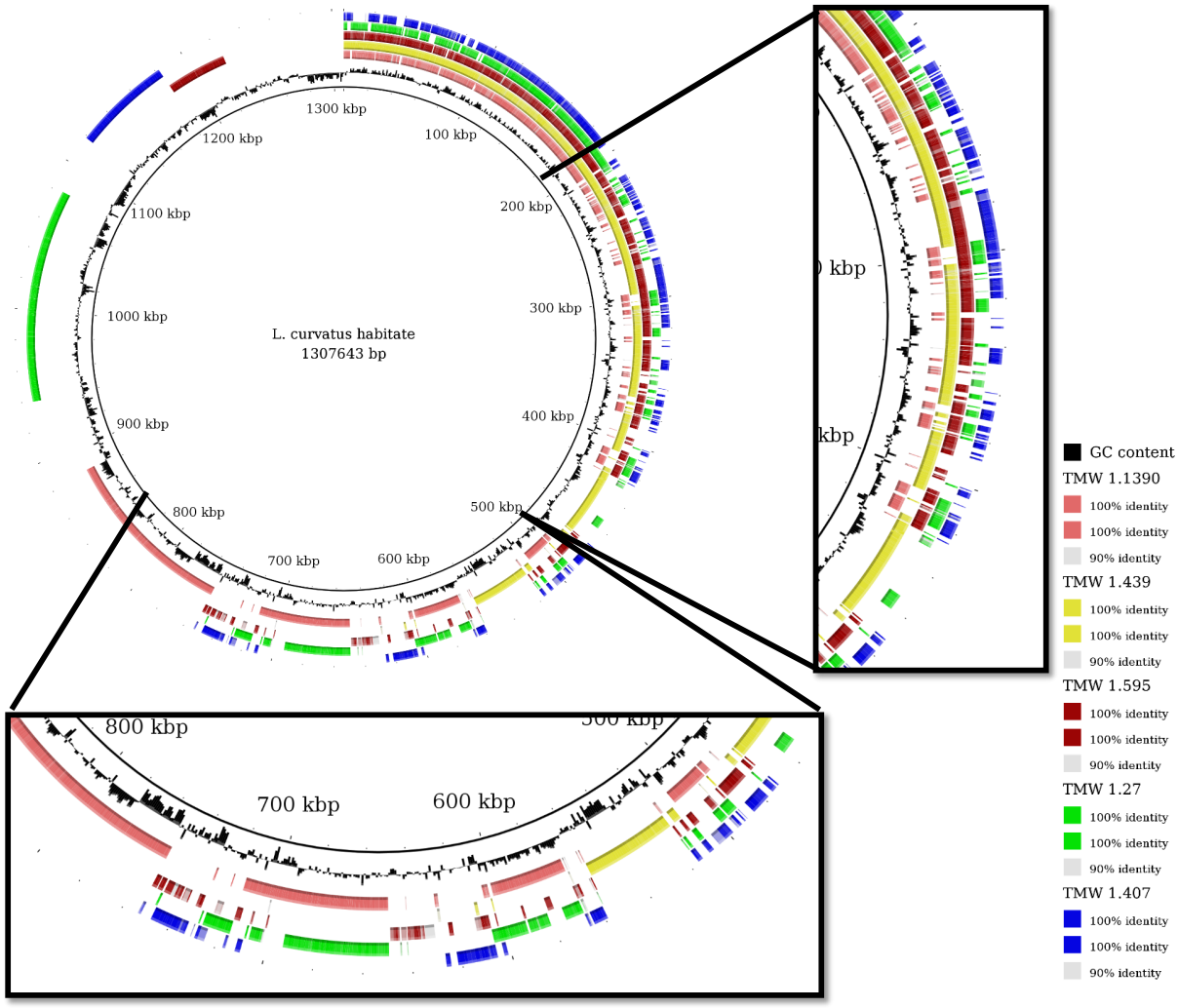

Figure 54: Complementary accessory-genome of tested starter strain set including *L. curvatus* TMW 1.27, TMW 1.407, TMW 1.595, TMW 1.439 and TMW 1.1390.

Still, within *L. sakei* and *L. curvatus* this possibility appears to only be exploitable within strains of the same species, because *L. sakei* and *L. curvatus* harbour too many (also non-annotated) differncies to enable interspecies partner prediction. The principle, which is proposed from the finding of this work for the selection of such strain combinations, should be the combination of as many as possible different assertiveness functions in as few as possible strains. It further appears that among the identified assertiveness functions

promoting colonization resistance and competitive exclusion there are stronger and weaker function. The strongest one may be judged as (multi) bacteriocin production, followed by arginine metabolism of *L. sakei*. Other such functions cannot be sorted along their quantitative contribution to assertiveness.

Taken together, this work shows that the principles of colonization resistance and competitive exclusion are a currently underestimated if not neglected in the strategies of starter culture development, which in many cases is just focussing on a rapid pH drop to ensure microbial safety. As a fast pH drop and application of only single strains limits the effectiveness and variety of metabolic functions, one could also expect an enhanced sensorical richness of a product derived from multi strain starter applications. So the exploitation of the idea of complementary accessory genomes presents a new age in starter culture development in many facettes.

4.13 Conclusion

Assertiveness in the raw meat matrix of sausage fermentation is a truly multifactorial trait, which can be correlated with genomic settings, rather than sources of isolation. This is because strains of *L. sakei* and *L. curvatus* can be isolated from many environments, while it is mostly unknown, whether these ecological niches, i.e. points of isolation, were true habitats in a sense that the strains had reached high numbers as a result of adaptation. For the time being, it cannot even be demonstrated that strains isolated from commercial cultures display assertiveness in sausage fermentation or have a specific set of “assertiveness traits”. This may be caused by the fact that strain specific tracking of a starter strain, hardly was achievable before, and autochthonous strains of the same species may have outcompeted the starter strain upon the fermentation and ripening. This work provides deep genomic insight and DMGs for the selection of strains with interesting sets of traits contributing to their assertiveness. This enables an essential move from an empirical trail and error approach to a knowledge-based starter culture development of single strains as well as of complementary strain sets. The general aim in such an approach must be the occupation by strain (sets) of

as many as possible ecological niches in the rich meat habitat by well-defined starter strains and leave no space for unwanted autochthonous strains with unknown properties.

The results of this work on comparative genomics were correlated with competition experiments done and described by Janßen *et al.* (Janßen et al., 2020; Janßen, Ehrmann, et al., 2018; Janßen, Eisenbach, et al., 2018). the results suggest that the assertiveness of the starter cultures is not determined by one special metabolic or physiological property, but multifactorial. Indeed, results of assertiveness monitoring suggest that it is unlikely that one strain can occupy all the niches of meat and thus express colonization resistance alone. Rather, this can be achieved by pairs or even groups of complementary strains with respective settings in their accessory genomes.

For strains of both *L. curvatus* and *L. sakei* species it was observed that strains are assertiveness in a co-existence (Janßen, Eisenbach, et al., 2018). As an example, *L. curvatus* TMW 1.439 and TMW 1.1390 are co-dominant during raw sausage fermentation. Genomic comparison of the accessory-genome reflects complementary (metabolic) traits in different strains of one species (Figure 15). Indeed, both strains encoded genes, which are not encoded in the genome of the other strain, e.g., nucleoside phosphorylases, phosphopentomutase, adenosine deaminase, ribose transporters. The results revealed that both strains are complementary based on their genomic properties and physiological strategies, which enables a co-existence and, furthermore, a co-dominance. Moreover, it was shown that one single strain of an assertive set is not able to be dominant during raw sausage fermentation if the second strain is missing (Janßen, Eisenbach, et al., 2018). Moreover, these results suggest a cooperation of the strains. Additionally, for *L. sakei* the same observations were done. *L. sakei* TMW 1.417 and TMW 1.1398 are co-dominant and differ in citrate, furthermore, *L. sakei* TMW 1.46 and TMW 1.578 assertive in a competitive experiment and they are different based on agmatine metabolism (Eisenbach, Geissler, Ehrmann, & Vogel, 2019; Janßen, Ehrmann, et al., 2018; Janßen). Actually, it has recently been demonstrated that *L. sakei* strains will generally outcompete *L. curvatus* strains in competitive interspecies competition (Janßen et al., 2020). This corroborates the general

importance of arginine/agmatine metabolism in *L. sakei versus* its absence in *L. curvatus* as the only general interspecies metabolic difference.

Still, properties exist, which can override the general principles of (i) assertive strain sets expressing colonization resistance and (ii) *L. sakei* as the faster growing species in meat, as observed for the multi-bacteriocin producer *L. curvatus* TMW 1.624, and for *L. sakei* TMW 1.1396. For the latter strain, single-strain assertiveness could not be so clearly explained. Still, *L. sakei* TMW 1.1396 produces a HePS, which can promote assertiveness, and it displayed tolerance to class II bacteriocins. So again, the role of bacteriocins is underlined, whenever it need not always be their production, but also or alternatively the immunity against them.

5 Summary

The traditional raw sausage fermentation is a complex process. Indeed, safe conversion of raw meat to a reproducible product is a challenge, as the raw material harbors autochthonous baceteria with unknown properties. For maintenance of the raw product character these cannot be inactivated before fermentation by heat treatments, and thus can take over fermentation, or pathogens are not sufficiently supressed by a slow onset of pH decrease. To get a non-biohazard, reproducible raw sausage, starter culture preparations lacking unwanted properties, basically biogenic amine formation of transmissible antibiotic resistance, are added to the sausage batter in high numbers. Such starter culture preparations comprise a combination of coagulase negative staphylococci, namely *Staphylococcus (S.) carnosus* and *S. xylosus* and lactobacilli. The latter quickly reduce the pH of the meat batter, which results in an acid environment and a reduced growth of autochthonous bacteria. Moreover, the pH reduction enables the sliceability of the sausage. The favoured lactobacilli for raw sausage starter cultures are strains of *Lactobacillus (L.) sakei* and *Lactobacillus (L.) curvatus* during raw sausage fermentation. Strains of both species are well adapted to the meat as environment. Both, *L. sakei* and *L. curvatus* can be isolated from at a high range of different sources, e.g., meat, sausages, sourdough, sauerkraut and kimchi. This ubiquitous occurrence suggests that there is a wide biodiversity within both species. The overall aim of this study was the characterization of biodioversity of *L. sakei* and *L. curvatus* at genomic level, and the identification of the main strategies, which contribute to assertiveness of specific strains during the raw sausage fermentation, to enable a predictive, knowledge-based raw sausage starter culture development.

To achieve this goal, 51 strains of *L. sakei* and 31 *L. curvatus* strains were screened by using different genomic methods and physiological experiments. As a starting point, results of RAPD-PCR fingerprinting, which had been done in previous studies, was used. Additionally, the strains were clustered based on their sub-proteome patterns generated by using MALDI-ToF-MS. Moreover, the physiological diversity of the strains was characterised by further

experiments. Firstly, the growth was observed after cold shock induction for 2 hours at -20°C and recovery, as compared to growth behaviour without any cold stress. Secondary, the growth in presence of oxidative stress, induced by addition of H_2O_2 (0 mM, 1.5 mM, and 3 mM), was determined. All generated data of each strain was used to analyse and visualize the biodiversity of both species *L. sakei* and *L. curvatus* by DAPC analysis.

Based on this analysis and the clusters generated by RAPD-PCR and MALDI-Tof MS, 10 representative strains of each species were selected for genomic analysis. High molecular DNA of the strains was isolated and the whole genome was sequenced with SMRT sequencing technology. In following steps, the generated genome sequences were established using assemblies, circularisation and resequencing, and finally annotated by RAST and NCBI annotation services. These annotations were used for further analysis of the selected strains. The genomic diversity was verified by basic comparisons, e.g., ANI calculation, identification of CRISPR-Cas sequences, putative bacteriocin gene clusters and putative prophage gene clusters at the genomes. Moreover, general genomic data of the sequenced genomes were compared like genome length, GC-content, number of coding sequences (CDS), number of identified plasmids. For a more detailed analysis the open reading frames (ORF) were used to establish the pan-genome, and to differentiate the core and accessory-genomes for each species by using CMG Biotools and BADGE. It was demonstrated that the selected strains are indeed representative for their respective species at the genomic level. This data pool enabled a more detailed comparison of the selected strains of each species, with the result to identify the genomic diversity.

First the metabolic properties were analysed with the focus on pathways, which were judged as tentatively important to growth in the meat environment and assertiveness during raw sausage fermentation. All enzymes important for the glycolysis are part of the core-genome, and all strains are predictively able to use glucose by a catabolic metabolism. Still, growth experiments revealed differences based on length of the detected lag phases and growth rates. Genes, associated with the catabolic glycerol metabolism, showed point mutations, which predict that the function of encoded enzymes is impaired, and the glycerol metabolism

is affected. These differences were also observed by a growth experiment, which showed physiological differences in the catabolic glycerol metabolism. An additional important substrate is ribose. It was shown that the ribose operon is not part of the core-genome of *L. curvatus*, whereas it is highly conserved and encoded in the core-genome of *L. sakei*. For the ribose operon of *L. curvatus* major differences were detected in the genomic structure and the encoded transporter system. A growth experiment in chemically defined medium in combination with a HPLC analysis revealed that the *rbsUDKR* (phosphotransferase transporter system (PTS)) operon results in a more efficient and faster ribose uptake and growth compared to the *RDACBK* (ABC transporter system) operon. This genomic and physiological difference is a predicted advantage for the assertiveness of a strain during raw sausage fermentation.

For *L. sakei* metabolic differences were also detectable. Strains could be grouped into three groups, which encoded no citrate cluster, or encoded either citrate cluster I or cluster II. Both clusters differ based on the transporter system (Mg^{2+}/citrate complex transporter or citrate permease). Moreover, within each “citrate cluster”-group genomic differences were detected. Mutations in transporter sequences resulted in changed transmembrane transporter structures and differences of citrate uptake efficiency. Also, mutations in sequences of regulatory gene components suggest changes in citrate uptake efficiency. These physiological differences predictively influence the assertiveness and occupation of ecological niches in meat. A second important metabolic pathway in *L. sakei*, is the arginine-diminase (ADI-) and agmatine-deiminase pathway. ADI-pathway is encoded in the core-genome of *L. sakei*, whereas it was not identified at any genome of *L. curvatus* strains. Moreover, the genes associated with the agmatine-deiminase pathway were identified in the genome of four *L. sakei* strains. A few genes carried mutations in the sequences and physiological experiments revealed that these mutations changed the function of the encoded enzymes. This results in an incomplete functionality of the agmatine-deiminase pathway. Nevertheless, both pathways enable a regulation of the milieu’s pH. This dedicated

compensation of acid stress and energy generation in the ADI pathway predict an generally enhanced assertiveness during the raw sausage fermentation of *L. sakei* over *L. curvatus*.

Further physiological properties characterize the adaptation to a defined environment and the assertiveness during raw sausage fermentation. As an example, the reaction to and regeneration upon cold shock. Starter cultures are freeze-dried for storage and encounter low temperature at the beginning of raw sausage fermentation. It was possible to detect differences between strains of both species based on the membrane damage and growth after cold shock induction and regeneration for 2 hours. Strains of both species could be differentiated within two groups because of the observed membrane damage after cold shock. All strains expressed the ability to regenerate the membrane damage after 2 hours of regeneration. These physiological observations and a genomic comparison revealed that there are diagnostic marker genes, which may be characteristic for each group and exert differences in their assertiveness in sausage fermentation.

Another predicted factor for adaptation to defined environment is the ability of adhesion to a defined surface. Specific surface proteins and the ability to form exopolysaccharides (EPS) influenced this property. *L. curvatus* TMW 1.27 and TMW 1.1390 encoded a gene cluster associated with the formation of flagella, and physiological experiments demonstrated motility for both strains. Moreover, it was possible to identify genomic differences of the encoded flagellin, which predictively influences the adhesion properties, because of the protein structure. Indeed, this difference was observed along the adhesion to collagen I.

Furthermore, the analysis of the strains revealed differences based on EPS production. On the one hand, a few strains are able to form HoPS in presence of sucrose, on the other hand a few strains encoded gene clusters associated with the production of HePS. Some of these (predicted) HePS and HoPS producers appeared to express the abilty to adhere to either hydrobobic or hydrophilic surfaces or collagen I under defined conditions. However, there was no significant correlation detectable between the (predicted) ability to produce EPS and the ability to adhere to defined surfaces.

With *L. curvatus* TMW 1.624 a special multi-bacteriocin producing strain could be characterized, which was able to suppress virtually all other strains of *L. sakei* and *L. curvatus*. Still, some strains expressing resistance to class II bacteriocins, delineate bacteriocin resistance as underestimated assertiveness marker in sausage fermentation.

Taken together, the genomic and physical analysis suggests that both *L. curvatus* and *L. sakei* are diverse, and their biodiversity reflects the adaption capability to many habitats. The comparison of the genomic data of this work with sausage fermentations involving the same strains in competitive settings, revealed clear correlations of genomically predicted assertiveness functions to real assertiveness in sausage fermentation. While no defined single marker gene encoding “assertiveness” could be found, a set of complementary strains as predicted by their complementary accessory genomes is suggested to occupy as many as possible niches in the rich meat habitat. These partner strains can effectively suppress the growth of unwanted autochthonous strains. Alternatively, rare multi-bacteriocin producing strains as *L. curvatus* TMW 1.624 can mostly override the sausage microbiota of lactobacilli.

6 Zusammenfassung

Die traditionelle Form der Rohwurstreifung ist ein komplexer Prozess. Die größte Herausforderung stellt das Ausgangsmaterial, das rohe Fleisch dar, weil es autochthone Bakterien mit unbekannten Eigenschaften enthält. Diese können vor der Fermentation nicht durch Wärmebehandlung des Rohwurstbräts inaktiviert werden, ohne den rohen Charakter der Würste zu verlieren. In der Folge können diese den Fermentationsverlauf bestimmen, oder Pathogene werden durch zu langsam absinkenden pH nicht ausreichend unterdrückt. Für die reproduzierbare Herstellung einer sicheren Rohwurst, werden dem Brät Starterkulturen ohne unerwünschte Eigenschaften, insbesondere biogene Aminbildung und übertragbare Antibiotikaresistenz in hohen Zellzahlen zugegeben. Diese Starterkulturen bestehen meist aus einer Mischung Koagulase-negativer Staphylokokken und Laktobazillen. Auf Seiten der Laktobazillen werden häufig Stämme von *Lactobacillus (L.) sakei* und

Lactobacillus (L.) curvatus eingesetzt. Beide Spezies sind an Fleisch als Medium angepasst. Stämme der beiden Spezies können aus einer Vielzahl verschiedener Habitate – sowohl mit Fleisch als auch Pflanzen assoziierte – isoliert werden. Dieses verbreitete Vorkommen lässt eine hohe Diversität der genetischen Ausstattungen der Stämme vermuten. Das Ziel dieser Arbeit war es die Biodiversität von *L. sakei* und *L. curvatus* auf genomischer Ebene zu erfasssen und die zur Durchsetzungsfähigkeit, während der Rohwurstfermentation beitragenden Eigenschaften zu identifizieren, und damit eine wissensbasierte, zielgerichtete Starterkulturentwicklung zu ermöglichen.

Daher wurden zunächst 51 *L. sakei* und 31 *L. curvatus* Stämme mit verschiedenen Experimenten genetisch und physiologisch gescreent. Als Ausgangspunkt wurde das RAPD-PCR Fingerprinting aus einem vorausgegangenen Projekt genutzt (Dissertation, S. Freiding, TUM). Zusätzlich wurden alle Stämme basierend auf dem stammspezifischen Sub-Proteom, welches mit Hilfe des MALDI-ToF-MS erstellt wurde, in Gruppen zusammengefasst. Zusätzlich wurde mit weiterführenden Experimenten die physiologische Diversität der Stämme untersucht. Zum einen wurde das Wachstumsverhalten nach einer Kälteschock-Induzierung mit einer Dauer von 2 Stunden bei -20°C im Vergleich zu einem Wachstum ohne Kälteeinwirkung aufgezeichnet. Zum anderen wurde das Wachstumsverhalten unter Einfluss verschiedener Konzentration von H_2O_2 (O mM, 1,5 mM und 3 mM) ausgewertet. All diese gewonnen Daten zu den Stämmen wurden genutzt, um die Biodiversität der beiden Spezies mit Hilfe einer DAPC Analyse auszuwerten und darstellen.

Basierend auf dieser Analyse und den Clustern aus der RAPD-PCR und MALDI-ToF-MS wurden jeweils 10 repräsentative Stämme pro Spezies für die folgende Genomanalysen ausgewählt. Zunächst wurden die hochmolekulare DNA dieser Stämme isoliert und mit Hilfe der SMRT Sequenzierung das gesamte Genom jedes Stammes sequenziert. Anschließend wurden diese Genomdaten durch Assemblierung, Zirkularisierung und Resequenzierung vorbereitet, um die gewonnenen Genomseqeunzen sowohl durch RAST als auch NCBI zu annotieren. Die Annotationen wurden dann für die weiteren Analysen der Stämme genutzt. Um zunächst die Diversität der Stämme zu erfassen wurden erste grundlegende Vergleiche

durchgeführt, wie z.B. die ANI-Kalkulation, CRISPR/Cas Sequenzen, potenzielle Bakteriozin-Gencluster und Nachweise für Prophagen-Sequenzen wurden in den Genomen identifiziert. Auch die Daten der jeweiligen Sequenzen wurden verglichen (Genomlänge, GC-Gehalt, Anzahl der kodierenden Sequenzen, Anzahl identifizierter Plasmide etc.). Mit Hilfe von CMG Biotool und BADGE wurden im folgenden Schritt die annotierten ORF genutzt, um das Pan-Genom beider Spezies zu bestimmen und dieses in das Core- und Accessory-Genom aufzuteilen. Es konnte gezeigt werden, dass die ausgewählten Stämme repräsentativ für die genomische Vielfalt von *L. sakei* und *L. curvatus* sind.

Basierend auf diesen Daten war es möglich, die Stämme der jeweiligen Spezies genauer miteinander zu vergleichen, mit dem Ziel die Diversität auf Genomebene zu identifizieren. Zunächst wurde der Fokus auf die grundlegenden Stoffwechselwege gelegt, die auch im Medium Fleisch wichtig sind. Erste Analysen zeigten, dass alle Stämme im Core-Genom die wichtigen Enzyme der Glykolyse codieren und somit auch physiologisch die gleiche Voraussetzung haben. Gleichwohl konnten Unterschiede im Wachstum bezüglich der zeitlichen Länge der Wachstumsphasen beobachtet werden. Bei den Genen, die mit dem Glycerolmetabolismus assoziiert werden konnten, wurden Punktmutationen identifiziert, die vermuten lassen, dass die Funktion einzelner Enzyme verändert ist, was wiederum Einfluss auf den katabolen Metabolismus des Glycerols hat. Diese Unterschiede konnten auch in einem Wachstumsexperiment nachgewiesen werden, das zeigte, dass nicht alle Stämme gleichermaßen in der Lage sind, Glycerol für das Zellwachstum zu nutzen. Ein weiteres wichtiges Substrat ist Ribose. Es konnte gezeigt werden, dass das Ribose Operon nicht im Kern-Genom von *L. curvatus* kodiert wird, sondern Teil des Akzessorischen Genom ist. Gleichwohl ist dieses Operon hochkonserviert im Core-Genom von *L. sakei* zu finden. Andererseits konnten für die Stämme von *L. curvatus* zwei Hauptunterschiede ausgemacht werden. Zum einen unterscheiden sich beide Operons in ihrer Struktur und zum anderen konnten zwei unterschiedliche Transportersysteme identifiziert werden. Ein Wachstumsexperiment in Kombination mit einer HPLC-Analyse zeigte, dass Stämme, die das Operon *rbsUDKR* (Phosphotransferasesystem (PTS) als Tranporter) in ihrem Genom

tragen, in der Aufnahme von Ribose effizienter bzw. schneller waren, im Vergleich zu den Stämmen, die das Operon *rbsRDACBK* (ABC Transporter System) im Genom kodieren. Dieser genetische und physiologische Unterschied ist ein wichtiger Vorteil bei der Konkurrenz mit anderen Mikroorganismen im gleichen Habitat und somit auch ein wichtiger Faktor bei der Durchsetzungsfähigkeit in einem komplexen System, wie der Rohwurstreifung.

Für die Stämme von *L. sakei* konnten ebenfalls metabolische Unterschiede identifiziert werden. Zum einen konnten die sequenzierten Stämme in drei Gruppen unterteilt werden, die entweder eines von zwei verschiedene Citrat-Genclustern kodieren oder keines. Auch hier gibt es Unterschiede basierend auf dem Transporter System (Mg^{2+}/Citrat-Komplex Transporter oder Citrat-Permease). Darüber hinaus konnten auch innerhalb dieser drei Gruppen genetische Unterschiede identifiziert werden. Mutationen in Transporter-Sequenzen führen zu Änderungen der Transporter-Struktur und damit voraussichtlich zu Unterschieden in der Effizienz der Citrate-Aufnahme. Auch die Mutation eines regulatorisch-wirksamen Gens zeigt eine Veränderung der Aufnahme des Citrates. Auch diese physiologischen Unterschiede können sich auf die Durchsetzungsfähigkeit und Besetzung einer ökologischen Nische im Fleisch auswirken. Weitere Unterschiede für die metabolischen Fähigkeiten in *L. sakei* konnten im Arginin-Deiminase (ADI-) und Agmatin-Deiminase Weg beobachtet werden. Alle Genome der *L. sakei* Stämme kodieren den ADI-Weg, welcher in keinem der *L. curvatus* Genome gefunden wurde. Darüber hinaus konnten in vier Stämmen von *L. sakei* auch Gene identifiziert werden, die mit dem Agmatine-Deiminase Pathway assoziiert sind. Einige Gene weisen jedoch Mutationen auf und physiologische Experimente zeigen, dass diese Mutationen die Funktion der entsprechenden Enzyme verändern, so dass nicht alle der 4 Stämme einen voll funktionsfähigen Agamtine-Deiminase Weg kodieren. Beide Stoffwechselwege ermöglichen den Stämmen eine Regulierung des pH im umgebenden Milieu. Eine erfolgreiche Kompensierung des Säurestresses und die zusätzliche Möglichkeit zur Energiegewinnung beeinflusst die Möglichkeit sich gegen Konkurrenten in einer sauren Umgebung durchzusetzen und ist somit ebenfalls ein wichtiger Faktor in der

Durchsetzungsfähigkeit von *L. sakei* in der Rohwurstfermentation, der auch die grundsätzliche Überlegenheit von *L. sakei* gegenüber *L. curvatus* begründet.

Neben den metabolischen Fähigkeiten gibt es auch noch weitere physiologische Aspekte, die sich auf die Durchsetzungsfähigkeit und Anpassung an die Umgebung in der Rohwurstfermentation auswirken. So zum Beispiel die Reaktion auf und Regeneration nach einem Kältestress. Starterkulturen werden zum einen zur Lagerung gefriergetrocknet und, zum anderen zu Beginn der Fermentation niedrigen Temperaturen ausgesetzt. Es konnten Unterschiede für Stämme beider Spezies in Bezug auf die Membranschädigung als auch auf das Wachstum nach einem Kälteschock und einer Regeneration nach 2 Stunden beobachtet werden. Stämme beider Spezies konnten in zwei Gruppen aufgeteilt werden, basierend auf der Membranschädigung direkt nach der Kälteschockanwendung. Alle Stämme zeigten eine Fähigkeit zur Regeneration der Schäden nach 2 Stunden. Diese physiologischen Beobachtungen in Kombination mit einem genetischen Vergleich, ermöglichten eine Identifizierung von diagnostischen Marker Genen, die möglicherweise charakteristisch für die jeweilige Gruppe sind.

Ein weiterer Einflussfaktor für die erfolgreiche Anpassung an das Habitat der Rohwurst ist die Adhäsion. Diese wird durch Oberflächenproteine, oder auch Exopolysaccharide (EPS) beeinflusst. Für *L. curvatus* TMW 1.27 und *L. curvatus* TMW 1.1390 konnte die Fähigkeit zur Motilität durch die Bildung von Flagellen nachgewiesen werden. Zudem unterscheiden sich beide Stämme genetisch aufgrund des kodierten Flagellins, welches wiederum aufgrund seiner Proteinstruktur die Adhesionseigenschaften einer Zelle beeinflusst. Diese Unterschiede zur Adhesion an Collagen I konnten in einem Experiment nachgewiesen werden.

Zusätzlich konnten Unterschiede in der EPS Bildung festgestellt werden. Zum einen sind einige Stämme in der Lage in Anwesenheit von Sucrose Homopolysaccharide zu bilden, zum anderen konnte ein Heteropolysaccharid-Gencluster in einigen Genomen identifiziert werden. Einige dieser EPS Produzenten zeigten auch unter definierten Bedingungen Adhesionsfähigkeiten entweder zu einer hydrophoben oder hydrophilen Oberfläche oder zu

Collagen I. Allerdings konnte keine eindeutige Korrelation zwischen der Fähigkeit zur EPS Produktion und der Adhesion nachgewiesen werden.

Mit *L. curvatus* TMW 1.624 konnte ein Multi-Bakteriozin Produzent charakterisiert werden, der in der Lage war nahezu alle anderen *L. sakei* and *L. curvatus* Stämme zu unterdrücken. Dennoch exprimierten einige Stämme eine Resistenz gegenüber Class II Bakteriozinen und zeigten damit an, dass unabhängig von der Bakteriozinbildung die Bakteriozinresistenz ein unterschätzter Faktor in der Durchsetzungsfähigkeit in der Rohwurstfermentation sein kann.

Zusammenfassend zeigt die genomische und physiologische Analyse, dass sowohl *L. curvatus* als auch *L. sakei* divers sind, und diese Biodiversität ihre Anpassungsfähigkeit an unterschiedliche Habitate begründet. Der Vergleich der genomischen Daten aus dieser Arbeit mit Rohwurstexperimenten, in denen dieselben Stämme unter Wettbewerbsbedingungen eingesetzt wurden, zeigte klare Korrelationen von genomisch vorhergesagten Determinanten mit deren tatsächlicher Durchsetzungsfähigkeit in der Fermentation. Während kein einzelnes Markergen für “Durchsetzungsfähigkeit” gefunden werden konnte, war es entlang komplementärer Akzessorischer Genome von Stämmen, Partner vorherzusagen, die eine möglichst große Breite der ökologischen Nischen im reichen Habitat Rohwurst besetzen können. Diese Partnerstämme können effektiv das Wachstum unerwünschter autochthoner Stämme durch die Ausprägung einer Kolonisierungsresistenz unterdrücken. Alternativ können seltene Multi-Bakteriozin Bildner wie *L. curvatus* TMW 1.624 die Laktobazillen Mikrobiota in der Rohwurstmatrix weitgehend beherrschen.

7 References

Alikhan, N.-F., Petty, N. K., Zakour, N. L. B., & Beatson, S. A. (2011). BLAST Ring Image Generator (BRIG): simple prokaryote genome comparisons. *BMC Genomics, 12*(402).

Altschul, S., Gish, W., Miller, W., Myers, E., & Lipman, D. (1990). Basic local alignment search tool. *J Mol Biol, 215*, 403-410.

Annous, B. A., Kozempel, M. F., & Kurantz, M. J. (1999). Changes in membrane fatty acid composition of *Pediococcus* sp. strain NRRL B-2354 in response to growth conditions and its effect on thermal resistance. In (Vol. 65, pp. 2857-2862): Appl. Environ. Microbiol.

Archibald, F. S., & Fridovich, I. (1981). Manganese, superoxide dismutase, and oxygen tolerance in some lactic acid bacteria. In (Vol. 146, pp. 928-936): J. Bacteriol.

Arndt, D., Grant, J. R., Marcu, A., Sajed, T., Pon, A., Liang, Y., & Wishart, D. S. (2016). PHASTER: a better, faster version of the PHAST phage search tool. *Nucleic Acids Research, 44*.

Axelsson, L., & Ahrne, S. (2000). Lactic acid bacteria. In (pp. 365-386): Applied microbial systematics. Kluwer Academic Publishers, Dodrecht.

Aziz, R. K., Bartels, D., Best, A. A., DeJongh, M., Disz, T., Edwards, R. A., Formsma, K., Gerdes, S., Glass, E. M., Kubal, M., Meyer, F., Olsen, G.J., Olson, R., Osterman, A.L., Overbeek, R.A., McNeil, L.K., Paarmann, D., Paczian, T., Parrello, B., Pusch, G.D., Reich, C., Stevens, R., Vassieva, O., Vonstein, V., Wilke, A., Zagnitko, O. (2008). The RAST Server: rapid annotations using subsystems technology. *BMC Genomics, 9*, 75. doi:10.1186/1471-2164-9-75

Bardy, S. L., Ng, S. Y., & Jarrell, K. F. (2003). Prokaryotic motility structures. *Microbiology, 149*(Pt 2), 295-304. doi:10.1099/mic.0.25948-0

Behr, J., Geissler, A. J., Preissler, P., Ehrenreich, A., Angelov, A., & Vogel, R. F. (2015). Identification of ecotype-specific marker genes for categorization of beer-spoiling *Lactobacillus brevis*. *Food Microbiol, 51*, 130-138. doi:10.1016/j.fm.2015.05.015

Behr, J., Geissler, A. J., Schmid, J., Zehe, A., & Vogel, R. F. (2016). The Identification of novel diagnostic marker genes for the detection of beer spoiling *Pediococcus* damnosus strains using the BlAst Diagnostic Gene findEr. *PLoS One, 11*(3), e0152747. doi:10.1371/journal.pone.0152747

Benito, M. J., Martin, A., Aranda, E., Perez-Nevado, F., Ruiz-Moyano, S., & Cordoba, M. G. (2007). Characterization and selection of autochthonous lactic acid bacteria isolated from traditional Iberian dry-fermented salchichon and chorizo sausages. *J Food Sci, 72*(6), M193-201. doi:10.1111/j.1750-3841.2007.00419.x

Berthier, F., Zagorec, M., Champomier-Verges, M. C., & Morel-Deville, F. (1996). High frequency transformation of *Lactobacillus sake* by electroporation. In (Vol. 142, pp. 1273-1279): Microbiology.

Bobay, L.-M., Touchon, M., & Rocha, E. P. C. (2014). Pervasive domestication of defective prophages by bacteria. *PNAS, 111*(33), 12127-12132.

Boorsma, A., van der Rest, M. E., Lolkema, J. S., & Konings, W. N. (1996). Secondary transporters for citrate and the Mg2+ - citrate complex in *Bacillus subtilis* are homologous proteins. *Journal of Bacteriology, 178*(21), 6216-6222.

Bourret, R. B., Charon, N. W., Stock, A. M., & West, A. H. (2002). Bright lights, abundant operons--fluorescence and genomic technologies advance studies of bacterial locomotion and signal transduction: review of the BLAST meeting, Cuernavaca, Mexico, 14 to 19 January 2001. *J Bacteriol, 184*(1), 1-17.

Bover-Cid, S., Hugas, M., Izquierdo-Pulido, M., & Vidal-Carou, M. C. (2001). Amino acid-decarboxylase activity of bacteria isolated from fermented pork sausages. *Int J Food Microbiol, 66*(3), 185-189.

Buntin, N., de Vos, W. M., & Hongpattarakere, T. (2017). Variation of mucin adhesion, cell surface characteristics, and molecular mechanisms among *Lactobacillus plantarum*

isolated from different habitats. *Appl Microbiol Biotechnol, 101*(20), 7663-7674. doi:10.1007/s00253-017-8482-3

Camacho, C., Coulouris, G., Avagyan, V., Ma, N., Papadopoulos, J., Bealer, K., & Madden, T. L. (2009). BLAST+: architecture and applications. In (Vol. 10, pp. 421): BMC Bioinformatics.

Chagnot, C., Venien, A., Renier, S., Caccia, N., Talon, R., Astruc, T., & Desvaux, M. (2017). Colonisation of meat by *Escherichia coli* O157:H7: Investigating bacterial tropism with respect to the different types of skeletal muscles, subtypes of myofibres, and postmortem time. *Front Microbiol, 8*, 1366. doi:10.3389/fmicb.2017.01366

Chaillou, S., Champomier-Verges, M. C., Cornet, M., Crutz-Le Coq, A. M., Dudez, A. M., Martin, V., Beaufils, S., Darbon-Rongere, E., Bossy, R., Loux, V., Zagorec, M. (2005). The complete genome sequence of the meat-borne lactic acid bacterium *Lactobacillus sakei* 23K. *Nat Biotechnol, 23*(12), 1527-1533. doi:10.1038/nbt1160

Chaillou, S., Daty, M., Baraige, F., Dudez, A. M., Anglade, P., Jones, R., Alpert, C.A., Champomier-Verges, M.C., Zagorec, M. (2009). Intraspecies genomic diversity and natural population structure of the meat-borne lactic acid bacterium *Lactobacillus sakei*. *Appl Environ Microbiol, 75*(4), 970-980. doi:10.1128/AEM.01721-08

Champomier Verges, M. C., Zuniga, M., Morel-Deville, F., Perez-Martinez, G., Zagorec, M., & Ehrlich, S. D. (1999). Relationships between arginine degradation, pH and survival in *Lactobacillus sakei*. *FEMS Microbiol Lett, 180*(2), 297-304.

Champomier-Vergès , M.-C., Maguin , E., Mistou , M.-Y., Anglade, P., & Chich , J.-F. (2002). Lactic acid bacteria and proteomics: current knowledge and perspectives. In (Vol. 771, pp. 329-342): J. Chromatogr.

Champomier-Vergès, M.-C., Maguin, E., Mistou, M.-Y., Anglade, P., & Chich, J.-F. (2002). Lactic acid bacteria and proteomics: current knowledge and perspectives. In (Vol. 771, pp. 329-342): J. Chromatogr.

Chin, C. S., Alexander, D. H., Marks, P., Klammer, A. A., Drake, J., Heiner, C., Clum, A., Copeland, A., Huddleston, J., Eichler, E.E., Turner, S.W., Korlach, J. (2013). Nonhybrid, finished microbial genome assemblies from long-read SMRT sequencing data. *Nat Methods, 10*(6), 563-569. doi:10.1038/nmeth.2474

Claesson, M. J., van Sinderen, D., & O'Toole, P. W. (2007). The genus Lactobacillus--a genomic basis for understanding its diversity. *FEMS Microbiol Lett, 269*(1), 22-28. doi:10.1111/j.1574-6968.2006.00596.x

Cocolin L., D. P., Rantisou K. (2011). Biodiversity and dynamics of meat fermentation: the contribution of molecular methods for a better comprehension of a complex ecosystem. In (Vol. 89, pp. 296-302): Meat science.

Condon, S. (1987). Responses of lactic acid bacteria to oxygen. In (Vol. 46, pp. 269-280): FEMS Microbiol. Rev.

Cousin, F. J., Lynch, S. M., Harris, H. M., McCann, A., Lynch, D. B., Neville, B. A., Irisawa,T., Okada, S., Endo, A., O'Toole, P. W. (2015). Detection and genomic characterization of motility in *Lactobacillus curvatus*: confirmation of motility in a species outside the *Lactobacillus salivarius* clade. *Appl Environ Microbiol, 81*(4), 1297-1308. doi:10.1128/AEM.03594-14

Dal Bello, F., Walter, J., Hammes, W. P., & Hertel, C. (2003). Increased complexity of the species composition of lactic acid bacteria in human feces revealed by alternative incubation condition. In (Vol. 45, pp. 455-463): Micron. Ecol.

de Jong, A., van Hijum, S. A., Bijlsma, J. J., Kok, J., & Kuipers, O. P. (2006). BAGEL: a web-based bacteriocin genome mining tool. *Nucleic Acids Res, 34*(Web Server issue), W273-279. doi:10.1093/nar/gkl237

de Man, J. D. R., M.; Sharpe, M.E. (1960). A medium for the cultivation of lactobacilli. *J Appl Bact., 23*, 130-135.

Delauney, A. J., Cheon, C. I., Snyder, P. J., & Verma, D. P. (1990). A nodule-specific sequence encoding a methionine-rich polypeptide, nodulin-21. In (Vol. 14, pp. 449-451): Plant Mol. Biol.

Derzelle, S., Hallet, B., Ferain, T., Delcour, J., & Hols, P. (2002). Cold shock induction of the cspL gene in *Lactobacillus plantarum* involves transcriptional regulation. *J Bacteriol, 184*(19), 5518-5523.

Derzelle, S., Hallet, B., Francis, K. P., Ferain, T., Delcour, J., & Hols, P. (2000). Changes in cspL, cspP, and cspC mRNA abundance as a function of cold shock and growth phase in *Lactobacillus plantarum*. *J Bacteriol, 182*(18), 5105-5113.

Diep, D. B., Skaugen, M., Salehian, Z., Holo, H., & Nes, I. F. (2007). Common mechanisms of target cell recognition and immunity for class II bacteriocins. *Proc Natl Acad Sci U S A, 104*(7), 2384-2389. doi:10.1073/pnas.0608775104

Drider, D., Bekal, S., & Prevost, H. (2004). Genetic organization and expression of citrate permease in lactic acid bacteria. *Genetics and molecular Research, 3*(2), 273-281.

Duwat, P., Ehrlich, S. D., & Gruss, A. (1995). The recA gene of *Lactococcus lactis*: characterization and involvement in oxidative and thermal stress. In (Vol. 17, pp. 1121-1131): Mol. Microbiol.

Eid, J., Fehr, A., Gray, J., Luong, K., Lyle, J., Otto, G., Peluso, P., Rank, D., Baybayan, P., Bettman, B., Bibillo, A., Bjornson, K., Chaudhuri, B., Christians, F., Cicero, R., Clark, S., Dalal, R., Dewinter, A., Dixon, J., Foquet, M., Gaertner, A., Hardenbol, P., Heiner, C., Hester, K., Holden, D., Kearns, G., Kong, X., Kuse, R., Lacroix, Y., Lin, S., Lundquist, P., Ma, C., Marks, P., Maxham, M., Murphy, D., Park, I., Pham, T., Phillips, M., Roy, J., Sebra, R., Shen, G., Sorenson, J., Tomaney, A., Travers, K., Trulson, M., Vieceli, J., Wegener, J., Wu, D., Yang, A., Zaccarin, D., Zhao, P., Zhong, F., Korlach, J., Turner, S. (2009). Real-time DNA sequencing from single polymerase molecules. *Science, 323*(5910), 133-138. doi:10.1126/science.1162986

Eisenbach, L., Geissler, A. J., Ehrmann, M. A., & Vogel, R. F. (2019). Comparative genomics of *Lactobacillus sakei* supports the development of starter strain combinations. *Microbiol Res, 221*, 1-9. doi:10.1016/j.micres.2019.01.001

Eisenbach, L., Janßen, D., Ehrmann, M. A., & Vogel, R. F. (2018). Comparative genomics of *Lactobacillus curvatus* enables prediction of traits relating to adaptation and strategies of assertiveness in sausage fermentation. *Int J Food Microbiol, 286*, 37-47.

Engesser, D. M., & Hammes, W. P. (1994). Non-heme catalase activity of lactic acid bacteria. In (Vol. 17, pp. 11-19): Syst. Apple. Microbiol.

Fernandez Murga, M. L., Bernie, D., Font de Valdez, G., & Disalvo, A. E. (1999). Permeability and stability properties of membranes formed by lipids extracted from *Lactobacillus acidophilus* grown at different temperatures. In (Vol. 364, pp. 115-121): Arch. Biochem. Biophys.

Fraunhofer, M. E. (2018). Characterization of EPS-producing brewery-associated lactobacilli. *Technische Universität München, Germany*.

Fraunhofer, M. E., Geissler, A. J., Jakob, F., & Vogel, R. F. (2017). Multiple genome sequences of exoploysaccharide-producing, brewery-associated *Lactobacillus brevis* strains. *american society for microbiology, 5*(26).

Freiding, S., Gutsche, K. A., Ehrmann, M. A., & Vogel, R. F. (2011). Genetic screening of *Lactobacillus sakei* and *Lactobacillus curvatus* strains for their peptidolytic system and amino acid metabolism, and comparison of their volatilomes in a model system. *Syst Appl Microbiol, 34*(5), 311-320. doi:10.1016/j.syapm.2010.12.006

Fu, D., Beeler, T., & Dunn, T. (1994). Sequence mapping and disruption of CCC1, a gene that cross-complements the Ca^{2+}-sensitive phenotype of *csg1* mutants. In (Vol. 10, pp. 515-521): Yeast.

Geissler, A. J., Behr, J., & Vogel, R. F. (2016). Multiple genome sequences of the important beer-spoiling species *Lactobacillus backii*. *Genome Announc, 4*(4). doi:10.1128/genomeA.00826-16

Geissler, A. J., Behr, J., von Kamp, K., & Vogel, R. F. (2016). Metabolic strategies of beer spoilage lactic acid bacteria in beer. *Int J Food Microbiol, 216*, 60-68. doi:10.1016/j.ijfoodmicro.2015.08.016

Geissler, A. J., Celano, G., Minervini, F., Gobbetti, M., & Vogel, R. F. (2017). Genomic diversity of Lactobacillus sanfranciscensis. *4th International Conference on Microbial Diversity, October 24.-26. 2017, Bari, Italy*.

Glaser, P., Frangeul, L., Buchrieser, C., Amend, A., Baquero, F., Berche, P., Bloecker, H.,

Brandt, P., Chakraborty, T., Charbit, A., Chetouani, F., Couve, E., de Daruvar, A., Dehoux, P., Domann, E., Dominguez-Bernal, G., Duchaud, E., Durand, L., Dussurget, O., Entian, K.-D., Fsihi, H., Garcia-Del Portillo, F., Garrido, P., Gautier, L., Goebel, W., Gomez-Lopez, N., Hain, T., Hauf, J., Jackson, D., Jones, L.-M., Karst, U., Kreft, J., Kuhn, M., Kunst, F., Kurapkat, G., Madueno, E., Maitournam, A., Mata Vicente, J., Ng, E., Nordsiek, G., Novella, S., de Pablos, B., Perez-Diaz, J.-C., Remmel, B., Rose, M., Rusniok, C., Schlueter, T., Simoes, N., Tierrez, A., Vazquez-Boland, J.-A., Voss, H., Wehland, J., Cossart, P. (2001). Comparative genomics of Listeria species. In (Vol. 294, pp. 849-852): Science.

Gottesman, S., Roche, E., Zhou, Y., & Sauer, R. T. (1998). The ClpXP and ClpAP proteases degrade proteins with carboxylate-terminal peptide tails added by the SsrA-tagging system. In (Vol. 12, pp. 1338-1347): Genes Dev.

Graumann, P., & Marahiel, M. A. (1996). Some like it cold: response of microorganisms to cold shock. *Arch Microbiol, 166*, 293-300.

Graumann, P., & Marahiel, M. A. (1998). A superfamily of proteins that contan the coldshock domain. *TIBS, 23*, 286-290.

Grissa, I., Vergnaud, G., & Pourcel, C. (2007). The CRISPRdb database and tools to display CRISPRs and to generate dictionaries of spacers and repeats. *BMC Bioinformatics, 8*, 172. doi:10.1186/1471-2105-8-172

Gryllos, I., Levin, J. C., & Wessels, M. R. (2003). The CsrR/CsrS two-component system of group A *Streptococcus* responds to environmental Mg^{2+}. In (Vol. 100, pp. 4227-4232): Proc. Natl. Acad. Sci. USA.

Guerzoni, M. E., Lanciotti, R., & Cocconcelli, P. S. (2001). Alteration in cellular fatty acid composition as a response to salt, acid, oxidative and thermal stresses in *Lactobacillus helveticus*. In (Vol. 147, pp. 2255-2264): Microbiology.

Hammes W.P., H. C. (1998). New developments in meat starter cultures. In (Vol. 49S1, pp. 125-138): Meat science.

Hammes, W. P., Bantleon, A., & Min, S. (1990). Lactic acid bacteria in meat fermentation. *FEMS Microbiology Reviews, 87*, 165-174.

Harshey, R. M. (2003). Bacterial motility on a surface: many ways to a common goal. *Annu Rev Microbiol, 57*, 249-273. doi:10.1146/annurev.micro.57.030502.091014

Hebert, E. M., Raya, R. R., & de Giori, G. S. (2004). Nutritional requirements of *Lactobacillus delbrueckii* subsp. *lactis* in a chemically defined medium. *Curr Microbiol, 49*(5), 341-345. doi:10.1007/s00284-004-4357-9

Hebert, E. M., Saavedra, L., Taranto, M. P., Mozzi, F., Magni, C., Nader, M. E., Font de Valdez, G., Sesma, F., Vignolo, G., Raya, R. R. (2012). Genome sequence of the bacteriocin-producing *Lactobacillus curvatus* strain CRL705. *J Bacteriol, 194*(2), 538-539. doi:10.1128/JB.06416-11

Hertel, C., Schmidt, G., Fischer, M., Oellers, K., & Hammes, W. P. (1998). Oxygen-dependent regulation of the expression of the catalase gene katA of *Lactobacillus sakei* LTH677. In (Vol. 64, pp. 1359-1365): Environ. Microbiol.

Horvath, P., & Barrangou, R. (2010). CRISPR/CAS, the immune system of bacteria and archaea. *Sciences Des Aliments, 327*.

Hugenholtz, J. (1993). Citrate metabolism in lactic acid bacteria. *FEMS Microbiology Reviews, 12*, 165-178.

Igarashi, T., Kono, Y., & Tanaka, K. (1996). Molecular cloning of manganese catalase from *Lactobacillus plantarum*. In (Vol. 271, pp. 29521-29524): J. Biol. Chem.

Janßen, D., Dworschak, L., Ludwig, C., Ehrmann, M. A., & Vogel, R. F. (2020). Interspecies assertiveness of *Lactobacillus curvatus* and *Lactobacillus sakei* in sausage fermentations. *International Journal of Food Microbiology, 331*, 108689. doi:https://doi.org/10.1016/j.ijfoodmicro.2020.108689

Janßen, D., Ehrmann, M. A., & Vogel, R. F. (2018). Monitoring of assertive *Lactobacillus sakei* and *Lactobacillus curvatus* strains in raw fermented sausage using MALDI-TOF MS. *Journal of Applied Microbiology*.

Janßen, D., Eisenbach, L., Ehrmann, M. A., & Vogel, R. F. (2018). Assertiveness of *Lactobacillus sakei* and *Lactobacillus curvatus* in a fermented sausage model. *Int J Food Microbiol, under review*.

Jones, P. G., Van Bogelen, R. A., & Neidhardt, F. C. (1987). Induction of proteins in response to low temperature in *Escherichia coli*. *J Bacteriol, 169*(5), 2092-2095.

Jänsch, A., Freiding, S., Behr, J., & Vogel, R. F. (2011). Contribution of the NADH-oxidase (Nox) to the aerobic life of *Lactobacillus sanfranciscensis* DSM20451^T. In (Vol. 28, pp. 29-37): Food Microbiol.

Kaiser, D. (2000). Bacterial motility: How to do pili pull? *Current Biology, 10*, R777-R780.

Klein, G., Dicks, L. M. T., Pack, A., Hack, B., Zimmermann, K., Dellaglio, F., & Reuter, G. (1996). Emended descriptions of *Lactobacillus sake* (Katagiri, Kitahara, and Fukami) and *Lactobacillus curvatus* (Abo-Elnaga and Kandler): Numerical classification revealed by protein fingerprinting and identification based on biochemical patterns and DNA-DNA hybridizations. *International Journal of Systematic Bacteriology, 46*(2), 367-376.

Knauf, H. J., Vogel, R. F., & Hammes, W. P. (1992). Cloning, sequence, and phenotypic expression of katA, which encodes the catalase of *Lactobacillus sake* LTH677. In (Vol. 58, pp. 832-839): Appl. Environ. Microbiol.

Kono, Y., & Fridovich, I. (1983). Isolation and characterization of the pseudocatalase of *Lactobacillus plantarum*. In (Vol. 258, pp. 6015-6019): J. Biol. Chem.

Koort, J., Vandamme, P., Schillinger, U., Holzapfel, W., & Bjorkroth, J. (2004). *Lactobacillus curvatus* subsp. *melibiosus* is a later synonym of *Lactobacillus sakei* subsp. *carnosus*. *Int J Syst Evol Microbiol, 54*(Pt 5), 1621-1626. doi:10.1099/ijs.0.63164-0

Krumsiek, J., Arnold, R., & Rattei, T. (2007). Gepard: a rapid and sensitive tool for creating dotplots on genome scale. In (Vol. 23, pp. 1026-1010-1028): Bioinformatics.

Kröckel, L., Schillinger, U., Franz, C.M., Bantleon, A., Ludwig, W. (2003). *Lactobacillus versmoldensis* sp. nov., isolated fram raw fermented sausage. In (Vol. 53, pp. 513-517): International journal of systematic and evolutionary microbiology.

Laikova, O. N., Mironov, A. A., & Gelfand, M. S. (2001). Computational analysis of the transcriptional regulation of pentose utilization systems in the gamma subdivision of Proteobacteria. *FEMS Microbiol Lett, 205*, 315-322.

Macnab, R. M. (2003). How bacteria assemble flagella. *Annu Rev Microbiol, 57*, 77-100. doi:10.1146/annurev.micro.57.030502.090832

Marty-Teysset, C., de la Torre, F., & Garel, J. (2000). Increased production of hydrogen peroxide by *Lactobacillus delbrueckii* subsp. *bulgaricus* upon aeration: involvement of an NADH oxidase in oxidative stress. In (Vol. 66, pp. 262-267): Apple. Environ. Microbiol.

Mayo, B., Derzelle, S., Fernandez, M., Leonard, C., Ferain, T., Hols, P., Suarez, J.E., Delcour, J. (1997). Cloning and characterization of *cspL* and *cspP*, two cold-inducible genes from *Lactobcaillus plantarum*. *J. Bacteriologie, 179*, 3039-3042.

Maze, A., Boel, G., Zuniga, M., Bourand, A., Loux, V., Yebra, M. J., Monedero, V., Correia, K., Jacques, N., Beaufils, S., Poncet, S., Joyet, P., Milohanic, E., Casaregola, S., Auffray, Y., Perez-Martinez, G., Gibrat, J. F., Zagorec, M., Francke, C., Hartke, A., Deutscher, J. (2010). Complete genome sequence of the probiotic *Lactobacillus casei* strain BL23. *J Bacteriol, 192*(10), 2647-2648. doi:10.1128/JB.00076-10

McCarthy, A. (2010). Third generation DNA sequencing: pacific biosciences' single molecule real time technology. In (Vol. 17, pp. 675-676): Chem Biol.

McLeod, A., Brede, D. A., Rud, I., & Axelsson, L. (2013). Genome sequence of *Lactobacillus sakei* subsp. *sakei* LS25, a commercial starter culture strain for fermented sausage. *Genome Announc, 1*(4). doi:10.1128/genomeA.00475-13

McLeod, A., Nyquist, O. L., Snipen, L., Naterstad, K., & Axelsson, L. (2008). Diversity of *Lactobacillus sakei* strains investigated by phenotypic and genotypic methods. *Syst Appl Microbiol, 31*(5), 393-403. doi:10.1016/j.syapm.2008.06.002

McLeod, A., Zagorec, M., Champomier-Verges, M. C., Naterstad, K., & Axelsson, L. (2010). Primary metabolism in *Lactobacillus sakei* food isolates by proteomic analysis. *BMC Microbiol, 10*, 120. doi:10.1186/1471-2180-10-120

Morishita, T., Deguchi, Y., Masako, Y., Sakurai, T., & Yura, T. (1981). Multiple nutritional requirements of lactobacilli: genetic lesions affecting amino acid biosynthetic pathways. *Journal of Bacteriology, 148*(1), 64-71.

Neville, B. A., Forde, B. M., Claesson, M. J., Darby, T., Coghlan, A., Nally, K., Ross, R.P., O'Toole, P. W. (2012). Characterization of pro-inflammatory flagellin proteins produced by *Lactobacillus ruminis* and related motile lactobacilli. *PLoS One, 7*(7), e40592. doi:10.1371/journal.pone.0040592

Nwodo, U. U., Green, E., & Okoh, A. I. (2012). Bacterial exopolysaccharides: functionality and prospects. *Int J Mol Sci, 13*(11), 14002-14015. doi:10.3390/ijms131114002

Nyquist, O. L., McLeod, A., Brede, D. A., Snipen, L., Aakra, A., & Nes, I. F. (2011). Comparative genomics of *Lactobacillus sakei* with emphasis on strains from meat. *Mol Genet Genomics, 285*(4), 297-311. doi:10.1007/s00438-011-0608-1

Overbeek, R., Olson, R., Pusch, G. D., Olsen, G. J., Davis, J. J., Disz, T., . Edwards, R.A., Gerdes, S., Parrello, B., Shukla, M., Vonstein, V., Wattam, A.R., Xia, F., Stevens, R. (2014). The SEED and the Rapid Annotation of microbial genomes using Subsystems Technology (RAST). In (Vol. 42, pp. 206-214): Nucleic. Acids Res.

Pebay, M., Holl, A. C., Simonet, J. M., & Decaris, B. (1995). Characterization of the gor gene of the lactic acid bacterium *Streptococcus thermophilus* CNRZ368. In (Vol. 146, pp. 371-383): Res. Microbiol.

Phadtare, S., Janivette, A., & Inouye, M. (1999). Cold-shock response and cold-shock proteins. *Current Opinion in Micriobiology, 2*, 175-180.

Prechtl, R. M., Janssen, D., Behr, J., Ludwig, C., Kuster, B., Vogel, R. F., & Jakob, F. (2018). Sucrose-Induced proteomic response and carbohydrate utilization of *Lactobacillus sakei* TMW 1.411 during dextran formation. *Front Microbiol, 9*, 2796. doi:10.3389/fmicb.2018.02796

Prechtl, R. M., Wefers, D., Jakob, F., & Vogel, R. F. (2018). Cold and salt stress modulate amount, molecular and macromolecular structure of a *Lactobacillus sakei* dextran. In (Vol. 82, pp. 73-81): Food Hydrocolloids.

Prieto-Alamno, M. J., Jurado, J., Gallardo-Madueno, R., F., M.-C., Holmgren, A., & Pueyo, C. (2000). Transcriptional regulation of glutaredoxin and thioredoxin pathways and related enzymes in response to oxidative stress. In (Vol. 275, pp. 13398-13405): J. Biol. Chem.

Rallu, F., Gruss, A., Ehrlich, S. D., & Magnin, E. (2000). Acid- and multi stress-resistant mutants of *Lactococcus lactis:* identification of intracellular stress signals. In (Vol. 35, pp. 517-528): Mol. Microbiol.

Rimaux, T., Riviere, A., Illeghems, K., Weckx, S., De Vuyst, L., & Leroy, F. (2012). Expression of the arginine deiminase pathway genes in *Lactobacillus sakei* is strain dependent and is affected by the environmental pH. *Appl Environ Microbiol, 78*(14), 4874-4883. doi:10.1128/AEM.07724-11

Rimaux, T., Vrancken, G., Pothakos, V., Maes, D., De Vuyst, L., & Leroy, F. (2011). The kinetics of the arginine deiminase pathway in the meat starter culture *Lactobacillus sakei* CTC 494 are pH-dependent. *Food Microbiol, 28*(3), 597-604. doi:10.1016/j.fm.2010.11.016

Rimaux, T., Vrancken, G., Vuylsteke, B., De Vuyst, L., & Leroy, F. (2011). The pentose moiety of adenosine and inosine is an important energy source for the fermented-meat starter culture *Lactobacillus sakei* CTC 494. *Appl Environ Microbiol, 77*(18), 6539-6550. doi:10.1128/AEM.00498-11

Schuster, J. A., Vogel, R. F., & Ehrmann, M. A. (2019). Characterization and distribution of CRISPR–Cas systems in *Lactobacillus sakei*. *Archives of Microbiology, 201*(3), 337-347. doi:10.1007/s00203-019-01619-x

SF, A., W, S., W, M., EW, M., & DJ, L. (1990). Basic local alignment search tool. *J Mol Biol, 215*, 403-410.

Starrenburg, M. J. C., & Hugenholtz, J. (1991). Citrate fermentation by *Lactococcus* and *Leuconostoc* spp. *Appl Environ Microbiol, 57*, 3535-3540.

Stentz, R., & Zagorec, M. (1999). Ribose utilization in *Lactobacillus sakei*: analysis of the regulation of the rbs operon and putative involvement of a new transporter. *J Mol Microbiol Biotechnol, 1*(1), 165-173.

Stewart, E. J., Aslund, F., & J., B. (1998). Disulfide bond formation in the *Escherichia coli* cytoplasm: an *in vivo* role reversal for the thioredoxins. In (Vol. 17, pp. 5543-5550): EMBO J.

Szurmant, H., & Ordal, G. W. (2004). Diversity in chemotaxis mechanisms among the bacteria and archaea. *Microbiol Mol Biol Rev, 68*(2), 301-319. doi:10.1128/MMBR.68.2.301-319.2004

Tichaczek, P. S., Nissen-Meyer, J., Nes, I. F., Vogel, R. F., & Hammes, W. P. (1992). Characterization of the bacteriocins Curvacin A from *Lactobacillus curvatus* LTH1174 and Sakacin P from *L. sake* LTH673. *Syst Appl Microbiol, 15*, 460-468.

Torriani, S., Van Reenen, G. A., Klein, G., Reuter, G., Dellaglio, F., & Dicks, L. M. (1996). *Lactobacillus curvatus* subsp. *curvatus* subsp. nov. and *Lactobacillus curvatus* subsp. *melibiosus* subsp. nov. and *Lactobacillus sake* subsp. *sake* subsp. nov. and *Lactobacillus sake* subsp. *carnosus* subsp. nov., new subspecies of *Lactobacillus curvatus* Abo-Elnaga and Kandler 1965 and *Lactobacillus sake* Katagiri, Kitahara, and Fukami 1934 (Klein et al. 1996, emended descriptions), respectively. *Int J Syst Bacteriol, 46*(4), 1158-1163.

Turner, M. S., Woodberry, T., Hafner, L. M., & Giffard, P. M. (1999). The bspA locus of *Lactobacillus fermentum* BR11 encodes an L-cystine uptake system. In (Vol. 181, pp. 2192-2198): J. Bacteriol.

van de Guchte, M., Ehrlich, S. D., & Magnin, E. (2001). Production of growth-inhibiting factors by *Lactobacillus delbrueckii*. In (Vol. 91, pp. 147-153): J. Appl. Microbiol.

van de Guchte, M., Penaud, S., Grimaldi, C., Barbe, V., Bryson, K., Nicolas, P., Robert, C., Oztas, S., Mangenot, S., Couloux, A., Loux, V., Dervyn, R., Bossy, R., Bolotin, A., Batto, J. M., Walunas, T., Gibrat, J.F., Bessieres, P., Weissenbach, J., Ehrlich, S.D., Maguin, E. (2006). The complete genome sequence of *Lactobacillus bulgaricus* reveals extensive and ongoing reductive evolution. *Proc Natl Acad Sci U S A, 103*(24), 9274-9279. doi:10.1073/pnas.0603024103

van de Guchte, M., Serror, P., Chervaux, C., Smokvina, T., Ehrlich, S. D., & Maguin, E. (2002). Stress responses in lactic acid bacteria. In (Vol. 82, pp. 187-216): Antonie van Leeuwenhoek.

Villani, F., Casaburi, A., Pennacchia, C., Filosa, L., Russo, F., & Ercolini, D. (2007). Microbial ecology of the soppressata of Vallo di Diano, a traditional dry fermented sausage from southern Italy, and in vitro and in situ selection of autochthonous starter cultures. *Appl Environ Microbiol, 73*(17), 5453-5463. doi:10.1128/AEM.01072-07

Yi, X., Kot, E., & Bezkorovainy, A. (1998). Properties of NADH oxidase from *Lactobacillus delbrueckii* ssp. *bulgaricus*. In (Vol. 78, pp. 527-534): J. Sci. Food Agric.

Zheng, J., Wittouck, S., Salvetti, E., Franz, C. M. A. P., Harris, H. M. B., Mattarelli, P., O'Toole, P.W., Pot, B., Vandamme, P., Walter, J., Watanabe, K., Wuyts, S., Felis, G.E., Gänzle, M.G., Lebeer, S. (2020). A taxonomic note on the genus *Lactobacillus*: Description of 23 novel genera, emended description of the genus *Lactobacillus* Beijerinck 1901, and union of *Lactobacillaceae* and *Leuconostocaceae*. *International Journal of Systematic and Evolutionary Microbiology, 70*(4), 2782-2858. doi:https://doi.org/10.1099/ijsem.0.004107

8 Supplementary

8.1 MALDI-Tof MS

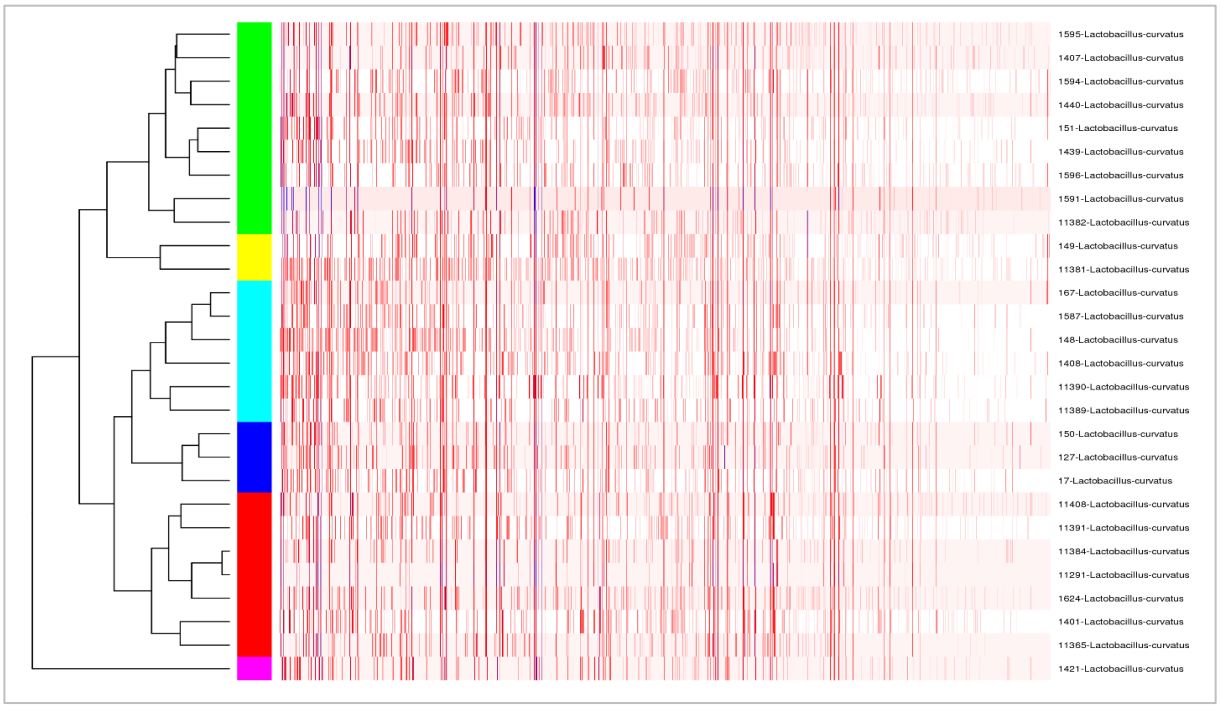

supplementary Figure 1: Cluster of all tested strains of *L. curvatus* during the initial screening. The Cluster reflects the biodiversity of the species based on the sub-proteom. Moreover, two main groups are detectable within this species.

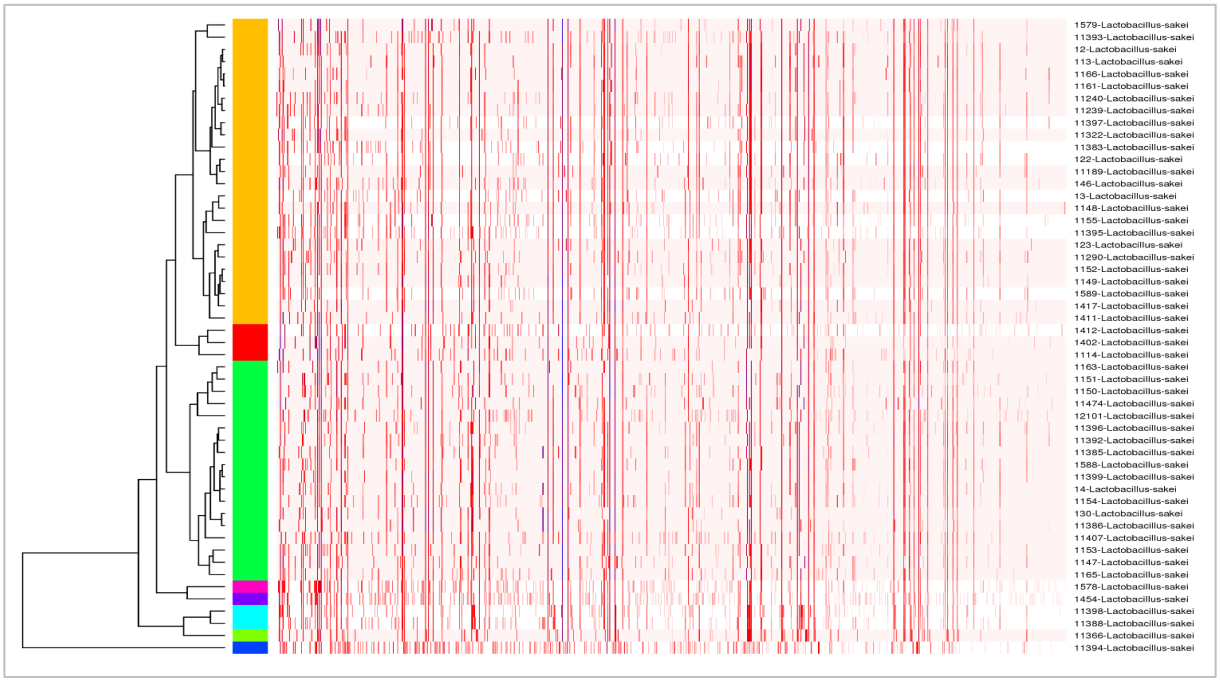

supplementary Figure 2: Cluster of all tested strains of *L. sakei* during the initial screening. The Cluster reflects the biodiversity of the species based on the sub-proteom. Moreover, three main groups are detectable within this species.

8.2 Amino acid Matrices and Codon Usage heat maps

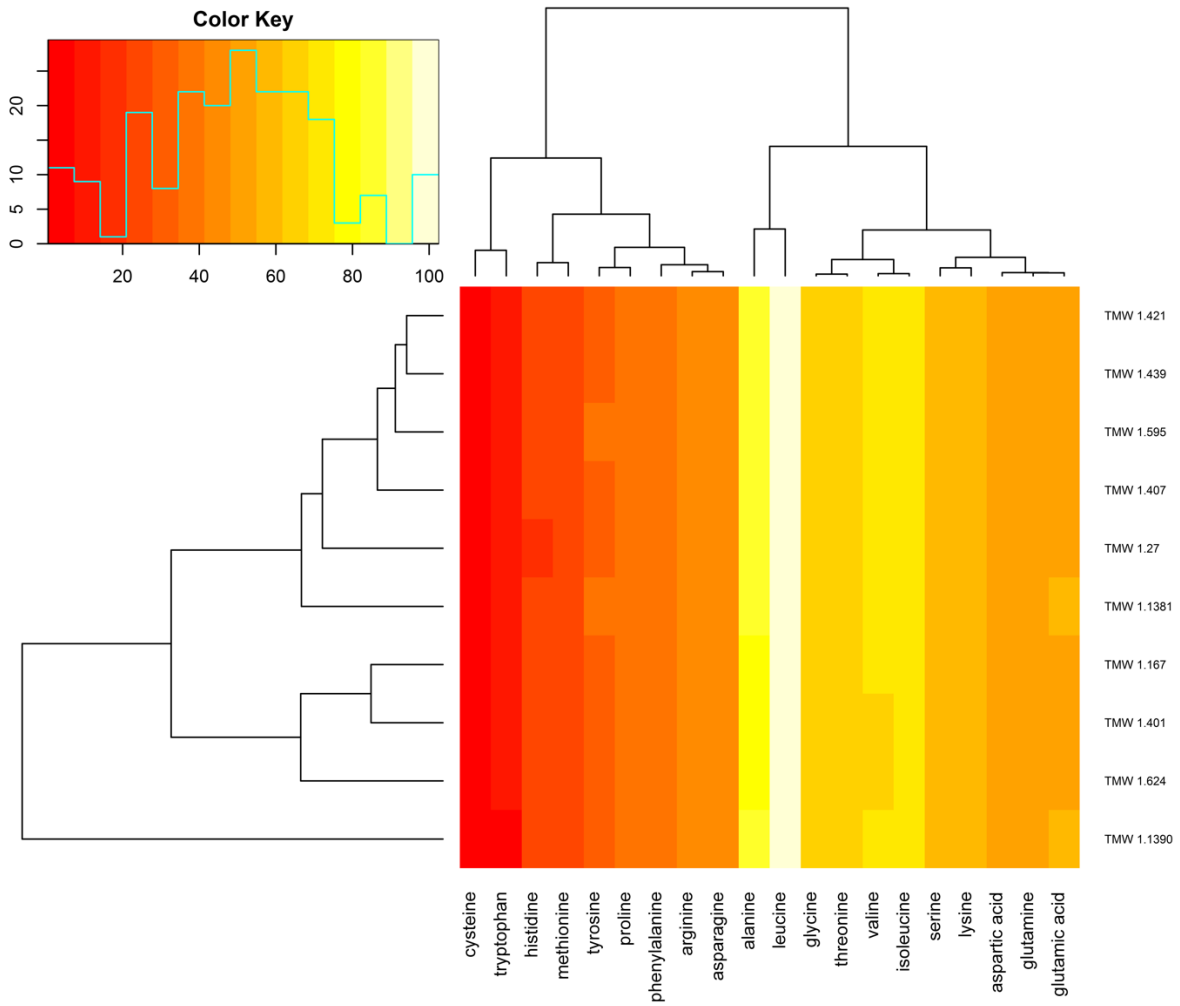

supplementary Figure 3: Cluster of *L. curvatus* strains based on the encoded amino acid by codons. The strains are clustered in two main groups, but three smaller groups. Indeed, *L. curvatus* TMW 1.1390 forms a single group. Interestingly, the cluster correlates not with other clusters based on the genomic comparison, e.g., ANI-calculation, pan-genome comparison etc.

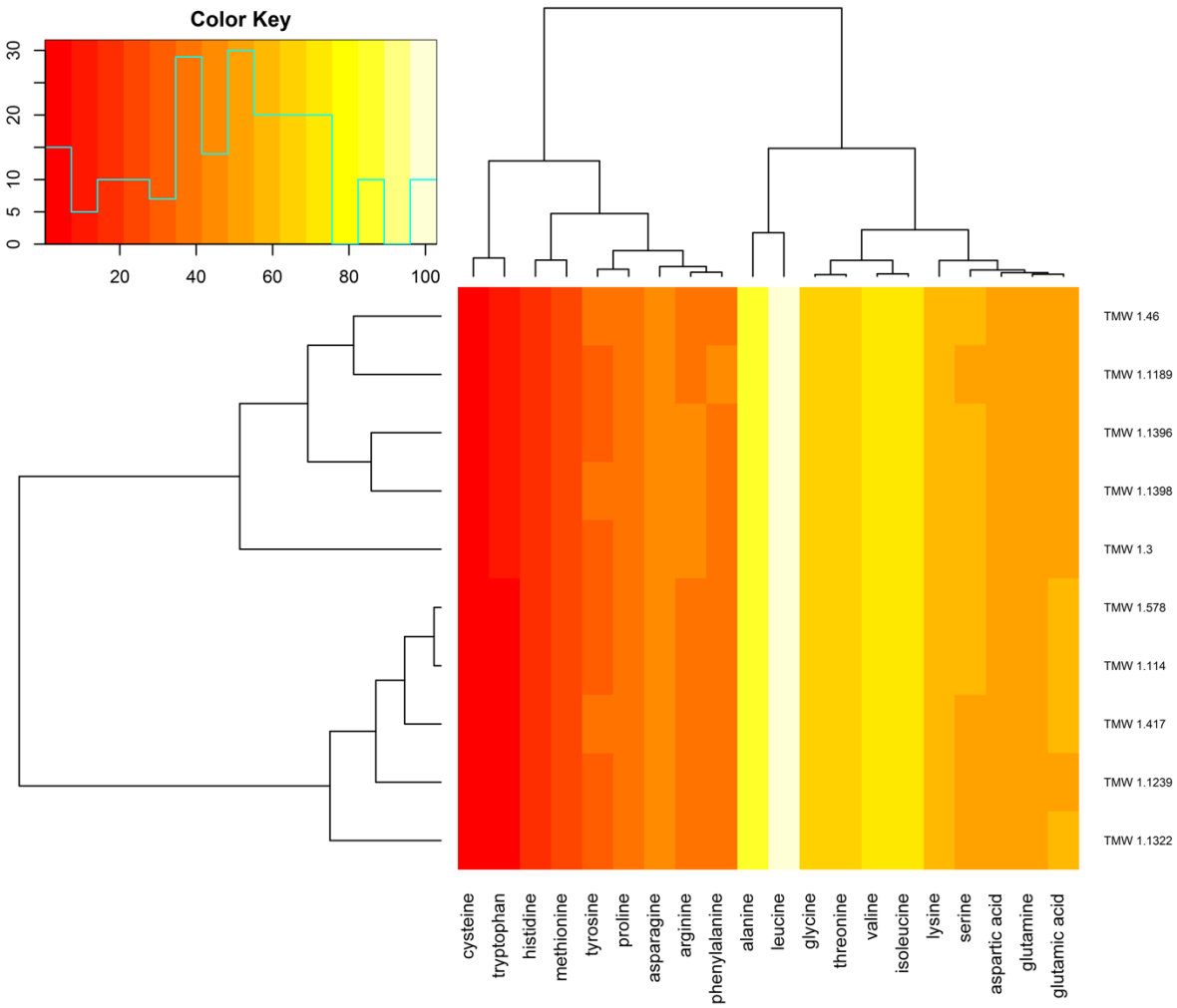

supplementary Figure 4: Cluster of *L. sakei* strains based on the encoded amino acid by codons. The strains are clustered in two main groups. Indeed, Interestingly, the cluster correlates not with other clusters based on the genomic or physiological comparison, e.g., ANI-calculation, pan-genome comparison, MALDI-ToF MS etc.

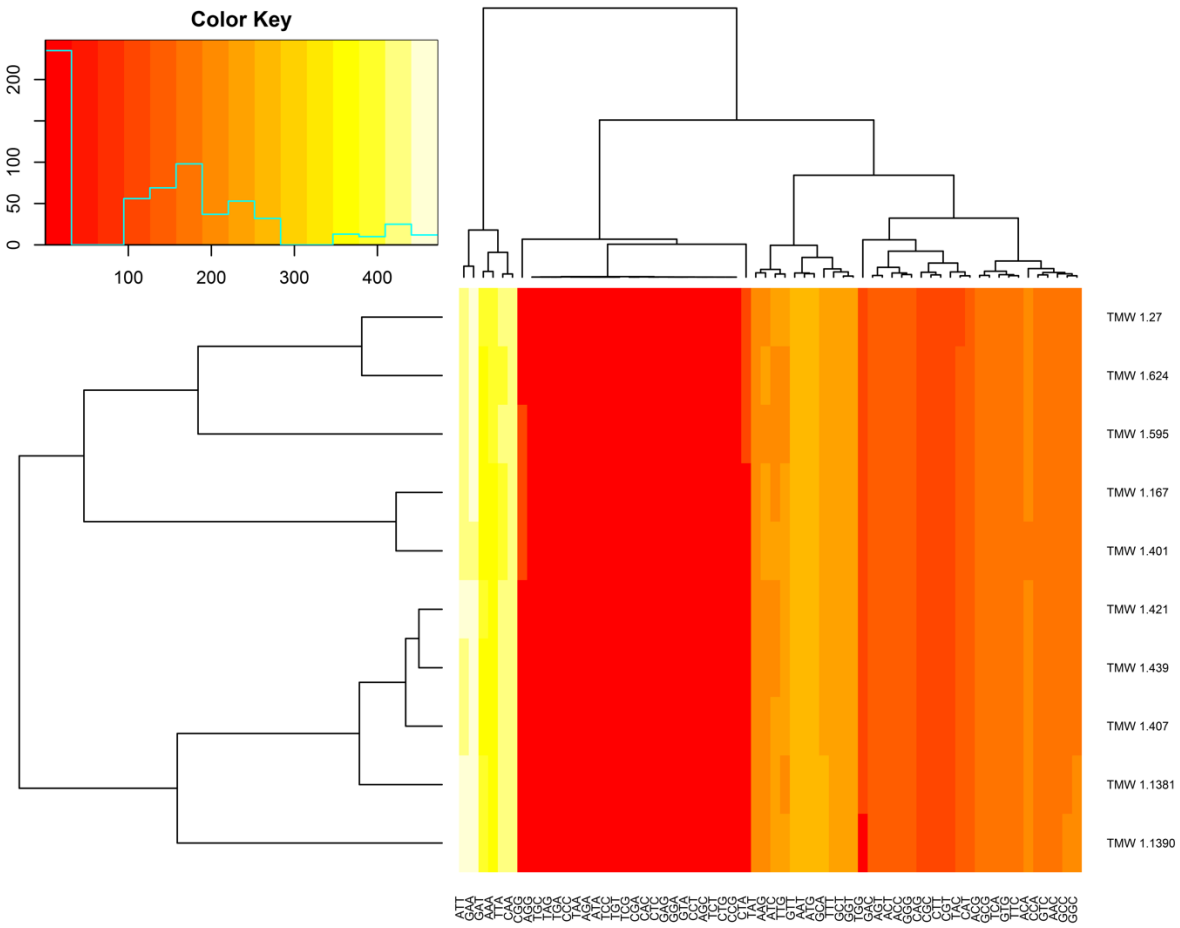

supplementary Figure 5: Cluster of *L. curvatus* strains based on codon usage. The strains are clustered in two main groups, but three smaller groups. Interestingly, the cluster correlates not with other clusters based on the genomic comparison, e.g., ANI-calculation, pan-genome comparison etc.

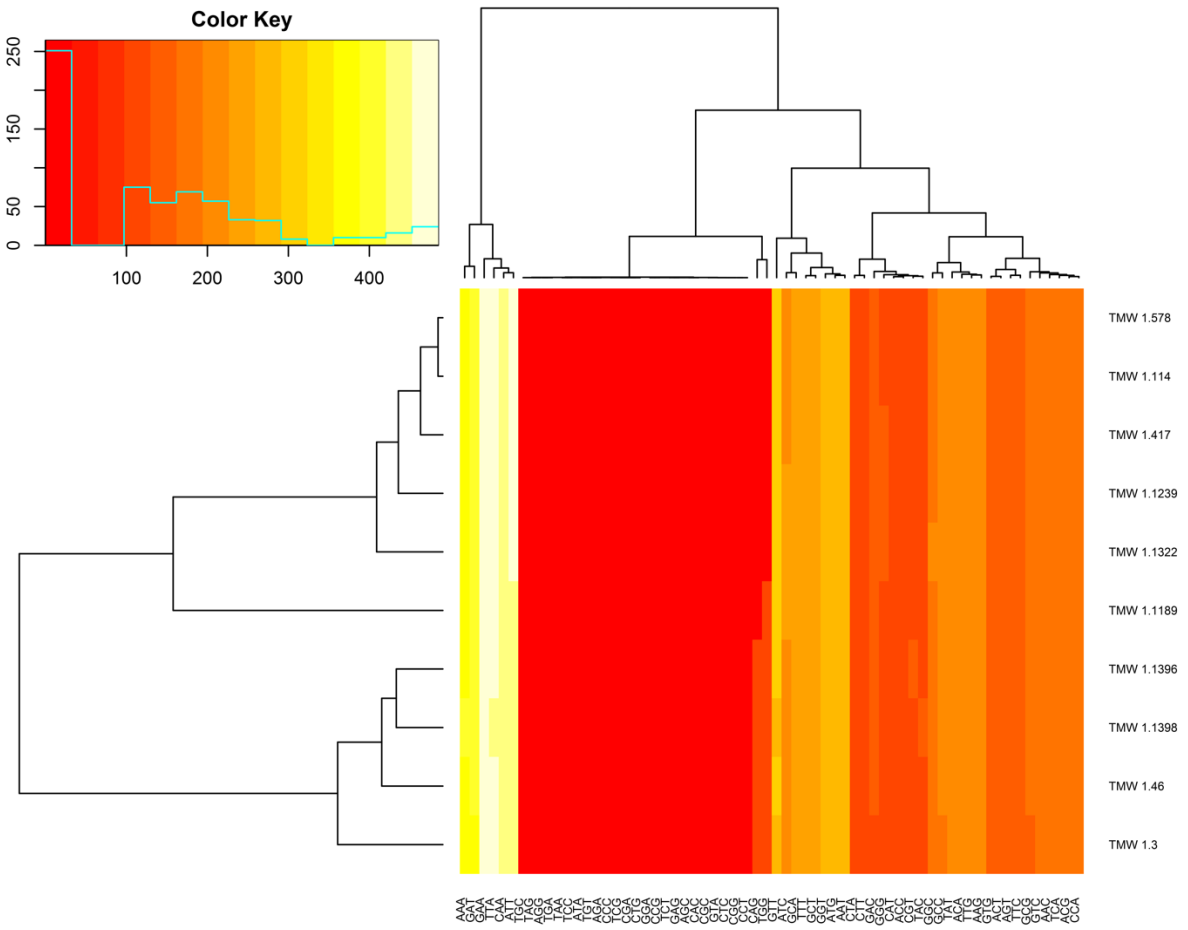

supplementary Figure 6: Cluster of *L. sakei* strains based on the codon usage. The strains are clustered in two main groups, but three smaller groups. Indeed, *L. sakei* TMW 1.1189 forms a single sub-group. Interestingly, the cluster correlates not with other clusters based on the genomic comparison, e.g., ANI-calculation, pan-genome comparison etc.

8.3 Supplementary 2: Proteomic comparison

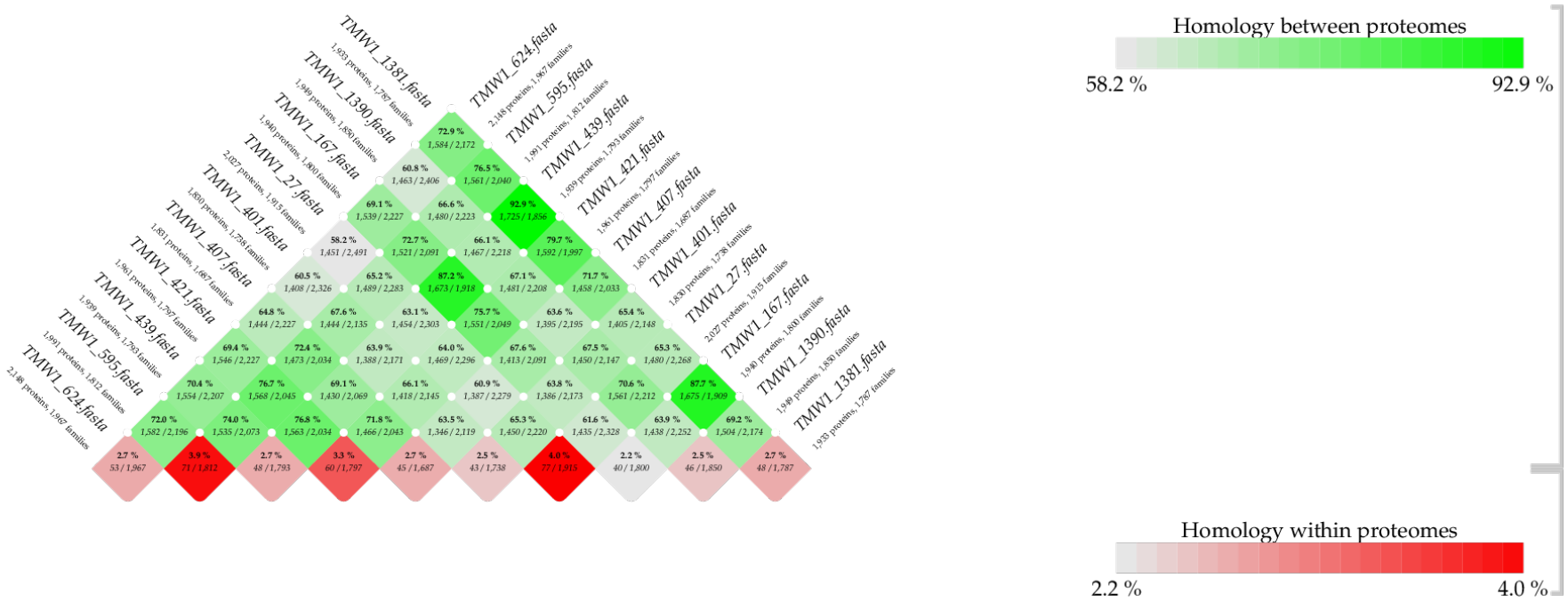

supplementary Figure 7: Comparison of the encoded proteome of *I. curvatus* enables to identify close related or similar strains based on the proteomic characteristics. Interestingly, strains which suggest a close genomic relationship indicates a high similarity based on the proteomic comparison.

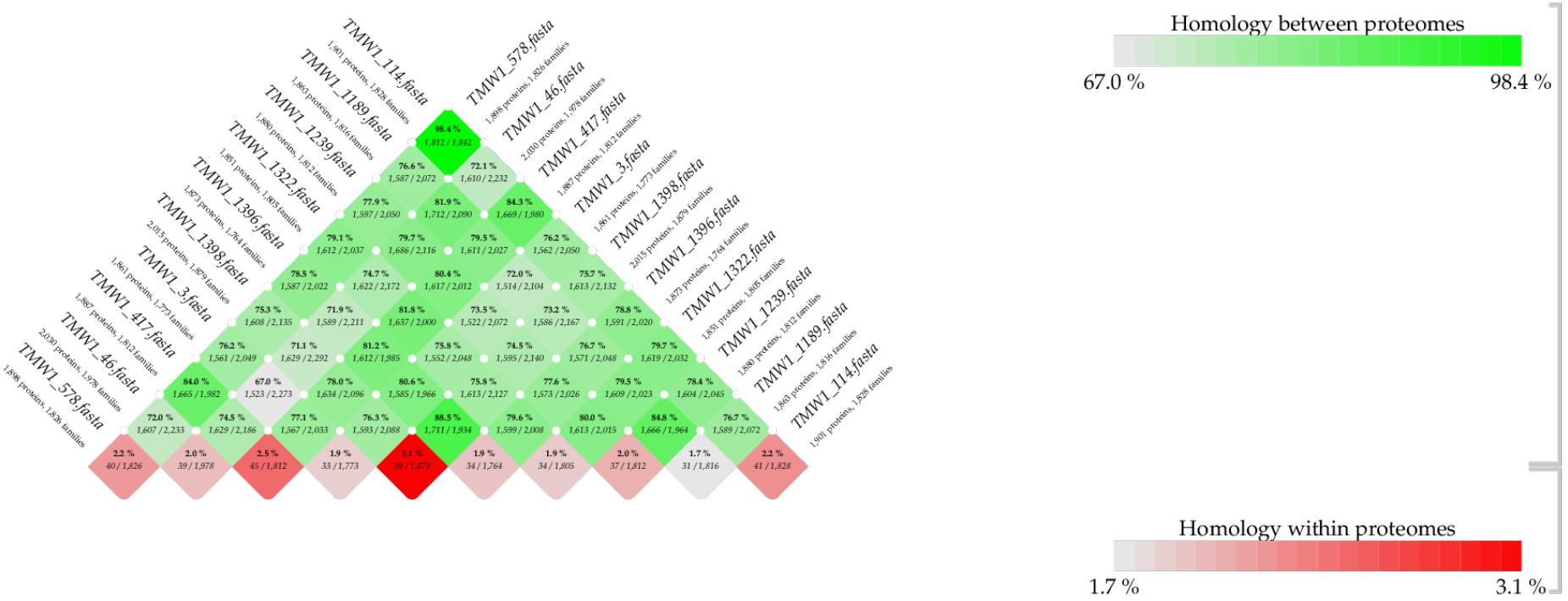

supplementary Figure 8: Comparison of the encoded proteome of *L. sakei* enables to identify close related or similar strains based on the proteomic characteristics. Interestingly, strains which suggest a close genomic relationship indicates a high similarity based on the proteomic comparison.

9 Appendix

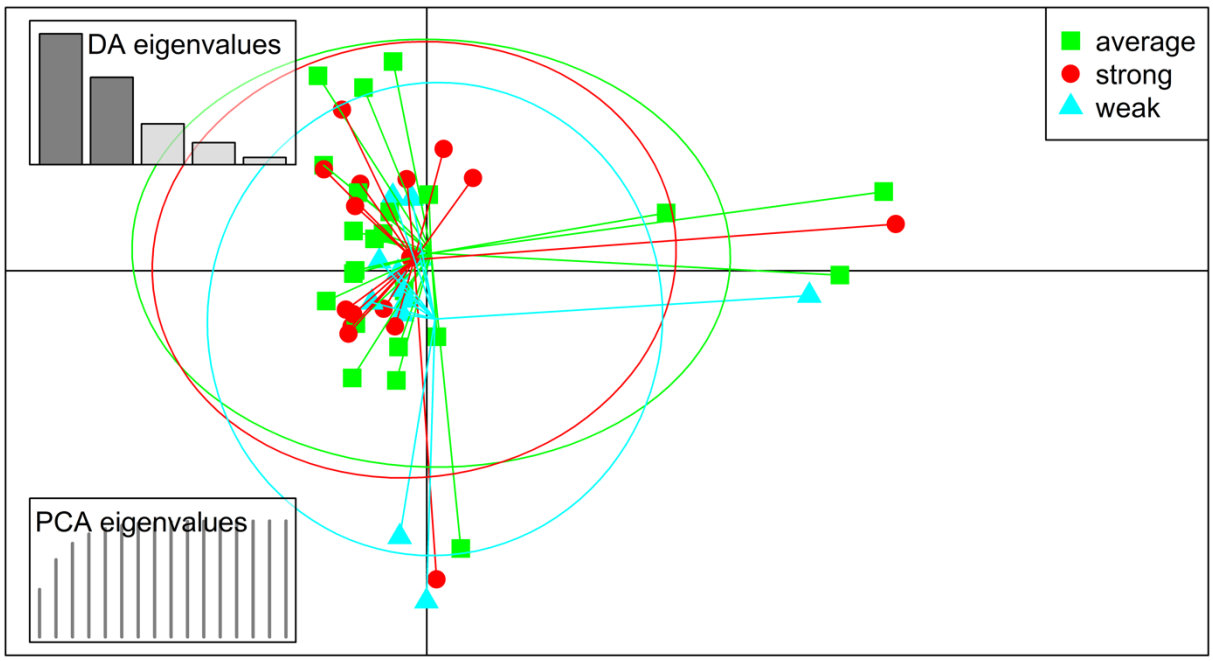

supplementary Figure 9: DAPC Cluster of *L. sakei* based on main criteria assertiveness prediction

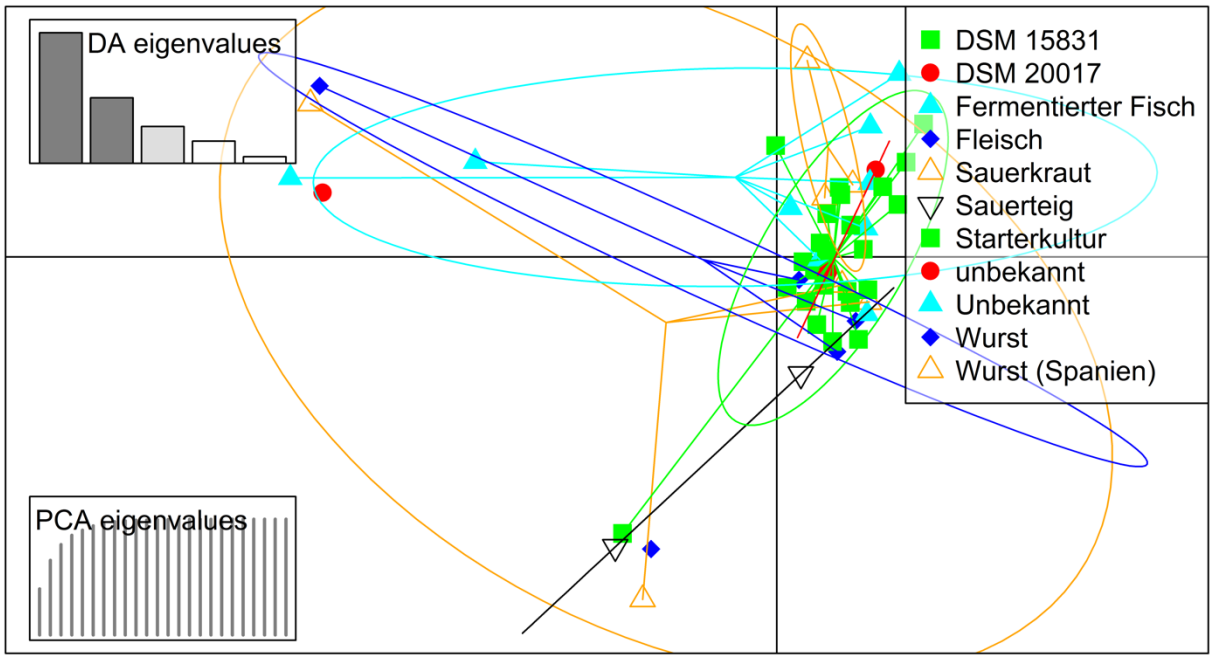

supplementary Figure 10: DAPC Cluster of *L. sakei* based on main criteria source of isolation

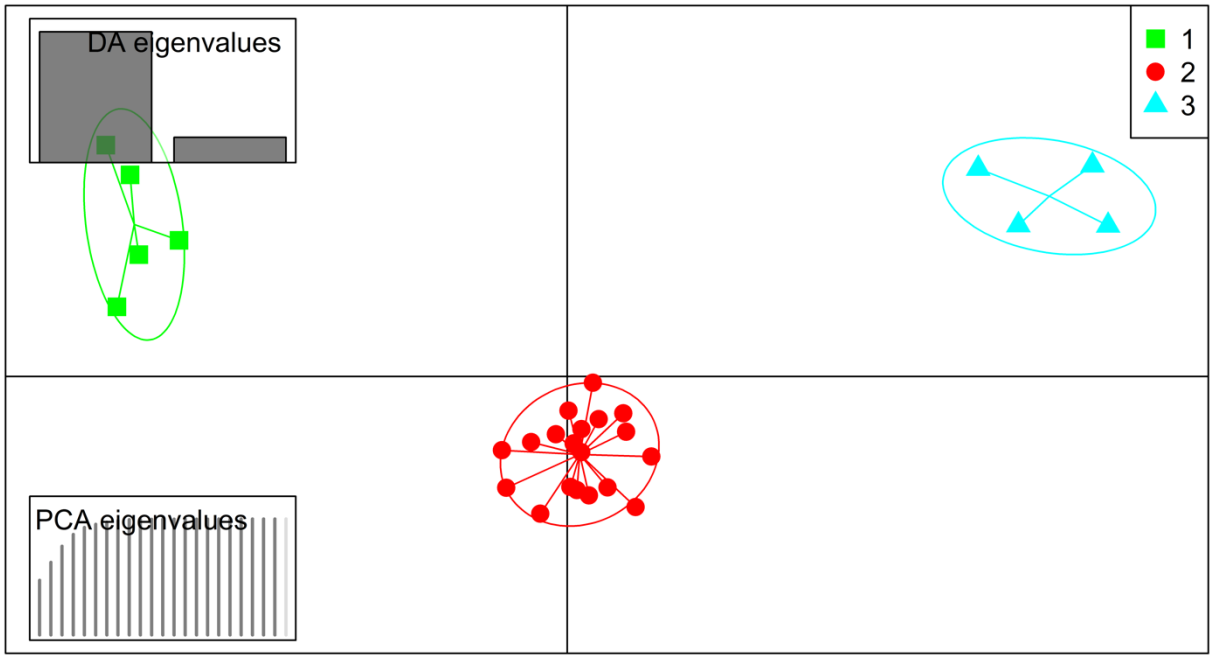

supplementary Figure 11: DAPC Cluster of *L. curvatus* based on physiological criteria and set to three groups instead of two.

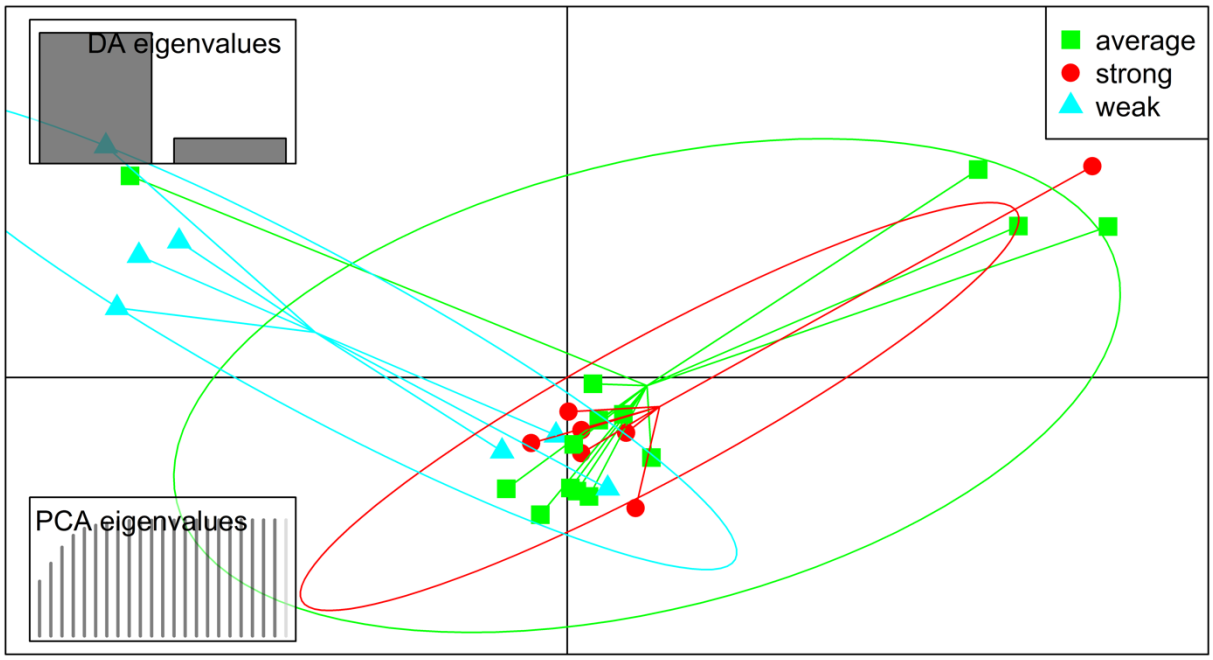

supplementary Figure 12: DAPC Cluster of *L. curvatus* based on main criteria assertiveness prediction.

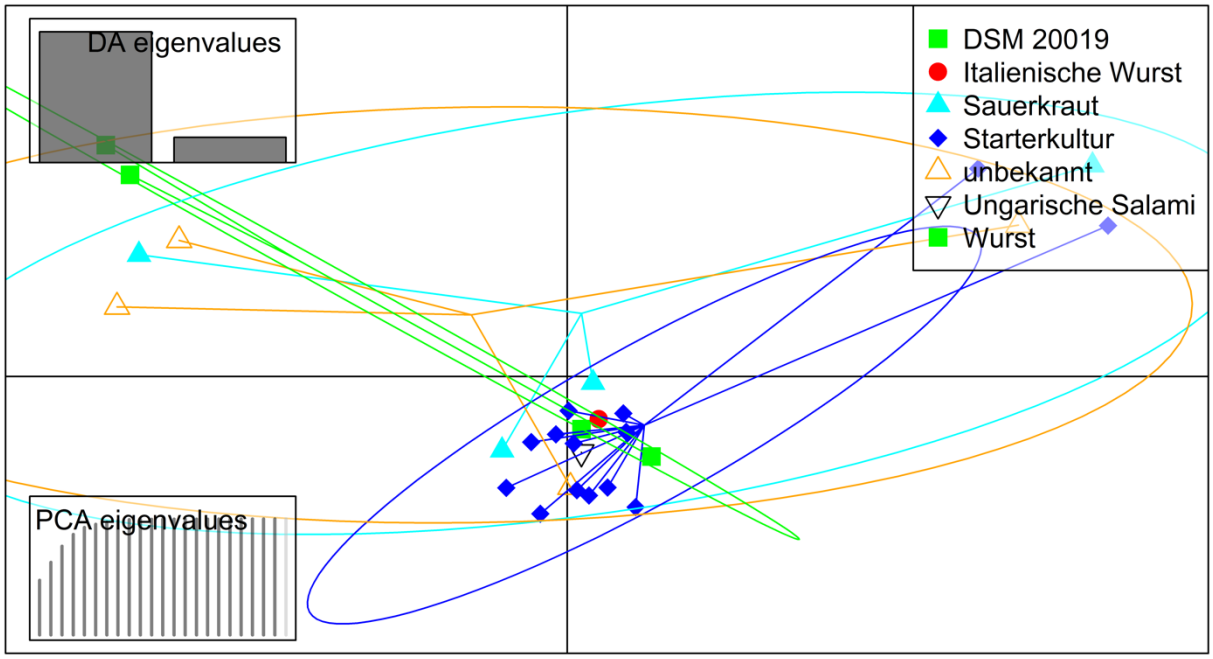

supplementary Figure 13: DAPC Cluster of *L. curvatus* based on main criteria source of isolation.

supplementary Table 1: Average nucleotide identity results for *L. sakei* and *L. curvatus*

ANI\GGDC	TMW 1.3	TMW 1.46	TMW1.114	TMW 1.417	TMW 1.578	TMW 1.1189	TMW 1.1239	TMW 1.1322	TMW 1.1396	TMW 1.1398	TMW 1.27	TMW 1.167	TMW 1.401	TMW 1.407	TMW 1.421	TMW 1.439	TMW 1.595	TMW 1.624	TMW 1.1381	TMW 1.1390
TMW 1.3	100,00	97,18	98,41	98,48	98,37	97,15	97,22	98,17	99,53	99,55	83,15	83,62	83,29	83,49	84,31	83,68	83,95	84,22	83,82	83,02
TMW 1.46	97,18	100,00	97,20	97,15	97,22	99,25	99,02	97,25	97,14	97,17	83,66	84,10	84,21	83,83	83,87	84,33	84,26	84,03	83,86	83,70
TMW1.114	98,41	97,20	100,00	99,08	100,00	97,06	97,20	98,22	98,51	98,42	83,75	84,24	84,16	83,49	84,60	84,32	84,31	83,79	84,12	83,68
TMW 1.417	98,48	97,15	99,08	100,00	99,06	97,17	97,25	98,26	98,53	98,63	83,59	83,92	83,89	84,31	84,08	84,20	84,24	83,75	84,00	83,88
TMW 1.578	98,37	97,22	100,00	99,06	100,00	97,05	97,18	98,22	98,51	98,45	83,74	84,34	84,11	83,77	84,43	84,49	84,16	84,07	83,92	83,87
TMW 1.1189	97,15	99,25	97,06	97,17	97,05	100,00	99,00	97,27	97,11	97,19	82,76	83,71	83,19	83,68	83,81	83,80	83,83	83,47	83,58	83,24
TMW 1.1239	97,22	99,02	97,20	97,25	97,18	99,00	100,00	97,21	97,23	97,17	83,13	83,75	83,41	83,63	83,52	83,95	83,43	83,39	83,38	83,32
TMW 1.1322	98,17	97,25	98,22	98,26	98,22	97,27	97,21	100,00	98,07	98,14	83,22	83,37	83,18	84,02	83,43	83,94	83,32	83,18	83,78	82,91
TMW 1.1396	99,53	97,14	98,51	98,53	98,51	97,11	97,23	98,07	100,00	99,90	83,47	84,40	83,73	84,25	84,04	84,40	84,15	84,17	83,84	83,39
TMW 1.1398	99,55	97,17	98,42	98,63	98,45	97,19	97,17	98,14	99,90	100,00	83,71	84,20	83,94	84,23	84,38	84,65	84,84	84,29	84,49	83,54
TMW 1.27	83,15	83,66	83,75	83,59	83,74	82,76	83,13	83,22	83,47	83,71	100,00	99,06	99,42	99,02	99,10	99,04	99,06	98,98	99,05	99,50
TMW 1.167	83,62	84,10	84,24	83,92	84,34	83,71	83,75	83,37	84,40	84,20	99,06	100,00	99,06	99,37	99,56	99,98	99,50	99,57	99,98	99,02
TMW 1.401	83,29	84,21	84,16	83,89	84,11	83,19	83,41	83,18	83,73	83,94	99,42	99,06	100,00	99,01	99,11	99,09	99,05	99,04	99,10	99,51
TMW 1.407	83,49	83,83	83,49	84,31	83,77	83,68	83,63	84,02	84,25	84,23	99,02	99,37	99,01	100,00	99,39	99,37	99,40	99,41	99,37	99,02
TMW 1.421	84,31	83,87	84,60	84,08	84,43	83,81	83,52	83,43	84,04	84,38	99,10	99,56	99,11	99,39	100,00	99,57	99,52	99,57	99,58	99,08
TMW 1.439	83,68	84,33	84,32	84,20	84,49	83,80	83,95	83,94	84,40	84,65	99,04	99,98	99,09	99,37	99,57	100,00	99,54	99,56	99,99	99,05
TMW 1.595	83,95	84,26	84,31	84,24	84,16	83,83	83,43	83,32	84,15	84,84	99,06	99,50	99,05	99,40	99,52	99,54	100,00	99,44	99,53	99,10
TMW 1.624	84,22	84,03	83,79	83,75	84,07	83,47	83,39	83,18	84,17	84,29	98,98	99,57	99,04	99,41	99,57	99,56	99,44	100,00	99,54	99,04
TMW 1.1381	83,82	83,86	84,12	84,00	83,92	83,58	83,38	83,78	83,84	84,49	99,05	99,98	99,10	99,37	99,58	99,99	99,53	99,54	100,00	99,03
TMW 1.1390	83,02	83,70	83,68	83,88	83,87	83,24	83,32	82,91	83,39	83,54	99,50	99,02	99,51	99,02	99,08	99,05	99,10	99,04	99,03	100,00

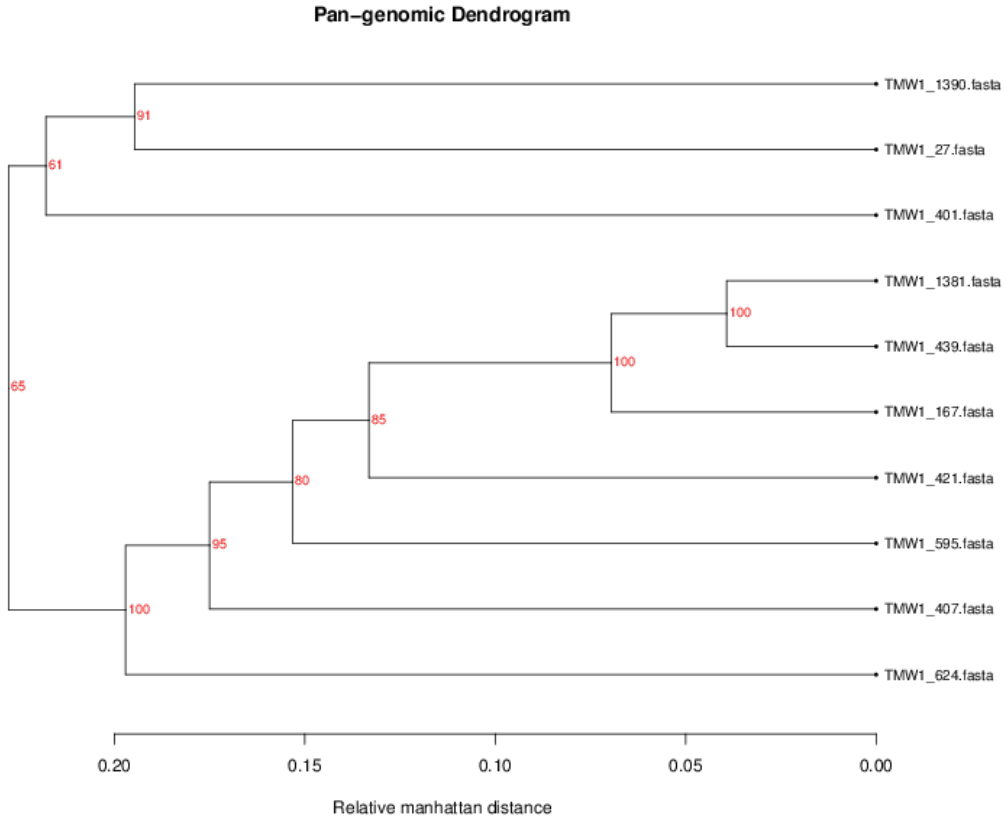

supplementary Figure 14: pan-genomic dendogram of sequenced *L. curvatus* strains.

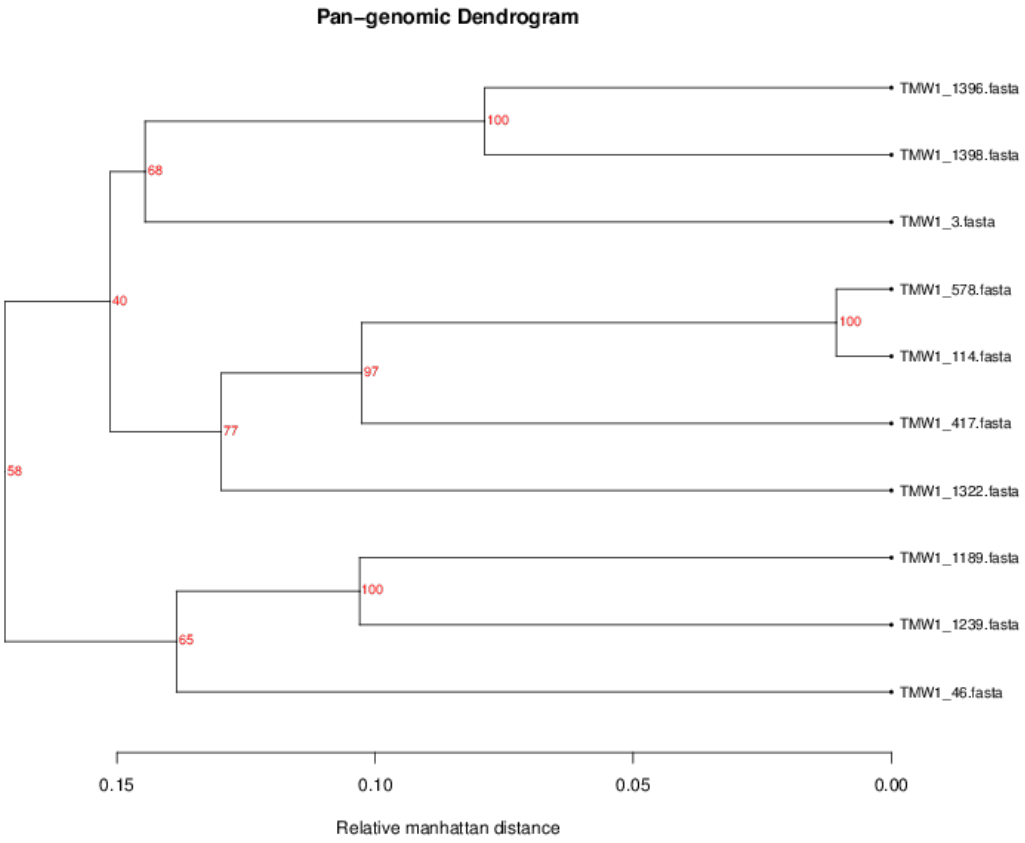

supplementary Figure 15: pan-genomic dendogram of sequenced *L. sakei* strains.

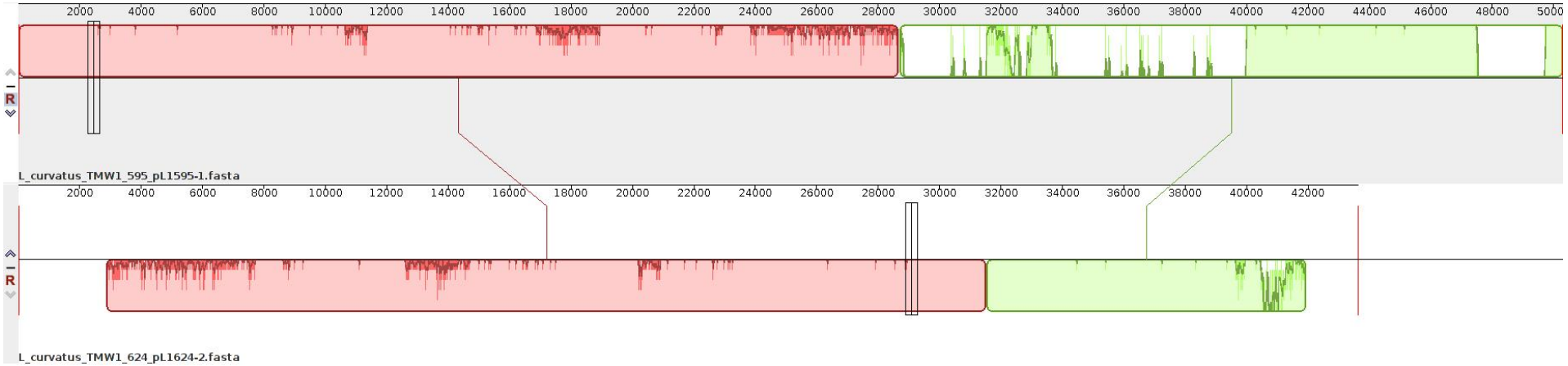

supplementary Figure 16: Genomic comparison of plasmids pL1595-1 and pL1624-2 revealed close genomic relation. Both genes are encoded within strains of *L. curvatus.*

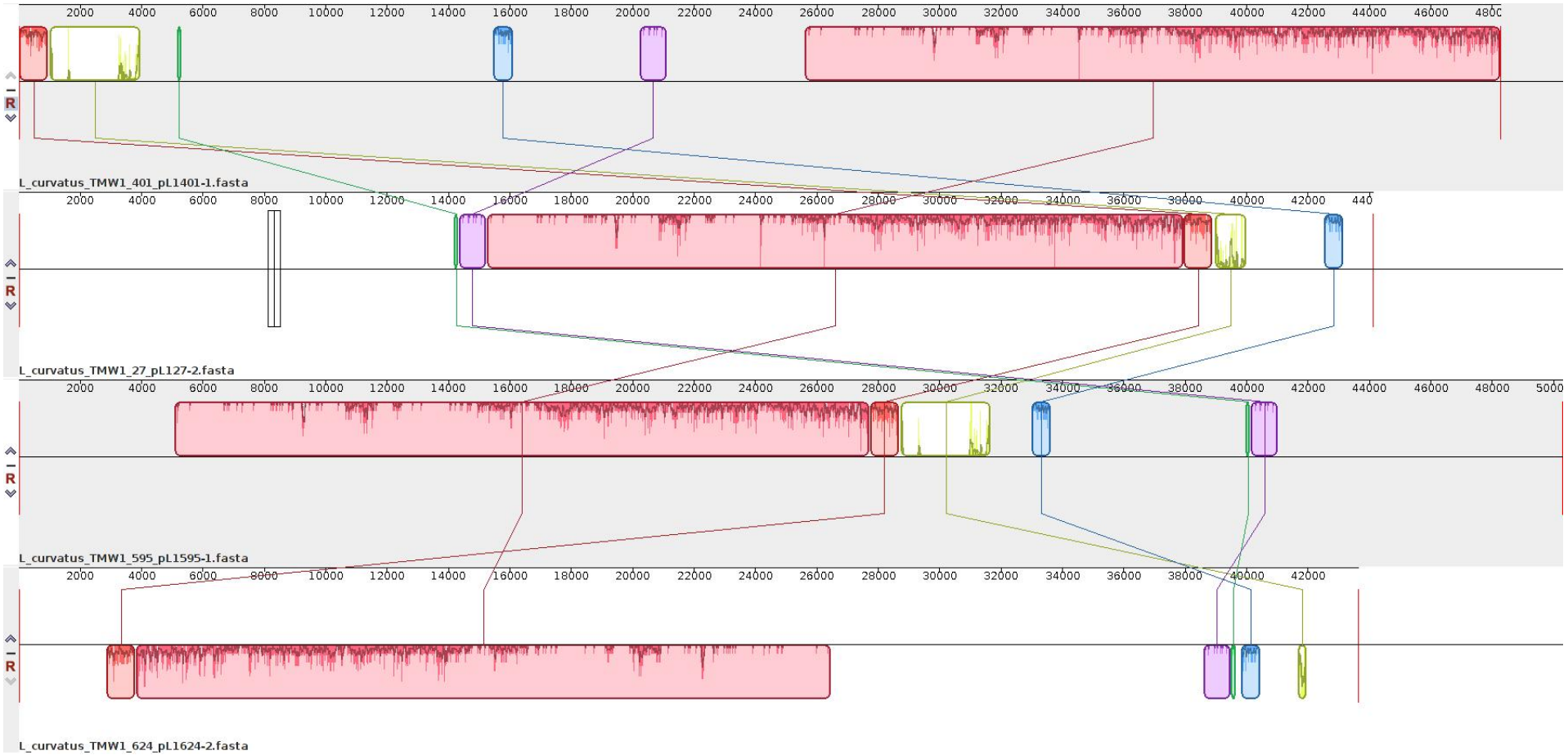

supplementary Figure 17: Genomic comparison of plasmids pL1401-1, pL127-2, pL1595-1 and pL1624-2 revealed a genomic relation. Both genes are encoded within strains of *L. curvatus.*

supplementary Figure 18: Genomic comparison of plasmids pL1114-1, pL11396-1, pL11398-2, pL146-1 and pL1578-1 revealed a genomic relation. Both genes are encoded within strains of *L. sakei.*

supplementary Figure 19: Genomic comparison of plasmids pL1114-1, pL11396-1, pL11398-1, pL11398-2 and pL11398-3 revealed a genomic relation. Both genes are encoded within strains of *L. sakei.*

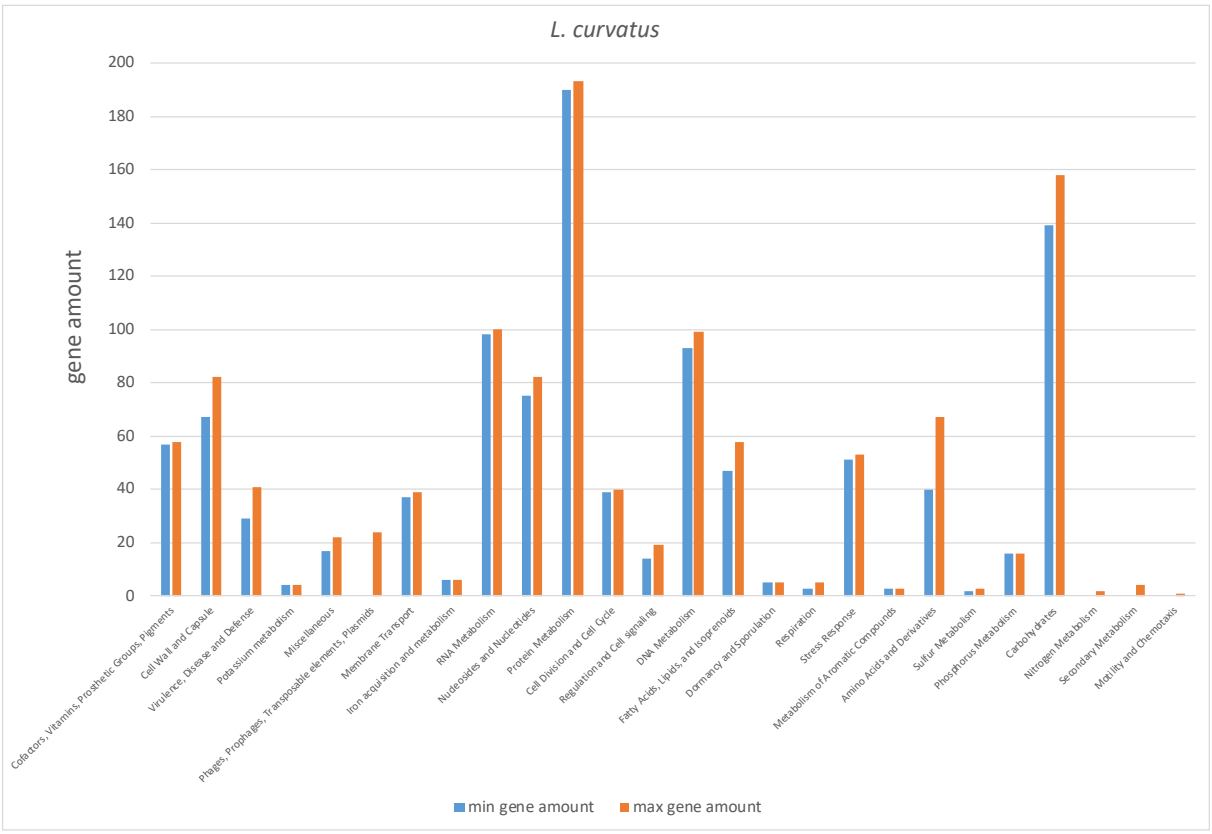

supplementary Figure 20: gene amount of *L. curvatus* based on categories defined by RAST annotation and Seed viewer.

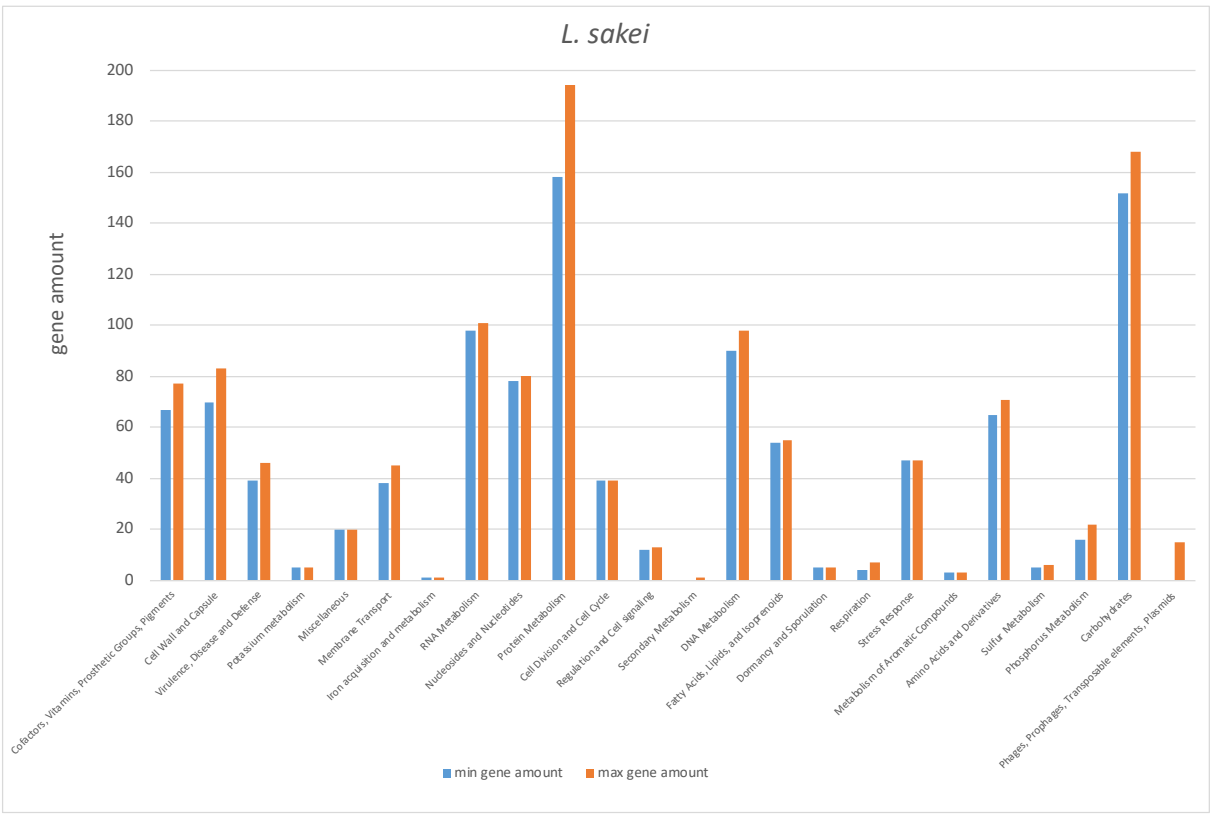

supplementary Figure 21: gene amount of *L. sakei* based on categories defined by RAST annotation and Seed viewer.

supplementary Table 2: Predicted prophage gene clusters encoded in genomes of *L. curvatus* and identified by web-based tool PHASTER.

strain	Region	Region length [kb]	Completeness	Region position [bp]	specific keywords	contig/ accession number
TMW 1.27	1	48.7	questionable	901927-950652	tail, head, portal, terminase	chromosome CP016467
	2	55.3	questionable	1043103-1098488	NA	chromosome CP016467
	1	9.6	incomplete	37404-47015	integrase	plasmid CP016468
TMW 1.167	1	22.8	incomplete	1018718-1041547	recombinase, transposase	chromosome CP016472
	2	45.9	questionable	1336757-1382662	tail, lysin, head, integrase	chromosome CP016472
	3	6.1	questionable	1792265-1798372	transposase	chromosome CP016472
TMW 1.401	1	10.4	incomplete	86529-96961	transposse, capsid	chromosome CP016216
	2	30.7	incomplete	861092-891880	transposase, recombinase	chromosome CP016216
	3	5.7	incomplete	1425674-1431449	head, transposase	chromosome CP016216
	4	8.8	questionable	1453146-1462041	transposase, head	chromosome CP016216
TMW 1.407	1	11	intact	130831-141847	protease, transposase	chromosome CP016218
	2	19	incomplete	1423645-1442657	head, transposase	chromosome CP016218
	1	8.9	incomplete	1124-10043	transposase, integrase, protease	plasmid CP016219
TMW 1.421	1	6.4	incomplete	140931-147396	transposase	chromosome CP016221
	2	11.3	incomplete	1386643-1397984	plate, transposase	chromosome CP016221
	3	4.5	incomplete	1493512-1498011	head, transposase	chromosome CP016221

strain	Region	Region length [kb]	Completeness	Region position [bp]	specific keywords	contig/ accession number
TMW 1.421	1	27.7	intact	15629-43393	integrase, transposase	plasmid CP016222
TMW 1.439	1	6.1	questionable	149837-155946	transposase	chromosome CP015489
	2	36.1	questionable	565215-601352	integrase, tail, lysin	chromosome CP015489
TMW 1.595	1	26.6	questionable	775842-802466	transposase, lysin	chromosome CP016470
	2	47.3	intact	907376-954693	integrase, terminase, portal, capsid, head, tail, lysin	chromosome CP016470
	3	7.8	incomplete	1929261-1937093	transposase, head	chromosome CP016470
	1	7.4	incomplete	39993-47483	transposase	plasmid CP016471
TMW 1.624	1	27.9	questionable	153484-181481	transposase	chromosome CP015490
	2	50.8	intact	574972-625781	integrase, transposase, tail, lysin	chromosome CP015490
	3	40.9	intact	1133047-1173971	lysin, tail, head, capsid, portal, terminase, integrase	chromosome CP015490
	1	26.5	incomplete	15543-42085	integrase, transposase	plasmid CP015491
	2	7.3	incomplete	72786-80184	protease	plasmid CP015491
	1	11.1	incomplete	32138-43321	transposase	plasmid CP015492
TMW 1.1381	1	45.9	questionable	1337062-1382972	tail, lysin, integrase	chromosome CP015493
	2	6.1	questionable	1792628-1798737	transposase	chromosome CP015493
TMW 1.1390	1	37.1	intact	1275957-1313100	lysin, tail, capsid, terminase, integrase	chromosome CP015494

strain	Region	Region length [kb]	Completeness	Region position [bp]	specific keywords	contig/ accession number
TMW 1.1390	2	26	questionable	1384892-1410955	lysin, tail, portal, terminase	chromosome CP015494

supplementary Table 3: Predicted prophage gene clusters encoded in genomes of *L. sakei* and identified by web-based tool PHASTER.

strain	Region	Region length [kb]	Completeness	Region position	specific keywords	contig/accession number
TMW 1.3	1	6.9	incomplete	390883-397813	transposase, protease	chromosome/CP016465
	2	9.8	incomplete	689343-699170	NA	
	3	6.4	incomplete	1021344-1027767	NA	
	4	7.2	incomplete	1319385-1326591	transposase	
	5	9.3	incomplete	1874295-1883672	NA	
	1	21.7	incomplete	4169-25941	integrase, transposase	plasmid/CP016466
TMW 1.46	1	39.6	intact	852024-891679	terminase, head, tail, capsid, lysin	chromosome/CP015487
	2	29.3	questionable	1197847-1227163	lysin, capsid, tail, portal, terminase	
	1	9.6	intact	10058-19712	plate, transposase, recombinase	plasmid/CP015488
TMW 1.114	1	5.6	incomplete	221965-227616	transposase	chromosome/CP017566
	2	8.9	incomplete	1506985-1515929	tail, transposase	

strain	Region	Region length [kb]	Completeness	Region position	specific keywords	contig/accession number
TMW 1.114	1	6.2	questionable	8100-14342	transposase, integrase	plasmid/CP017567
	2	8.5	incomplete	24698-33294	transposae	
TMW 1.417	1	5.6	incomplete	231470-237087	transposase	chromosome/CP017568
	1	9.0	questionable	4499-13540	transposase, integrase	plasmid/CP017569
	2	6.0	incomplete	37535-43622	transposase	
	3	8.0	incomplete	51498-59508	transposase	
TMW 1.578	1	5.6	incomplete	221961-227612	transposase	chromosome/CP017570
	2	8.9	incomplete	1506964-1515908	tail, transposase	
	1	7.2	incomplete	1-7220	transposase	plasmid/CP017571
	2	12.2	questionable	17424-29707	transposase, integrase	
DSM 20017^T	1	9.7	intact	120034-129776	plate, transposase, recombinase	chromosome/CP017271
	2	28.2	incomplete	1029921-1058176	integrase, protease	
TMW 1.1239	1	9.3	incomplete	10683-20057	NA	chromosome/CP017272
	2	8.2	incomplete	720819-729111	NA	
	3	6.9	questionable	1188070-1195052	transposase	
	4	6.5	incomplete	1558819-156330	NA	

strain	Region	Region length [kb]	Completeness	Region position	specific keywords	contig/accession number
TMW 1.1322	1	7.7	incomplete	1134936-1142684	tail, transposase	chromosome/NC_007576
TMW 1.1396	1	6.2	incomplete	359295-365576	transposase, head	chromosome/CP017273
	2	6.8	questionable	1097765-1104617	plate, transposase	
	1	12.4	incomplete	4211-16660	transposase	plasmid/CP017274
TMW 1.1398	1	40.5	intact	789443-829994	transposase, terminase, portal, capsid, head, tail	chromosome/CP017275
	2	6.9	questionable	848394-855366	transposase, plate	
	3	8.1	incomplete	1534648-1542839	transposase, tail	
	4	6.2	incomplete	1594777-1601058	head, transposase	
	1	12.3	incomplete	5024-17369	transposase	plasmid/CP017277
	1	12.4	incomplete	5561-18008	transposase	plasmid/CP017278

L_curvatus_TMW1_1390_A4W74_09505 catalase

Sequence ID: **Query_68050** Length: **481** Number of Matches: **1**

Range 1: 1 to 473 Graphics ▼ Next Match ▲ Previous Match

Score	Expect	Method	Identities	Positives	Gaps
916 bits(2367)	0.0	Compositional matrix adjust.	435/473(92%)	455/473(96%)	0/473(0%)

```
Query  1    MTNQLTTNEGQPWADNQHSQTAGQRGPVLIQDYQLLEKLAHFNRERIPERVVHAKGAGAK  60
            +T + TTNEGQPWADNQHSQTAGQRGPVLIQDY LLEKLAHFNRERIPERVVHAKGAGAK
Sbjct  1    IT*RFTTNEGQPWADNQHSQTAGQRGPVLIQDY*LLEKLAHFNRERIPERVVHAKGAGAK  60

Query  61   GYFKVTKDMSAYTKAAVFSGVGKKTPLITRFSQVAGEAGYPDTYRDVRGFAVKFYTEEGN  120
            GYF++TKDMSAYTKAA+FSG GKKTP+I RFSQVAGEAGYPDTYRDVRGFA+KFYTEEGN
Sbjct  61   GYFQLTKDMSAYTKAAIFSGAGKKTPMIARFSQVAGEAGYPDTYRDVRGFALKFYTEEGN  120

Query  121  YDIVGNNTPVFFVNDPLKFPDFIHSQKRDPRTHARSQDMQWDFWSLSPESVHQVTILMSD  180
            YDIVGNNTPVFFVNDPLKFPDFIHSQKRDPRTHARSQDMQWDFWSLSPESVHQVTILMSD
Sbjct  121  YDIVGNNTPVFFVNDPLKFPDFIHSQKRDPRTHARSQDMQWDFWSLSPESVHQVTILMSD  180

Query  181  RGIPASYRMMHGFGSHTFKWVNAQGEQFWVKYHFKTNQGIHNLSNELADELAGKDTDYLQ  240
            RGIPASYRMMHG+GSHTFKWVNA GEQFWVKYHFKTNQG+HNLSNELA ELAGKDTDYLQ
Sbjct  181  RGIPASYRMMHGYGSHTFKWVNAAGEQFWVKYHFKTNQGVHNLSNELAAELAGKDTDYLQ  240

Query  241  NDLFDAIETGDYPSWTVAVQLVPYEDGLNYPQDIFDVTKVISQKDYPLIEIGQMVLDENP  300
            NDLFDAIETGD+PSWTVAVQLVPYE GLNYPQDIFDVTKVISQKDYPLIEIGQMVLDENP
Sbjct  241  NDLFDAIETGDHPSWTVAVQLVPYEAGLNYPQDIFDVTKVISQKDYPLIEIGQMVLDENP  300

Query  301  TNNFEDIQELAFSPANLVPGIEASPDKLLQGRLFGYKDAERYRLGANYEQLPVNRPKVPV  360
            TNNFEDI+ELAFSPANLVPGIEASPDKLLQGRLFGYKDAERYRLGANYEQLPVNRPKVPV
Sbjct  301  TNNFEDIEELAFSPANLVPGIEASPDKLLQGRLFGYKDAERYRLGANYEQLPVNRPKVPV  360

Query  361  HNYERDGAMAQNQATGVNYEPNSQDGPTEVPAAKIHGDQLSGTTGNFSADPDYYSAAGKL  420
            HNYERDG MA+NQ TGVNYEPNS+DGP EVP+AKIHGDQLSG TGN+ ADPDYYSAA KL
Sbjct  361  HNYERDGIMAKNQETGVNYEPNSEDGPKEVPSAKIHGDQLSGQTGNYPADPDYYSAADKL  420

Query  421  YRLLSADEQTRLIENIRMNLGQVTKPEIQIREVKQFYQADPEYGRRVATSVKL  473
            Y LL+ +EQ RLIENIR+NLGQVTKPEIQIREVKQFYQADPEYGRRVAT++ L
Sbjct  421  YNLLTDEEQDRLIENIRLNLGQVTKPEIQIREVKQFYQADPEYGRRVATALNL  473
```

supplementary Figure 22: Blast comparison of katA gene (Query) of *L. sakei* LTH677 (Knauf et al., 1992) and *L. curvatus* TMW 1.1390 catalase gene (Sbjct). Alignment revealed that identified catalase of *L. curvatus* is a hemedependent catalase like it is described by Knauf *et al.* (Knauf et al., 1992).

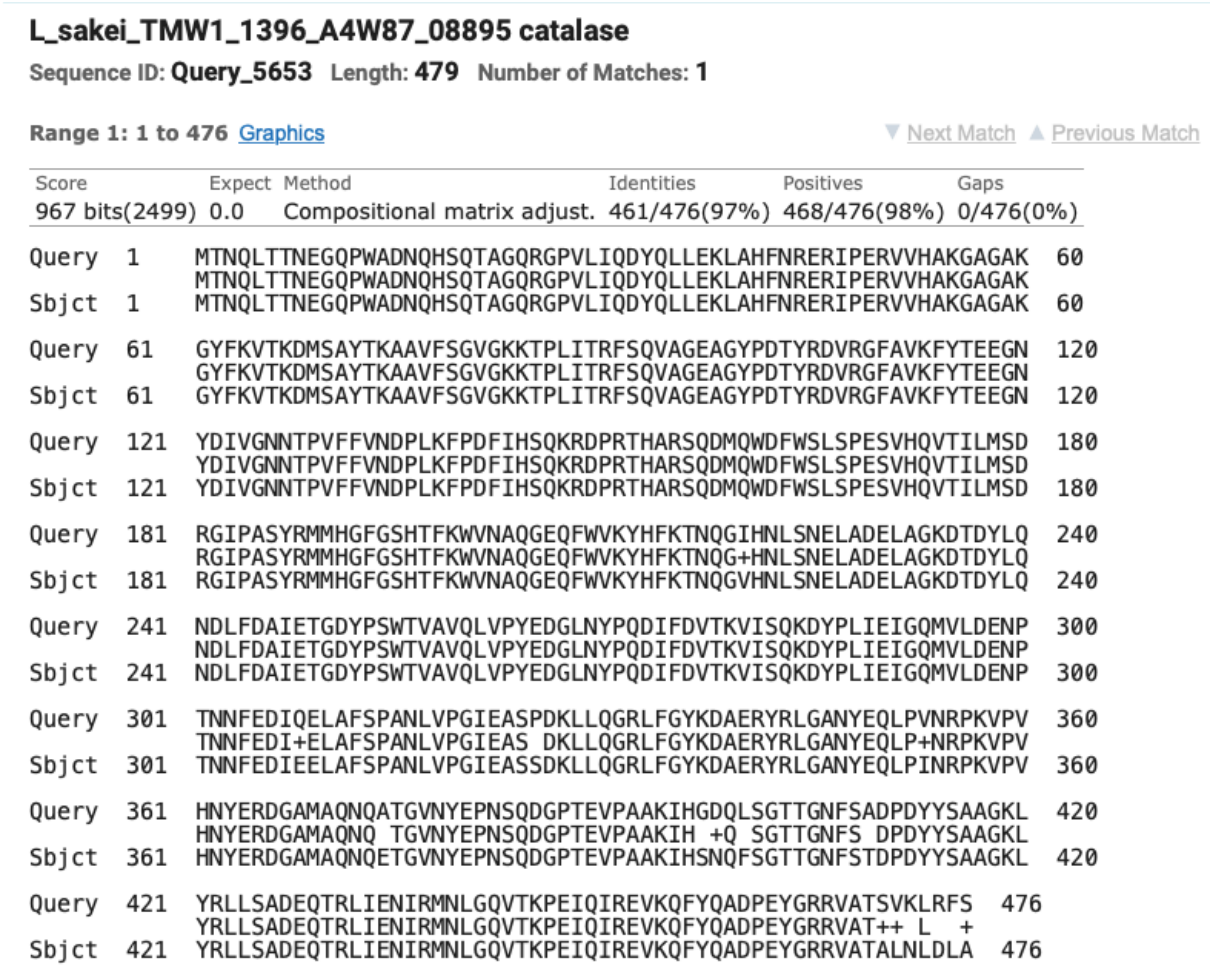

L_sakei_TMW1_1396_A4W87_08895 catalase

Sequence ID: **Query_5653** Length: **479** Number of Matches: **1**

Range 1: 1 to 476 Graphics ▼ Next Match ▲ Previous Match

Score	Expect	Method	Identities	Positives	Gaps
967 bits(2499)	0.0	Compositional matrix adjust.	461/476(97%)	468/476(98%)	0/476(0%)

```
Query  1    MTNQLTTNEGQPWADNQHSQTAGQRGPVLIQDYQLLEKLAHFNRERIPERVVHAKGAGAK  60
            MTNQLTTNEGQPWADNQHSQTAGQRGPVLIQDYQLLEKLAHFNRERIPERVVHAKGAGAK
Sbjct  1    MTNQLTTNEGQPWADNQHSQTAGQRGPVLIQDYQLLEKLAHFNRERIPERVVHAKGAGAK  60

Query  61   GYFKVTKDMSAYTKAAVFSGVGKKTPLITRFSQVAGEAGYPDTYRDVRGFAVKFYTEEGN  120
            GYFKVTKDMSAYTKAAVFSGVGKKTPLITRFSQVAGEAGYPDTYRDVRGFAVKFYTEEGN
Sbjct  61   GYFKVTKDMSAYTKAAVFSGVGKKTPLITRFSQVAGEAGYPDTYRDVRGFAVKFYTEEGN  120

Query  121  YDIVGNNTPVFFVNDPLKFPDFIHSQKRDPRTHARSQDMQWDFWSLSPESVHQVTILMSD  180
            YDIVGNNTPVFFVNDPLKFPDFIHSQKRDPRTHARSQDMQWDFWSLSPESVHQVTILMSD
Sbjct  121  YDIVGNNTPVFFVNDPLKFPDFIHSQKRDPRTHARSQDMQWDFWSLSPESVHQVTILMSD  180

Query  181  RGIPASYRMMHGFGSHTFKWVNAQGEQFWVKYHFKTNQGIHNLSNELADELAGKDTDYLQ  240
            RGIPASYRMMHGFGSHTFKWVNAQGEQFWVKYHFKTNQG+HNLSNELADELAGKDTDYLQ
Sbjct  181  RGIPASYRMMHGFGSHTFKWVNAQGEQFWVKYHFKTNQGVHNLSNELADELAGKDTDYLQ  240

Query  241  NDLFDAIETGDYPSWTVAVQLVPYEDGLNYPQDIFDVTKVISQKDYPLIEIGQMVLDENP  300
            NDLFDAIETGDYPSWTVAVQLVPYEDGLNYPQDIFDVTKVISQKDYPLIEIGQMVLDENP
Sbjct  241  NDLFDAIETGDYPSWTVAVQLVPYEDGLNYPQDIFDVTKVISQKDYPLIEIGQMVLDENP  300

Query  301  TNNFEDIQELAFSPANLVPGIEASPDKLLQGRLFGYKDAERYRLGANYEQLPVNRPKVPV  360
            TNNFEDI+ELAFSPANLVPGIEAS DKLLQGRLFGYKDAERYRLGANYEQLP+NRPKVPV
Sbjct  301  TNNFEDIEELAFSPANLVPGIEASSDKLLQGRLFGYKDAERYRLGANYEQLPINRPKVPV  360

Query  361  HNYERDGAMAQNQATGVNYEPNSQDGPTEVPAAKIHGDQLSGTTGNFSADPDYYSAAGKL  420
            HNYERDGAMAQNQ TGVNYEPNSQDGPTEVPAAKIH +Q SGTTGNFS DPDYYSAAGKL
Sbjct  361  HNYERDGAMAQNQETGVNYEPNSQDGPTEVPAAKIHSNQFSGTTGNFSTDPDYYSAAGKL  420

Query  421  YRLLSADEQTRLIENIRMNLGQVTKPEIQIREVKQFYQADPEYGRRVATSVKLRFS  476
            YRLLSADEQTRLIENIRMNLGQVTKPEIQIREVKQFYQADPEYGRRVAT++ L  +
Sbjct  421  YRLLSADEQTRLIENIRMNLGQVTKPEIQIREVKQFYQADPEYGRRVATALNLDLA  476
```

supplementary Figure 23: Blast comparison of katA gene (Query) of *L. sakei* LTH677 (Knauf et al., 1992) and *L. sakei* TMW 1.1396 catalase gene (Sbjct). Alignment revealed that identified catalase of *L. sakei* is a hemedependent catalase like it is described by Knauf *et al.* (Knauf et al., 1992).

supplementary Table 4: Several orfs were identified at the genome of *L. curvatus* strains associated with bacteriocin and bacteriocin immunity protein using BADGE.

ORF_ID	ORF_length	annotation	contig	start	stop
L_curvatus_TMW1_1381_A4W73_07565	186	bacteriocin	L_curvatus_TMW1_1381_CP015493	1453556	1453371
L_curvatus_TMW1_167_A4W76_07565	186	bacteriocin	L_curvatus_TMW1_167_CP016472	1453236	1453051
L_curvatus_TMW1_27_A4W75_09655	186	bacteriocin	L_curvatus_TMW1_27_CP016468	62399	62214
L_curvatus_TMW1_401_A4W77_02545	186	bacteriocin	L_curvatus_TMW1_401_CP016216	509407	509592
L_curvatus_TMW1_421_A4W79_02490	186	bacteriocin	L_curvatus_TMW1_421_CP016221	487373	487558
L_curvatus_TMW1_439_A4W71_02535	186	bacteriocin	L_curvatus_TMW1_439_CP015489	494991	495176
L_curvatus_TMW1_595_A4W80_07765	186	bacteriocin	L_curvatus_TMW1_595_CP016470	1514017	1513832
L_curvatus_TMW1_1381_A4W73_07590	348	bacteriocin immunity protein	L_curvatus_TMW1_1381_CP015493	1457616	1457963
L_curvatus_TMW1_1390_A4W74_07635	348	bacteriocin immunity protein	L_curvatus_TMW1_1390_CP015494	1470443	1470790
L_curvatus_TMW1_167_A4W76_07590	348	bacteriocin immunity protein	L_curvatus_TMW1_167_CP016472	1457295	1457642
L_curvatus_TMW1_421_A4W79_02470	348	bacteriocin immunity protein	L_curvatus_TMW1_421_CP016221	484360	484013
L_curvatus_TMW1_439_A4W71_02510	348	bacteriocin immunity protein	L_curvatus_TMW1_439_CP015489	490931	490584
L_curvatus_TMW1_595_A4W80_07785	348	bacteriocin immunity protein	L_curvatus_TMW1_595_CP016470	1517030	1517377
L_curvatus_TMW1_624_A4W72_02650	348	bacteriocin immunity protein	L_curvatus_TMW1_624_CP015490	516802	516455
L_curvatus_TMW1_1390_A4W74_07630	288	bacteriocin immunity protein	L_curvatus_TMW1_1390_CP015494	147032	1470033

ORF_ID	ORF_length	annotation	contig	start	stop
				0	
L_curvatus_TMW1_167_A4W76_07525	277	bacteriocin immunity protein	L_curvatus_TMW1_167_CP016472	144951	1449240
				6	
XTRA_L_curvatus_TMW1_1381_L_curvatus_TMW1_167_A4W76_0752	277	bacteriocin immunity protein	L_curvatus_TMW1_1381_CP015493	144983	1449560
5				6	
L_curvatus_TMW1_27_A4W75_09605	280	bacteriocin immunity protein	L_curvatus_TMW1_27_CP016468	54495	54216
L_curvatus_TMW1_401_A4W77_02575	280	bacteriocin immunity protein	L_curvatus_TMW1_401_CP016216	512435	512714
L_curvatus_TMW1_421_A4W79_02530	280	bacteriocin immunity protein	L_curvatus_TMW1_421_CP016221	491399	491678
XTRA_L_curvatus_TMW1_439_L_curvatus_TMW1_167_A4W76_07525	277	bacteriocin immunity protein	L_curvatus_TMW1_439_CP015489	498711	498987
L_curvatus_TMW1_595_A4W80_07730	280	bacteriocin immunity protein	L_curvatus_TMW1_595_CP016470	151110	1510821
				0	
XTRA_L_curvatus_TMW1_624_L_curvatus_TMW1_167_A4W76_07525	280	bacteriocin immunity protein	L_curvatus_TMW1_624_CP015490	522126	522405
L_curvatus_TMW1_27_A4W75_09675	348	bacteriocin immunity protein	L_curvatus_TMW1_27_CP016468	65412	65759
L_curvatus_TMW1_401_A4W77_02525	348	bacteriocin immunity protein	L_curvatus_TMW1_401_CP016216	506396	506049
L_curvatus_TMW1_401_A4W77_00445	357	bacteriocin immunity protein	L_curvatus_TMW1_401_CP016216	97385	97029
L_curvatus_TMW1_624_A4W72_00665	186	bacteriocin	L_curvatus_TMW1_624_CP015490	134825	134640

supplementary Table 5: Several orfs were identified at the genome of *L. sakei* strains associated with bacteriocin immunity protein and bacteriocin using BADGE.

ORF_ID	ORF_length	annotation	contig	start	stop
L_sakei_TMW1_114_A4W83_03015	348	bacteriocin immunity protein	L_sakei_TMW1_114_CP017566	593266	592919
L_sakei_TMW1_1189_BHU02_03230	348	bacteriocin immunity protein	L_sakei_TMW1_1189_CP017271	652972	652625
L_sakei_TMW1_1239_A4W86_03145	348	bacteriocin immunity protein	L_sakei_TMW1_1239_CP017272	646491	646144
L_sakei_TMW1_1322_LCA_RS02865	348	bacteriocin immunity protein	L_sakei_TMW1_1322_NC_007576	575788	575441
L_sakei_TMW1_1396_A4W87_06780	348	bacteriocin immunity protein	L_sakei_TMW1_1396_CP017273	1338660	1339007
L_sakei_TMW1_1398_A4W88_02920	348	bacteriocin immunity protein	L_sakei_TMW1_1398_CP017275	577815	577468
L_sakei_TMW1_3_A4W81_06700	348	bacteriocin immunity protein	L_sakei_TMW1_3_CP016465	1329518	1329865
L_sakei_TMW1_417_A4W84_03010	348	bacteriocin immunity protein	L_sakei_TMW1_417_CP017568	600850	600503
L_sakei_TMW1_46_A4W82_03055	348	bacteriocin immunity protein	L_sakei_TMW1_46_CP015487	616771	616424
L_sakei_TMW1_578_A4W85_03015	348	bacteriocin immunity protein	L_sakei_TMW1_578_CP017570	593261	592914
L_sakei_TMW1_114_A4W83_03030	186	bacteriocin	L_sakei_TMW1_114_CP017566	595816	596001
L_sakei_TMW1_578_A4W85_03030	186	bacteriocin	L_sakei_TMW1_578_CP017570	595811	595996
L_sakei_TMW1_114_A4W83_03070	327	bacteriocin immunity protein	L_sakei_TMW1_114_CP017566	601605	601931
L_sakei_TMW1_578_A4W85_03070	327	bacteriocin immunity protein	L_sakei_TMW1_578_CP017570	601600	601926
L_sakei_TMW1_114_A4W83_03075	280	bacteriocin immunity protein	L_sakei_TMW1_114_CP017566	601950	602229
L_sakei_TMW1_578_A4W85_03075	280	bacteriocin immunity protein	L_sakei_TMW1_578_CP017570	601945	602224
L_sakei_TMW1_417_A4W84_03035	333	bacteriocin immunity protein	L_sakei_TMW1_417_CP017568	605821	606153
L_sakei_TMW1_1189_BHU02_03265	297	bacteriocin immunity protein	L_sakei_TMW1_1189_CP017271	657314	657610
L_sakei_TMW1_1239_A4W86_03180	297	bacteriocin immunity protein	L_sakei_TMW1_1239_CP017272	650833	651129
L_sakei_TMW1_1396_A4W87_06700	297	bacteriocin immunity protein	L_sakei_TMW1_1396_CP017273	1328841	1328545
L_sakei_TMW1_1398_A4W88_02960	297	bacteriocin immunity protein	L_sakei_TMW1_1398_CP017275	583584	583880

ORF_ID	ORF_length	annotation	contig	start	stop
L_sakei_TMW1_3_A4W81_06615	297	bacteriocin immunity protein	L_sakei_TMW1_3_CP016465	1316480	1316184
L_sakei_TMW1_417_A4W84_03040	297	bacteriocin immunity protein	L_sakei_TMW1_417_CP017568	606163	606459
L_sakei_TMW1_46_A4W82_03090	276	bacteriocin immunity protein	L_sakei_TMW1_46_CP015487	621122	621397
L_sakei_TMW1_1322_LCA_RS02905	288	hypothetical protein	L_sakei_TMW1_1322_NC_007576	581106	581393
L_sakei_TMW1_1189_BHU02_03260	333	enterocin immunity protein	L_sakei_TMW1_1189_CP017271	656972	657304
L_sakei_TMW1_1239_A4W86_03175	333	enterocin immunity protein	L_sakei_TMW1_1239_CP017272	650491	650823
L_sakei_TMW1_1322_LCA_RS02900	333	hypothetical protein	L_sakei_TMW1_1322_NC_007576	580755	581087
L_sakei_TMW1_1396_A4W87_06705	333	enterocin immunity protein	L_sakei_TMW1_1396_CP017273	1329183	1328851
L_sakei_TMW1_1398_A4W88_02955	333	enterocin immunity protein	L_sakei_TMW1_1398_CP017275	583242	583574
L_sakei_TMW1_3_A4W81_06620	333	enterocin immunity protein	L_sakei_TMW1_3_CP016465	1316822	1316490
L_sakei_TMW1_417_A4W84_03035	333	bacteriocin immunity protein	L_sakei_TMW1_417_CP017568	605821	606153
L_sakei_TMW1_46_A4W82_03085	333	enterocin immunity protein	L_sakei_TMW1_46_CP015487	620771	621103

10 List of Publications and Student Theses

Peer-reviewed journals

Eisenbach, L. et al. (2018), Comparative genomics of *Lactobacillus curvatus* enables prediction of traits relating to adaptation and strategies of assertiveness in sausage fermentation, Int. J. Food Microbiol.

Eisenbach, L. et al. (2019), Comparative genomics of *Lactobacillus sakei* supports the development of starter strain combinations, Microbiological Research

Janßen, D. et al (2018), Assertiveness of *Lactobacillus sakei* and *Lactobacillus curvatus* in a fermented sausage model, Int. J. Food Microbiol.

Lauterbach et al. (2018), Novel diagnostic marker genes differentiate *Saccharomyces* with respect to their potential application, J. Inst. Brew.

Xu, D. et al. (2019), Lifestyle of *Lactobacillus hordei* isolated from water kefir based on genomic, proteomic and physiological characterization, Int. J. Food Microbiol.

Oral presentation

Eisenbach, L., Janßen D. Ehrmann, M.A., Vogel, R. F., (2017), Comparative genomics of *Lactobacillus sakei* and *Lactobacillus curvatus* suggests the use of strain starter sets, 3rd International Symposium on Fermented Meat, Clermont-Ferrand

Poster presentation

Eisenbach[x], L., Janßen[x], D., Ehrmann, M., Vogel, R. F., (2016), Biodiversity of *Lactobacillus sakei* and *Lactobacillus curvatus*, Food Micro, Dublin, PO2-SB-236

x: shared authorship